

AD-A067 736

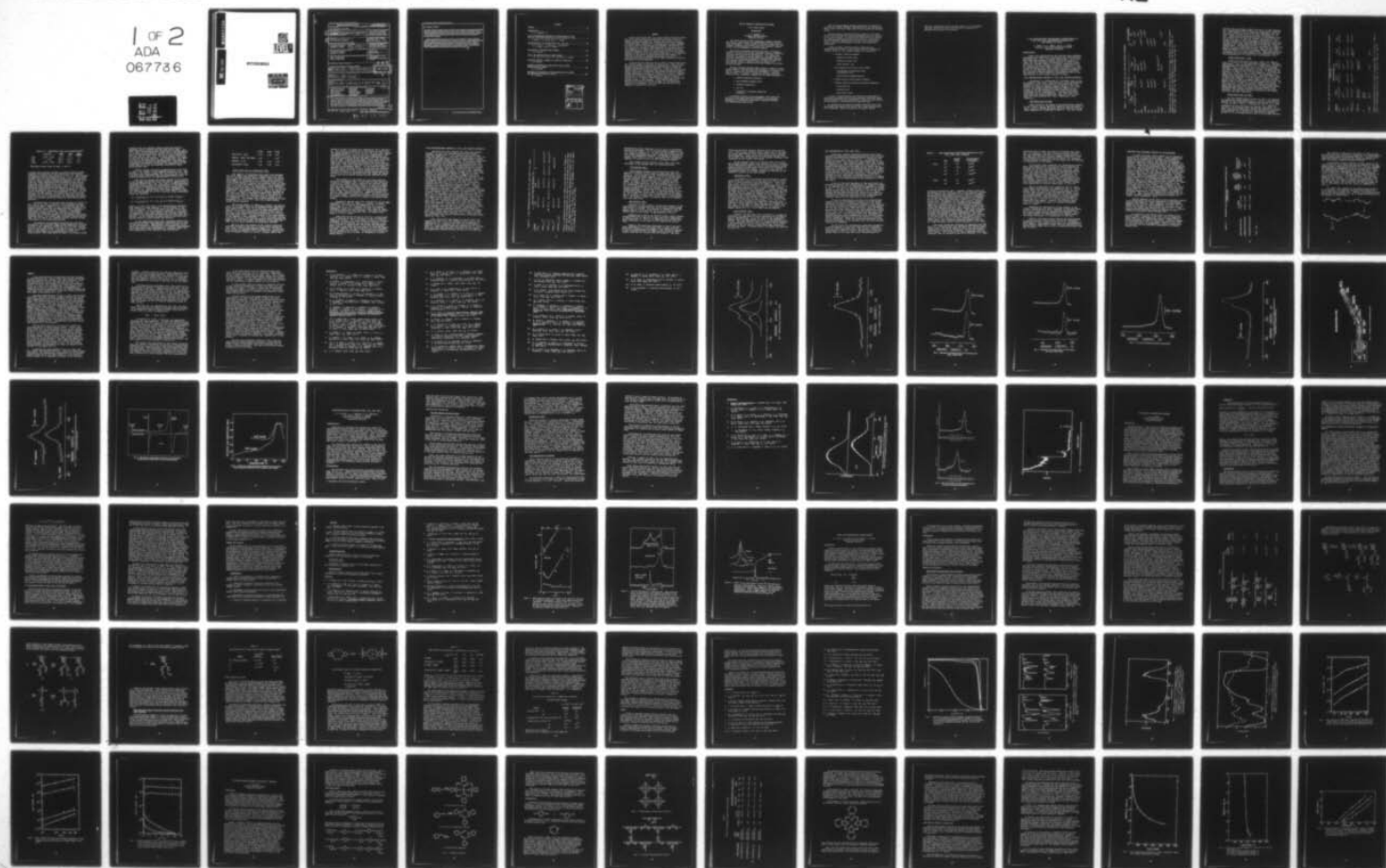
NAVAL RESEARCH LAB WASHINGTON D C
THE NRL PROGRAM ON ELECTROACTIVE POLYMERS. (U)
MAR 79 L B LOCKHART
NRL-MR-3960

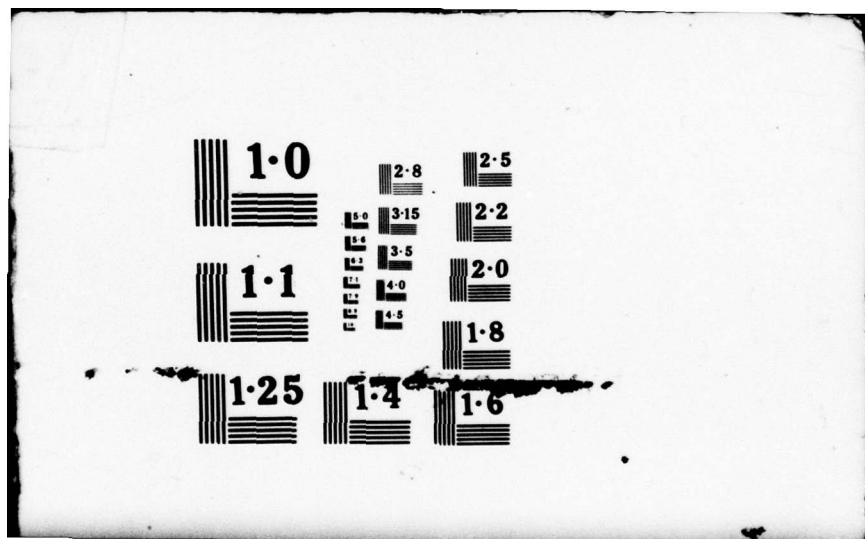
F/G 7/3

UNCLASSIFIED

NL

1 OF 2
ADA
067736





DDC FILE COPY

ADA067736

MARCH 30 1979

LEVEL II

12



SECURITY CLASSIFICATION OF THIS PAGE (When Data Entered)

REPORT DOCUMENTATION PAGE		READ INSTRUCTIONS BEFORE COMPLETING FORM
1. REPORT NUMBER NRL Memorandum Report 3960	2. GOVT ACCESSION NO.	3. RECIPIENT'S CATALOG NUMBER
4. TITLE (and Subtitle) THE NRL PROGRAM ON ELECTROACTIVE POLYMERS FIRST ANNUAL REPORT		5. TYPE OF REPORT & PERIOD COVERED Progress Report for the Period Oct 1, 1977 - Sept 30, 1978
7. AUTHOR(s) Luther B. Lockhart, Jr., Editor		8. CONTRACT OR GRANT NUMBER(s) 30 Mar 79
9. PERFORMING ORGANIZATION NAME AND ADDRESS Naval Research Laboratory Washington, D.C. 20375		10. PROGRAM ELEMENT, PROJECT, TASK AREA & WORK UNIT NUMBERS NRL Problem C03-34 & C04-12 PE 61153N-13; RR 013-02-43
11. CONTROLLING OFFICE NAME AND ADDRESS Naval Research Laboratory Washington, D.C. 20375		12. REPORT DATE March 30, 1979
14. MONITORING AGENCY NAME & ADDRESS (if different from Controlling Office) Office of Naval Research Arlington, Virginia 22217		13. NUMBER OF PAGES 179
		15. SECURITY CLASS. (of this report) UNCLASSIFIED
		15a. DECLASSIFICATION/DOWNGRADING SCHEDULE
16. DISTRIBUTION STATEMENT (of this Report) Approved for public release; distribution unlimited.		
16 RR 01302		17 RR 0230243
17. DISTRIBUTION STATEMENT (of the abstract entered in Block 20, if different from Report) 14 NRL-MR-3960		
18. SUPPLEMENTARY NOTES Annual rept. no. 1.1 Oct 77-30 Sep 78		
19. KEY WORDS (Continue on reverse side if necessary and identify by block number)		
Organic semiconductors	Charge-transfer	Ion implantation
Organic superconductors	Polyacetylenes	Piezoelectricity
Photoconductors	Polyphthalocyanines	Pyroelectricity
Inorganic polymers	Phosphorus nitrides	Intercalation
Polyconjugated polymers	Sulfur nitrides	
20. ABSTRACT (Continue on reverse side if necessary and identify by block number) The general objective of this program is to develop new classes of polymeric materials that have unique and useful electrical properties suitable for application to Naval devices and systems. A subsidiary objective is to develop theory and guidelines relating electrical properties to the molecular nature and morphology of polymeric materials to permit the design of such materials with predictable properties for use in Naval applications. Specific material objectives are to synthesize, characterize, and evaluate for Naval applications (a) polymers that have substantially inorganic		
(Continues)		

DD FORM 1 JAN 73 1473

EDITION OF 1 NOV 65 IS OBSOLETE
S/N 0102-014-6601

SECURITY CLASSIFICATION OF THIS PAGE (When Data Entered)

79 04 18 041

20. Abstract (Continued)

main-chains that exhibit metallic or semiconductivity; (b) polyconjugated and organometallic polymers that exhibit metallic or semiconductivity; (c) organic polymers capable of forming inter- or intramolecular charge-transfer complexes through electron donor and acceptor moieties within or attached to the polymer chain; and (d) polymers that exhibit piezoelectric, pyroelectric, photovoltaic, or memory-switching properties.

Specific items addressed in this first year's effort are the application of advanced analytical techniques to develop an understanding of the composition and structure of state-of-the-art polymeric conductors and superconductors, the development of computer models of electron mobility in polymeric structures which would provide guidance to the synthetic effort, and the synthesis of polyacetylenes, conjugated polyphthalocyanines and charge-transfer polymers for development of a better understanding of structure-property relationships in these systems.

CONTENTS

PREFACE.	iv
INTRODUCTION.	1
L. B. Lockhart, Jr.	
X-RAY PHOTOELECTRON SPECTROSCOPIC INVESTIGATION OF (SN) AND (CH) _x AND RELATED MATERIALS AND ESR STUDIES OF (CH) _x	4
P. Brant, D. C. Weber, and C. T. Ewing	
CHARACTERIZATION OF HALOGEN-DOPED (CH) _x AND (SN) _x	39
W. N. Allen, J. J. DeCorpo, F. E. Saalfeld, J. R. Wyatt, and D. C. Weber	
NMR STUDIES OF ELECTROACTIVE POLYMERS.	42
H. A. Resing.	
PHOTO- AND SEMICONDUCTING POLYMER SYSTEMS.	58
R. B. Fox, T. R. Price, O-K. Kim and R. F. Cozzens	
CONJUGATED NETWORK POLYMERS AS ELECTRICAL CONDUCTORS.	80
T. R. Walton	
ELECTRICAL PROPERTIES OF METAL-FREE, DIANIL-LINKED PHTHALOCYANINE POLYMERS.	98
J. P. Reardon	
PROBLEMS AND PROSPECTS OF FUTURE ELECTROACTIVE POLYMERS AND "MOLECULAR" ELECTRONIC DEVICES.	121
F. L. Carter	

ACCESSION for	
NTIS	White Section <input checked="" type="checkbox"/>
DDC	Buff Section <input type="checkbox"/>
UNANNOUNCED	<input type="checkbox"/>
JUSTIFICATION _____	
BY _____	
DISTRIBUTION/AVAILABILITY CODES	
Dist. AVAIL. and/or SPECIAL	
A	

PREFACE

Recent work has shown that, as a class, polymeric materials possess many of the useful electrical properties that are found in the non-polymeric metals and inorganics. Moreover, the polymers possess potential advantages: notably, ease of fabrication into films, filaments and complex shapes; variability in molecular design; general availability and low cost; and high strength and toughness. The objective of this program is to develop an understanding of the molecular structure and configuration in polymers that confers the unusual and desirable electrical properties and to use this knowledge to develop new polymer systems with improved utility and greater versatility. It is envisioned that many of the present day Naval applications that depend on the electrical properties of non-polymeric materials will benefit significantly by having available a wider range of materials having new and unusual electrical properties.

The Naval Research Laboratory and the Office of Naval Research have had a direct interest in this area for several years. About two years ago both organizations independently reevaluated their programs and decided that expanded effort was warranted. At NRL, this involved drawing together several small projects into a larger more well-focussed effort in this area. Concurrently, ONR through its Advanced Polymer Program significantly increased its activity in the areas of conducting polymers and piezoelectric polymers. Coordination of the two programs was carried out through the Navy Committee on Advanced Polymers, chaired by Dr. K. J. Wynne of ONR's Chemistry Branch, and through joint internal reviews of both programs. A joint ONR-NRL Symposium on Electroactive Polymers held at NRL on August 25, 1978 highlighted efforts in these programs. Much of the NRL work discussed at that Symposium is contained in this report.

THE NRL PROGRAM ON ELECTROACTIVE POLYMERS

First Annual Report

INTRODUCTION

L. B. Lockhart, Jr.
Polymeric Materials Branch
Chemistry Division

The entire spectrum of Navy technology in weapons, platforms, and logistics relies heavily on sophisticated electronic devices. These technologies, in turn, depend on a variety of metals and other inorganic substances that serve as electrical conductors, semiconductors, and electromagnetic or acoustic sensors.

The utility of available electronic materials is frequently limited by such factors as weight, mechanical fragility, fabrication problems, corrosion, scarcity and high cost. As a result, Navy scientists are looking to the development of a new generation of electronic components and systems employing non-metallic materials which we call "electroactive polymers." Although these materials have long been known to chemists, efforts to exploit their extraordinary electrical properties have been attempted only within the last few years.

The Naval Research Laboratory (NRL) research program in electroactive polymers is directed toward the development of synthetic, non-metallic polymers with electrical and electromagnetic properties that are equal to or superior to those of conventional materials (metals and their compounds), combined with the added advantages of

- o greatly simplified fabrication
- o high strength-to-weight ratios
- o unlimited availability
- o low cost
- o variability in molecular design and properties

A subsidiary objective is the development of new theory and guidelines which relate electrical properties to the molecular structures and morphological properties of polymeric materials.

Note: Manuscript submitted January 22, 1979.

NRL's current program of research on electroactive polymers is concerned with THEORY, SYNTHESIS, CHARACTERIZATION, and APPLICATIONS. Each of these interrelated tasks draws on prior capabilities developed at NRL.

Existing theories relating electrical properties to molecular structure and describing how electrical phenomena operate in polymers are not well developed. To correct these deficiencies, NRL chemists are comparing quantum-theory models with electronic energy levels and other molecular parameters derived from electron spectroscopy (ESCA), carbon-13 nuclear magnetic resonance, and conductivity measurements.

Polymer synthesis, guided by parallel theoretical and characterization studies, is being directed toward both organic and inorganic materials. The following examples are illustrative:

- o Inorganic conducting polymers
 - Phosphorus nitrides $(\text{PN})_x$
 - Phosphorus borides $(\text{PB})_x$
 - Carbon sulfides $(\text{CS})_x$
- o Polyconjugated linear and network polymers
 - Ion-implanted and chemically doped polyacetylene $(\text{CH})_x$
 - Dianil-linked polyphthalocyanines
- o Charge-transfer (donor-acceptor) polymers
- o Polymers exhibiting stimulated electrical phenomena ...
 - piezoelectricity
 - pyroelectricity
 - photovoltaic effect

A variety of physicochemical and spectroscopic measurements is being used to determine the electrical properties, mechanical properties and molecular structures of materials. Results of these studies provide guidance to the theoretical and synthesis tasks.

As promising new electroactive polymeric materials evolve from the program, applications which exploit their unique characteristics will be examined. Beyond the potential for improved sensors,

detectors, semiconductors and solid-state devices, it is anticipated that these studies will lead to the discovery of important new phenomena and exciting new technologies.

X-RAY PHOTOELECTRON SPECTROSCOPIC INVESTIGATION OF
(SN)_x AND (CH)_x AND RELATED MATERIALS AND
ESR STUDIES OF (CH)_x

P. Brant, D. C. Weber, and C. T. Ewing
Inorganic and Electrochemistry Branch
Chemistry Division

INTRODUCTION

Both X-ray photoelectron and electron spin resonance techniques were utilized to investigate the electroactive materials (SN)_x, (CH)_x, and their derivatives. It was felt that these spectroscopic methods could give greater insight into the electronic configurations of these unique molecules, thereby leading to a greater understanding of the reasons for their unique electrical properties. Such an understanding would then be used as a guide in the synthesis of new materials with similar electrical properties but with much improved physical and chemical properties. The progress of these studies is discussed as well as the implications of the results obtained to date.

X-RAY PHOTOELECTRON SPECTRA OF (SN)_x AND RELATED MATERIALS

Polythiazyl is synthesized by "cracking" S₄N₄ in the gas phase to form clear, colorless S₂N₂, which subsequently polymerizes in the solid state to the golden (SN)_x (1). Exposure of (SN)_x to bromine vapors results in the formation of the highly conducting material (SNBr_{0.4})_x (2,3). As part of the Electroactive Polymer Program, we have undertaken an XPS investigation of several derivatives containing the SN repeating unit. Gas phase and solid state data have been recorded for S₂N₂, and solid state data have been obtained for (SN)_x, (SNBr_{0.05})_x, and (SNBr_{0.4})_x.

Gas Phase Data on S₂N₂

High resolution gas phase X-ray photoelectron spectra of the S 2p_{1/2}, 2p_{3/2}, and N 1s levels in S₂N₂ are shown in Figs. 1 and 2, and the gas phase XPS data for this and related compounds are organized in Table I. The line widths

TABLE I - GAS PHASE XPS DATA FOR S₂N₂ AND SOME RELATED COMPOUNDS

	BINDING ENERGY, eV			CALC. CHARGES	
	S 2p _{1/2}	2p _{3/2}	N 1s	Q _S	Q _N
S ₂ N ₂	173.64(1.09) ^{a,c}	172.44(1.08) ^a	405.86(1.09) ^a	0.13 ^k	-0.13 ^k
N ₂			409.9 ^d		0.00
NSF ₃		176.8 ^{b,e}	406.23 ^{b,e}	0.82 ^{e,k}	-0.44 ^{e,k}
C ₆ H ₅ NH ₂			4.05.31 ^{a,f}		-0.187 ^k
SF ₆		180.4 ^{a,g}		1.14 ^{e,k}	
OCS		170.6 ^{a,g}		-0.03 ^{e,k}	
CS ₂		169.8 ^{a,g}		-0.04 ^{e,k}	
(NPF ₂) ₃			405.29(1.07) ^{b,h}		
CH ₃ CN			405.9 ⁱ		-0.15 ^k
S ₈		170.5 ^{a,j}		0.00	

^aRelative to Ar 2p_{3/2} 248.62 eV; ^bRelative to Ar 2p_{3/2} 248.45 eV; ^cValues in parentheses are peak full width at half maxima in eV; ^dRef. 28; ^eRef. 30; ^fRef. 31; ^gRef. 32; ^hRef. 33; ⁱRef. 34; ^jRef. 35; ^kCHELEQ method, see Ref. 36.

of the S $2p_{1/2}$ and $2p_{3/2}$ peaks, and the N $1s$ peak approach the natural line width of the Al-K α X-ray source (0.95 eV) (4). The symmetric narrow peaks are consistent with the presence of a single form of nitrogen and sulfur (1) in S_2N_2 . Empirical charge-binding energy relationships (5,6) for S and N indicate that the charges on sulfur and nitrogen in S_2N_2 are $\sim +0.15e$ and $-0.15e$, respectively. Dr. Joseph A. Hashmall, who is working as an outside consultant on this project, has completed MNDO calculations which give charges on the sulfur and nitrogen of +0.402 and -0.402, respectively. Calculations for S_2N_2 by others (7) employing SCF-X α , ab initio LCAO Hartree-Fock, INDO, and INDO-type ASMO-SCF methods give N and S charges ranging from -0.21 to -0.48 and +0.21 to +0.48, respectively. The experimentally determined and calculated charges are consistent with the electronegativities of sulfur (1.9) and nitrogen (2.5).

Solid State Data: S_2N_2

Solid state XPS data for S_2N_2 , $(SN)_x$, and $(SNBr_y)_x$ with $y \approx 0.05$ or 0.4 are summarized in Table II. For these experiments, S_2N_2 was sprayed onto a sample probe cooled to approximately 77°K and its S $2p$, S $2s$, and N $1s$ spectra recorded. These core levels have binding energies roughly the same as reported by Sharma et al (8). In addition, an intense O $1s$ peak at 533.2 eV was observed. It is believed that the O $1s$ peak is due to water which presumably condensed onto the probe with the S_2N_2 . Electron energy loss features are associated with the primary S $2p$, S $2s$, and N $1s$ core level signals. A broad feature situated approximately 22-24 eV from the primary peak is present in all the spectra and is attributed to a bulk plasmon excitation. In the S $2p$ (Fig. 3) and S $2s$ spectra, weaker and narrower satellites are also observed 6.2 eV from the primary peaks. These weak satellites are tentatively attributed to an intramolecular valence electron transition during photoemission. The molecular orbitals involved in the transition have not been identified.

Solid State Data on $(SN)_x$

In situ polymerization of S_2N_2 to $(SN)_x$ was achieved by raising the probe temperature to $\sim 300^\circ K$. S $2p$ and N $1s$ spectra of the polymerized product are compared with those of S_2N_2 in Figs. 3 and 4. Although the $S-N-S$ and $N-S-N$ topologies of S_2N_2 and $(SN)_x$ are similar (see Table III), and the S and N ground state charges are expected to be the same, some marked differences in the spectra are observed. In particular, the S $2p$ and S $2s$ peaks broaden approximately 0.4 eV on polymerization, and the N $1s$ peak develops

TABLE II - SOLID STATE XPS DATA FOR COMPOUNDS WITH THE REPEATING SN UNIT AND FOR RELATED DERIVATIVES

Compound	Binding Energies, eV			
	S 2p _{3/2}	S 2s	N 1s	O 1s
S ₂ N ₂	165.8(2.3) ^{a,b}	229.2(2.9) ^b	399.6(1.7) ^b	284.4(1.9) 532.6(1.9)
S ₄ N ₄	164.4 ^c		397.1 ^c	285.0
(SN) _x	165.0(3.0) ^d	229.1(3.6) ^d	398.3(1.8) ^d	284.4(1.7) 531.4(2.0)
(SNBr _{0.04}) _x	165.0(3.4) ^e	229.1(3.3) ^e	398.3(2.4) ^e	284.4(1.4) 284.4 531.1(1.5)
(SNBr _{0.4}) _x	168.7(2.4) ^f 164.7(2.7)		401.4(1.9) ^f 398.2(2.0)	
S ₈	164.2 ^g 163.9 ^h			
S ₄ (NH) ₄	164.8 ⁱ		399.1 ⁱ	285.0

^aValues in parentheses are peak full width at half maxima (fwhm) in eV; ^bRef. 8; ^cRef. 41; ^dRef. 8; ^eValues reported in Ref. 14; ^fRef. 37; ^gRef. 38; ^hRef. 39; ⁱRef. 40.

TABLE III - STRUCTURAL DATA FOR SN DERIVATIVES^a

	<u>S-N (\AA)</u>	<u><NSN</u>	<u><SNS</u>	<u>Bond Order</u>
S_2N_2	1.657, 1.651	89.6	90.4	1.5
S_4N_4	1.616	105.5	113.5	1.5
$(\text{SN})_x$	1.593, 1.628	106.2	119.9	~1.3

^aStructural data found in Refs. 1 and 37.

a strong well-resolved shoulder at higher binding energy. Gaussian deconvolution of the primary peak and shoulder resulted in relative peak areas of 2.0 to 1.0. The shoulder is separated from the primary peak by 2.4 eV. Other investigators have utilized electron energy loss (EEL) spectroscopy to examine plasmon dispersion phenomena in $(\text{SN})_x$ (10). A strong, sharp dispersion peak propagated along the SN chain was found separated by 2.5 eV from the elastically scattered monoenergetic electrons, while a weak plasmon dispersion peak propagated perpendicular to the SN chains was found separated by 1.5 eV. These plasmons are related to the anisotropic electrical properties of $(\text{SN})_x$. On the basis of the EEL studies, the broadening of the S 2p and 2s peaks and the shoulder in the N 1s spectrum from polymerization of S_2N_2 to polythiazyl are attributed to excitation of a plasmon transition along the chain during photoemission.

Polymerization of the S_2N_2 also results in a shift of the S 2p, N 1s, and S 2s peaks to lower binding energies. In a recent paper, Sharma et al. (8) attributed the lower binding energies in $(\text{SN})_x$ to more efficient dissipation of sample surface charge by the conducting $(\text{SN})_x$ compared to S_2N_2 which is not a conductor. However, a reasonable alternative explanation is that the decreased binding energies and, with the exception of the plasmon loss peaks discussed above, the broader peak envelopes associated with $(\text{SN})_x$ are the result of a greater valence electron relaxation effect in the conducting polymer.

In addition to providing the energy for S_2N_2 polymerization, the increased sample probe temperature resulted in loss of the intense O 1s peak at 533.5 eV while giving rise to a new, much weaker O 1s peak at 531.5 eV. Correlation of the relative O 1s, S 2p, and N 1s peak areas (11) gave an approximate O:S:N stoichiometric ratio of 0.04:1.0:1.0. The large shift to lower O 1s binding energy

suggests that the adsorbed oxygen-containing material (probably water) reacted with the S_2N_2 and/or $(SN)_x$. In fact, other investigators have identified a hydride impurity in $(SN)_x$ by mass spectral studies and it was speculated that the hydride arose from reaction of small amounts of H_2O with S_2N_2 or $(SN)_x$ (12). No oxide impurity was found in the mass spectral analysis. We believe the O 1s signal recorded in the spectrum on in situ polymerized $(SN)_x$ to be a previously unobserved oxide impurity. Unfortunately, independent information concerning the composition of the oxide impurity is not yet available from XPS or other spectroscopic data.

Before, during, and after polymerization of the S_2N_2 to $(SN)_x$, the carbon 1s peak remained extremely weak. Comparison of the carbon 1s peak area with the S 2p, S 2s and N 1s peak areas indicated that the stoichiometric ratio of carbon:nitrogen:sulfur was approximately 0.05:1.0:1.0.

The very low carbon and oxygen content on the surface of the in situ polymerized $(SN)_x$ provided an opportunity to accurately measure the S 2p, S 2s, and N 1s photoionization intensity ratios without the complication of selective overlayer signal attenuation of lower kinetic energy photoelectrons (13). Standardized area ratios determined for this sample are compared below with those reported by Wagner (11) and Nefedov et al (13), and with ratios calculated using the equations

$$I_x = I_{ox} \sigma_x \eta_x \lambda_x(\epsilon_i) [1 + (0.5 \beta_x)(1.5 \sin^2 \varphi - 1)] D_x(\epsilon_i)$$

$$I_y = I_{oy} \sigma_y \eta_y \lambda_y(\epsilon_i) [1 + (0.5 \beta_y)(1.5 \sin^2 \varphi - 1)] D_y(\epsilon_i)$$

where I_0 is the x-ray flux, σ the photoelectron cross-section relative to some standard, η is the density of the atom of interest, $\lambda(\epsilon_i)$ is the mean free path of an electron of energy ϵ_i in the substance examined, β is an orbital parameter, φ the angle between the incident radiation and path of the detected photoelectrons (in this case, 90°), and $D(\epsilon_i)$ is the fraction of photo-ejected electrons with kinetic energy ϵ_i which reaches the detector.

As the comparisons below show, agreement between the calculated and three experimentally determined sets of data is only qualitative. Experimental values probably do not agree well because of differences in overlayer contributions, x-ray anode and window contamination, variable sample surface compositions, and satellite loss differences.

	<u>S 2p</u>	<u>S 2s</u>	<u>N 1s</u>
This work, (SN) _x	2.10	1.00	1.83
Wagner, (K ₂ SO ₄ and KNO ₃)	3.04	-	1.83
Nefedov, et al	5.28	1.00	2.50
Calculated (AlK _α)	3.26	1.00	1.05

Solid State Data on Brominated (SN)_x

Two samples of brominated (SN)_x have been examined. The first sample was prepared by bromination of an (SN)_x film in the spectrometer sample chamber, while the second was prepared by bromination of an (SN)_x single crystal to form (SNBr_{0.4})_x according to the literature method (10a). In the first instance, bromine was condensed onto the (SN)_x film at 77°K and the sample was warmed to room temperature over a one-hour period. The approximate S:N:Br stoichiometry at the film surface was ascertained to be 1:1:0.04 by standardized area comparisons of the S 2p, N 1s, and Br 3d peaks (11). Although the quantity of bromine absorbed by the (SN)_x was small, discernible changes were observed in the core level spectra, including loss of definition of the plasmon peak at 2.4 eV higher binding energy in the N 1s spectrum. The changes were largely manifested as peak broadening (ca. 0.2-0.3 eV), with only slight binding energy shifts observed.

The second sample, an (SNBr_{0.4})_x crystal, was held in place on the sample wheel by an aluminum spacer planchette and a gold screen. Prior to XPS analysis, the sample had been stored in vacuo for a period of approximately three months. It had been prepared by exposure of the (SN)_x to Br₂ vapor from undistilled bromine according to the literature procedure (10a). During transfer to the spectrometer, it was exposed to the atmosphere. Due to the small surface area of the crystal and the area of gold screen covering the sample, the core level peaks recorded for this sample are weak, but the gross features are adequately defined.

The N 1s and S 2p spectra of the crystal exhibited striking differences from all of the previous spectra of S₂N₂, (SN)_x, and in situ prepared (SNBr_{0.04})_x. In addition to S 2p and N 1s peaks at 164.7 and 398.2 eV, respectively, which correspond roughly to those of undoped (SN)_x, new,

strong S 2p and N 1s peaks were observed at 168.7 and 401.4 eV. The relative intensities of the higher to lower binding energy (E_b) peaks in the S 2p and N 1s core level regions are approximately 0.7:1.0 and 1.0:0.7, respectively. The additional N 1s peak which arises after bromination has also been observed by Sharma and Iqbal (14), who attribute the new peak to ammonium ions (NH_4^+) which form on the surface of $(\text{SN})_x$ films during bromination and which they report have been identified by infrared and X-ray diffraction data. (The salt identified from the X-ray powder pattern data is presumably NH_4Br .) In the previous report, a separate higher binding energy S 2p peak was not observed, but this may be due both to lower resolution and to lower relative intensity of the higher binding energy peaks, as reflected in the N 1s spectrum where the higher E_b component is only two-thirds as intense as that observed in our study.

The position of the higher E_b S 2p peak which we observe in brominated $(\text{SN})_x$ is the same as that found for a variety of sulfate salts. Based on the relative intensities of the higher binding energy N 1s and S 2p components and their binding energy values, we believe at this point that the additional peaks are due to ammonium sulfate, $(\text{NH}_4)_2(\text{SO}_4)$, which forms from substantial decomposition of $(\text{SN})_x$ during bromination. Ammonium bromide, as well as other ammonium salts (see below), may also be present in the sample. Independent evidence for the presence of either of these salts in the sample is presently being sought.

Bromine 3d spectra were also recorded for the in situ brominated $(\text{SN})_x$ and the $(\text{SNBr}_{0.4})_x$ crystal. In both instances, a Br 3d signal was centered at 68.8 ± 0.2 eV with a fwhm of 2.2 eV. Although the peak is slightly asymmetric, there is no evidence for more than one form of bromine within the peak envelope. This peak is indicative of bromine in an unreacted (Br_2) or reduced (Br_n^- where $n = 1$ or 3) state.

Along with the Br 3d peak at 68.8 eV, a second peak is also observed in the Br 3d region of the air-exposed $(\text{SNBr}_{0.4})_x$ crystal. The second peak, which is of variable intensity, is observed at 75.6 eV with a fwhm of 2.0 eV. It is believed at present that the higher binding energy peak is an Al 2p signal which arises from the aluminum plate used, along with the gold screen, to hold the sample in place. However, the peak could be due to an oxidized form of bromine such as BrO_3^- . Discrimination between the two possibilities will be made by changing to a silver sample holder.

X-RAY PHOTOELECTRON SPECTRA OF $(CH)_x$ AND RELATED MATERIALS

XPS data have been compiled for $(CH)_x$ and several halogen (F_2 , Cl_2 , Br_2) and AsF_5 -treated derivatives. Recently, Baughman et al (15) reported XPS results for $(CH)_x$ and $(CHI_{0.22})_x$. Our data are presented in Table IV. A gold screen was placed over the mounted sample in most cases to eliminate sample charging. Under these conditions, binding energies were measured with the assumption that sample charging was negligible. The polyacetylene used was prepared via Ziegler-Natta polymerization with a mixture of $Ti(n-OBu)_4$ and $AlEt_3$ in vacuum-distilled toluene (16). The polymer films were washed with dry n-pentane until the washings were clear. In some cases, measurable quantities of titanium remained trapped in the $(CH)_x$ film; however, no aluminum was detected. XPS and ion back-scattering measurements indicate that the titanium in "dirty" polyacetylene films comprised less than 2% of the polymer by weight. The $Ti 2p_{3/2}$ binding energy for "dirty" air-exposed $(CH)_x$ was 458.2 eV. By comparison, that reported for pure TiO_2 (17) is 458.5 eV. We therefore conclude that the titanium in the air-exposed $(CH)_x$ is present in an oxidized form (probably Ti^{+4}). "Clean" polyacetylene films did not exhibit core level signals for titanium or aluminum. These films, including one from Prof. MacDiarmid at the University of Pennsylvania, exhibit a single narrow (fwhm 1.2-1.8 eV), intense C 1s line at 284.4 eV, in agreement with previously reported data (15). This value is the same within experimental error as the C 1s binding energy reported for polyethylene (284.6 eV) (19). The peak is markedly skewed to higher binding energies (Fig. 5). The only other core level photoelectron peak found between 50 and 1000 eV is that due to oxygen (O 1s) at 532.4 eV. Using the C 1s and O 1s peaks, area ratio analyses indicate that the carbon:oxygen molar ratio on the surface of a freshly prepared, clean sample is 1.0:0.05. Samples which have been exposed to the atmosphere for several days have much more intense O 1s peaks and carbon:oxygen ratios approach 1:0.5. These results are consistent with earlier observations concerning oxygen uptake by $(CH)_x$ (20).

$(CH)_x$ films have been doped (F_2 , Cl_2 , Br_2 , AsF_5) by exposure of the film to the halogen or AsF_5 gas at room temperature (21). Each of the films was subsequently analyzed by XPS techniques and the results are shown in Table IV. Mass spectral data were obtained by Dr. William Allen and have been discussed elsewhere in this report. The approximate halogen content in each of the films was

TABLE IV. X-RAY PHOTOELECTRON DATA FOR (CH)_x AND DOPED (CH)_x FILMS

Polymer	Core Level Binding Energies, eV		
	C 1s	O 1s	\bar{x}
(CH) _x	284.5(1.2) ^a	532.4(2.1)	
(CHBr _{0.3}) _x ^b	284.9(1.9)	531.9(1.9)	69.4(2.7) ^c 182.5(1.8) ^d
(CHCl _{0.3}) _x ^b	286.3(1.9), 284.9(1.7)	532.0(2.7)	202.0(1.5) 200.2(1.5) ^e
(CHF _{0.3}) _x ^b	286.0(1.8)	532.4(1.9)	686.8(2.6) ^f
[CH(AsF ₅) _{0.3}] _x ^b	284.9(1.8)		

^aValues in parentheses are peak full width at half maxima in eV; ^bCarbon to halogen molar ratio determined from relative C 1s and halogen core-level peak areas. The photoionization cross-section scaling factors of Wagner (11) were used; ^cBr 3d; ^dBr 3p_{3/2}; ^eCl 2p_{1/2}; ^fF 1s; ^gBaughman, et al (15) report a C 1s binding energy of 284.4 eV for (CH)_x.

determined by area comparison (11) of the C 1s and appropriate halogen peak. In all the halogenated samples, the C:X ratio is roughly 3:1. As shown by the strong O 1s signal, oxygen is present as a major component (contaminant) in all the halogenated samples. Its abundance relative to carbon varies from 1:1 in the fluorinated and brominated samples, to 0.14:1.0 (O:C) in the chlorinated sample.

The effects of the halogen on the $(CH)_x$ film vary according to the halogen used, as indicated below:

Fluorinated $(CH)_x$

Fluorination bleaches the polyacetylene film and results in a shift in the carbon 1s peak from 284.4 eV to 286.0 eV. The C 1s peak of the fluorinated polymer also broadens, for different samples, 0.2 to 0.6 eV and loses the well-defined "tail" which extends to 288 eV in the undoped polymer, thus taking on a more symmetric peak shape. A single, broad F 1s peak is found at 686.6 eV. Due to the high reactivity and electronegativity of F_2 , the bleaching of the film, and the net C 1s shift of 1.4 eV, it is concluded that the fluorine reacts with the conjugated backbone of the polyacetylene, saturating it at random positions. Indeed, the C 1s binding energy of the fluorinated polymer is the same as that calculated (286.1 eV) for a mean C 1s shift due to replacement of one hydrogen by fluorine on every third carbon atom in polyethylene (18). The single, broad F 1s peak at 686.6 eV is consistent with this view.

Chlorinated $(CH)_x$

Exposure of $(CH)_x$ film to chlorine gas results in the generation of a strong shoulder on the high binding energy side of the C 1s peak. The shoulder is separated from the larger peak by 1.5 eV and the ratio of the area of the smaller peak to the larger is approximately 0.8:1.0.

Examination of the Cl 2p binding energy region reveals exceptionally well resolved Cl 2p_{1/2} and 2p_{3/2} components, as shown in Fig. 6. The 1.5 eV separation of the two spin-orbit components is the same as that reported by others (22).

Based on the excellent resolution of the Cl 2p spin-orbit components, it is concluded that a single form of chlorine is present in the polymer. Mass spectral analyses of the Cl₂-doped polymer at temperatures as high as 340°C suggest that the Cl₂ reacted with the polymer. The only

chlorine-containing species observed below 340°C was HCl (23). The Cl $2p_{3/2}$ binding energy (200.2 eV) is the same as others reported for mono- and dichloro aryls, olefins, and aliphatics. Based on the mass spectral and XPS data, it is clear that chlorination of the polymer backbone, with formation of C-Cl bonds, took place.

At the present time it is believed that the resolvable higher binding energy peak observed in the C 1s region of the chlorinated sample is due to the chlorinated carbon atoms as well as those carbon atoms which are adjacent to two chlorinated carbon atoms. In such a case, the unchlorinated carbon 1s binding energies are shifted by the inductive effects of the CHCl groups.

Brominated (CH)_x

In contrast to fluorination and chlorination, bromination does not result in a large shift in part or all of the C 1s peak associated with polyacetylene. After exposure to Br₂ vapor and formation of (CHBr_{0.3})_x, the C 1s peak shifts to 284.9 from 284.5 eV and broadens 0.2-0.7 eV. The asymmetry present in the C 1s peak of (CH)_x remains sensibly unaltered after bromination. A single Br 3d peak is found at 69.3 eV. Mass spectral analysis shows Br₂ and HBr loss from the sample at temperatures less than 300°, suggesting that substantial amounts of the bromine do not covalently add to the polymer backbone (23). Combined, the mass spectral and XPS data indicate that the bromine is present in the (CH)_x as Br₂ or Br_n⁻ (n = 1 or 3). The results we have obtained for brominated (CH)_x are very similar to those reported for (CHI_{0.22})_x by Baughman et al (15) who, on the basis of Raman and XPS data, argue that the iodine is present in the polymer as I_n⁻ where n = 3. Higher values of n (5, 7 or 9) may also be possible.

AsF₅-treated (CH)_x

Finally, XPS data have been recorded for a sample of [CH(AsF₅)_{0.3}]_x provided by Prof. MacDiarmid of the University of Pennsylvania. As in the case of the brominated sample, the C 1s peak shifts to 284.9 eV and broadens 0.2-0.6 eV. The peak remains skewed to higher binding energies. A well-defined As 3d or As $3p_{3/2}$ peak could not be found, although in the 3d region, a very broad weak feature at 44.5 eV was noted. A strong broad F 1s signal was observed at 686.5 eV.

ION IMPLANATION OF $(CH)_x$ AND $(SN)_x$

Previously, highly conducting materials have been obtained by chemically doping polyacetylene films and polythiazyl films and single crystals with a variety of molecules (Br_2 , I_2 , AsF_5 , etc.) (2,3,21). In principle, it should be possible to achieve the same results by ion implantation (24). While chemical dopants have been limited to compounds with high vapor pressures, and control of the dopant concentration and placement in the matrix can be difficult or impossible, ion implantation offers the advantages that any element in the Periodic Table can be added to the polymers and that the ion flux, energy, and spacial resolution can be rigorously controlled. Accordingly, a program has been initiated in collaboration with Dr. C. Carosella of the Radiation Technology Division, to examine the effects of ion implantation on the properties of $(CH)_x$ and $(SN)_x$.

A list of the ions implanted to date with their implantation energies and concentrations is compiled in Table V. A schematic of the ion implantation apparatus is shown in Fig. 7. In order to evaluate the effects of ion implantation on the $(CH)_x$ and $(SN)_x$ polymers, all but one of the initial studies have involved the use of Br^+ as dopant, because the chemically brominated products have been sufficiently well characterized that direct comparisons of chemical doping and ion implantation can be made.

In the ion-implantation process, the translational energy of the ion is degraded on impact with the target. Localized increases in vibrational energy of the target can result in bond breaking with consequent target degradation as well as loss of target material. Once implanted, the ion can either react with the target material, become neutralized in the grounded target and combine with itself (e.g., $2 Br \rightarrow Br_2$), or become neutralized and react with the target (24). In the second case, the recombined implanted material might subsequently react with the target, remain trapped but unreactive in the target, or diffuse out of the target. Under the conditions employed in the present experiment, it is expected that the third alternative will be dominant.

In the first Br^+ implantation experiment attempted, a single crystal of $(SN)_x$ was subjected to a rastered beam of 46-keV bromonium ions. The visible results were encouraging in that the crystal changed from a lustrous golden color to the deep blue color characteristic of

TABLE V - ION-IMPLANTATION CONDITIONS EMPLOYED TO DOPE
(CH)_x AND (SN)_x POLYMERS

	<u>Ion</u>	<u>Energy (keV)</u>	<u>Concentration (ions/cm²)</u>
(CH) _x	Pd ⁺	90	2x10 ¹⁶
	Br ⁺	41.6	3x10 ¹⁵
	Br ⁺	25	5x10 ¹⁵
	Br ⁺	25	3.4x10 ¹⁶
(SN) _x	Br ⁺	46	5x10 ¹⁵
	Br ⁺	25	5x10 ¹⁵

chemically brominated (SN)_x. However, bromine could not be detected in the crystal by XPS or mass spectral studies, and no changes were observed in the S 2p and N 1s peaks. The absence of detectable bromine is likely a consequence of the low bulk concentration of bromine in the crystal and of the large mean free path (~1000 Å) of 46 keV bromonium ions. Presumably for the same reasons, bromine could not be detected in two subsequent ion-implanted samples of polyacetylene, nor could bromine be detected (XPS, mass spectral analysis) in a second attempt at bromonium ion implantation into (SN)_x, though the S 2p and N 1s spectra changed significantly. Both peaks broadened and very weak new peaks were observed at higher binding energies due perhaps to sample degradation. The most striking information acquired from the XPS data, however, is the fact that the N 1s peak area decreased relative to that of S 2p by a factor of three compared with pure, clean (SN)_x. The decreased intensity suggests that the Br⁺ beam treatment causes nitrogen depletion of the (SN)_x.

The first successful detection of implanted ions was made for a polyacetylene film implanted with 90-keV palladium ions. The Pd 3d region of the X-ray photoelectron spectrum of the specimen contained a strong but unstructured signal. The Pd 3d_{3/2} and 3d_{5/2} components were not resolved, and the breadth of the Pd 3d envelope (7 eV fwhm)

indicated that at least two forms of palladium were present. In addition, film embrittlement resulted from the Pd^+ beam treatment, and the C 1s signal suggested that the Pd^+ beam had inflicted extensive damage on the $(\text{CH})_x$ film. Film conductivity (four-point probe method) did increase several orders of magnitude, but the reason for the increase in conductivity is not known.

In the most recent bromonium ion implantation experiment, some experimental difficulties were eliminated by mounting the $(\text{CH})_x$ to be implanted on a 3/8" rod. Slow rotation of the rod combined with near tangential impact of the Br^+ beam with the $(\text{CH})_x$ film, low beam energy (25 keV), high beam concentration (3.4×10^{16} ions/cm²), and long beam exposure times, resulted in implantation of a measurable concentration of bromine near the surface of the sample. XPS of this sample shows a moderately strong Br 3d signal centered at 70.3 eV. The approximate mean C:Br stoichiometric ratio in the surface region, derived from comparisons of relative peak areas, is 1.0:0.07.

The Br 3d spectrum of Br^+ implanted and Br_2 chemically doped polyacetylene are compared in Fig. 8. As the figure shows, the envelope shapes of the peaks are very similar, but the peak in the ion-implanted sample is at 1.0 eV higher binding energy than that of the Br_2 chemically doped sample. The difference in binding energies indicates that the implanted bromine is not present as Br_2 or Br_n^- ($n = 1, 2$) as it is in the case for the Br_2 chemically doped sample. However, the binding energy (70.3 eV) is similar to that of a bromine covalently bound to carbon.

Bromonium ion implantation causes changes in the carbon 1s spectrum; the major component of the peak shifts to 285.0 eV (from 284.4 eV for pristine polyacetylene) and a minor higher energy component also appears. It is not known whether the changes are due to target damage, ion-target reactions, or a combination of the two.

Finally, four-point probe conductivity measurements of various regions of the surface of the Br^+ implanted polyacetylene, when compared with those for an unimplanted $(\text{CH})_x$ sample, consistently showed that the conductivity of the implanted sample was an order of magnitude greater than that of $(\text{CH})_x$.

ELECTRON SPIN RESONANCE STUDIES OF POLYACETYLENE

In 1960 there was a brief report of the results of an esr study on polyacetylene (25a). Since polymerized acetylene is expected to be diamagnetic according to simple valence bond theory, the fact that the polymer possesses unpaired electron spin density is somewhat surprising. There have followed reports of esr studies of a variety of substituted acetylenes (25b) such as polyphenylacetylene, and of irradiated diacetylene single crystals (26). In collaboration with Dr. A. Snow, presently a post-doctoral fellow at NRL, and Prof. N.-L. Yang at City University of New York, we have obtained esr data for polyacetylene films under a variety of conditions. The data for $(CH)_x$ films are summarized in Table VI and examples of X-band spectra for air-exposed and unexposed samples are shown in Fig. 9. All the films exhibit a strong, sharp, slightly asymmetric signal (peak-to-peak width 4-8 G) which contains no hyperfine features and is centered at the nearly spin-free g value 2.0030. The intensity of the esr signal from the film's paramagnetic centers was found to be dependent on the extent of exposure of the films to oxygen (Fig. 9). For an unexposed sample, the number of unpaired spins/mole at room temperature is calculated to be 1×10^{19} . The g value and unpaired spin density are comparable to those reported for polyphenylacetylene ($g = 2.0027$; 1×10^{19} spins/mol) (25b).

Initial exposure of the film to the atmosphere results in an irreversible threefold enhancement in the polymer unpaired spin density. After exposure, the peak becomes symmetric and the line width increases ~ 1 G (Fig. 9). Although the increase in spin density is retained, evacuation of the sample cell narrows the line to 2.4 G. Similar oxygen pressure-dependent signal broadening has been observed in pyrolytic carbon systems (29).

In contrast to the marked effect of oxygen on the polymer signal, exposure of the $(CH)_x$ film to ammonia or water vapor at room temperature does not affect the esr signal intensity or peak-to-peak width. Variable temperature measurements of the esr signal intensity from -162° to $+22^\circ\text{C}$ show that the paramagnetic centers follow Curie law behavior and are therefore attributed to a doublet ground state.

TABLE VI - ELECTRON SPIN RESONANCE DATA FOR POLYACETYLENE AND DERIVATIVES

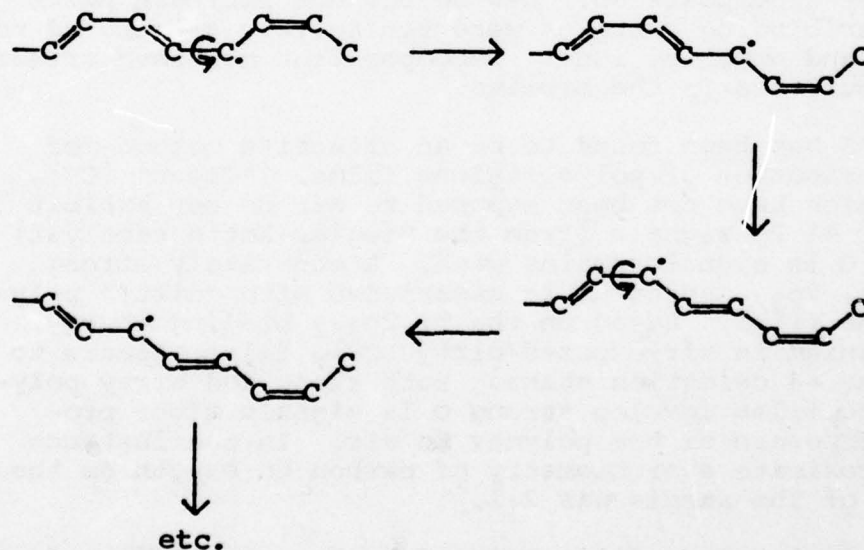
	g value	Peak Width (Gauss)	Spin Density (Spins/mole) $\frac{10^{18}}$	Conductivity (mho/cm) $\frac{10^{-9}}$
<u>cis</u> -polyacetylene	2.0030 ± 0.002	4-8	10^{18}	10^{-9}
<u>trans</u> -polyacetylene	2.0030 ± 0.002	4-8	10^{19}	10^{-5}
polyphenylacetylene ^a	2.0027 ± 0.0001	10-13	$10^{18}-10^{19}$	$10^{-18}-10^{-15}$

^aRef. 25b.

The effects of the active ^1H nuclei in $(\text{CH})_x$ on the esr line width was examined by comparison with perdeuterated polyacetylene which was prepared from C_2D_2 . It was found that perdeuteration decreases the signal linewidth 2G, while the signal intensity remains constant.

Differential thermal analysis of $(\text{CH})_x$ shows an exothermic peak at 145°C which has been attributed to the cis-trans polymer isomerization process (27). We have examined the temperature dependence of the esr signal up to 200°C for polyacetylene films prepared at -78° and 20°C . Based on the preparation temperature, the sample prepared at -78°C is believed to be 98% cis and the sample prepared at 20°C is believed to be a 60%-40% mixture of the cis and trans polymer isomers. For both polymers, the esr signal intensity was followed as a function of temperature. It was found that the signal intensity increased tenfold for the 98% cis isomer, and twofold for the 60% cis isomer at 150°C . The results for the two films are displayed in Fig. 10.

In view of the relatively low unpaired spin density in the polymer, the unpaired electrons are believed to arise from defect states (29). Indeed, these defect states may provide the mechanism for cis to trans isomerization of the polymer as shown below:



SUMMARY

X-ray photoelectron spectroscopy has been utilized to characterize S_2N_2 , $(CH)_x$, $(SN)_x$, and several chemically modified products of the $(CH)_x$ and $(SN)_x$ polymers. From the gas phase and solid state XPS data for S_2N_2 , the charges on sulfur and nitrogen are empirically estimated to be +0.15 and -0.15, respectively. The charges calculated for S and N in S_2N_2 using the electronegativity equalization method incorporated in the CHELEQ program are +0.05 and -0.05, respectively, while the values determined from MINDO calculations are ± 0.40 .

In situ polymerization of S_2N_2 to $(SN)_x$ was followed using XPS. The most striking changes observed during and after polymerization are the increases in all core-level peak widths which arise at least in part from new plasmon peaks. In the N 1s spectrum, a strong well-resolved plasmon peak is found 2.5 eV from the primary peak. The in situ generated $(SN)_x$ film was subsequently treated with bromine in the spectrometer. A film of approximate composition $(SNBr_{0.05})_x$ was formed. The only discernible effect of this light bromination was loss of plasmon resolution and broadening of the primary peaks. In contrast to the in situ bromination, a sample of $(SNBr_{0.4})_x$ prepared on a vacuum line and stored under nitrogen showed extensive decomposition. New sulfur and nitrogen peaks at higher binding energies were tentatively attributed to sulfate and ammonium ions. Decomposition may have arisen from impurities in the bromine.

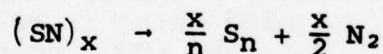
XPS has been found to be an effective method for characterization of polyacetylene films. "Clean" $(CH)_x$ films which have not been exposed to air do not exhibit Ti 2p or Al 2p signals (from the Ziegler-Natta catalyst) and the O 1s signal remains weak. A moderately strong Ti $2p_{1/2}$, $2p_{3/2}$ spectrum is associated with "dirty" polyacetylene films. Based on the Ti $2p_{3/2}$ binding energy, the titanium in air-exposed dirty $(CH)_x$ films appears to be in the +4 oxidation state. Both clean and dirty polyacetylene films develop strong O 1s signals after prolonged exposure of the polymer to air. In one instance the approximate stoichiometry of carbon to oxygen on the surface of the sample was 2:1.

Polyacetylene films exposed to F_2 , Cl_2 , Br_2 , and AsF_5 vapors were studied with XPS. Based on relative peak intensities, the approximate stoichiometry of the halogen-treated films was in all cases $(CHX_{0.3})_x$ (C:H stoichiometry assumed to be unchanged from that in the untreated

polymer). Whereas fluorine and chlorine appeared to have reacted with the polymer backbone, forming discrete C-X bonds, the bromine apparently intercalated into the polymer, forming Br_n^- species where n is 1 or 3. Similarly, the AsF_5 appeared to have intercalated into the polymer, but information on the fate of the AsF_5 is not yet available.

Ion-implantation experiments have been performed as an alternative method for doping $(\text{CH})_x$ and $(\text{SN})_x$. In the experiments using $(\text{CH})_x$, implanted 40-keV Br^+ and 90-keV Pd^+ ions were detectable by XPS. The Pd^+ ion implantation appeared to cause extensive damage to the polymer surface and the palladium was present in a variety of states. However, XPS indicates that the sample implanted with Br^+ ions had sustained minimal surface damage and that the bromine was present in a single chemical environment but not the same environment as that of bromine chemically added to $(\text{CH})_x$ as Br_2 .

Thus far, Br^+ ion implantation into $(\text{SN})_x$ has been found to preferentially deplete nitrogen from the polymer. It is postulated that the energy transfer from ions to target leads to polymer decomposition:



A detailed esr study of both cis- and trans-polyacetylene has been completed. Results show that there are approximately 10^{18} - 10^{19} spins per mole of acetylene depending on the particular preparation and that the paramagnetic centers have doublet ground states. The ESR signal increases roughly threefold in intensity due to exposure of the $(\text{CH})_x$ to oxygen. Spin density-temperature correlations show a marked increase (2x for the predominantly trans isomer and 10x for the predominantly cis isomer) in polymer spin density at 150°C . This increase in spin density is correlated with the cis-trans isomerization process which, from differential thermal analysis experiments, has been reported to occur between 150 and 155°C .

The results and conclusions of the studies conducted thus far provide a foundation for analysis of future data. Techniques for preparing clean films of polyacetylene have been developed. The fundamental utility of XPS in characterizing polymer films and single crystals and in evaluating chemical effects and surface composition of $(\text{CH})_x$ and $(\text{SN})_x$ treated with various dopants has been demonstrated.

In the near future we will obtain gas phase and solid state XPS data for S_4N_4 to complete a systematic study of charge variation in the S_2N_2 , S_4N_4 , $(SN)_x$ series. We also expect to record the gas phase sulfur and nitrogen core level spectra of the $(SN)_4$ species formed on volatilization of $(SN)_x$. A special Knudsen cell has been designed for the spectrometer sample chamber for this purpose.

At the present time the effects of halogens and AsF_5 on the electrical properties of $(CH)_x$ and $(SN)_x$ are reasonably well known. We plan to extend the investigation of chemical dopants to include SF_5Br , $S_2F_2O_6$, and SF_5OCl . These dopants may result in greater film stability toward oxygen and moisture.

Initial results of the unique application of ion implantation for controlled doping of $(SN)_x$ and $(CH)_x$ have been encouraging. Indeed, our qualified success with this technique has led to its utilization for doping polyphthalocyanines. The ion implantation effect will be vigorously extended over the next few months. In this time critical questions such as "What are the effects of varying implanted ion energy and dosage per unit area?" and "Can the electrical properties of these or other polymers be rigorously controlled?" will be addressed. An important point to keep in mind which is related to the questions above is that $(SN)_x$ and $(CH)_x$ polymers hold promise as electrical devices if the electrical properties of the polymers can be "fine-tuned" for specific applications by controlling implanted dopant levels and spatial resolution of implanted ions. For example, it may be possible to construct a diode or triode from a $(CH)_x$ film by implanting donor and acceptor ions in spatially resolved regions of the film. As part of the implantation effort, we will begin examining the effects of implantation of transition metal ions into polyacetylene. The metal d orbitals offer the possibility of stable π complex formation with the polymer backbone. One might reasonably expect back π bonding to increase the conductivity of the polymer.

Electron spin resonance studies of $(CH)_x$ thus far completed have demonstrated the presence of delocalized defect states in the polymer and their probable role in polymer isomer conversion. The fate of the defect states on doping is not yet known.

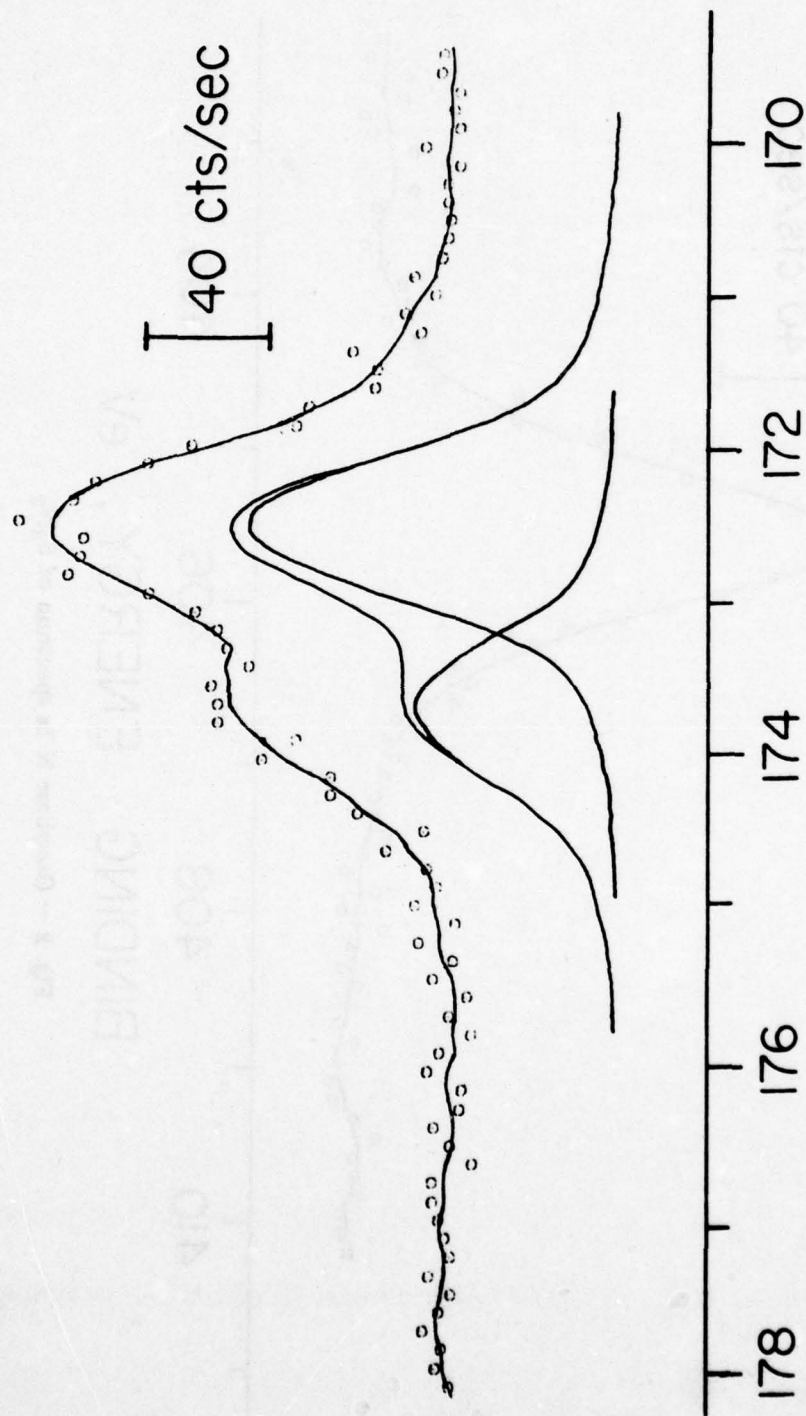
REFERENCES

1. C. M. Mikulski, P. J. Russo, M. S. Saran, A. G. MacDiarmid, A. F. Garito, and A. J. Heeger, *J. Amer. Chem. Soc.* 97, 6358 (1975).
2. M. Akhtar, J. Kleppinger, A. G. MacDiarmid, J. Milliken, M. J. Moran, C. K. Chiang, M. J. Cohen, A. J. Heeger, and D. L. Peebles, *Chem. Comm.* 473 (1977).
3. G. B. Street, W. D. Gill, R. H. Geiss, R. L. Greene, and J. J. Mayerle, *Chem. Comm.* 407 (1977).
4. H. Fellner-Feldegg, U. Gelius, B. Wannberg, A. G. Nilsson, E. Basilier, and K. Siegbahn, *J. Electron Spectroscopy* 5, 643 (1974).
5. B. J. Lindberg, K. Hamrin, G. Johansson, U. Gelius, A. Fahlman, C. Nardling and K. Siegbahn, *Phys. Scripta* 1, 286 (1970).
6. K. Siegbahn, C. Nordling, A. Fahlman, R. Nordberg, K. Hamrin, J. Hedman, G. Johansson, T. Bergmark, S. E. Karlsson, I. Lindgren, and B. Lindberg, *ESCA; Atomic, Molecular, and Solid State Structure Studies by Means of Electronic Spectroscopy*, Allquist and Wiksells, Uppsala, Sweden, 1970.
7. (a) S. Suhait and J. Ladik, unpublished results; (b) D. R. Salahub and R. P. Messmer, *J. Chem. Phys.* 64, 2039 (1976); (c) T. Yamabe, K. Tanaka, K. Fukui and H. Kato, *J. Phys. Chem.* 81, 727 (1977); (d) I. Batra, S. Ciraci, and W. E. Rudge, *Phys. Rev.* B15, 5858 (1977); (e) K. Tanaka, T. Yamabi, A. Tachibana, H. Kato and K. Fukui, *J. Phys. Chem.* 82, 21, 2121 (1978).
8. J. Sharma, D. S. Downs, Z. Iqbal, and F. J. Owens, *J. Chem. Phys.* 67, 3045 (1977).
9. P. Mengelt, P. M. Grant, W. E. Rudge, B. H. Schechtman and D. W. Rice, *Phys. Rev. Lett.* 35, 1803 (1975).
10. (a) C. H. Chen, J. Silcox, A. F. Garito, A. J. Keeger, and A. G. MacDiarmid, *Phys. Rev. Lett.* 36, 525 (1976); (b) J. Ruvalds, F. Brosens, L. F. Lemmens, and J. T. Devreese, *Solid St. Comm.* 23, 243 (1977).
11. C. D. Wagner, *Anal. Chem.* 44, 1050 (1972).

12. R. D. Smith, J. R. Wyatt, J. J. DeCorpo, F. E. Saalfeld, M. J. Moran, and A. G. MacDiarmid, Chem. Phys. Lett. 41, 362 (1976).
13. V. I. Nefedov, N. P. Serguishin, I. M. Band, and I. Trzhaskovskaya, J. Electron Spectroscopy 2, 383 (1973).
14. J. Sharma and Z. Iqbal, Chem. Phys. Lett. 56, 373 (1978).
15. S. L. Hsu, A. G. Signorelli, G. P. Pez, and R. H. Baughman, J. Chem. Phys., 0000 (1978).
16. C. K. Chiang, C. R. Fincher, Y. W. Park, A. J. Heeger, H. Shirakawa, E. J. Louis, S. C. Gau and A. G. MacDiarmid, Phys. Rev. Lett. 39, 1098 (1977).
17. V. I. Nefedov, Y. V. Salyn, A. A. Chertkov, and L. N. Padurets, Russ. J. Inorg. Chem. 19, 785 (1974).
18. J. J. Pireaux, J. Riga, R. Caudano, J. M. Andre, J. Delhalle, S. Delhalle, and J. Verbist, J. Electron Spectroscopy 5, 531 (1974).
19. W. L. Jolly, in Electron Spectroscopy; Theory, Techniques and Applications, Vol. 1, C. R. Brundle and A. D. Baker, eds., Academic Press, N.Y. 1977.
20. M. Hatano, S. Kambara, and S. Okamoto, J. Polymer Sci., 51, S26 (1961).
21. C. K. Chiang, M. A. Druy, S. C. Gau, A. J. Heeger, E. J. Louis, A. G. MacDiarmid, Y. W. Park, and H. Shirakawa, J. Amer. Chem. Soc. 100, 1013 (1978).
22. R. A. Walton, Coord. Chem. Rev. 21, 63 (1976).
23. W. Allen, et al., Progress Report, Chemical Diagnostics Branch, Chemistry Division, Naval Research Laboratory, Washington, D.C., November 1978.
24. J. A. Taylor, G. M. Lancaster, and J. W. Rabalais, J. Electron Spectroscopy 13, 435 (1978).
25. (a) T. Masuda, N. Sasaki, and T. Higashimura, Macromolecules 8, 717 (1975); (b) G. M. Holob, P. E. Ehrlich and R. D. Allendorfes, Macromolecules 5, 569 (1972).

26. Y. Hori and L. D. Kispert, Abstract 163, Physical Chemistry Section, National ACS Meeting, Miami Beach, Fla., September 1978.
27. T. Ito, H. Shirakawa, and S. Ikeda, J. Polymer Sci. and Polymer Chem. 13, 1943 (1975).
28. P. Finn, R. K. Pearson, J. M. Hollander and W. L. Jolly, Inorg. Chem. 10, 378 (1971).
29. L. S. Singer, "Proceedings of the Fifth Carbon Conferences," Pergamon Press (1961), 37.
30. W. L. Jolly, M. S. Lazarus and O. Glemser, Z. Anorg. Allg. Chem. 406, 209 (1974).
31. R. G. Cavell and D. A. Allison, J. Amer. Chem. Soc. 99, 4203 (1977).
32. K. Siegbahn, C. Nordling, G. Johansson, J. Hedman, P. F. Heden, K. Hamrin, U. Gelius, T. Bergmark, L. O. Werme, R. Mann, and Y. Baer, ESCA Applied to Free Molecules, North-Holland Publishing Co., Amsterdam, 1969.
33. S. C. Avanzino, W. L. Jolly, T. F. Schaaf, and H. R. Allcock, Inorg. Chem. 16, 2046 (1977).
34. M. Barber, P. Baybutt, J. A. Connor, I. H. Hillier, W. N. E. Meredith, and V. R. Saunders, in Electron Spectroscopy, D. A. Shirley, ed., New York, 1972, p. 753.
35. M. S. Banna, D. C. Frost, C. A. McDowell, and B. Walloank, Chem. Phys. Lett. 43, 426 (1976).
36. W. L. Jolly and W. B. Perry, J. Amer. Chem. Soc. 95, 5442 (1973).
37. B. Sharma and J. Donohue, Acta. Cryst. 16, 891 (1963).
38. B. J. Lindberg, K. Hamrin, G. Johansson, U. Gelius, A. Fahlman, C. Nordling and K. Siegbahn, Phys. Scripta 1, 286 (1970).
39. W. J. Stec, W. E. Moddeman, R. G. Albridge, and J. R. VanWazer, J. Phys. Chem. 75, 3975 (1971).

40. A. Barrie, H. G. Fernandez, H. G. Heal, and R. J. Ramsey, J. Inorg. Nucl. Chem. 37, 311 (1975).
41. V. W. Lidy, W. Sundermeyer and W. Verbeek, Z. Anorg. Allg. Chem. 406, 228 (1974).
42. D. R. Penn, J. Electron Spectroscopy, 9, 29 (1976).
43. J. H. Scofield, J. Electron Spectroscopy, 8, 129 (1976).



BINDING ENERGY, eV

Fig. 1 — Gas-phase S $2p_{1/2}$, $2p_{3/2}$ spectrum of S_2N_2

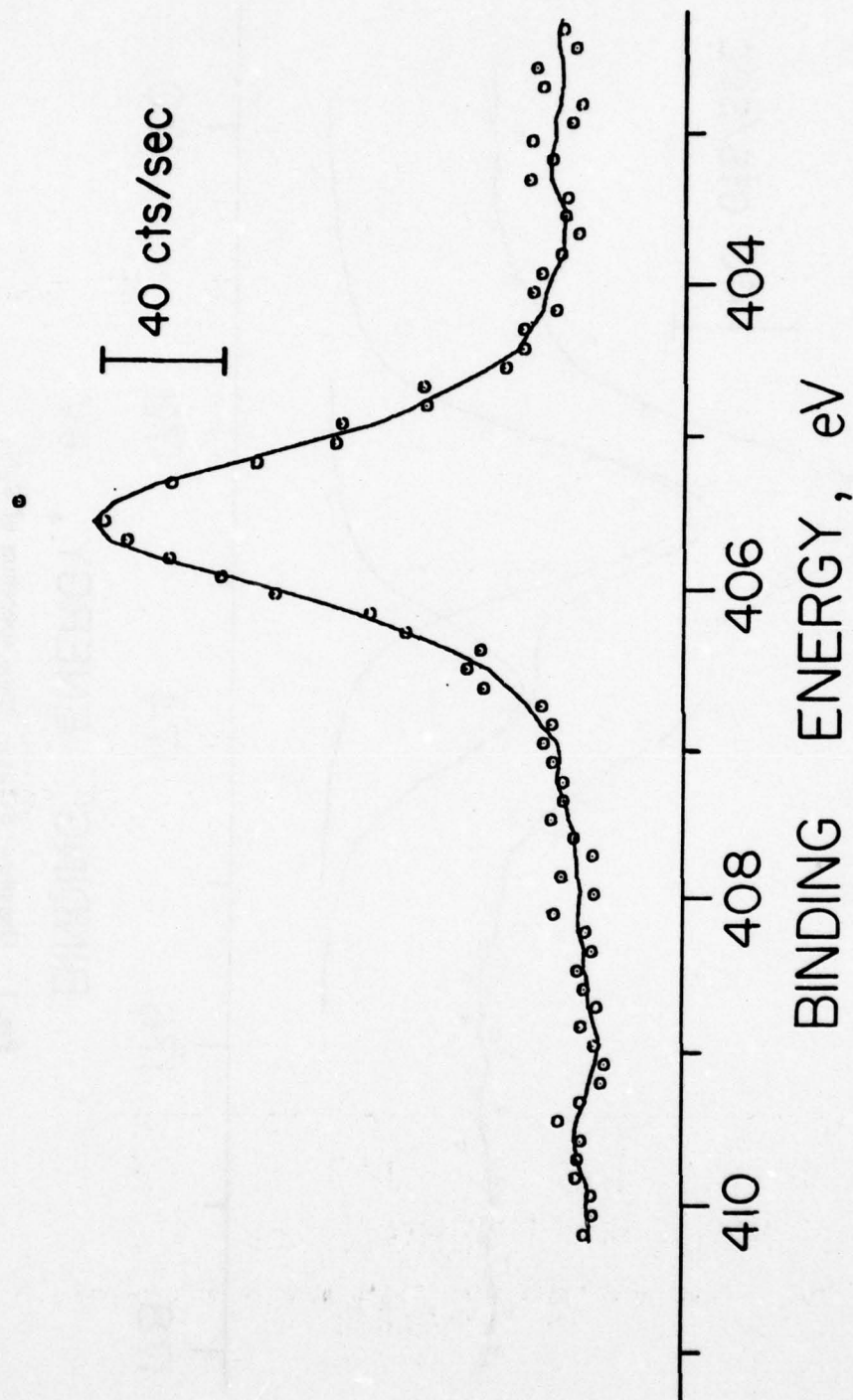


Fig. 2 - Gas-phase N 1s spectrum of S_2N_2

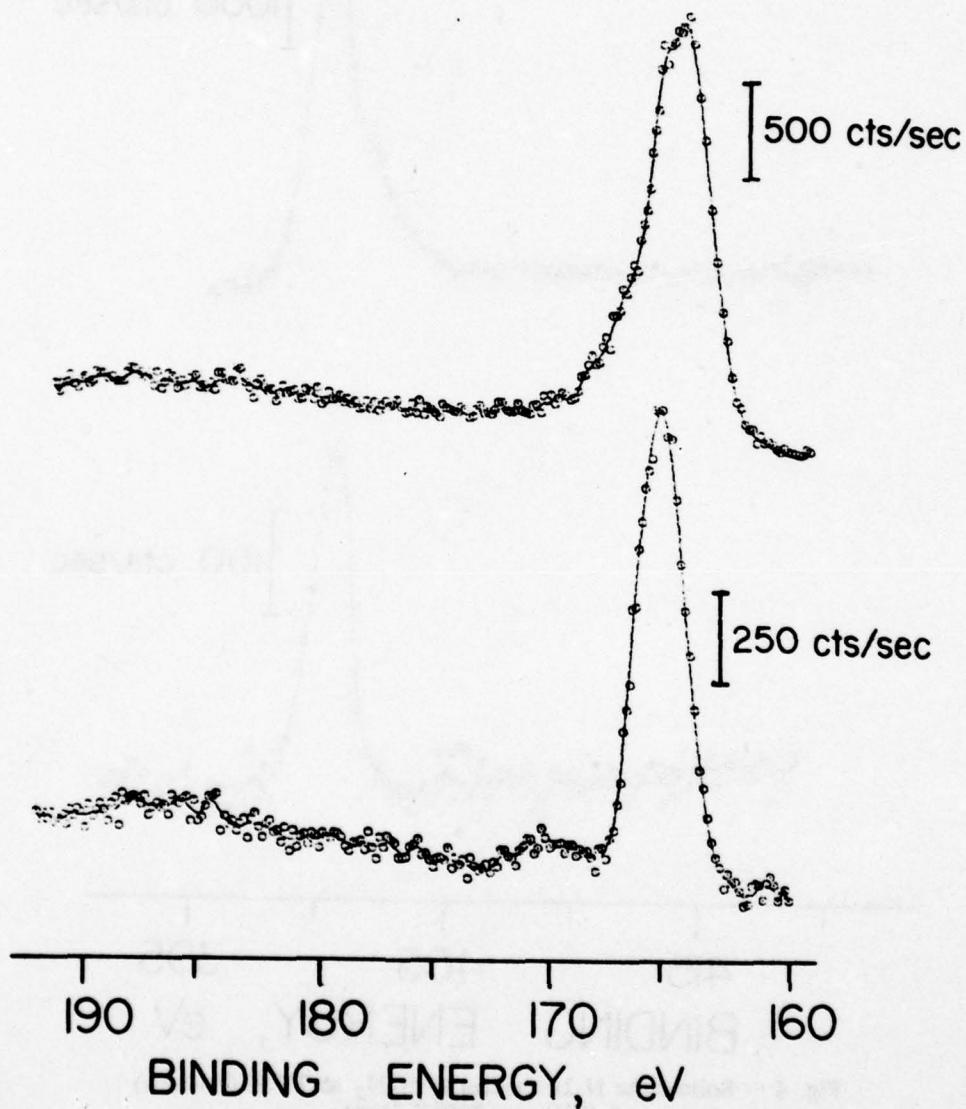


Fig. 3 — Solid-state S 2p spectra of S_2N_2 at 77°K (bottom) and $(\text{SN})_x$ at 300°K (top)

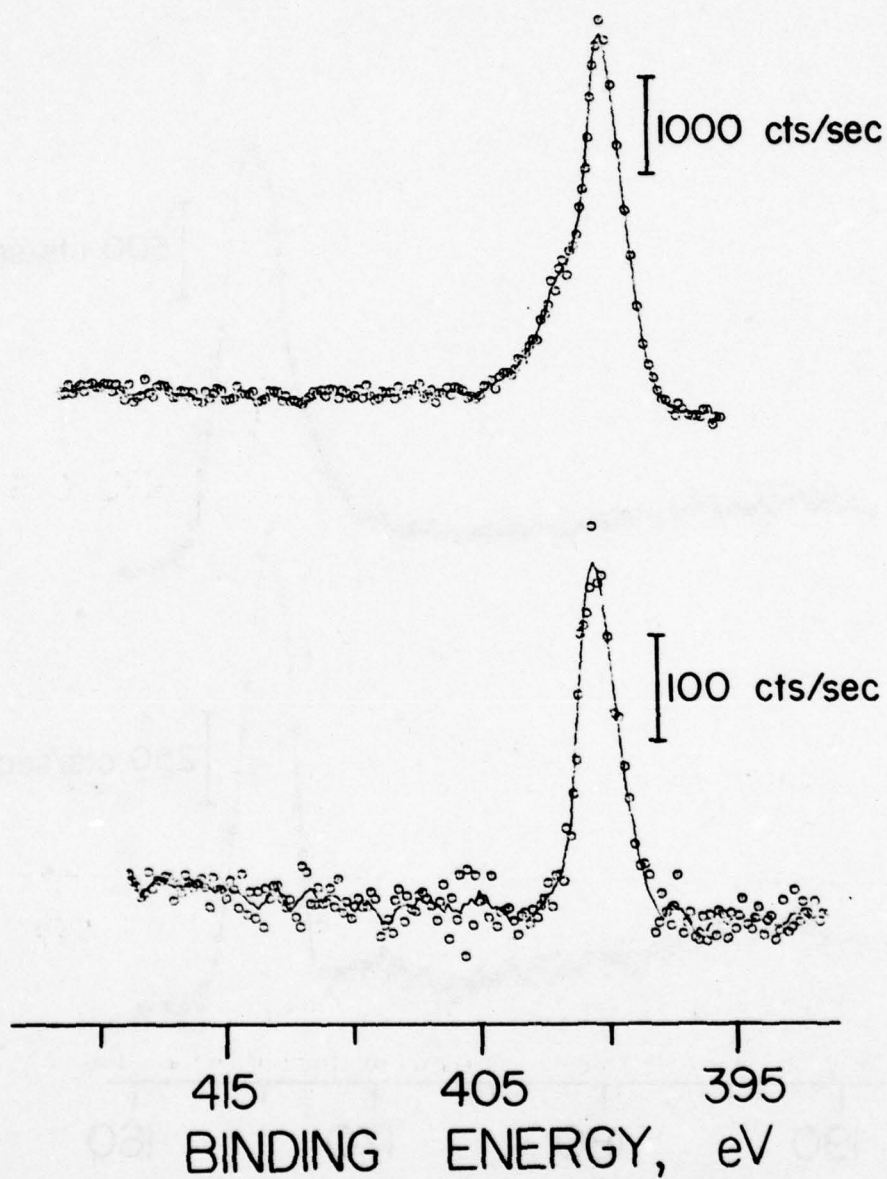


Fig. 4 — Solid-state N 1s spectra of S_2N_2 at 77°K (bottom) and $(\text{SN})_x$ at 300°K (top)

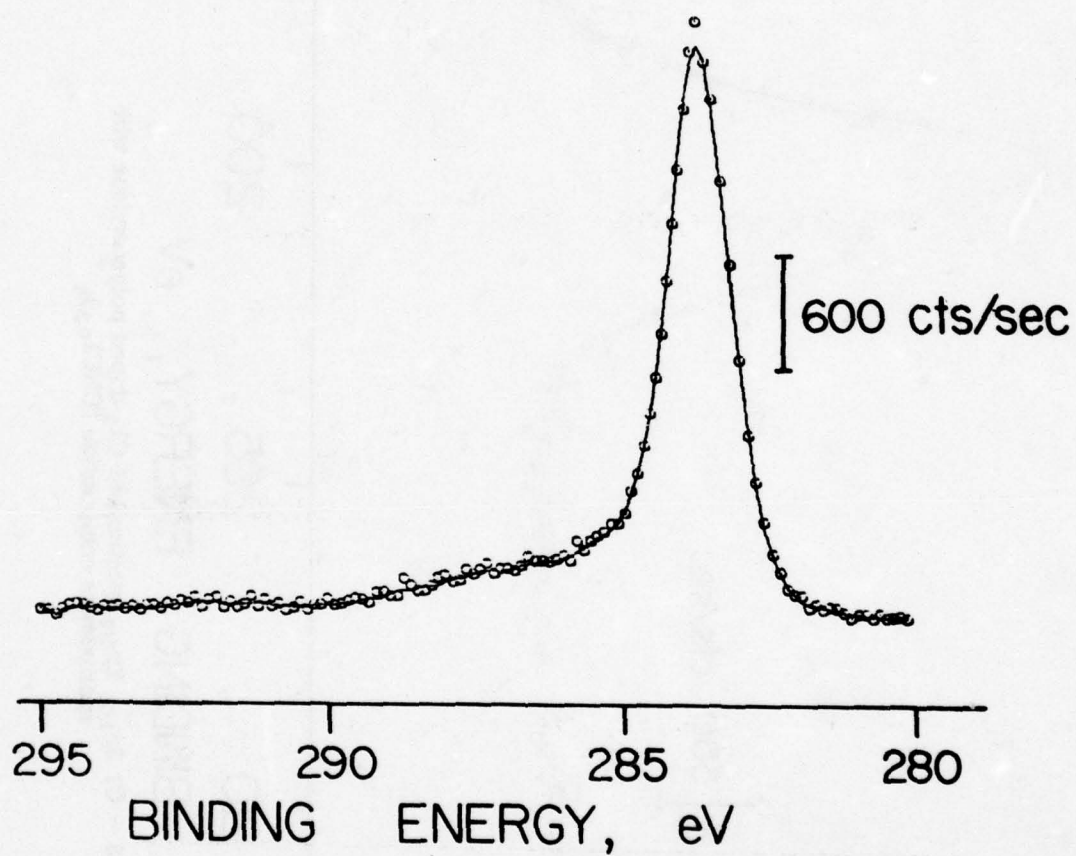


Fig. 5 - C 1s X-ray photoelectron spectrum of polyacetylene

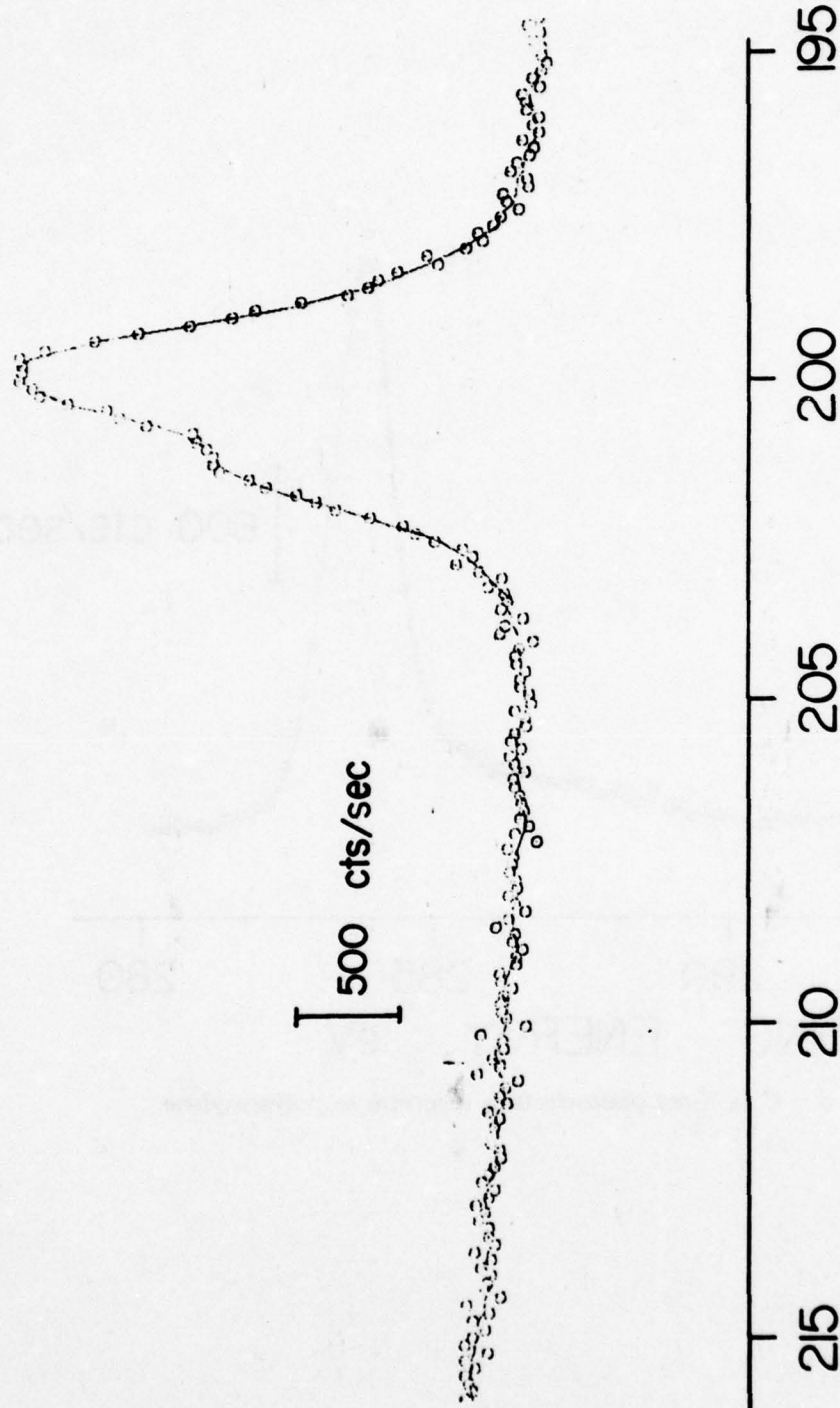


Fig. 6 - C1 $2p_{1/2}$, $2p_{3/2}$ spectrum of C_{12} -doped polyacetylene with approximate composition $(CHC_{10.3})_x$

ION IMPLANTATION SYSTEM

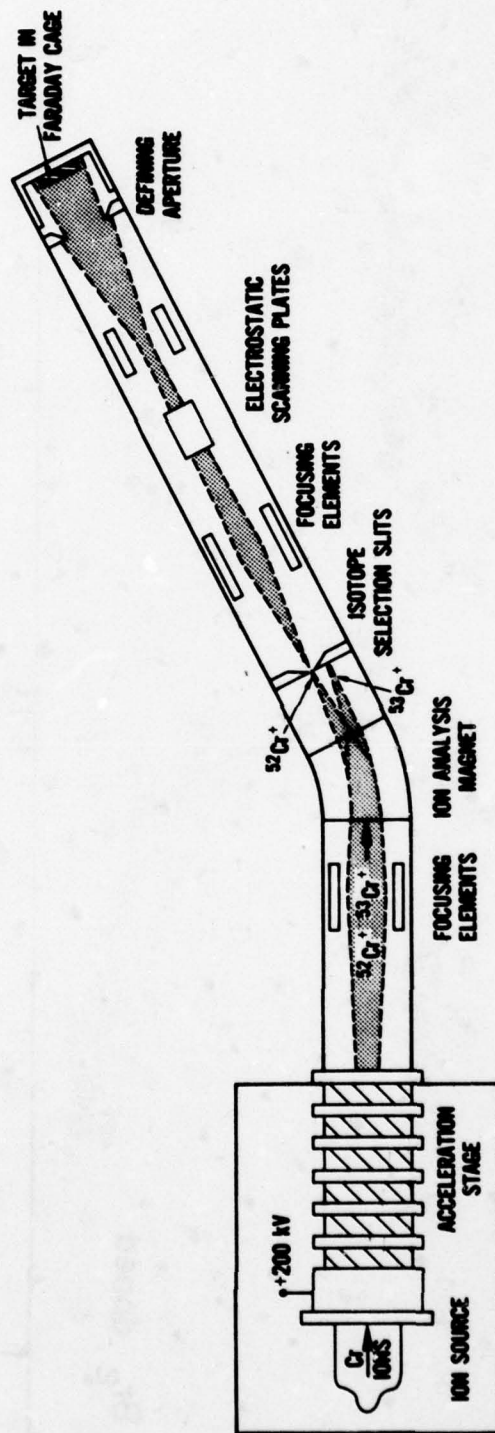


Fig. 7 — Schematic of the ion-implantation system

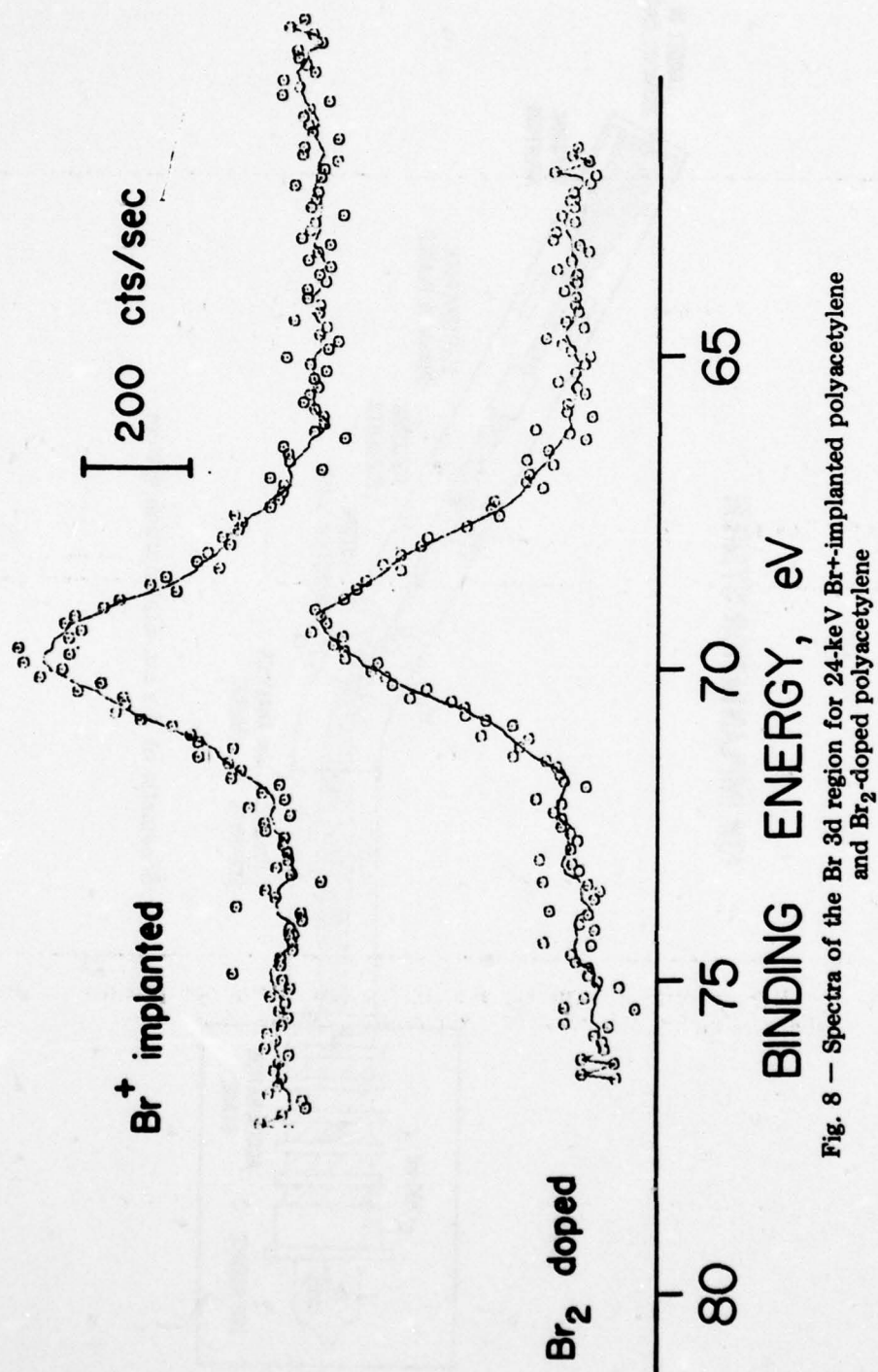


Fig. 8 — Spectra of the Br 3d region for 24-keV Br⁺-implanted polyacetylene and Br₂-doped polyacetylene

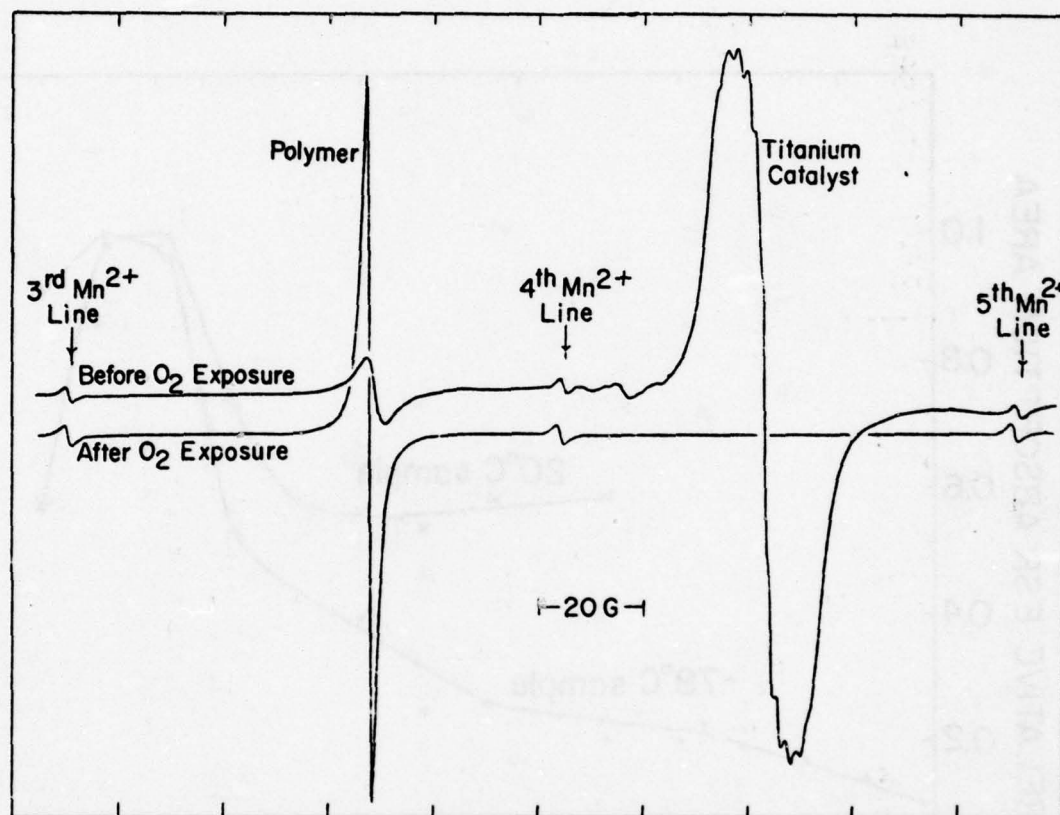


Fig. 9 — ESR spectra of polyacetylene and titanium tetraisopropoxide-triethylaluminum catalyst before and after oxygen exposure

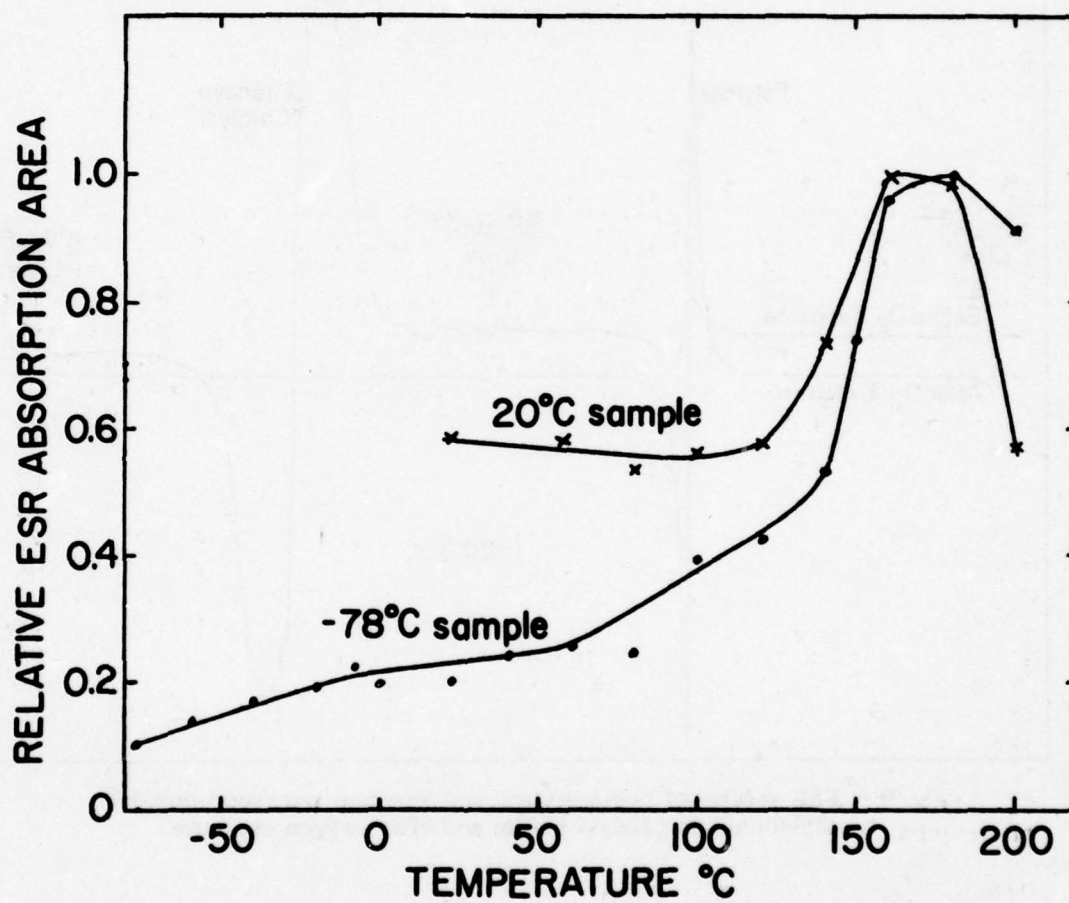


Fig. 10 — Relative spin density dependence on heating above polyacetylene sample preparation temperature; X, 20°C sample, o, -78°C sample

CHARACTERIZATION OF HALOGEN-DOPED $(CH)_x$ AND $(SN)_x$

W. N. Allen, J. J. DeCorpo, F. E. Saalfeld,
J. R. Wyatt, and D. C. Weber*
Chemical Diagnostics Branch
Chemistry Division

INTRODUCTION

Electroactive polymers have become the subject of considerable research effort in recent years, not only as scientifically interesting materials, but also for potential applicability in the electronics industry. Some of the most extensively studied ones are polythiazyl, $(SN)_x$, polyacetylene, $(CH)_x$, and their doped derivatives. While pure polyacetylene behaves as a large bandgap semiconductor (1), doping with iodine can increase its conductivity by more than seven orders of magnitude (2).

Our laboratory has carried out studies in the past on $(SN)_x$ and its brominated derivatives, using mass spectroscopy^x to characterize the vapor species associated with the crystalline material when it is heated. The previous work (3) identified a persistent hydrogen impurity in $(SN)_x$, and gave structural information about $(SN)_4$, the major species produced when $(SN)_x$ is vaporized. We have also characterized the vapor species associated with brominated $(SN)_x$ (4). In this report, we present results of studies on^x halogenated polyacetylenes, as well as some preliminary findings about ion-implanted polyacetylenes and polythiazyls.

EXPERIMENTAL

Polyacetylene was prepared using the method of Shirakawa, et al. (5). Samples of pure polyacetylene were then doped by exposing them to vapors of either iodine, chlorine, bromine, or fluorine. The mass spectrometric studies of the polyacetylenes were done with Hewlett-Packard 5985A Mass Spectrometer using a direct insertion probe. Most of this

* Inorganic and Electrochemistry Branch

work was done with electron-impact (EI) ionization; some samples were examined with chemical ionization, and this data supplemented the EI data. Mass spectra were taken over the temperature range 40 to 340°C, 340° being the maximum temperature for the direct insertion probe. The maximum temperature in this study is just below that at which pure polyacetylene begins to decompose.

RESULTS AND DISCUSSION

Halogen-Doped Polyacetylenes

Examination of the mass spectra of iodine-doped polyacetylene as it is heated to a constant rate (20°C/min) shows that the principal iodine-containing species evolved are I_2 and HI. Their intensities in the mass spectra are of comparable magnitude, (I_2 intensity ~40% of HI intensity) with the I_2 being evolved at a lower average temperature than HI. A slight "double peaking" in the I_2 temperature profile (Fig. 1) suggests that the I_2 may be associated with the polymer in more than one form.

Mass spectra of brominated polyacetylene similarly show Br_2 and HBr to be the principal bromine-containing species evolved from the sample. However, Br_2 is in a much lower abundance relative to HBr (~5% of HBr intensity) than in the case of iodine-doped material.

Chlorinated polyacetylene yields mass spectra in which Cl_2 is not detectable and only HCl was clearly identifiable as a chlorine-containing species. Fluorination of polyacetylene is apparently so vigorous that what results is a fluorinated hydrocarbon, as indicated by fluorine appearing in the mass spectra only as carbon-fluorine ions.

Thus, the trend observed in the mass spectra of the various halogenated polyacetylenes is one of decreasing proportion of molecular halogen associated with the polymer as one goes up Group VIIA in the periodic table from iodine to fluorine. This trend can be correlated with reported conductivities (6) of these materials.

The iodine-doped polyacetylene exhibits the greatest conductivity with successively lower values for the brominated and chlorinated species. The conductivity of the fluorinated compound has not been measured. The conductivities do show a trend which correlates with relative abundance of molecular halogen observed in the mass spectra. The iodinated material having the highest conductivity has the greatest abundance of molecular halogen. Spectroscopic data

(7) suggest that iodine resides principally as I_3^- in the polyacetylene crystal with some evidence for the presence of a second type of iodine in the crystal - either I_5^- or intercalated I_2 . The mass spectrometric results support two types of iodine species because the I_2 ion temperature profile shows a small initial rise followed by a much larger rise in ion intensity. We interpret this as indicating I_2 evolution at lower temperature from either intercalated I_2 or a decomposition of I_5^- followed at higher temperature by decomposition of I_3^- to produce I_2 .

Brominated (SN)_x

Previous studies (3) found a persistent hydride impurity (~2-7 atom percent) associated with (SN)_x. Bromination of (SN)_x converts the hydride impurity to hydrogen bromide (4). In an attempt to determine if there is any relationship between the presence of hydrogen bromide and the crystal's conductivity, we measured the conductivity of a sample of brominated (SN)_x, before and after removal of hydrogen bromide. The hydrogen bromide was removed by heating the crystal in a vacuum at 60° for 20 hours. This process removes virtually all (~90%) of the hydrogen bromide. It also causes some of the Br₂ to be lost from the crystal, changing its empirical formula from (SNBr_{0.4})_x to approximately (SNBr_{0.2})_x. Results of electrodeless conductivity measurements (8) indicate the crystal's conductivity decreased by a factor of ~2. This decrease is probably due to the loss of Br₂ from the crystal and not a result of hydrogen bromide removal. A further experiment, in which the conductivity is measured after re-exposing the crystal to Br₂, is in progress, and the results will be reported in the near future.

Ion-Implantation Studies

While chemical doping of electroactive polymers is successful, this process has inherent limitations with regard to what materials are usable as dopants and to what extent one can control the placement of the dopant in the crystal. In view of the well-known successes of ion implantation with semiconductors, we have begun an investigation into the use of this technique with electroactive polymers. This technique has the advantage that any material which can be ionized is usable as a dopant. Our results, which thus far are only preliminary, are encouraging.

We initially subjected a sample of polyacetylene film to a 90-keV beam of Pd ions for a period sufficient to give a total dosage of $\sim 1 \times 10^{16}$ ions/cm². Implanted materials

typically have a gaussian depth profile. We estimate by analogy with graphite that the mean depth of penetration at this energy is approximately 1000Å with a standard deviation of about 400Å.

The sample was examined after irradiation by both mass spectrometry and ESCA. The ESCA studies were done on a McPherson ESCA 36 Photoelectron Spectrometer equipped with a PDP 12 computer. Mass spectrometry detected no Pd-containing species. However, the ESCA data detected the presence of Pd and revealed, by examination of the C(1s) peak broadening (Fig. 2), that surface damage had occurred. This damage was apparently only on a molecular scale - no damage (or etching) was observable in a scanning electron micrograph of the surface. The Pd (3d) peak also showed considerable broadening over the same peak in pure Pd.

Four-probe DC conductivity measurements on the Pd-implanted sample before and after the irradiation showed an enhancement in conductivity of about three orders of magnitude.

Polyacetylene ion-implanted with bromine ions under similar conditions again showed broadening of the C(1s) peak. However, bromine could not be detected in the crystal either by ESCA or mass spectrometry analysis. As a further check for the presence of bromine in the crystal, we examined the sample by Rutherford back-scattering of α -particles (Fig. 3). The presence of bromine near the surface was confirmed by this technique. We were not able to measure the conductivity of bromine ion-implanted polyacetylene. Reliable conductivity measurements on these ion-implanted species are quite difficult due to the nature of the sample - the dopant is below the surface, making electrical contact with the doped portion difficult.

Finally, a sample of (SN)_x was ion-implanted with bromine. The surface exposed to the ion beam changed from the characteristic golden luster of (SN)_x to a bright blue, similar to the color of chemically brominated (SN)_x.

With these preliminary results, we feel that ion implantation shows promise for use with electroactive polymers. Further work is needed to characterize the structure and properties of these ion-implanted materials and is in progress in our Laboratory. Results of studies on ion-implanted (CH)_x and (SN)_x will be reported in the near future.

REFERENCES

1. Organic Semiconductors, F. Gutman and L. E. Lyons, John Wiley, NY, 1967.
2. H. Shirakawa, E. J. Louis, A. G. MacDiarmid, C. K. Chiang, and A. J. Heeger, J. C. S. Chem. Comm. 578 (1977).
3. R. D. Smith, J. R. Wyatt, J. J. DeCorpo, F. E. Saalfeld, M. J. Moran, and A. G. MacDiarmid, J. Am. Chem. Soc. 99, 1726 (1977).
4. W. N. Allen, J. J. DeCorpo, F. E. Saalfeld, and J. R. Wyatt, Chem. Phys. Lett. 54, 524 (1978).
5. a. H. Shirakawa and S. Ikeda, Polymer J. 2, 231 (1971).
b. H. Shirakawa, T. Ito, and S. Ikeda, Polymer J. 4, 460 (1973).
6. C. K. Chiang, M. A. Druy, S. C. Gau, A. J. Heeger, E. J. Louis, A. G. MacDiarmid, Y. W. Park, and H. Shirakawa, J. Am. Chem. Soc. 100, 1013 (1978).
7. S. L. Hsu, A. J. Signorelli, G. P. Pez, and R. H. Baughman, J. Chem. Phys. 69 (1), 106 (1978).
8. J. S. Lass and A. P. Pippard, J. Phys. E. 3, 137 (1970).

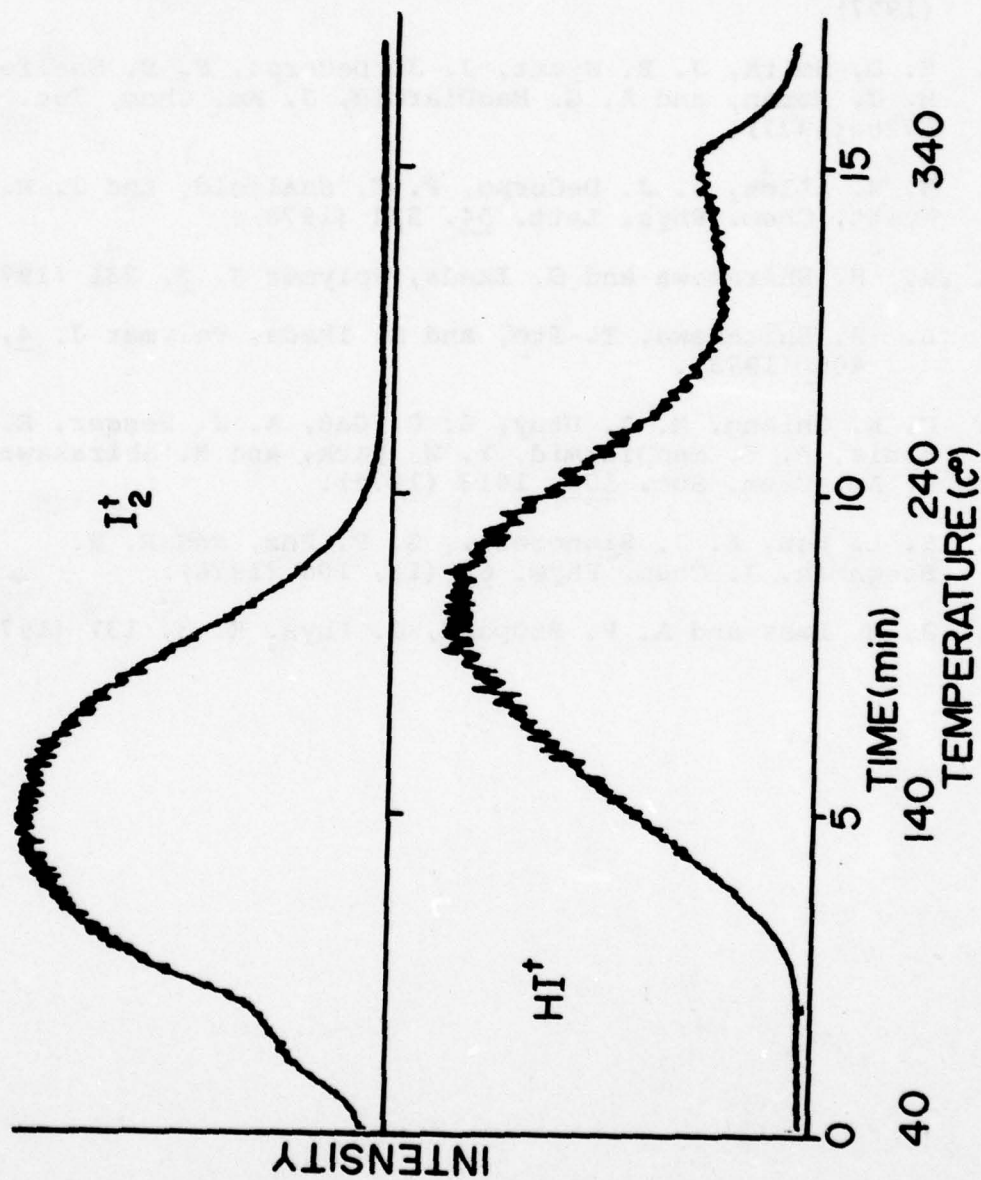


Fig. 1 - Iodine-doped polyacetylene. I_2^+ and HI^+ ion intensity vs. time (and temperature). See text for explanation of the initial rise in the I_2^+ profile.

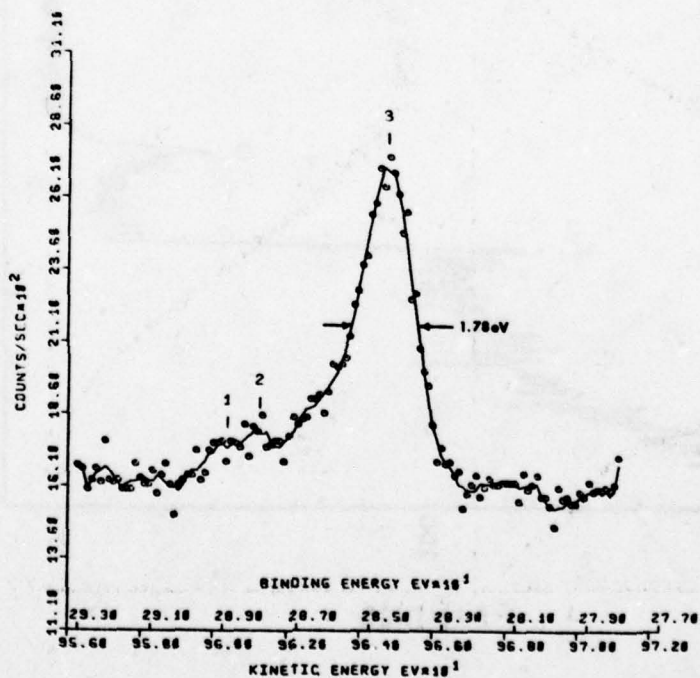
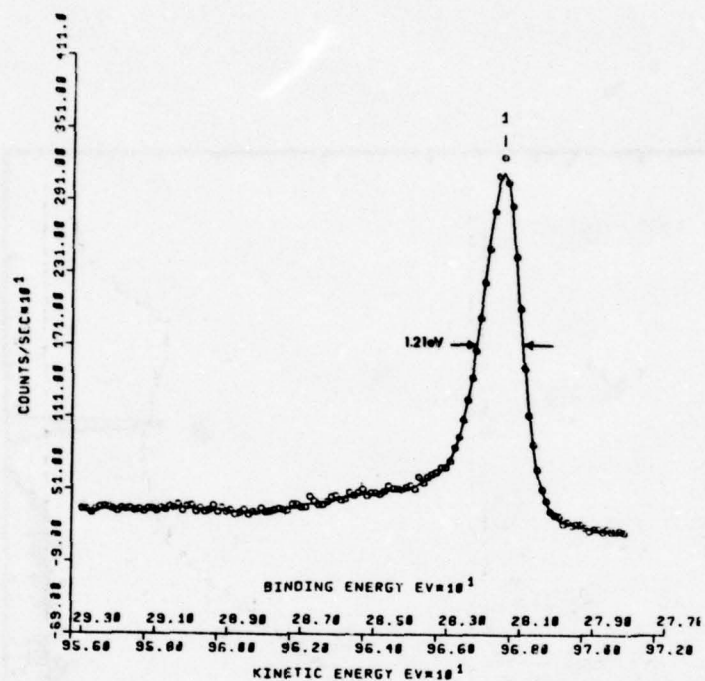


Fig. 2 — ESCA C(1s) Peaks in (a) pure polyacetylene and (b) palladium-implanted polyacetylene

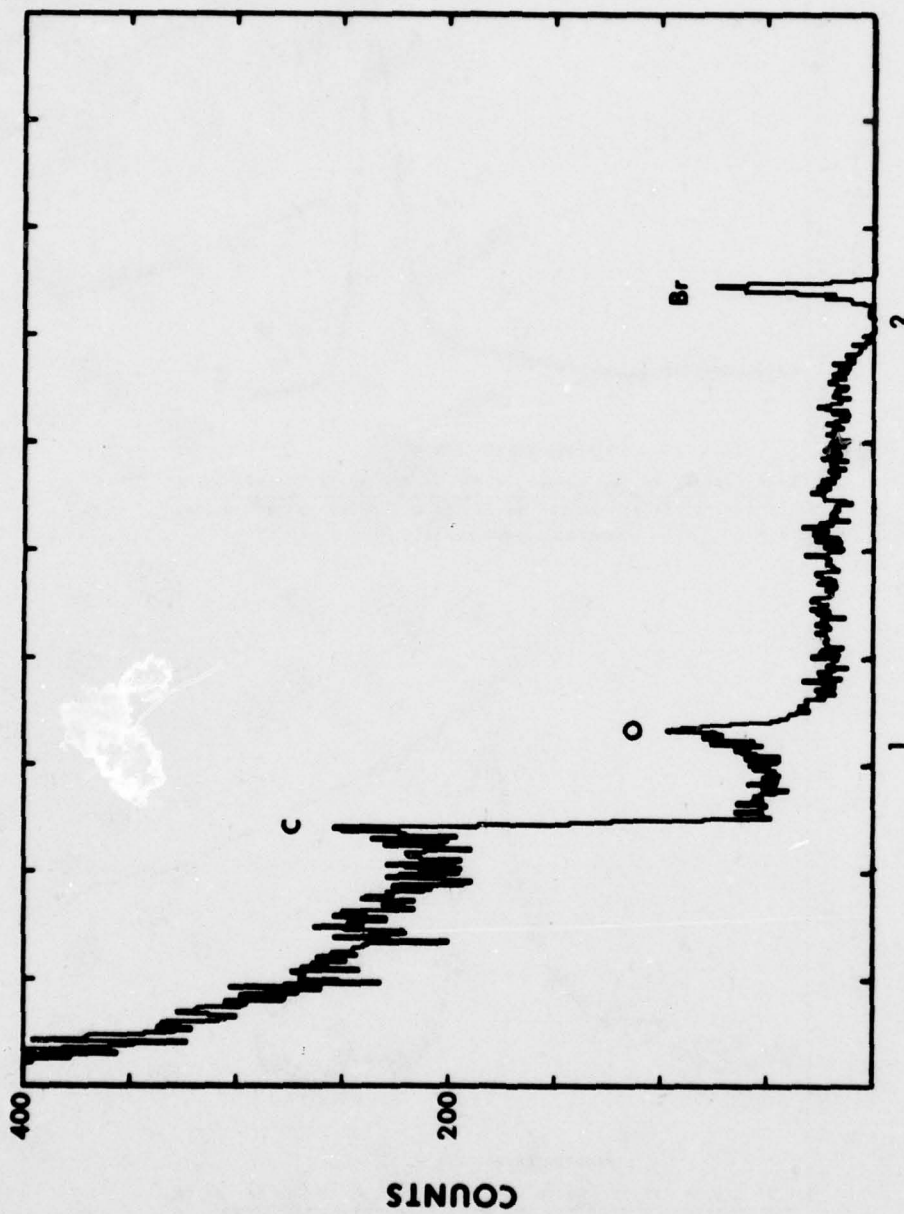


Fig. 3 — Rutherford backscattering from bromine-implanted polyacetylene

NMR STUDIES OF ELECTROACTIVE POLYMERS

H. A. Resing
Surface Chemistry Branch
Chemistry Division

INTRODUCTION

The piezoelectric (1) and electrical conductivity properties (2,3) of polymers are being, or appear ripe to be exploited for Naval and other technological purposes. Though the application of such electroactive materials must depend ultimately on detailed knowledge of molecular structure and dynamics as they relate to performance properties and stability, these details are in many cases not known or understood (2,3). Progress proceeds in Edisonian fashion. This report is concerned with attempts to understand the underlying causes of the desired electrical properties, attempts based for the most part on the use of the tool nuclear magnetic resonance (NMR). As these NMR studies are integrated with the preparative and characterization work of others - at NRL and elsewhere - it is intended that a coherent description of such materials as polyacetylene, intercalated graphite, and polyvinylidene fluoride will emerge, a description which will allow these materials to be used with confidence and profit.

Thus, we first describe exactly what parameters of interest become available by means of the various NMR techniques which have been developed recently or are in current use at the Naval Research Laboratory. Then we assess the possibility of formation of piezoelectric delrin, based on NMR relaxation measurements. Next we use NMR spectroscopy to qualitatively and quantitatively analyze polyacetylene for cis-trans ratio and impurities. Finally we list a rough outline of future possible experiments and materials of interest.

Nuclear Magnetic Resonance (NMR) techniques allow the motions and structures of molecules to be fruitfully characterized in polymeric and other states of matter. On the one hand, NMR relaxation measurements (4) suffice to determine equilibrium rates of molecular diffusion, rotation, or internal isomerization; and on the other, NMR spectroscopic techniques allow the number and kind of organic functional groups to be determined, even in the solid state (5). Herein we report recent application of the relaxation technique to ferroelectric trioxane and of the spectroscopic technique to semiconducting polyacetylene.

Relaxation

The random motion of one nuclear magnet with respect to another (caused by molecular diffusion, etc.) can be characterized by a

power spectrum $J(\omega) \sim \frac{K\tau}{1 + \omega^2\tau^2}$. Here K is an intensity factor,

depending on nuclear separations in a known way, τ is a correlation time, roughly the time between molecular diffusional or rotational jumps (between successive equilibrium positions) and ω is the frequency at which the power density is measured. It is this correlation time which is the main goal of the experiments on trioxane described below, although the intensity factor is also quite useful, as in molecular structure determinations. For nuclei of spin 1/2 (^1H , ^{13}C , ^{19}F) the nuclear magnetic system is only loosely coupled to its surrounding heat bath. When it is disturbed from equilibrium, as by absorption of energy at its resonant frequency ω_0 (usually ~ 10 -60 MHz), its relaxation to thermal equilibrium with the heat bath can be followed. It is well understood that the rate of relaxation T_1^{-1} is roughly

$$T_1^{-1} \sim J(\omega_0).$$

That is, the intensity of the motional power spectrum at the resonant frequency, $J(\omega_0)$, determines the relaxation rate. In addition to the spin lattice relaxation time T_1 , other measurable NMR parameters serve to determine $J(\omega)$ at other frequencies. Measurement of such a data suite generally overdetermines the molecular jump time (4).

Electroactive polymer systems in which molecular motion (hence NMR relaxation) is important are those in which small molecules intercalate into a fibrous (2) (polyacetylene) or interlammellar (3) (graphite) system and interact with the host in some as yet unknown way. Among such intercalants are SbF_5 , AsF_5 , Na, K, and benzene (6). All of these nuclei are subject to NMR motional analysis. Although such NMR work has been initiated in several labs, the data gathered has been fragmentary, and final interpretations remain to be made. Note that since the intercalants are mobile, the stability of the conductors formed may be limited by the lifetime against out-diffusion.

Spectroscopy

NMR spectroscopy has long been a tool for assessing the numbers and kinds of protons or ^{13}C -nuclei in molecules in the liquid state. Recently such high resolution spectroscopy has become possible in the solid state as well, most notably for carbon-13. This advance is made possible by the development of techniques to overcome the lack of molecular motion in the solid state; for it is molecular motions in the liquid state which average nuclear dipolar interactions and chemical shift interactions respectively to zero and to an average shift. For

carbon-13 nuclei at natural abundance (ca 1.11%) the dominant dipolar interaction is with protons; in the solid state this is averaged away by a strong r. f. field at the proton resonance frequency (proton decoupling) (5). The resulting broad "chemical shift anisotropy pattern" can then be averaged by "magic angle" spinning to achieve resolution sufficient for determination of functional groups (5). For polyacetylene and intercalated graphite, the goal is the observance of a very large shift due to conduction electrons - the Knight shift (7).

We point out that ^{13}C NMR spectroscopic analysis is complementary to the relaxation studies mentioned above. There we seek to investigate the intercalated molecules and find out their behavior. With ^{13}C NMR spectroscopy we look for chemical changes in the host materials, presumed to be the locus of the metallic conduction.

WILL FERROELECTRIC TRIOXANE SPONTANEOUSLY POLYMERIZE TO PIEZOELECTRIC DELRIN?

The unique success of polyvinylidene fluoride as a piezoelectric material is reportedly (8) due to the presence of ferroelectric microcrystalline blocks in the polymeric state, which blocks may be oriented in a poling field. The work on trioxane described in this section is motivated by another hypothesis, however, which is based on the fact that trioxane undergoes radiation-induced polymerization in the solid state (9). Trioxane crystallizes as a ferroelectric solid with molecules in stacks, and with all stacks having parallel electric moments. In any polycrystalline assembly the polycrystals form keeper domains as in a random ferromagnetic material (10). Suppose that liquid trioxane were crystallized as a thin film in a strong electric field. By hypothesis the film is ferroelectric with electric moment normal to the film. Suppose that this film is caused by radiation or otherwise to polymerize in the solid state and in the presence of the electric field. The hypothesis is further that a large fraction of the molecular electric dipole moment of the trioxane would then remain locked in place in the resulting delrin polymer. Finally, the hypothesis is that this resulting material would be piezoelectrically active. For purposes of application it would only be necessary to test the last part of the hypothesis, i.e. to carry through the preparative procedure as outlined above and to test for piezoelectric activity. This has not yet been done. As a preliminary estimate of the probability of success however, we have chosen to examine, theoretically, the polymerization act itself to see whether the molecular moment might be preserved in orientation in the polymerization process. To do this we compare the activation enthalpy for polymerization with that for molecular motion (11).

The NMR relaxation data is given in Figure 1. From this data and from dielectric studies we conclude that there is a molecular motion in solid trioxane which does not reorient the molecular electric moment; the jump time for this process is

$$\tau = 1.8 \times 10^{-17} \exp (15,000/RT) \text{ s.}$$

where R is in units of $\text{cal deg}^{-1} \text{ mol}^{-1}$. The solid lines in Figure 1 represent the fitting of this motional model to the data, as is discussed elsewhere. The fact that no dielectric loss is observed in trioxane at 1 kHz implies that at least 2 kcal more are required to reorient the molecular electric dipole moment. The hypothesis now becomes: if the activation enthalpy H_p for polymerization is less than 15 kcal/mol, it is likely that the orientation of the molecular electric dipole moment is preserved in the polymerization process and a polar polymer should result. If H_p is much greater than 15 kcal/mol, it is unlikely that intermolecular forces alone will keep the molecular moments aligned during the polymerization process (although the presence of the poling field must be of some help). The activation enthalpy for polymerization, H_p , has been found to be 40 kcal/mol; thus the likelihood of loss of molecular polarization during the polymerization process must be admitted.

The larger question is whether the details of the polymerization process affect the piezoelectric properties at all. If the NBS hypothesis (8) involving polymer chains with net dipole moment imbedded in crystalline blocks with net dipole moment is universally true (i.e. if such a condition is absolutely necessary for a piezoelectric effect of useful magnitude) then the only crystallization-polymerization details which should be of importance are those that govern the size and packing of the blocks. The existence of such a viable model for polyvinylidene fluoride tends to make other hypotheses, such as those upon which this trioxane study was based, appear more speculative. Nevertheless, the polymerization process proposed here for trioxane is simple and should be tested.

Finally, the NBS model for polyvinylidene fluoride (8) requires that the crystalline blocks have an electric moment which can be poled. The crystalline reorganization necessary for this requires molecular motion. It would be interesting to use NMR relaxation techniques on this polymer to search for these motions and test the model.

IS POLYACETYLENE METALLIC WHEN DOPED WITH BROMINE?

Metals are characterized by an appreciable density of electronic states at the Fermi level and by delocalized electrons. By way of a hyperfine or contact interaction these electrons cause a shift of the resonant frequency of the nuclei of the metal to a higher frequency for a given magnetic field - a deshielding of the nuclei (7). This Knight shift, measured in percent, is opposite in sign and much larger than the shift due to interaction of nuclei with electrons in fixed orbits, usually measured in tens of ppm. In the field of organic conductors, a Knight shift has been observed for the carbon nuclei of the TTF-TCNQ

complexes (12); the large conductivity induced by intercalated halogens in polyacetylene leads one to expect a Knight shift here as well. Thus far we have found none in two separate doping experiments with Br_2 .

At lower doping levels than necessary for maximum conductivity, polyacetylene shows the properties of a semiconductor. For semiconductors Knight shifts are not expected; chemical shifts should be the same as in any other diamagnetic solid. The two isomers of polyacetylene have ^{13}C chemical shifts different by about 10 ppm (trans 139 ppm, cis 129 ppm) with respect to tetramethyl silane (just as found elsewhere (13)). Two spectra obtained at NRL for a mixed trans-cis specimen are shown in Figure 2. In the upper spectrum, high-power proton decoupling has revealed the chemical shift powder anisotropy pattern. There the powder pattern deduced for the aromatic ^{13}C nuclei is sketched in, leaving the sharp line (a) in the aliphatic region and a broad line (b) in the region where oxygen- sp^3 carbon linkages normally manifest themselves. The effects of spinning at the magic angle are shown in the lowermost spectrum, where the broad aromatic pattern has been narrowed to the trans-cis doublet which is not quite resolved. The aliphatic region is somewhat narrowed as well. But the C-O region remains broad (and almost undiscernible in this spectrum) which may be an indication of a distribution of bonding arrangements such as alcohol, ether, epoxy etc. Some of these may be due to polymer oxidation, others to chemical incorporation of butoxy groups from the catalyst (14).

In Figure 3 the spectrum for the same sample after exposure to saturated Br_2 vapor for 10 minutes is given. The only noticeable effect is a sharpening or increase in resolution of the aromatic lines. This sharpening gradually disappeared in the course of 24 hours after bromination. No large shift signalling the onset of metallic behavior was observed. Since these NMR measurements were not accompanied by conductivity measurements, one may speculate that insufficient Br_2 was taken up. Better controlled conditions in future experiments are thus required. Since the spinning chambers currently in use at NRL are not hermetically sealable, the possible effects of air oxidation of polyacetylene (15) or of the bromine intercalant are difficult to avoid. Development of sealable spinning chambers is required.

In Figure 3 the integral for the polyacetylene spectrum is shown, which clearly reveals the intensity in the C-O bond region; almost one third of the observable carbons lie in this region. Fully one third of the carbons are not in polyacetylene per se, i.e. are not olefinic. In the two NRL preparations thus far investigated, this has been the case.

In summary, the ability of ^{13}C -NMR to quantitatively and qualitatively analyze polyacetylene has been demonstrated. No indication of metallic Knight shifts has yet been found. Work for the future includes (a) a survey of polyacetylene preparations from other laboratories, (b) investigation of samples doped under conditions in which conductivity

can be monitored, and (c) development of hermetically sealable spinning cases. The list of dopants includes halogens, AsF_5 and alkali metals; we will investigate the effects of chemical addition as compared to ion implantation.

We have observed that the proton relaxation times observable in polyacetylene are anomalously small and seemingly temperature independent. A more complete study here may reveal the very specific relaxation behavior expected for metals, i.e. the Korringa relation may be obeyed ($T_1 T = k$) where T_1 is the spin-lattice relaxation time and T is the absolute temperature (7).

SUMMARY AND PROGNOSIS

We have examined the role of molecular motion in the solid state polymerization of trioxane-delrin and concluded that it is unlikely that the orientation of the molecular electric dipole moment is preserved in the polymerization process in the absence of an external electric field. We have shown that a given polyacetylene sample contained both trans and cis isomers, oxide linkages and a predominant sp^3 linkage; no Knight shift was found. In the future we plan to investigate the systems and problems listed below via NMR techniques. Emphasis initially will be on establishing a more complete picture of the polyacetylene system; this task is broken into the more specific subtasks listed under polyacetylene. Schedule-wise, the intercalated graphite work will be interleaved with the polyacetylene program. We will also provide vigorous analytical support for in-house preparative work on polyphthalocyanines and other highly conjugated network systems. The remaining programs will be pursued when and if time permits.

Polyacetylene

1. Effect of intercalation on chemical shifts, comparison of chemical and ion-implantation doping; effect of conductivity on chemical shift for a given dopant.
2. Comparison of specimens from various laboratories (16) prepared by several techniques; determination of sp^3 carbon content, oxidation levels.
3. Measurement of carbon-carbon bond distance using polyacetylene prepared from ^{13}C -enriched acetylene.
4. Measurement of interproton spacing in cis-polyacetylene via proton NMR; test of structure as postulated in another laboratory (17).
5. Relation of motional behavior of intercalant AsF_5 to stability.

Graphite

1. Motional study of SbF_5 in highly crystalline graphite (3) as regards chemical stability.
2. Fluorine chemical shifts as a function of stage, i.e. of SbF_5 content, to find a diagnostic tool for routine assessment of doping level of graphite fibers intercalated with SbF_5 .
3. Fluorine chemical shift study of graphite fibers doped with SbF_5 : origin, preparation, and doping levels of fibers will be variables. Emphasis will be on fibers used in composites fabrication.
4. Search for metallic behavior as revealed by ^{13}C NMR Knight shift in HNO_3 -intercalated graphite, in K-benzene-intercalated graphite, etc.

Polyphthalocyanines

Carbon-13 NMR spectroscopic studies of the high conductivity preparations that are mentioned elsewhere in this report.

Polythiazyl $(\text{SN})_x$

Measurement of hydrogen content via proton NMR; comparison with mass spectrometric assessment (18).

Polydiacetylene

Search for metallic character via ^{13}C NMR chemical shift studies. Investigation of solid state polymerization process.

REFERENCES

1. R. Hayakawa and Y. Wada, *Advances in Polymer Science* 11, 1 (1973).
2. C. K. Chang, M. A. Druy, S. C. Gau, A. J. Heeger, E. J. Louis, A. G. MacDiarmid, Y. W. Park, and H. Shirakawa, *J. Am. Chem. Soc.* 100, 1013 (1978).
3. T. E. Thompson, E. R. Falardeau, and L. R. Hanlon, *Carbon* 15, 39 (1977); see also *Proc. Int'l. Conf. on Intercalation Compounds of Graphite*, *Mat. Sci. Eng.* 31, 1977.
4. N. Bloembergen, E. M. Purcell, and R. V. Pound, *Phys. Rev.* 73, 679 (1948); C. P. Slichter, *Principles of Magnetic Resonance*, Harper & Row, New York, 1963, Chapter 3 and 5.

5. A. Pines, M. G. Gibby and J. S. Waugh, J. Chem. Phys. 59, 569 (1973); C. C. Chang, A. Pines, J. J. Fripiat and H. A. Resing, Surf. Sci. 47, 661 (1975); A. N. Garroway, W. B. Moniz, and H. A. Resing, Preprints of the Div. of Organic Coatings and Plastics Chem. 36, 133 (1976).
6. L. Bonnetain, P. Touzain, and A. Hamwi, Mat. Sci. Eng. 31, 45 (1977).
7. A. Abragam, Principles of Nuclear Magnetism, Oxford, 1961, p. 199ff.
8. F. J. Mopsik and M. G. Broadhurst, J. Appl. Phys. 46, 4204 (1975); G. T. Davis, J. E. McKinney, M. G. Broadhurst, and S. C. Roth, *ibid*, in press.
9. G. Carazzolo, S. Legisa, and M. Mammi, Makromol. Chem. 60, 171 (1963).
10. V. Busetti, M. Mammi, and G. Carazzolo, Z. Kristallog 119, 310 (1963).
11. H. A. Resing and A. N. Garroway, Proc. 5th International Conf. on the Organic Solid State - A Volume of Mol. Cryst. and Liq. Cryst., in press.
12. E. F. Rybaczewski, L. S. Smith, A. F. Garito, A. J. Heeger, and B. G. Silbernagel, Phys. Rev. B 14, 2746 (1976).
13. M. M. Maricq, J. S. Waugh, A. G. MacDiarmid, H. Shirakawa, and A. J. Heeger, J. Am. Chem. Soc., in press.
14. G. Natta, G. Mazzauti, and P. Corradini, Rend. Accad. Nazl. Lincei 25, 2 (1978).
15. See for example A. Snow, N-L. Yang, P. Brant and D. Weber, Polymer Letters, submitted.
16. Specimens donated by G. P. Pez of Allied Chemical Co. (17) and A. G. MacDiarmid of the University of Pennsylvania have been obtained.
17. R. H. Baughman, S. L. Hsu, G. P. Pez and A. J. Signorelli, J. Chem. Phys. 68, 5405 (1978).
18. R. D. Smith, J. R. Wyatt, J. J. DeCorpo, F. E. Saalfeld, M. J. Moran, and A. G. MacDiarmid, J. Am. Chem. Soc. 99, 1726 (1977).

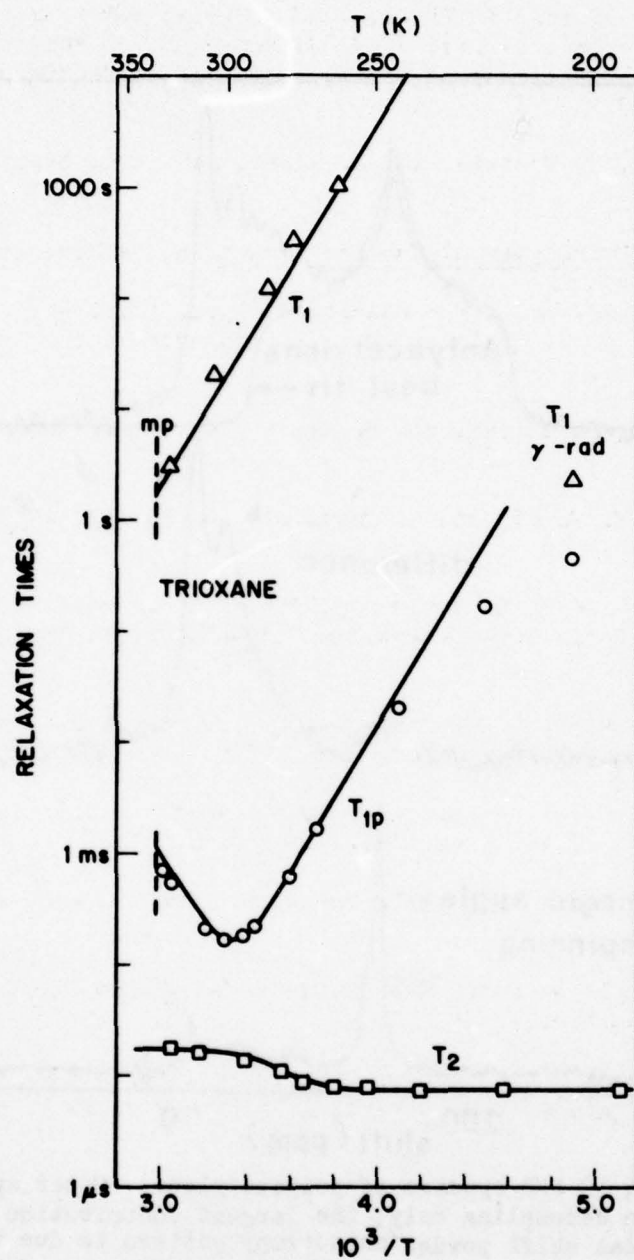


Figure 1: NMR relaxation times for trioxane in the solid as a function of reciprocal temperature. Solid lines compare theory with experiment. The various relaxation times T_1 , $T_{1\rho}$, and T_2 measure the power density spectrum due to molecular rotation for three frequencies at a given temperature. Rotation of the molecule is about the three-fold axis.

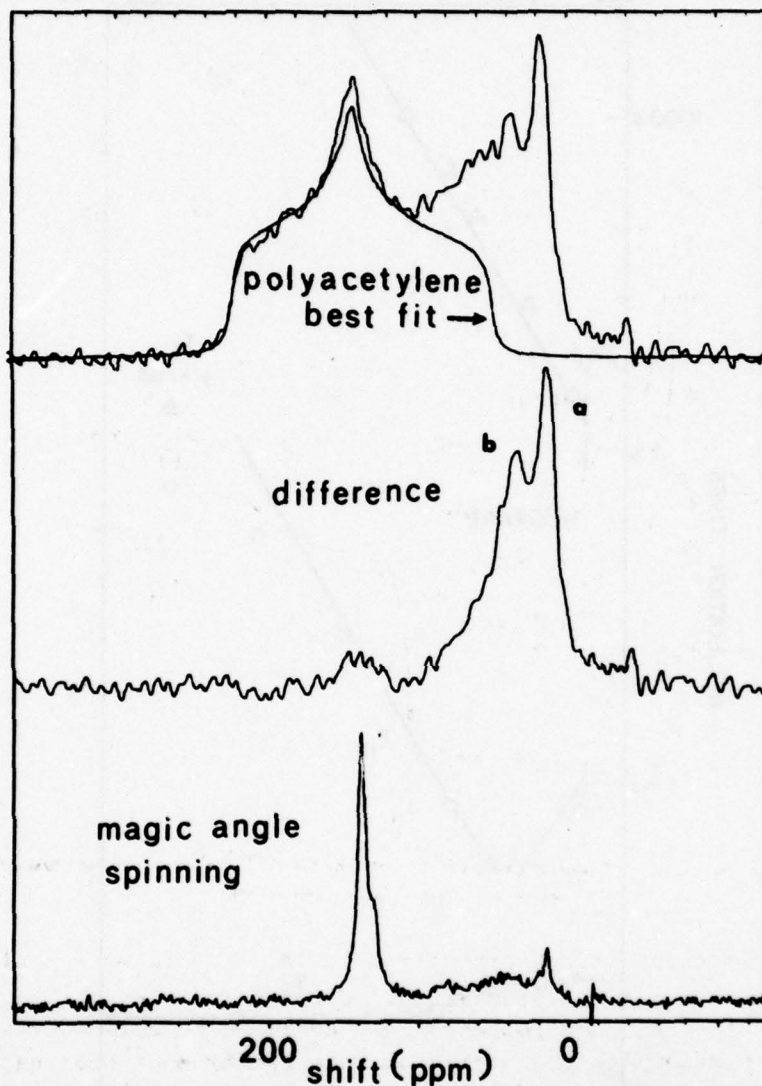


Figure 2: Carbon-13 NMR spectra of polyacetylene. Upper spectrum: proton decoupling only; the largest contribution to the chemical shift powder anisotropy pattern is due to the polyacetylene backbone, for which a theoretical spectrum is shown. Subtraction of the theoretical pattern leaves the center spectrum, a doublet, with lines (a) at 20 ppm and (b) at 50 ppm. In the lowermost spectrum, magic-angle spinning has narrowed the upper spectrum; the olefinic region (around 130 ppm) shows an unresolved doublet; the 50 ppm line is not narrowed; that at 20 ppm is.

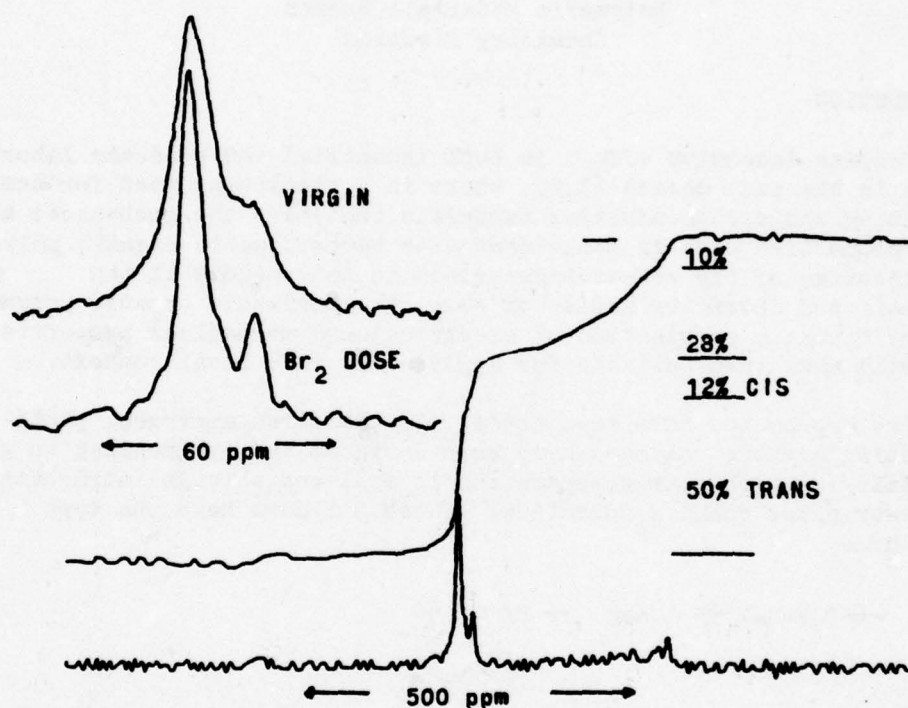


Figure 3: Effect of Br₂ intercalation on the ^{13}C high-resolution spectrum of polyacetylene. Upper left: olefinic region expanded; pure polyacetylene compared to Br₂-intercalated polyacetylene. Lower: complete spectrum of brominated polyacetylene and the integral thereof. Note the significant intensity of the broad 50-ppm line.

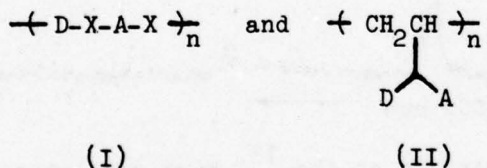
PHOTO- AND SEMICONDUCTING POLYMER SYSTEMS*

R. B. Fox, T. R. Price, O-K. Kim and R. F. Cozzens
Polymeric Materials Branch
Chemistry Division

INTRODUCTION

Despite intensive effort in both industrial and academic laboratories in the past decade (1,2), there is a continuing need for semiconducting and photoconducting materials that have the mechanical and other properties usually associated with thermoplastic organic polymers. The objective of the research described in this report is the synthesis and characterization of novel thermoplastic organic polymer systems having a combination of electrical and mechanical properties that will make them suitable for application in a Naval context.

Two approaches have been taken. In the first approach, photoconducting organic polymers have been designed and synthesized to give materials in which charge separation is achieved through intrachain charge-transfer complex formation. These polymers have the type structures



where D and A represent electron donor and acceptor moieties, respectively. The first structure is a condensation polymer in which X is an ester linkage. The second structure is an addition homopolymer with D and A incorporated into each repeating unit through a variety of organic groupings. In the second approach, semiconducting tetracyanoquinodimethane salt systems having the cation complexed with a macrocyclic ether are dispersed in a polymeric matrix to take advantage of the matrix mechanical properties and the increased solubility or dispersibility of the complexed salts in the matrix.

* This work was carried out under NRL Problem CO4-12.101

The present work is in no sense complete. Electrical measurements have been made on a screening basis, and materials characterization is incomplete. In this progress report, therefore, conclusions are to be utilized primarily in indicating future directions to be taken in the work.

EXPERIMENTAL

Infrared spectra were obtained by the KBr pellet technique with a Perkin-Elmer Model 267 Spectrometer. Ultraviolet-visible spectra were determined with a Shimadzu Spectronic 200 UV instrument.

Electrical conductivity measurements were made with a Keithley Model 610C electrometer connected in series with an Aminco high voltage power supply and an interdigital-grid type electrode system of vacuum-deposited chromium on quartz. Electrode spacing was 0.1 cm. The entire assembly was carefully shielded with copper screening and all electrical components were connected to a common ground along with the shield. Polymer films were cast by evaporation of solutions placed directly on the electrode system. Current as a function of applied electric field was measured in the dark as well as when the sample was irradiated through the quartz and electrode grid with the output from a 200-W high-pressure mercury arc lamp at a distance of 15 cm. Light output was filtered through water to minimize infrared heating of the sample.

RESULTS AND DISCUSSION

Photoconducting Homopolymers and Copolymers

The principle of charge separation through charge-transfer complex formation is well established; both ground-state and light-induced excited-state complexes are known. A wide variety of crystalline organic complexes of these types have been shown to exhibit semi- and photoconductivity when sufficient order is present to allow reasonable electron or hole mobilities under an applied electric field (3,4,5).

Organic polymeric systems are also known to form charge-transfer complexes; their electrophysical properties have been reviewed (6,7). The most extensively studied of the photoconducting systems is that of the poly(*N*-vinylcarbazole) (PVCA) complex with 2,4,7-trinitrofluorenone (TNF) (8). In these and related materials, appreciable charge transfer occurs in the excited state of the complex to produce ion-radical species that can act as charge carriers. Hole and electron transport takes place through the hopping of highly localized charge carriers. Mobility is strongly affected by the geometric relationships and orbital overlap of the interacting chromophores, the presence of trapping entities, and the extent of chemical and physical disorder in these generally amorphous systems. Complex formation itself is inhibited by steric hindrance that prevents the efficient alignment of the acceptor additive molecules with the closely packed donor moieties along the polymer chains. At

the same time, mechanical and other physical properties of the complexed polymers are less than optimum for most applications in which a flexible film-forming material is required.

With these constraints in mind, donor-acceptor polymer systems have been designed in the present work to allow electron transfer in the photo-excited state. Two types of polymers, (I) and (II), were noted in the introduction to this report, and others, such as a regularly alternating copolymer from a vinyl-donor and vinyl-acceptor monomer, are readily envisaged. For example, Inami and Morimoto (9) disclosed photoconducting addition copolymers of VCA (as donor) with 5-nitro-acenaphthylene (as acceptor), as well as other monomer combinations, although regular alternation was not claimed. Alternating copolymers from 2- and 4-vinylpyridine or 4-(dimethylamino)-styrene with trinitrostyrene have been reported (10); this report has been questioned (11). Recently, a 1:1 copolymer from 1-(2-anthryl)ethyl methacrylate (donor) and 2,4,7-trinitro-9-fluorenyl methacrylate (acceptor) has been described along with its spectral properties (12). The charge-transfer interaction in the copolymer was strongly enhanced relative to that observed with model compounds. In the field of condensation polymers, Sulzberg and Cotter (13) synthesized a low molar mass polyester from 2,5-dimethoxyphenyliminodiethanol and 5-nitro-isophthaloyl chloride; this material had a volume resistivity of about 10^{11} ohm-cm.

In our work, synthesis and screening for photoconductivity was undertaken with polyesters (polymer type (I)) based on 4,5-dinitro-fluorenone-2,7-dicarboxylic acid ($\text{DNF}(\text{COOH})_2$) (14) and its derivatives to provide the acceptor moiety. The dimethyl ester of this acid should have an electron affinity between that of TNF (1.0 eV) and 1,3,5-trinitrobenzene (0.7 eV) (14). Ionization potentials (in eV) of the donor moieties are exemplified by dimethylaniline 7.3, N-ethyl-carbazole 7.4, anthracene 7.4, fluorene 7.8, and naphthalene 8.1. Charge-transfer interaction in these systems would be expected to be weak in the ground state.

The synthesis of the polyesters was carried out by conventional procedures, with the acid chloride, $\text{DNF}(\text{COCl})_2$, providing better film-forming compositions than the dimethyl ester. In no case were high molar mass products obtained.

Of the many polyesters screened, that synthesized from $\text{DNF}(\text{COCl})_2$ and 9,10-anthracenebis(methanol) provided films with the highest photoconductive response. In Figure 1 are shown visible spectra of model compounds, their 1:1 mixture, and the purified polyester. A very weak charge-transfer band centering at about 525 nm is apparent in the model compound mixture. In the visible region, the polyester has intense absorption that overlaps this charge-transfer band. This absorption may result from a better geometric alignment of the chromophores in the polymer, where a very high local concentration exists, than in a

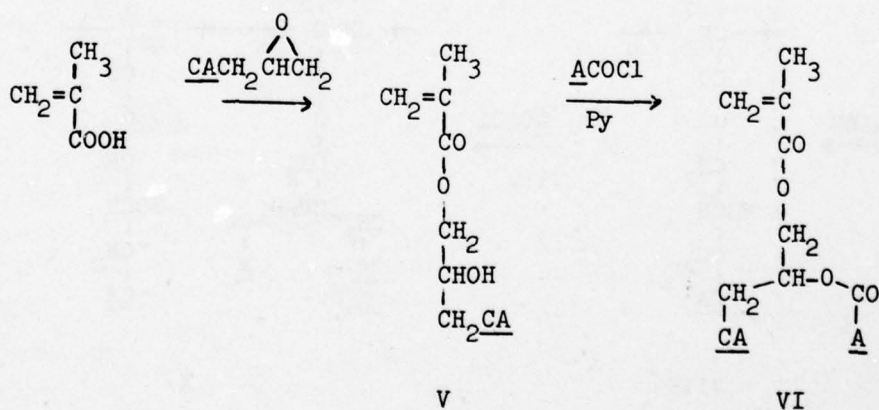
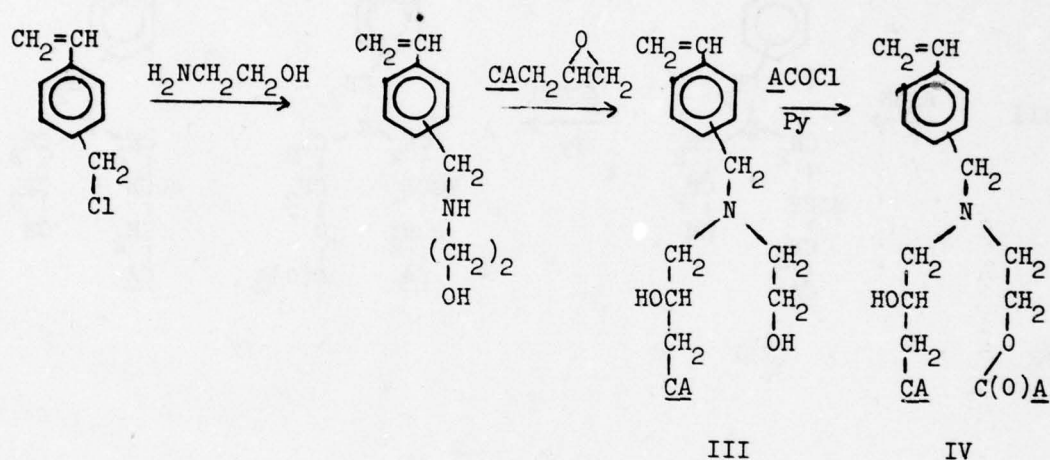
dilute mixture of the model compounds. Films of this polyester, as well as the other polyesters evaluated, were dark brown in color, and it is assumed that much of the color results from the excitation of charge-transfer ground states.

Films of the polyesters, as deposited, were generally weakly semiconducting and exhibited a photocurrent to dark current ratio of less than 10^2 . However, when these films are heated to about 150°C in vacuum, further polymerization may occur and certainly volatile impurities are removed. In certain cases, the dark current was drastically reduced while there was little effect on the photocurrent. Current-voltage plots were generally ohmic in the 100-500 V region.

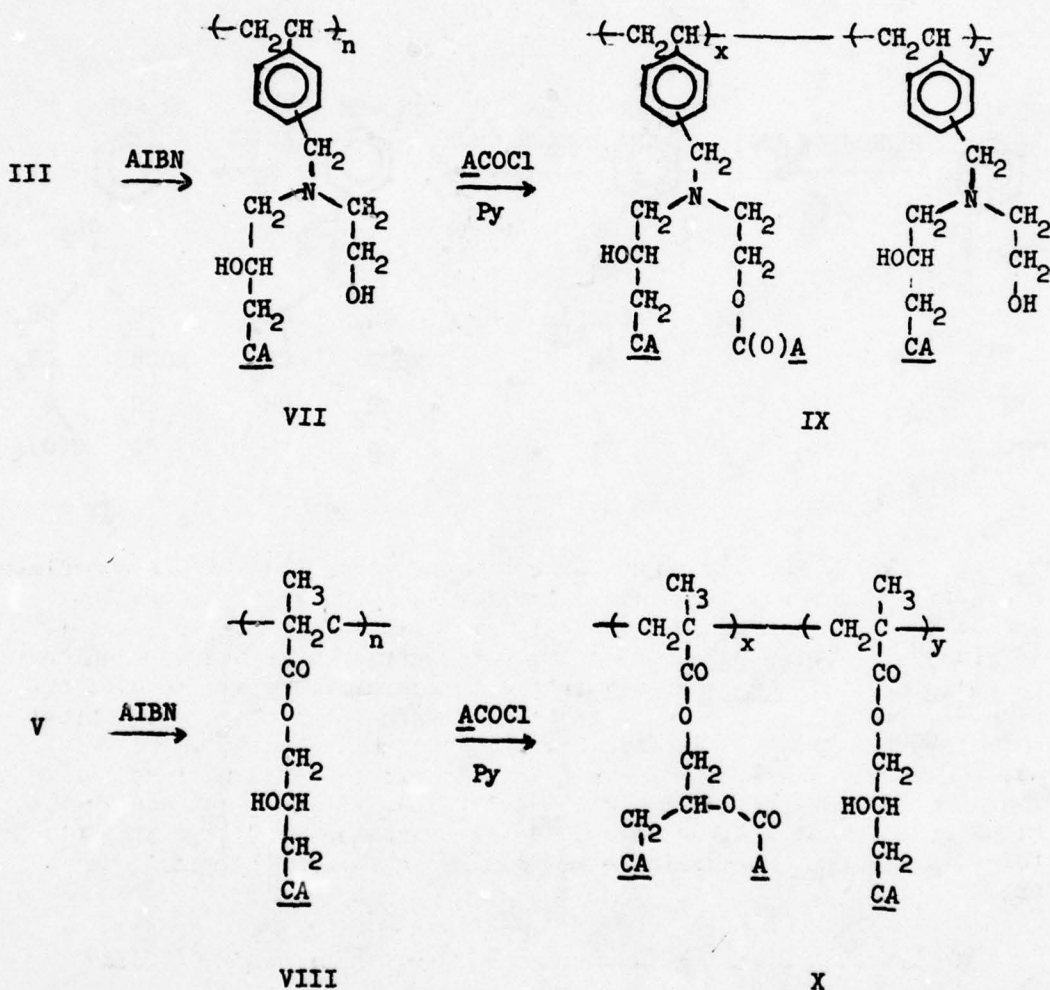
Typical screening photoconductivities that were obtained with polyester films that had been heated in vacuum are shown in Table I. Polymer A prior to heat treatment showed a photocurrent of 7×10^{-9} amp at 500 V and $I_{\text{PH}}/I_{\text{DK}}$ of only 2.5. After heating in vacuum from 55 to 155°C in the course of 2 hrs, followed by 1 hr at 155°C , this film had the values shown in the Table. The photoconductive response, $I_{\text{PH}}/I_{\text{DK}}$, of this film was similar to that of a reference PVCA-TNF (1:1) film, and it was a better dark insulator. Other samples of this polymer made by various methods that led to lower molar mass materials and/or poorer film-forming properties gave lower photoconductive responses. 2,7-Fluorenebis(methanol) gave a polyester related in structure to polymer A that was a poor photoconductor. Polyesters prepared from various diphenols and $\text{DNF}(\text{COCl})_2$ were less photoconductive than polymer A; polymer B is a typical example. Other polymers related to polymer B that gave similar results were synthesized from $\text{DNF}(\text{COCl})_2$ and 1,5-naphthalenediol or 9,10-anthracenediol. Polymers C and D are examples that show the effect of varying the acceptor moiety; polymer D has been previously reported (13), but without mention of electrical properties.

It is evident that certain donor-acceptor polyesters do provide film-forming materials with a reasonable photoconductive response. This response is dependent upon not only the nature of the donor and acceptor but upon their geometric relationship to each other both within a given chain and between adjacent chains in the solid material. From the results thus far obtained, it is clearly possible to design systems that have satisfactory electrical properties. However, as noted above, products of this type are difficult to obtain as high molar mass materials (13), possibly as a result of changed reactivity in a charge-transfer complex system. As a consequence of low molar mass, mechanical properties of the donor-acceptor polyesters were not satisfactory in themselves. An alternative is that they be used as dispersions, blends, or solutions with other polymers to provide materials with both electrical and mechanical properties in useful ranges.

Homopolymers and copolymers based on type structure II were also screened as photoconducting film-forming compositions. Synthetic routes leading to the monomers for these materials are shown in the following schemes, in which CA is 9-carbazoyl and A is a 2-(4,5,7-trinito-fluorenyl) radical:



In the presence of a free radical initiator (azobisisobutyronitrile, AIBN), homopolymers were obtained from III, IV, and V, but not from VI, and the polymers from III and V (VII and VIII, respectively) underwent partial reaction with AClCO to give the copolymers IX and X.



$$\text{IV} \xrightarrow{\text{AIBN}} \begin{array}{c} \text{---} \text{CH}_2 \text{---} \text{CH} \text{---} \text{---} \\ | \\ \text{C}_6\text{H}_4 \\ | \\ \text{CH}_2 \\ | \\ \text{N} \\ / \quad \backslash \\ \text{CH}_2 \quad \text{CH}_2 \\ | \quad \quad | \\ \text{OHCH} \quad \text{CH}_2 \\ | \quad \quad | \\ \text{CH}_2 \quad \text{O} \\ | \quad \quad | \\ \text{CA} \quad \text{C(O)A} \end{array}$$

Semiconducting Polymers Containing Dispersed TCNQ Salt-Crown Ether Complexes

65

Table II

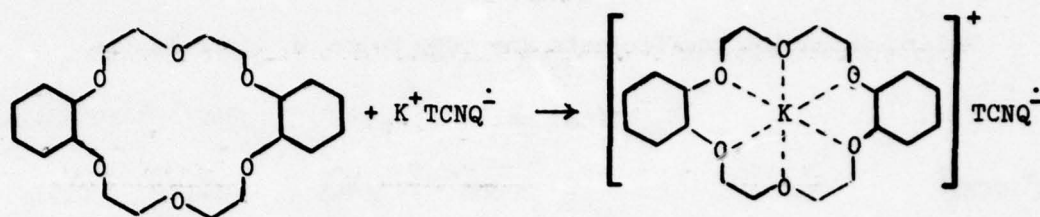
Photoconductivity of Donor-Acceptor Addition Polymer Systems

System	I_{Photo} (amp) at 500 V	$I_{\text{Photo}}/I_{\text{Dark}}^*$
VII (doped with ACl)	3.5×10^9	10^4
IX	7×10^{10}	10^4
XI	1.8×10^9	2×10^3
X	-	10^2

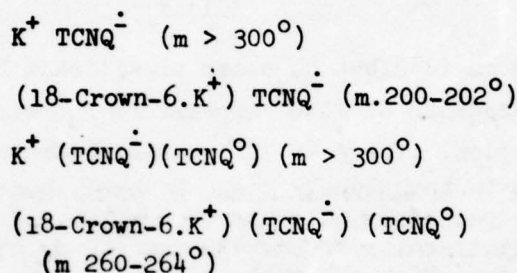
* After heating in vacuum

Two series of conducting radical-ion salts are formed with TCNQ. The first series, with the formula $M^{n+}(\text{TCNQ}^{\cdot-})_n$ (called "simple salts"), is formed with organic and metallic cations and has generally lower conductivities ($< 10^{-4} \Omega^{-1} \text{cm}^{-1}$) than the second series with the general formula $M^+(\text{TCNQ})_2$ or $M^+(\text{TCNQ})_2 \cdot (\text{TCNQ})$ (called "complex salts"), which have conductivities in the range 10^{-3} to $10^2 \Omega^{-1} \text{cm}^{-1}$. Where M is an alkali metal, only simple salts have been reported, and these have conductivities as high as $10^{-3} \Omega^{-1} \text{cm}^{-1}$. The alkali metal salts other than those from Li are extremely insoluble in organic solvents, but conducting dispersions of such salts in organic polymer films have been disclosed in the patent literature (17). In the case of organic cation complexes, solubility in organics is often greater, and as solubility in polymer film matrices increases, conductivity also increases (18).

The ability of multidentate macrocyclic compounds, particularly the so-called "crown ethers", to complex metallic cations and thereby increase the solubility of both inorganic and organic salts in organic solvents is well-established (19,20). Crown ether complexes of sodium and potassium salts of tetracyanoethylene have been studied (21), and one example involving a TCNQ salt, that of (dicyclohexyl-18-crown-6. K^+) (TCNQ $^{\cdot-}$), has been reported (22) without disclosure of conductivity data. The latter complex, unlike the uncomplexed salt, was soluble in an organic liquid crystal solvent and in methyltetrahydrofuran, in which infrared spectra of TCNQ $^{\cdot-}$ unperturbed by the cation were obtained. The reaction that probably occurs is



In the present work, the following crystalline complex salts



have been prepared, partially characterized, and their solutions or dispersions in poly(methyl methacrylate) films screened for their semi- and photoconducting properties. Other film-forming polymer matrices, such as polycarbonate, may also be used. It is evident that this work can be extended to a wide variety of macrocyclic complexing agents and TCNQ salts and complexes, and that the macrocyclic complexes of the TCNQ salts and complexes are of interest in themselves for their electrical properties.

Conventional procedures (15) were used to prepare $\text{K}^+ \text{TCNQ}^-$; the remaining compounds were easily prepared by simple mixing of solutions of $\text{K}^+ \text{TCNQ}^-$ with TCNQ^0 or 18-Crown-6, as appropriate. These substances were characterized through their absorption spectra. In all cases, the spectra were consistent with known or predicted spectra for each compound. The infrared spectra are shown in Figure 2. That for $\text{K}^+(\text{TCNQ}^-)(\text{TCNQ}^0)$ appears to be a superposition of the spectra of $\text{K}^+ \text{TCNQ}^-$ (23) and TCNQ, while the corresponding complexed salts contain bands ascribable to 18-Crown-6. Qualitatively, the visible spectra of the simple salt and its crown complex in acetonitrile are similar to those reported for TCNQ^+ (15,24) and for (dicyclohexyl18-Crown-6. K^+) (TCNQ^+) (22). With the corresponding complex salts (containing TCNQ^0), the 419 nm band maximum of the simple salts is shifted to 391 nm, but there is no change in the other band maxima. Extinction coefficients are given in Table III. The shift to 391 nm is reasonable, since TCNQ has a

Table III

Molar Extinction Coefficients for TCNQ Salts in Acetonitrile

	λ_{max} (nm)	419	742	842	$\epsilon_{419}/\epsilon_{842}$
$\text{K}^+ \text{TCNQ}^-$		20800	19700	36800	0.57
(18-Crown-6. K^+) (TCNQ^-)		25200	23600	43400	0.58
$\text{K}^+(\text{TCNQ}^-)$ (TCNQ^0)		67900 (391)	31100	59000	1.15
(18-Crown-6. K^+) (TCNQ^-) (TCNQ^0)		87500 (391)	18000	40000	2.19

strong λ_{max} at 395 nm (25) but no other significant bands up to 900 nm. In addition, the presence of TCNQ^0 appears to increase strongly the ϵ in the 400-nm region. The ϵ at 391 nm for 18-Crown-6. $\text{K}^+(\text{TCNQ}^-)$ - (TCNQ^0) appears to be anomalously high, however, suggesting that more than one TCNQ is present per molecule of complex. Melby et al (15) regarded the intensity ratio of the 420 and 850-nm bands as diagnostic for simple salts, for which the ratio was about 0.5.

The solubilization of the TCNQ salts in organic solvents by a crown ether is easily demonstrated by adding 18-Crown-6 to a suspension of $\text{K}^+ \text{TCNQ}^-$ in a solvent such as 1,2-dichloroethane; the bright green color of TCNQ^- becomes immediately apparent. In Figure 3, visible spectra are given to show these phenomena; $\text{K}^+ \text{TCNQ}^-$ is soluble in acetonitrile but not in dichloroethane.

For the purpose of making screening conductivity measurements, films were prepared by the slow evaporation of 1,2-dichloroethane solutions of a commercial poly(methyl methacrylate) (PMMA), Elvacite 2010, that contained appropriate amounts of the TCNQ salt or crown ether-complexed salt. In the absence of crown ether, very faintly greenish films containing suspended solids were obtained; there was little evidence of significant solubility for these salts in either the solvent-solute system or in the polymer film. Green solutions were obtained in the presence of 18-Crown-6 either as part of a previously formed complex or as an additive to a salt suspension. Solubility in the polymer film is less than in the solvent system. One percent by weight of (18-Crown-6. K^+) (TCNQ^-)(TCNQ^0) plus an equal weight of additional 18-Crown-6 in PMMA gave a clear green film, the spectrum of which is shown in Figure 4. This film underwent photobleaching in air during a one-hour exposure to the radiation, filtered through water to minimize heating, from a 200-W high pressure mercury lamp at a distance

of about 15 cm; the resulting spectrum is also shown in Figure 4. The same solute system at a weight concentration of 3% in PMMA gave a green film with widely scattered clusters of blue needles. At 6% or higher, the needle clusters were overlapping. Immersion of these films in water over a period of several days did not change their appearance.

As expected, films containing the complex salt or its crown ether complex were better conductors than films with the substances not having excess incorporated TCNQ. Therefore, the screening electrical measurements were centered on PMMA films containing $K^+(TCNQ^{\cdot-})(TCNQ^0)$ ("uncrowned salt"), (18-Crown-6. K^+)($TCNQ^{\cdot-}$)($TCNQ^0$) ("crowned salt"), and crowned salt with an equal weight of 18-Crown-6 ("crowned salt plus crown"). In no case was a significant photoconductive response observed. The observations that follow refer to dark currents produced at room temperature.

Initially, the films were electrically unstable. Application of the electric field tended to produce dark currents that varied with time, suggesting detrapping of charge carriers. Repeated application of the field, however, eventually resulted in stable and reproducible dark currents in films containing the crowned salt; stabilization was achieved more rapidly if excess crown ether was present. Stabilization was not achieved in films containing uncrowned salt. In Table IV are given the estimated dark conductivities at 5000 V cm^{-1} observed for these films at a number of salt concentrations. It is immediately

Table IV
Estimated Dark Conductivity of PMMA Films Containing
 $K^+(TCNQ^{\cdot-})(TCNQ^0)$ Systems

		$\sigma, \Omega^{-1} \text{ cm}^{-1}, \text{ at } 5000 \text{ V cm}^{-1}$	
<u>System</u>		<u>Initial</u>	<u>Stabilized</u>
Uncrowned Salt	1%	10^{-8}	(a)
	6%	10^{-8}	(a)
Uncrowned Salt, 6%, plus Crown Ether, 6%		10^{-5}	10^{-6}
Crowned Salt plus Crown	1%	10^{-10} (b)	-
	3%	10^{-7}	10^{-8}
	6%	10^{-5}	10^{-7}

^aStablization not achieved.

^bWithin an order of magnitude of a blank PMMA film.

apparent from these results that conductivity of the uncrowned salt is enhanced by the incorporation of the crown ether and that excess crown ether does not grossly change this conductivity. It is also clear that conductivity is not a simple function of solubility in the crown systems, since crystalline material was present in the films at the 3% and 6% levels.

Dark currents as a function of applied voltage are shown in Figure 5 for a film containing 6% crowned salt plus crown; the figure shows the effect of continued application of the electric field on this film. In the 100-500 V range, the response was approximately ohmic, but below this range the response became superohmic. The initial dark currents at any given voltage were fairly rapidly decreased with time of electric field application, and they recovered somewhat after standing for several hours in the dark in the absence of a field. After stabilization, however, dark currents did not vary with the duration of field application, and there was no back current when the field was removed.

The spectrum in Figure 4 indicates that these films are photosensitive. The effect of irradiation on field-induced dark currents in films containing 6% of the uncrowned salt is compared to that for the crowned salt plus crown in Figures 6 and 7. In general, the effect is to reduce the dark current at the time of application of the field (Figure 6). However, the time response of the current induced by a given voltage while the film is continuously irradiated is quite different for the two samples, as seen in Figure 7. It is clear that light has a profoundly degrading effect on the induced current when crown ether is absent, but the nature of the effect is unknown at present.

The foregoing is intended to be a phenomenological description. No attempt is made to adduce mechanisms or even to explain the results, since these represent preliminary data acquired with a screening device. Nonetheless, polymer films containing crown ether complexed TCNQ salts do show promise in the development of flexible semiconducting films. The crown ether does appear to be an essential element in this development.

SUMMARY

A series of polyesters having alternating electron donor and acceptor moieties have been synthesized and screened for their photoconducting and other properties. Photoconductive response in certain cases approaches that of 1:1 PVCA-TNF, a commercially useful polymeric photoconductor, but only low molar mass polymers were formed and as a consequence, mechanical properties were not satisfactory.

Addition polymers and copolymers containing pendant donor and acceptor groups were also synthesized and screened. These materials include a representative of a new class of addition polymers, those containing a strong donor and acceptor moiety in every structural

repeating unit. As with the condensation polyesters, good photoconductive response was observed with specific donor-acceptor addition polymer systems. Some of these materials were film-forming, but in general they were low molar mass polymers with poor mechanical properties.

The results with both condensation and addition donor-acceptor polymer systems indicate that it is possible to design photoconducting polymers based on intramolecular charge-transfer complex formation as a probable source of charge separation. In both cases, ways must be devised to increase polymer chain length to provide materials with useful mechanical properties.

Crown ether complexes of tetracyanoquinodimethane salts have been synthesized. They are found to be more soluble in organic solvents than the salts themselves. Solutions and dispersions of the complex salts in common film-forming polymers, such as poly(methyl methacrylate), provide flexible semiconducting films having conductivities several orders of magnitude greater than those for polymer dispersions of the salts in the absence of crown ethers. The crown ethers appear to have roles, such as that of electrical stabilizers, in addition to that of separation of the cation from the radical anion that functions as the conducting species.

REFERENCES

1. E. P. Goodings, *Quart. Rev.* 1975, 95.
2. V. S. Mylnikov, *Usp. Khim.* 43, 1821 (1974); *Russ. Chem. Rev.* 43, 862 (1974).
3. R. Foster, "Organic Charge-Transfer Complexes", Academic Press, New York (1969), Chapter 9 and Appendices.
4. V. M. Vincent and J. D. Wright, *Faraday Transactions I*, 1974, 58.
5. J. E. Katon, ed., "Organic Semiconducting Polymers", M. Dekker, New York (1968), p. 118-63.
6. S. I. Peredereeva, I. G. Orlov, and M. I. Cherkashin, *Usp. Khim.* 44, 602 (1975); *Russ. Chem. Rev.* 44, 295 (1975).
7. J. M. Pearson, *Pure and Applied Chem.* 49, 463 (1977).
8. W. D. Gill, Chap. 8 in "Photoconductivity and Related Phenomena", J. Mort and D. M. Pai, eds., Elsevier, New York (1976).
9. A. Inami and K. Morimoto, *U. S.* 3 418 116 (1968).
10. N. C. Yang and Y. Gaoni, *J. Am. Chem. Soc.* 86, 5022 (1964).

11. G. B. Butler and K. Sivaramakrishnan, *Polymer Preprints* 17(2), 608 (1976).
12. S. R. Turner and M. Stolka, *Macromols.* 11, 835 (1978).
13. T. Sulzberg and R. J. Cotter, *J. Pol. Sci. A-1*, 8, 2747 (1970).
14. T. Sulzberg and R. J. Cotter, *J. Org. Chem.* 35, 2762 (1970).
15. L. R. Melby, R. J. Harder, W. R. Hertler, W. Mahler, R. E. Benson, and W. E. Mochel, *J. Am. Chem. Soc.* 84, 3374 (1962).
16. B. P. Bespalov and V. V. Titov, *Usp. Khim.* 44, 2249 (1975); *Russ. Chem. Rev.* 44, 1091 (1975).
17. T. Suzuki and K. Mizoguchi, *Jap. Kokai* 75, 123 750; *Chem. Abstr.* 84, 75110.
18. T. Kamiya, J. Mizoguchi, E. Tsuchida and I. Shinohara, *Nip. Kagaku Kaishi* 1977, 1385.
19. C. J. Pedersen and H. K. Frensdorff, *Angew. Chem. Intl. Ed.* 11, 16 (1972).
20. J. J. Christensen, D. J. Eatough, and R. M. Izatt, *Chem. Rev.* 74, 351 (1974).
21. M. P. Eastman, Y. Chiang, G. V. Bruno, and C. A. McGuyer, *J. Phys. Chem.* 81, 1928 (1977) and earlier papers.
22. I. Haller and F. B. Kaufman, *J. Am. Chem. Soc.* 98, 1464 (1976).
23. Z. Iqbal and C. W. Christoe, *J. Chem. Phys.* 63, 4485 (1975).
24. H. T. Jonkman and J. Kommandeur, *Chem. Phys. Lett.* 15, 496 (1972).
25. D. S. Acker and W. R. Hertler, *J. Am. Chem. Soc.* 84, 3370 (1962).
26. T. Nakaya, T. Tomomoto, and I. Imoto, *Bull. Chem. Soc. Japan* 39, 1551 (1966).

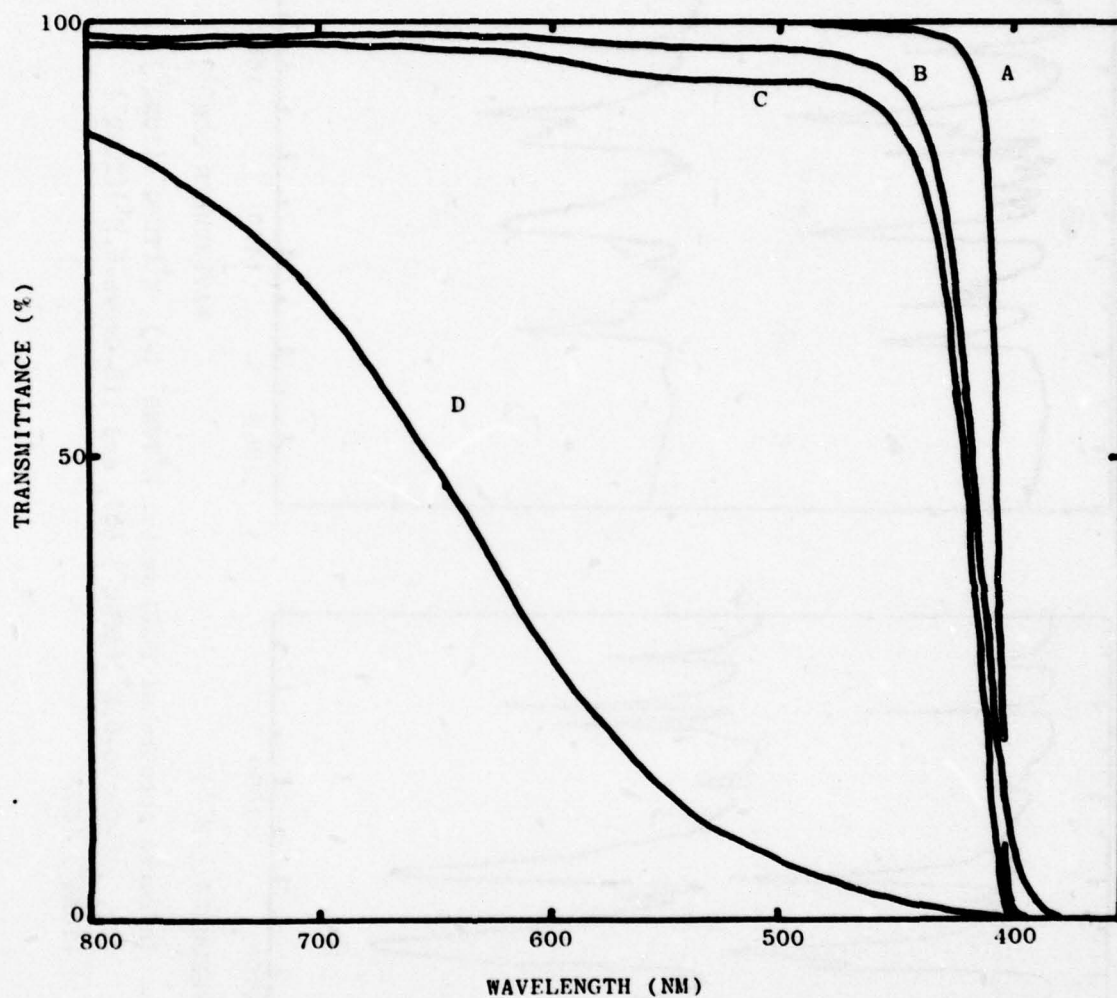


Fig. 1 Absorption spectra of 10^{-3} M dimethyl sulfoxide solutions of 9, 10-anthracenebis(methanol)(A), dimethyl 4,5-dinitrofluorenone-2,7-dicarboxylate (B), mixture of these compounds (C), and the condensation polymer from the diol and DNF (COCl_2) (D).

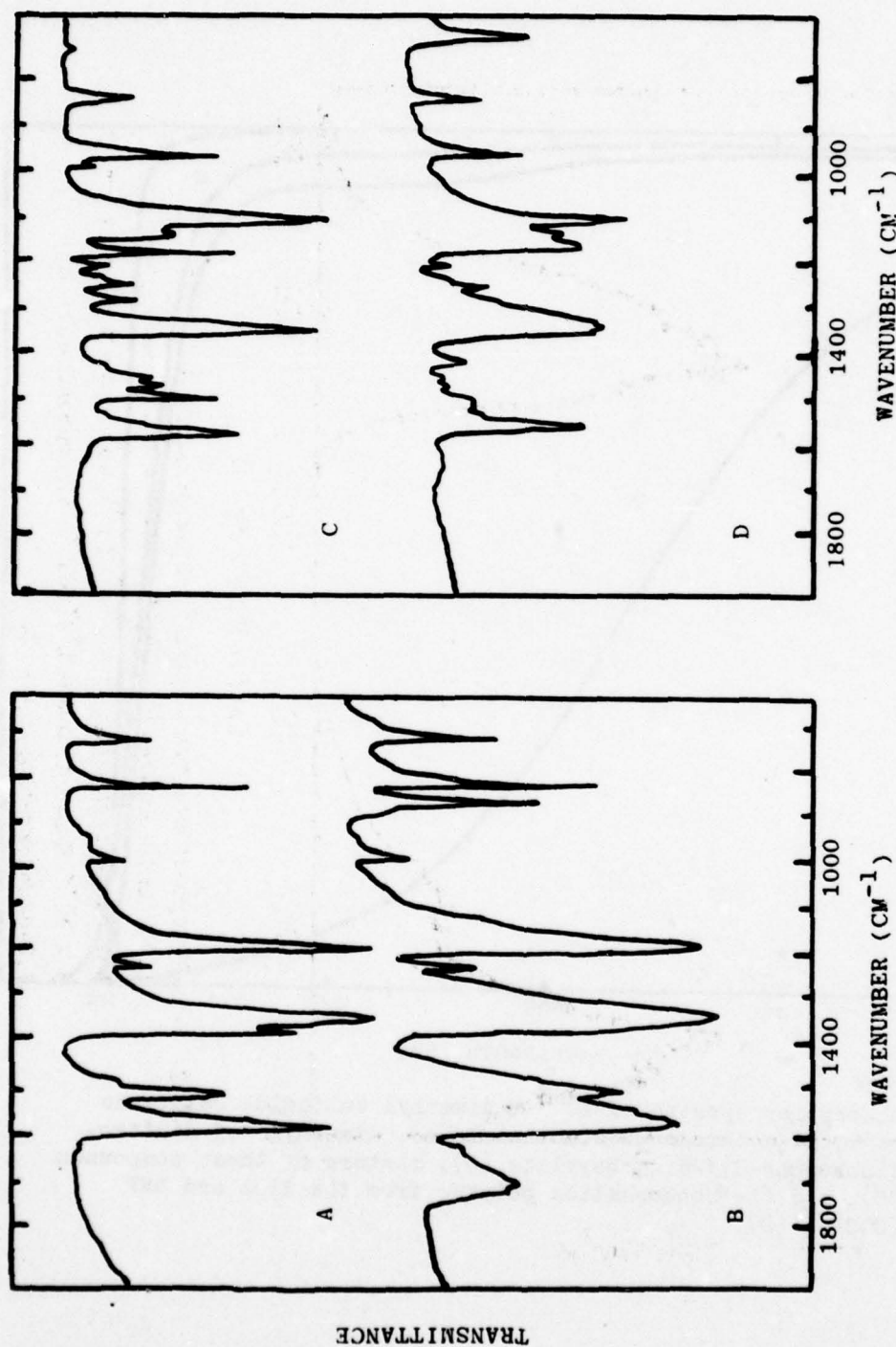


Fig. 2. Infrared spectra of TCNQ salts: K⁺TCNQ⁻ (A), K⁺(TCNQ⁻)(TCNQ⁰) (B), (18-Crown-6.K⁺)(TCNQ⁻) (C), and (18-Crown-6.K⁺)(TCNQ⁰) (D).

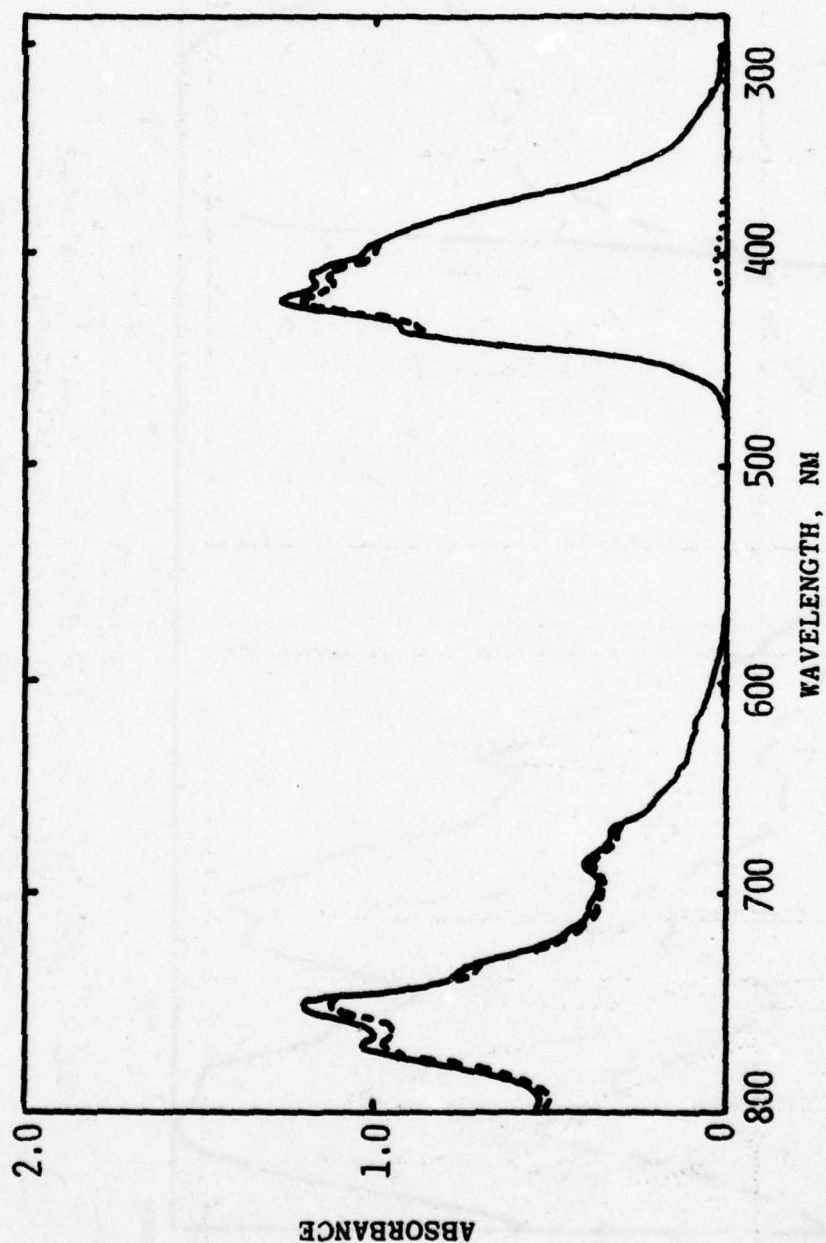


Fig. 3. Absorption spectra of a 10^{-3} M suspension of K^+TCNQ^- in 1,2-dichloroethane (.....); 5×10^{-5} M 18-Crown-6 added to the suspension (---); 5×10^{-5} M K^+TCNQ^- in acetonitrile or 5×10^{-5} M (18-Crown-6. K^+)($TCNQ^-$) in acetonitrile or 1,2-dichloroethane (----).

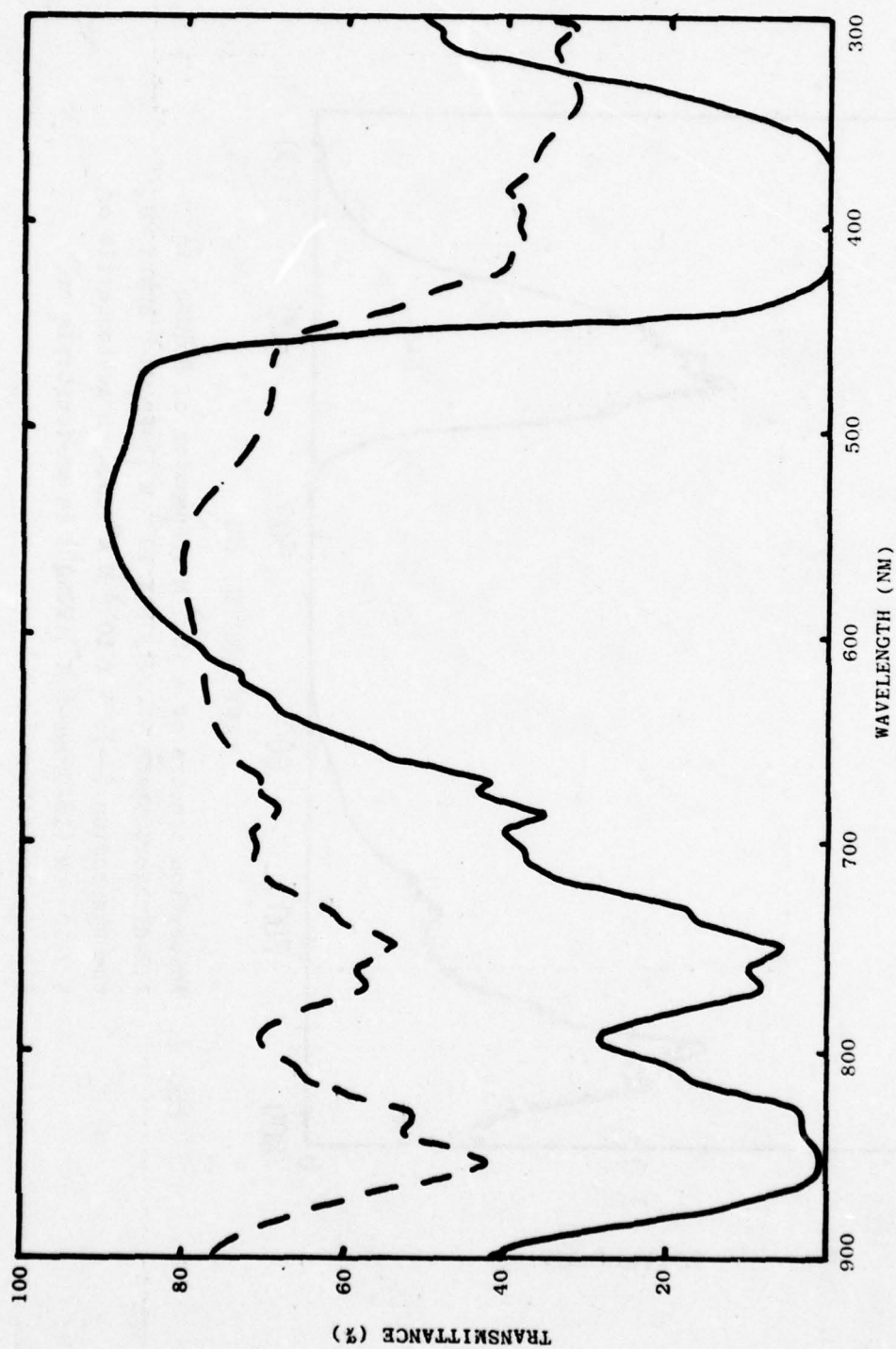


Fig. 4. Photobleaching of a 6 μ m PMMA film containing one weight percent each of (18-Crown-6.K⁺)(TCNQ⁻)(TCNQ⁰) and 18-Crown-6: before (----) and after (---) 60 min. UV irradiation.

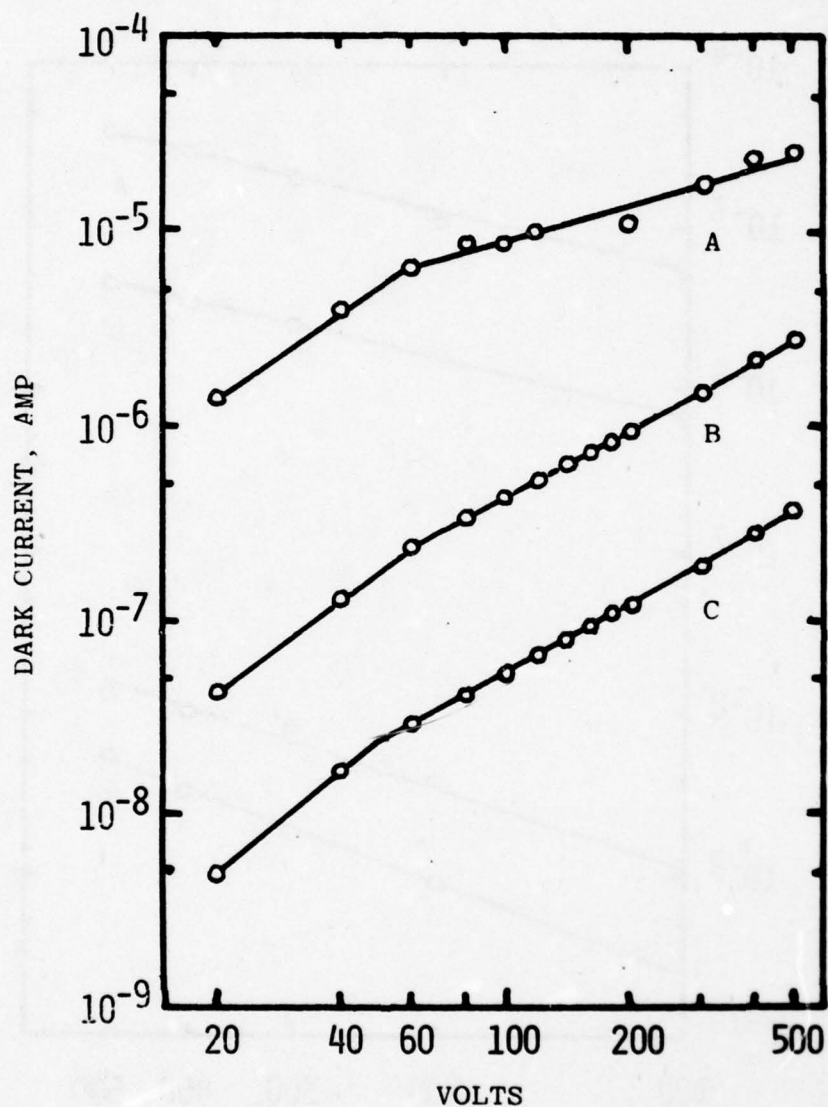


Fig. 5. Dark currents in PMMA films containing 6% (18-Crown-6.K⁺) (TCNQ)⁻(TCNQ⁰) plus 6% 18-Crown-6 as prepared (A); after 20 min. at 500 V (B); after electrical stabilization (C).

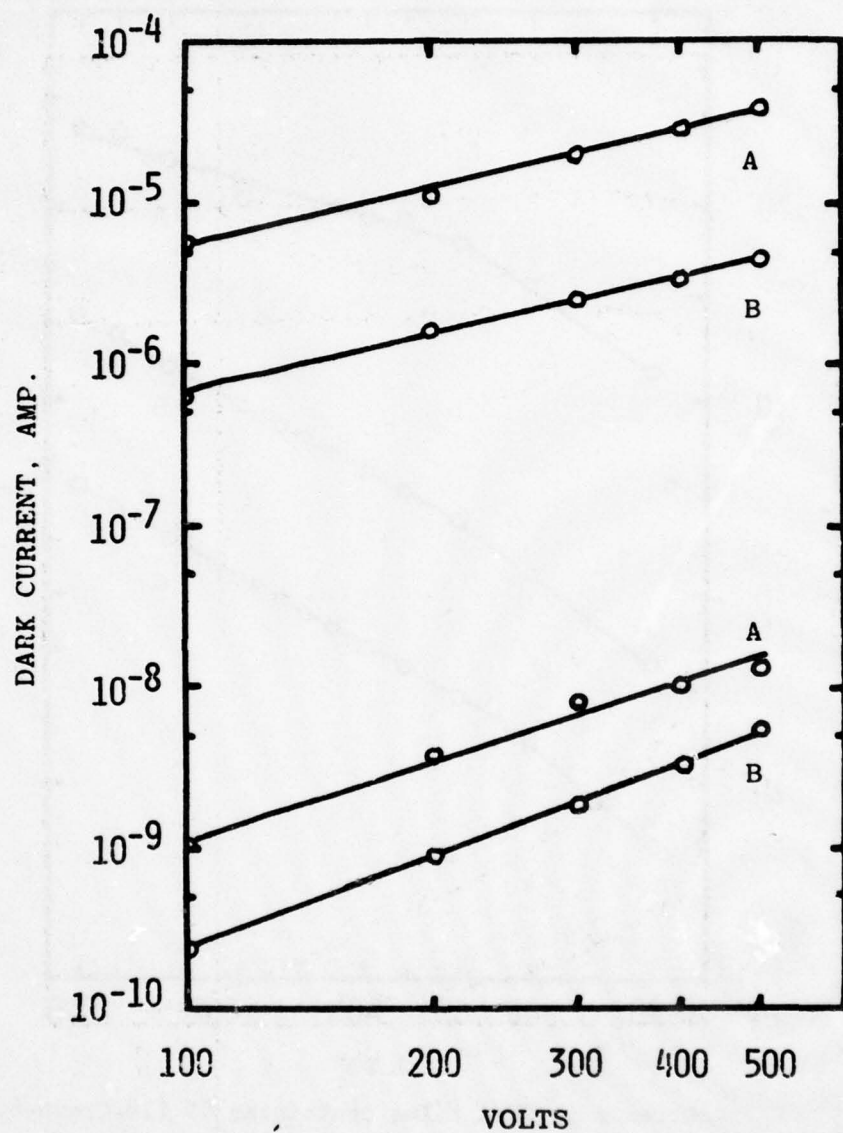


Fig. 6. Dark currents (A) before and (B) after irradiation of PMMA films containing 6% (18-Crown-6.K⁺)(TCNQ⁺)(TCNQ⁰) (lower plots).

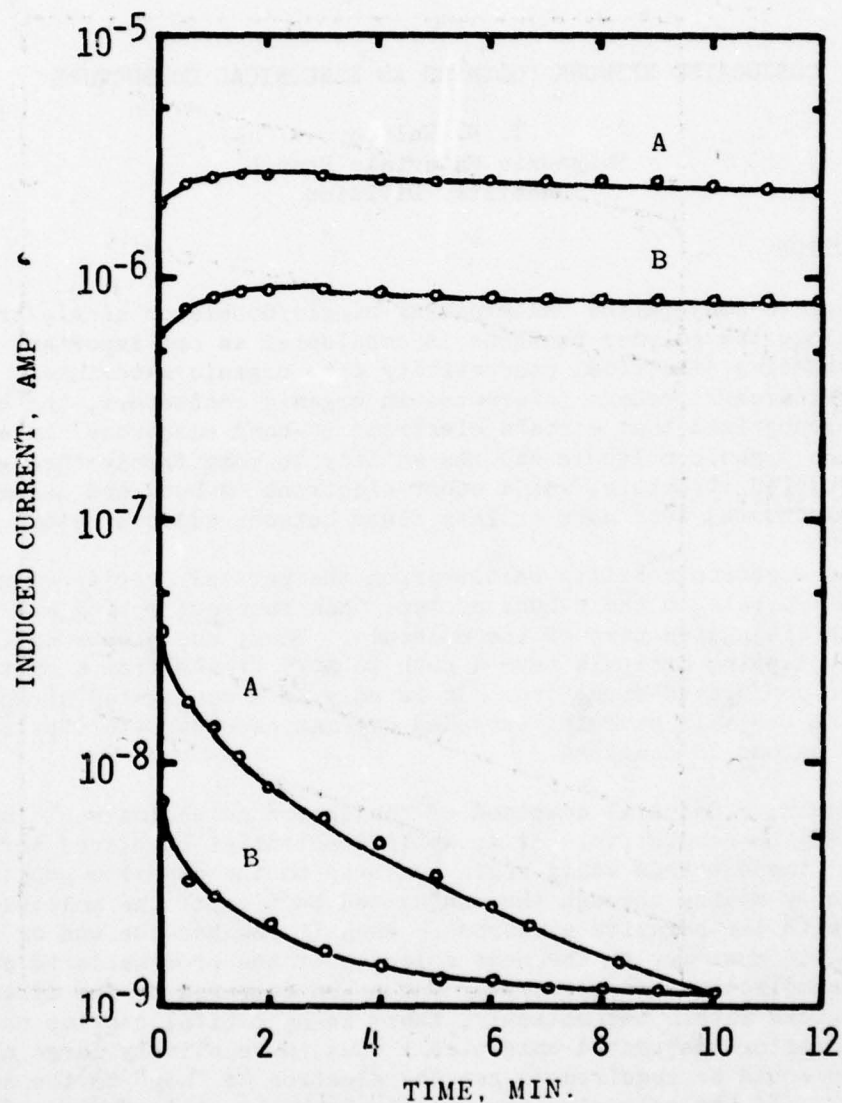


Fig. 7. Induced currents at 500 V (A) before and (B) after repeated field application during continuous UV irradiation of PMMA films containing 6% (18-Crown-6.K⁺)(TCNQ⁺)(TCNQ⁰) (upper plots) and 6% K⁺(TCNQ⁺)(TCNQ⁰) (lower plots).

CONJUGATED NETWORK POLYMERS AS ELECTRICAL CONDUCTORS

T. R. Walton
Polymeric Materials Branch
Chemistry Division

INTRODUCTION

Complete conjugation (alternating single/double or single/triple bonds) along the polymer backbone is considered as one important means for introducing electrical conductivity into organic materials. Long before researchers became interested in organic conductors, the organic chemist recognized that certain electrons (π -bond electrons) in a conjugated organic molecule had the ability to roam freely throughout the conjugated structure, while other electrons (σ -bond and isolated π -bond electrons) were more or less fixed between adjacent atoms.

This electron mobility results from the partial overlap of neighboring p orbitals in the π -bond system, thus interconnecting all π -bonds along the conjugated part of the molecule. Thus, the electrons in these overlapping orbitals have a path to move freely from atom to atom along the conjugated structure. It is only in a conjugated structure that these orbitals have the extended overlap necessary for the electrons to become delocalized.

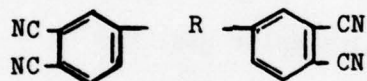
However, a material composed of conjugated molecules would not necessarily be conductive. If an applied potential is placed across the material, the electron would begin its trip to the opposite positive electrode by moving through the conjugated portion of the molecule in contact with the negative electrode. When it reaches the end of that molecule, it must get to the next molecule if the process is to continue. Since the molecules are relatively far apart compared to the distance between atoms within the molecule, there is no orbital overlap connecting neighboring conjugated molecules. Thus, a relatively large amount of energy would be required to get the electron to "hop" to the next molecule. If the molecules are relatively small, this "hopping" process would have to occur many times before the electron finally reached the opposite end of the material. Since a large amount of energy would be required for these numerous hopping processes, one would expect poor conductivity. On the other hand, if instead of a large number of small molecules, the material were composed of one huge, completely conjugated molecule, there would be no disruption of the conjugation path from one end of the material to the other, and one would expect high conductivity.

In practice one cannot prepare infinite network polymers; that is, polymerize all of the monomer (prepolymers) into a single molecule. Side reactions and/or immobility terminates polymer growth such that the material is generally composed of a number of very large polymer molecules rather than one single molecule. Nevertheless, the amount of hopping would be greatly reduced and increased conductivity would be expected as the polymer structure approached an infinite network. Since the extent of the polymer growth will control conductivity, polymerization reactions that lead to high molecular weight, network polymers are important requirements.

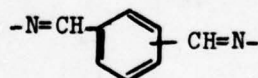
PREPOLYMER RESINS

Figure 1 shows three basic chemical reactions which, when utilized with the properly designed monomer molecule, would lead to three-dimensional, conjugated polymer networks. In each reaction a conjugated system of aromatic rings is formed.

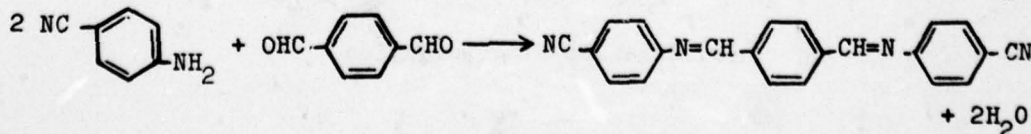
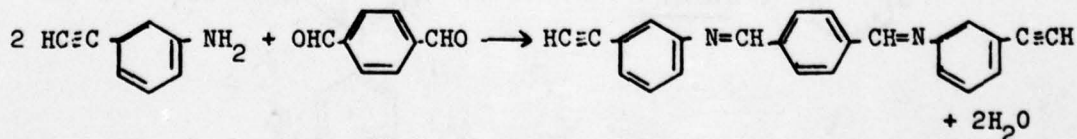
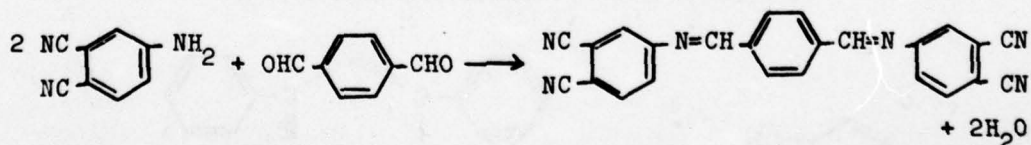
To utilize these reactions for polymer synthesis, two reactive groups must be linked together, as illustrated for the phthalonitrile structure:

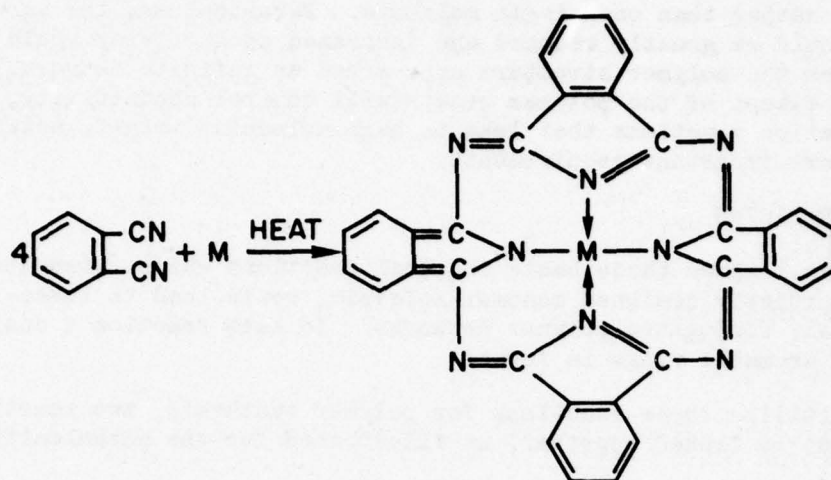


Since a completely conjugated network is desired, the linking R group must also be conjugated. The linking groups reported on in this paper have the structure:

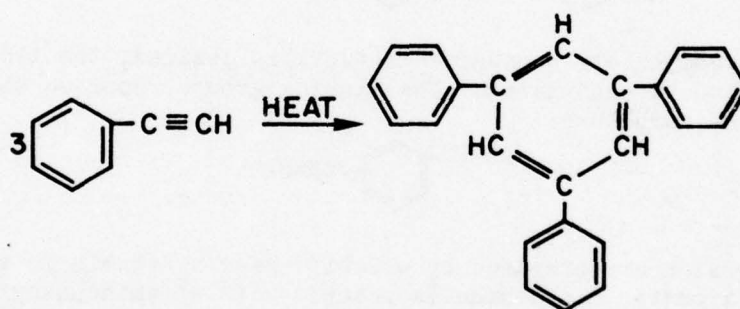


Prepolymer resins are prepared by a Schiff-base synthesis in which the appropriate aromatic dialdehyde is reacted with an aminophenyl orthodinitrile, nitrile, or acetylene, to produce a dianil linking structure:

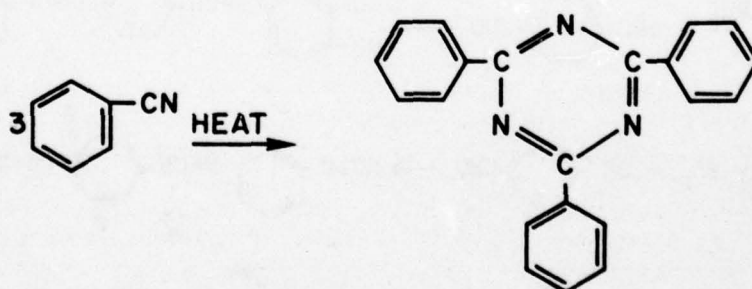




(a) Phthalocyanine Reaction



(b) Acetylenic Cycloaddition Reaction



(c) Triazine Ring Formation

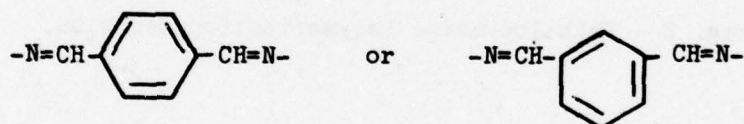
Fig. 1 - Synthesis Reaction.

Table 1 lists four prepolymer resins that have been prepared and the common names that will be used in the discussion to follow. In the synthesis of these materials, a slight excess of the amine is used to ensure reaction of both aldehyde groups. The preparations are generally carried out in refluxing toluene and the progress of the reaction is followed by measuring the amount of water collected during the reaction. In addition to carbon, hydrogen and nitrogen analysis, the infrared and nuclear magnetic resonance (NMR) spectra are used to verify the structures.

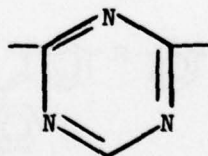
The presence of the imine linkage ($-\text{C}=\text{N}-$) introduces the possibility of cis-trans isomers in the structures of the prepolymers. Since there are two such linkages, three isomers are possible, a cis-cis, a trans-trans, and a cis-trans. Melting points and NMR indicate only one isomer is formed and this has the trans-trans structure.

POLYMERIZATION

The type of network polymer structure produced on thermal polymerization of the dianil phthalonitrile resin in the presence of a metal co-reactant, such as Cu, is shown in Fig. 2, and the product from the dianilphenylacetylene resin is shown in Fig. 3, where the R groups in both figures have the following structure:



The polymer from the dianil phenylnitrile resin would be similar to the acetylene polymer in Fig. 3 except that triazine rings would replace the Kekule benzene rings:



Since the R groups in Figs. 2 and 3 are completely conjugated, the polymer network is a totally conjugated (alternating single/double bonds) system. Furthermore, we would expect these polymers to be of high molecular weight due to the high functionality (multiple growth sites) of the polymerization reaction. Thus, with electron mobility provided by the extensive delocalization of the π -bond electrons throughout the structure, we might expect these systems to be electrically conducting. It should be kept in mind that the structures are much more complicated than illustrated. Further, the diagrams depict a planar configuration, but the actual structures are three-dimensional highly crosslinked networks.

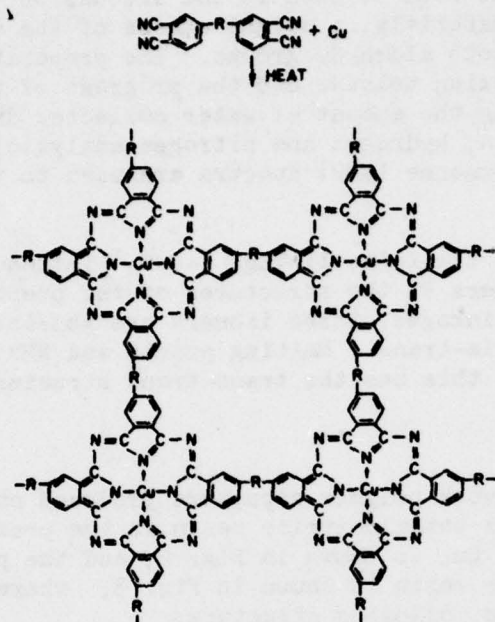


Fig. 2 - Phthalocyanine Polymerization Reaction.

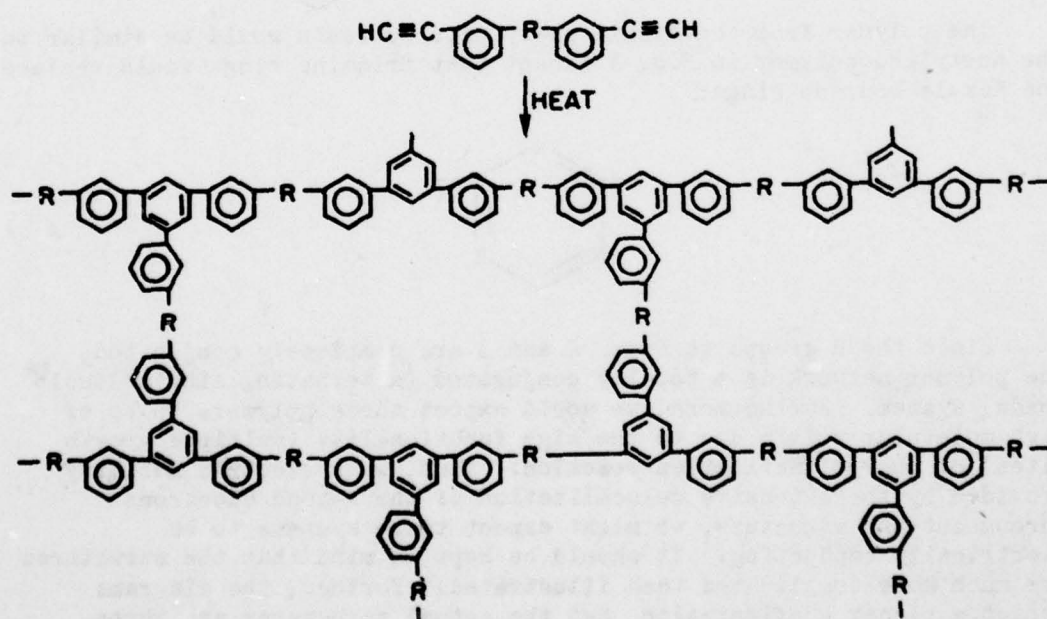


Fig. 3 - Acetylene Polymerization Reaction.

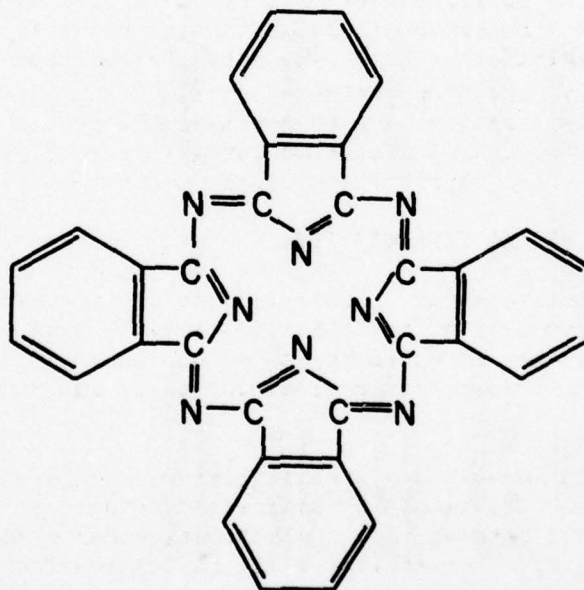
Table 1
Resins For Preparing Conductive Network Polymer

<u>Carbon/Hydrogen/Nitrogen Analysis</u>									
<u>Resin Prepolymer</u>	<u>Resin Common Name</u>	<u>Yield, %</u>	<u>Melting Point, °C</u>	<u>Calculated</u>			<u>Found</u>		
				<u>%C</u>	<u>%H</u>	<u>%N</u>	<u>%C</u>	<u>%H</u>	<u>%N</u>
$[(N \equiv C)_2 \text{N} = \text{CH}]_2$ para	Para-Dianil Phthalonitrile	70%	269-270°C	74.99	3.15	21.86	74.90	3.33	21.67
$[(N \equiv C)_2 \text{N} = \text{CH}]_2$ meta	Meta-Dianil Phthalonitrile	60%	255-257°C	74.99	3.15	21.86	74.86	3.26	21.64
$(\text{HC} \equiv \text{CN} = \text{CH})_2$ para	Para-Dianil Phenylacetylene	80%	139-140°C	86.72	4.85	8.43	85.75	5.00	8.24
$(N \equiv \text{CN} = \text{CH})_2$ para	Para-Dianil Phenylnitrile	78%	222-224°C	79.02	4.22	16.76	no data		

The phthalonitrile and acetylenic systems have been successfully polymerized. It appears that a catalyst will be necessary to effectively convert the dianilphenylnitrile resin into a triazine network polymer. In the case of the dianil phthalonitrile resins, the polymerization can be carried out in either the presence or absence of a metal or metal salt co-reactant. If a metal is present, it is incorporated into the phthalocyanine nucleus (see Fig. 2). The purpose of adding a metal co-reactant would be to modify the electrical properties, for example, from an n to p type semiconductor, as well as to accelerate the cure.

In the absence of a metal co-reactant, the resins are polymerized by simply heating them above their melting point, usually to 275-300°C. Gelation occurs in approximately 2 hours and the cure is continued for an additional 24 to 50 hours. The cured polymer is a dark brown color, changing to black during postcuring. The dark color is attributed to the conjugation of the system.

In the absence of a metal co-reactant, polymerization may lead to an alternate structure, called dehydrophthalocyanine:



This structure has been identified and also apparently exists in the case of certain metals which form hexavalent coordinate complexes.

Metal cures are somewhat more complex and the cure rate is generally greatly accelerated. With a free metal such as Cu, there is always some unreacted metal left which tends to settle out because of

the density difference. Metal chlorides can generally be more uniformly distributed, but partial ring chlorination may occur and HCl gas liberated.

Anhydrous tin dichloride, SnCl_2 , is an exception since it increases its valence to +4 and is inserted as $(\text{SnCl}_2)^{+2}$ without gas evolution. The melting point of the SnCl_2 is approximately the same as the resin (241°C), and both components are in the liquid state and mutually soluble at the polymerization temperature. The polymerization is extremely fast, gelation occurring within a few minutes after melting. The stoichiometry of the reaction requires one metal atom for each two resin molecules to have a metal atom in each phthalocyanine ring formed. However, since the polymerization occurs even in the absence of metals, one has the option of using less than stoichiometric amounts. Indeed the insertion of metal atoms into only a few of the phthalocyanine rings may be sufficient to modify the electrical properties of the polymer.

The dianil phenylacetylene resin can be polymerized at much lower temperatures than the dianil phthalonitrile resins. Generally, the acetylene resin is initially heated at 150°C for 1 hour during which time the liquid resin darkens in color and its viscosity slowly increases until gelation occurs. The resin is then further cured overnight at 200°C , and then postcured at 300°C for 50 hours. Although the acetylene polymerization may be catalyzed by certain metal or metal complexes, the metal cannot become an integral part of the polymer structure as with the polyphthalocyanines.

POSTCURE AND ELECTRICAL CONDUCTIVITY

Both the phthalocyanine polymer and the acetylene-based polymer are essentially non-conductive (resistivities greater than 10^{10} ohm-cm) after the initial cure. Postcuring these polymers at higher temperatures in a vacuum or inert atmosphere results in substantial increases in conductivity.

Resistance is measured in a straightforward manner with a Keithley 610A electrometer. The sample is sandwiched between soft conductive mats which are held between copper electrodes under a constant load of approximately 1.2 Kg. Resistivities are calculated from the measured resistance, sample thickness, and a conservative estimate of the contact area. The measurements are made in air and the apparatus is not shielded. With this setup, resistances in the range of 10^0 to 10^{10} ohms can be measured. Resistivity values determined in this manner agreed reasonably well with the more detailed measurements reported in the following paper by J. P. Reardon.

Initial examination of the postcure necessary to introduce conductivity into these new polymeric materials revealed that little change

occurs below 400°C. Even after several hundred hours at 400°C, resistivity was still greater than 10^{10} ohm-cm. However, at 500°C, resistivity rapidly dropped to 10^5 ohm-cm, and continued to decrease with time, leveling off at 10^2 - 10^3 ohm-cm after 800 hours (Fig. 4). At 600°C another rapid drop in resistivity to 10^0 to 10^1 ohm-cm occurred.

As expected, both temperature and time are important factors in controlling resistivity. Although the lower temperatures do not lead to rapid development of conductivity, they are important in developing the polymeric structure and in minimizing weight loss and the problem of sample cracking at the higher temperatures. With these preliminary results as guidelines, a standard heat treatment was adopted in which the cured polymers were first heated at 400°C for 100 hours, then 500°C for 100 hours, 600°C for 100 hours, etc. Thus, the samples have an accumulated history of the previous heat treatments. Further, to avoid temperature shock and minimize the development of thermal stresses in the sample during the postcure, slow heat-up and cool-down rates were used, ranging from 0.5°C/min. to 2°C/min.

In Table 2 are summarized some typical results on postcuring the para- and meta-dianil phthalocyanine polymers and the para-dianil phenylacetylene polymer. For ease of comparison, Fig. 5 shows a composite plot of the change in resistivity with temperature for the three polymers. In a qualitative sense the materials fall in the same conductivity range for a given temperature treatment.

In Figure 6, the weight losses for the materials in Table 2 are plotted as a function of the postcure temperature. In general, temperatures above 300-400°C are disastrous for most organic polymers, but these new polymeric materials show relatively low weight losses at 400-500°C and maintain a great deal of structural integrity even at 600-700°C. The implications of the high thermal stability is that these materials have the potential for operation in a high temperature environment.

An indication of the variation of properties between replicate samples can be obtained from the data in Table 3 for a series of identically cured and postcured polyphthalocyanines. Samples 1-4 were from one resin batch while 5 and 6 were from another. All samples were cured and postcured at the same time in the same furnace. Considering the variation in temperature that could exist at different positions in the furnace and the rapid change in electrical properties in the 400-500°C range (Figure 5), the agreement between samples is exceptional.

Up to this point we have considered only metal-free cured resins. However, as discussed earlier, the phthalonitrile resins can also be cured in the presence of a metal or metal chloride. Under these

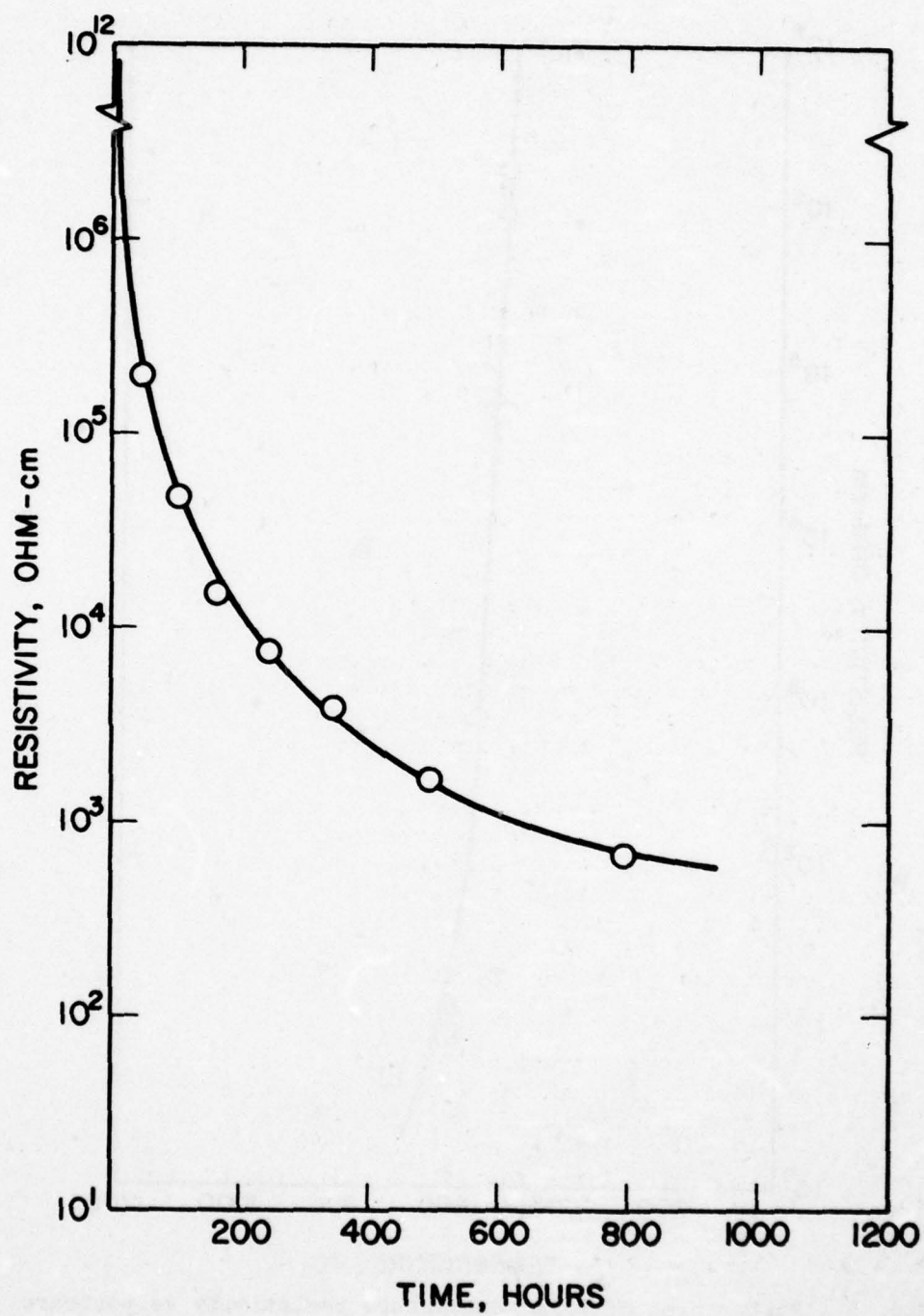


Fig. 4 - Room temperature resistivity vs. time of heating at 500°C for p-dianil phthalocyanine polymer.

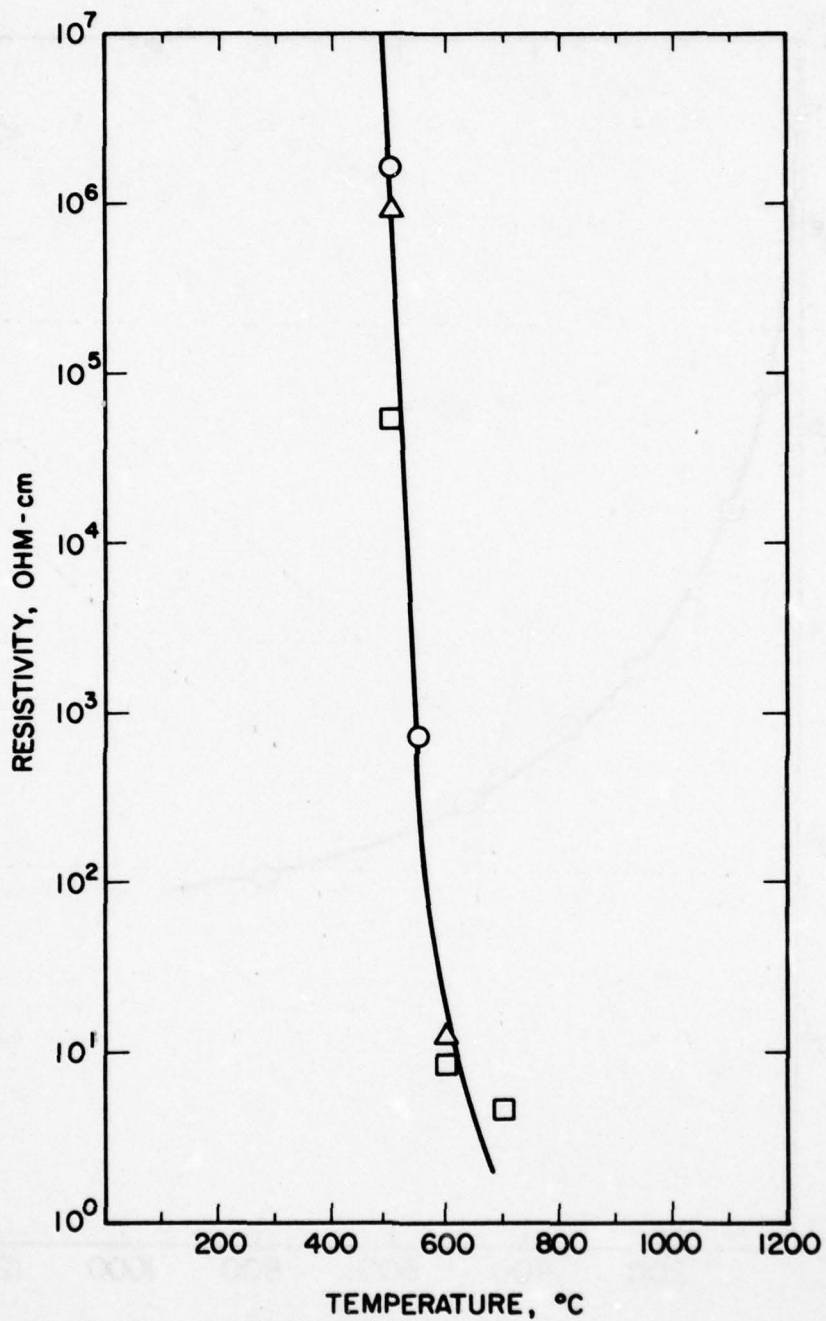


Fig. 5 - Master plot of room temperature resistivity vs postcure temperature for
(a) p-dianil phthalocyanine polymer, O;
(b) n-dianil phthalocyanine polymer, □;
(c) p-dianil phenylacetylene polymer, Δ.

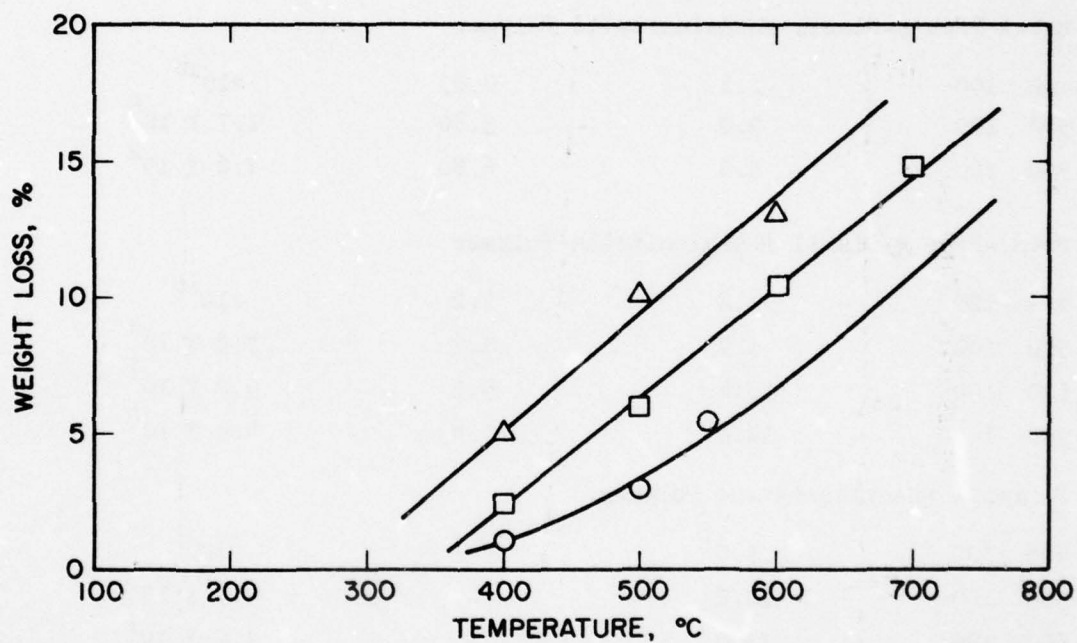


Fig. 6 - Thermal stability of conjugated polymers (cumulative weight loss after 100 hrs at each temperature). Samples initially cured 50 hrs at 300°C. (a) p-dianil phthalocyanine polymer, O; (b) n-dianil phthalocyanine polymer, □; (c) p-dianil phenylacetylene polymer, Δ.

AD-A067 736

NAVAL RESEARCH LAB WASHINGTON D C
THE NRL PROGRAM ON ELECTROACTIVE POLYMERS. (U)
MAR 79 L B LOCKHART
NRL-MR-3960

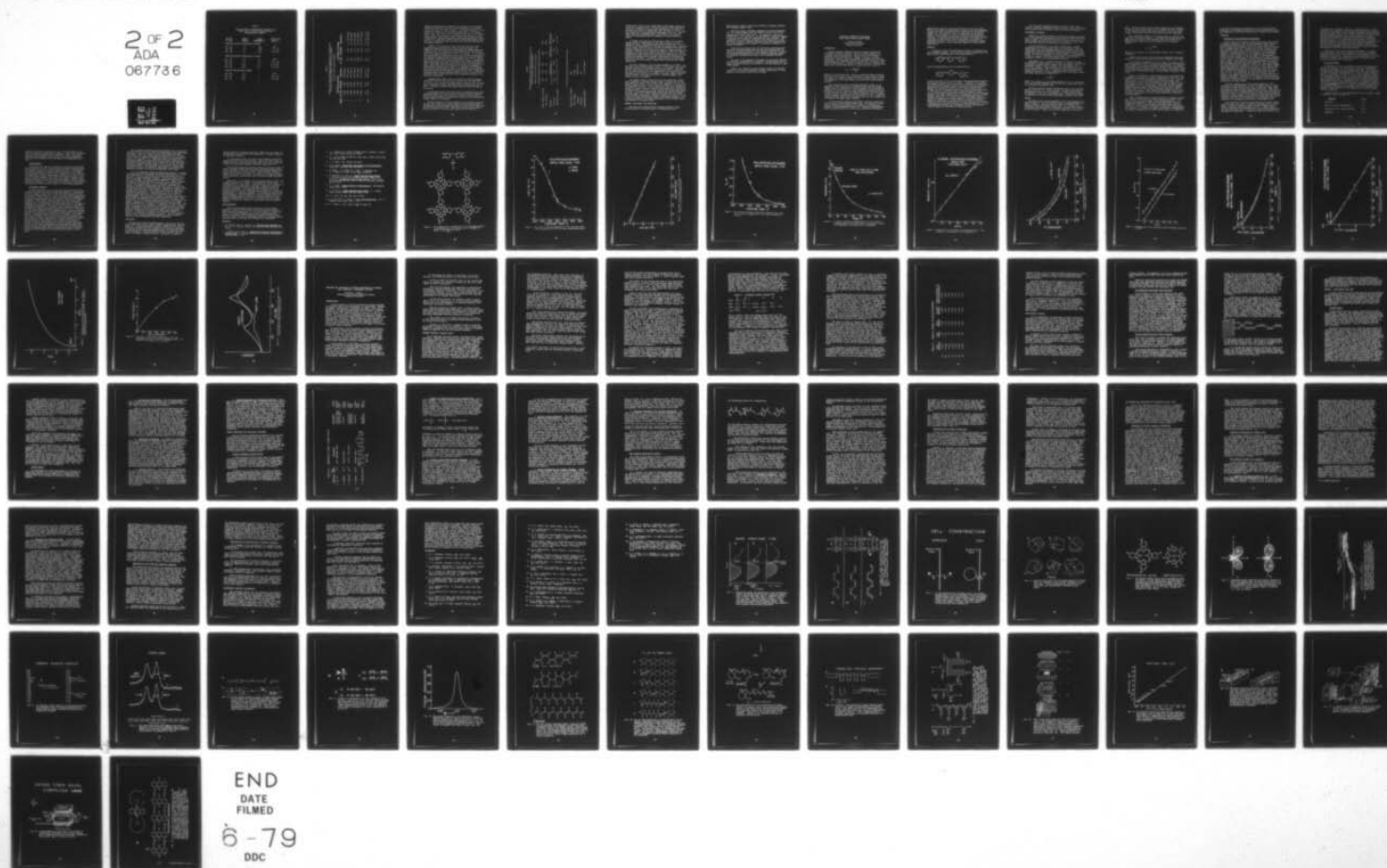
F/6 7/3

UNCLASSIFIED

NL

2 OF 2
ADA
067736

501



END
DATE
FILMED

6-79
DDC

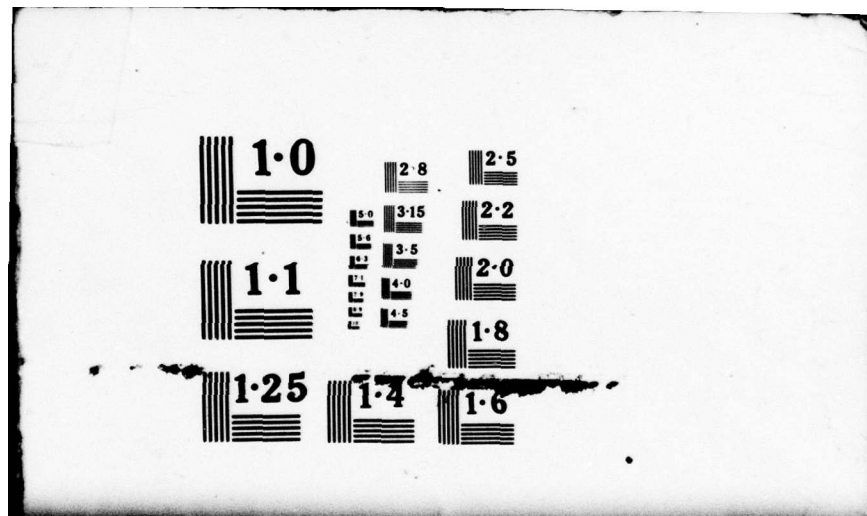


Table 2

Postcure Effects on Resistivity, Shrinkage, and
Weight Loss for Dianil Phthalocyanine and
Phenylacetylene Polymers

Postcure °C	Hrs	Weight Loss, %	Linear Shrinkage, %	Resistivity ohm-cm
Metal-Free p-Dianil Phthalonitrile Polymer				
400	100	1.1	0.85	$>10^{10}$
500	100	3.0	3.80	1.7×10^6
550	100	5.4	6.80	7.6×10^2
Metal-Free m-Dianil Phthalonitrile Polymer				
400	100	2.2	1.2	$>10^{10}$
500	100	5.9	5.2	5.8×10^4
600	100	10.4	9.1	9.0×10^0
700	100	14.8	11.4	4.8×10^0
P-Dianil Phenylacetylene Polymer				
400	100	5.0	-	$>10^{10}$
500	100	10.2	-	9.4×10^5
600	100	13.0	-	1.2×10^1

Table 3

Weight Loss, Linear Shrinkage and Resistivity for Identically
Cured and Postcured p-Dianil Phthalocyanine Polymers
(Initial Cure 50 Hours at 300°C)

Sample	400°C/100 hr Postcure			500°C/100 hr Postcure		
	Wt. Loss	Shrinkage	Resistivity	Wt. Loss	Shrinkage	Resistivity
1	1.25%	1.56%	$>10^{10}$ ohm-cm	-	-	-
2	1.09%	0.95%	$>10^{10}$ ohm-cm	3.40	4.62	6.1×10^5 ohm-cm
3	1.08%	0.85%	$>10^{10}$ ohm-cm	3.05	3.78	17×10^5 ohm-cm
4	1.19%	0.81%	$>10^{10}$ ohm-cm	2.59	4.16	19×10^5 ohm-cm
5	1.60%	1.43%	$>10^{10}$ ohm-cm	2.98	4.40	16×10^5 ohm-cm
6	1.99%	1.05%	$>10^{10}$ ohm-cm	3.55	4.60	2.6×10^5 ohm-cm
Avg.	1.37%	1.11%	$>10^{10}$ ohm-cm	3.11	4.31	12.1×10^5 ohm-cm

conditions the metal may be chemically incorporated into the phthalocyanine ring structure. Results of cures conducted in the presence of SnCl_2 and CuCl_2 are shown in Table 4. As discussed earlier, the tin expands its valence to +4 as the SnCl_2 becomes part of the phthalocyanine ring. With CuCl_2 , only the copper becomes part of the phthalocyanine ring and the chlorine is lost through other reactions as discussed earlier. When less than 100% of the theoretical amount of metal is used (i.e., less than one metal atom for every phthalocyanine ring that can be formed), both metal and metal-free rings will be present in the polymer structure.

Compared to the metal-free system, the SnCl_2 and CuCl_2 -cured polymers are more conductive at a given postcure treatment. For example, at 400°C the resistivity of the metal-free polyphthalocyanine is greater than 10^{10} ohm-cm, while the resistivities of the SnCl_2 and CuCl_2 -cured polyphthalocyanines are 10^6 to 10^7 ohm-cms. It is believed that the increase in conductivity results from an earlier development of the extended conjugated polymer network rather than a specific electrical influence of the metal in the phthalocyanine ring. It is observed that as the content of the metal co-reactant is increased, the gelation time decreases and lower resin loss occurs during the initial cure at 300°C . The weight loss during initial cure results from sublimation of some uncured resin, which is minimized by the earlier development of high molecular weight species. Thus, it is apparent that the polymer structure has developed more rapidly in the presence of the metals and this could account for the higher conductivities at 400°C . Although the extended polymer structure develops earlier, it does not rule out the possibility that the metal may also have an important influence of the electrical conductivity.

Although higher conductivities are obtained at lower processing temperatures with the SnCl_2 and CuCl_2 systems, there are undesirable side effects which include high weight losses during postcure, too rapid cure at high metal contents, and the production of HCl in the case of CuCl_2 . In addition, problems with sample cracking during postcure are more severe.

As discussed earlier, direct reaction of the phthalonitrile resins with metal powders (Cu and Zn) results in much of the metal remaining unreacted and settling to the bottom of the sample during the cure. Thus, an effective means for introducing a metal into the phthalocyanine polymer remains to be developed.

We have referred to the heat treatment used to introduce conductivity into these polymers as a postcure because of observations made on the metal-free cured phthalocyanine polymer structure after initial cure at 300°C and postcure at 550°C . ESCA (Electron Spectroscopy Chemical Analysis) analysis of the 300°C -cured polymer did not reveal the

Table 4

Postcure Effects on Resistivity and Weight Loss for
Metal Containing Polypthalocyanines

(Initial Cure at 300°C for 50 hours)

A. SnCl_2 -Cured p-Dianil Phthalonitrile Resin

	550°C/100 hrs			400°C/100 hrs		500°C/100 hrs
Mole % SnCl_2 of Theory	1.7%	11%	50%	100%		100%
Wt % of SnCl_2	0.4%	2.6%	11%	19%		19.8%
Postcure						
% Wt Loss	9.5%	9.4%	12.8%	9.2%		18%
Resistivity, ohm-cm	7.1×10^2	8.5×10^2	4.0×10^2	5.6×10^6		1.6×10^3

B. CuCl_2 -Cured p-Dianil Phthalonitrile Resin

Mole % CuCl_2 of Theory	100%
Wt % of CuCl_2	14.9%
Postcure	400°C/100 hrs
% Wt Loss	7%
Resistivity, ohm-cm	4.6×10^7 ohm-cm

characteristic spectra of the phthalocyanine ring bonding energies for carbon and nitrogen electron. After postcuring at 550°C, ESCA showed two types of nitrogens of almost equal concentration with distinct binding energy levels of approximately 398.4 and 399.8 eV, and a single type carbon with a binding energy of approximately 284.6 eV. These values agree with measurements made on the simple (non-polymeric) metal-free phthalocyanine and are comparable to values reported by others.

It appears that after the initial cure at 300°C, the conjugated polymer network of phthalocyanine rings shown in Figure 2 is not completely formed. Although infrared spectra show that most of the CN absorption has disappeared, ESCA indicates that phthalocyanine rings have not yet formed. Thus the flow of electrons is hindered by the lack of extended conjugation and electrons must undergo a "hopping process" from molecule to molecule to move through the material. Since the hopping mechanism is a high energy process, conductivity would be low. As the phthalocyanine rings form at the higher postcure temperatures and a more extensive conjugated network develops, less hopping is necessary and conductivity increases. In addition, during the postcure some weight loss occurs which may eliminate charge-carrier traps and thus increase conductivity.

The exact structures of the postcured polymers are not known. In the case of the polyphthalocyanine, there is a 5-8% weight loss at 550°C and some decrease in the nitrogen content of the polymer. This might indicate some deviation from the ideal structure shown in Figure 2, but it is also possible that the decomposition is at unreacted end-sites which would lead to little or no change in the basic polymer structure. At 900°C, where a 27% weight loss occurs, a definite change in the polymer structure is expected.

Our present feeling is that the bulk of the conductivity results from a conjugated, condensed aromatic, organic structure and not from the formation of carbon. Even at 900°C, this temperature is too low for graphite formation and the X-ray diffraction pattern is not indicative of a graphitic structure. At this temperature, ESCA still indicates the presence of organic structure; however, the phthalocyanine ring concentration appears to be 1/4 to 1/2 that observed for the materials heated at 550°C. A carbon-hydrogen-nitrogen analysis has not been obtained on the 900°C sample, but at 550°C values are 81.35%, 2.08%, and 16.69% (100.12% total), respectively, compared to theoretical values of 74.99%, 3.15%, and 21.86%. Although these results show carbon enrichment, it is a logical consequence of further aromatization of the structure rather than formation of inorganic carbon.

SUMMARY, CONCLUSIONS, AND FUTURE WORK

This paper has described several extended conjugated polymer networks based on the polymerization of orthodinitriles into

phthalocyanines, phenyl nitriles into triazines, and phenyl acetylene into condensed aromatic rings.

Under the concept of extended conjugation and network polymerization, new organic polymers have been prepared having conductivities ranging from 10^{-12} to 10^{+2} ohm⁻¹-cms⁻¹). For comparison, copper has a conductivity of 10^{+6} ohm⁻¹-cms⁻¹. The conductivity of these new polymers is controlled by the postcure (temperature and time) treatment. Thus, conductivity can be tailored to specific values required for a given application or device. Moreover, because of their high thermal stability, these polymers should be capable of operating at temperatures in excess of 300-400°C.

Future work will address means for effectively introducing metal atoms into the phthalocyanine ring structure and assessing their influence on electrical properties. More extensive study will be made of the acetylene-terminated resins and for finding an effective catalyst for converting the phenylnitrile resin into a conjugated triazine polymer.

The effect of the aggressive environments on the polymer stability and electrical properties will be evaluated. Information will also be sought to further elucidate the structure of the high temperature, post-cured polymers.

Finally, upon completion of more detailed analysis and characterization of the electrical properties, potential applications of these materials in electrical devices will be sought.

ELECTRICAL PROPERTIES OF METAL-FREE,
DIANIL-LINKED PHTHALOCYANINE POLYMERS

Joseph P. Reardon
Surface Chemistry Branch
Chemistry Division

INTRODUCTION

Charge carriers in organic molecules are readily generated by activation of π -bonded electrons. When the π -bonded electrons in a conjugated system are delocalized, they provide an intramolecular conduction path of high mobility. Polyene, $(-\text{CH}=\text{CH}-)_n$, and polymethinimine, $(-\text{CH}=\text{N}-)_n$, chains are examples of systems of delocalized π -electrons. Such conjugated systems lend themselves nicely to a simple quantum mechanical "free electron" calculation; thus, for example, one finds that the energy, E_a , required to raise an electron from the ground state to the first excited state in a polyene chain of n units is:

$$E_a = 19 \left(\frac{2n + 1}{2n^2} \right),$$

where E_a is in electron-volts. Hence, an increasing number of polyene units in the chain should yield a progressively lower activation energy. For values of n typical of polymers (~ 500), E_a becomes equal to kT at room temperature, which means that the excited levels become thermally populated.

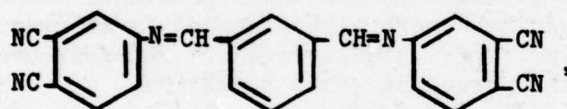
High conductivity within the polymer molecules, however, is no guarantee of high conductivity in the plastic made from that polymer. Polymer chains are ordinarily quite short compared with the macroscopic dimensions of a plastic article. Held together principally by weak van der Waals forces, the chains are widely separated on a molecular scale. To move from chain to chain, the conduction electrons rely on thermally-activated hopping, which means that their mobility is low. In general, though, mobility increases with long-range order, the very property that is lacking in the common organic polymers.

It was our desire to make an electrically conductive polymer that could be used for manufacturing useable items. The approach to doing this was spawned by our program in the synthesis of phthalocyanine polymers for high-temperature plastics (1). Polymeric phthalocyanines based on pyromellitonitrile (2,3) had been synthesized and exhibited

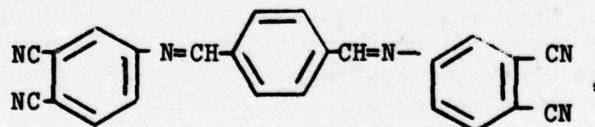
semiconducting properties with resistivities as low as a few ohm-cm. Being of a low degree of polymerization, however, they lacked mechanical strength and could be processed only by compression of the powdered polymer. As a consequence, a limit on conductivity was set by the contact resistance among the particles constituting the manufactured component. By contrast, the materials described in this paper are from a new class of phthalocyanine resins that liquify at the onset of polymerization and, so, can be cast or molded by conventional polymer processing techniques, thereby being made adaptable to many technical applications.

MATERIALS

A subclass of these new phthalocyanine resins is synthesized from fully conjugated monomers. The two specific polymers reported here were made from *N,N'*-isophthalylidene bis(3,4-dicyanoaniline),



and *N,N'*-terephthalylidene bis(3,4-dicyanoaniline),



and were described in the preceding paper ("Conjugated Network Polymers as Electrical Conductors" by T. R. Walton). Henceforth in this paper the polymers made from these monomers will be referred to as meta dianil and para dianil polyphthalocyanine, respectively, with meta and para denoting the substitution positions on the central benzene rings. Thermal curing of the monomers yields the polymer represented by Figure 1. The cure can be effected without a metal co-reactant; indeed, with a single exception the materials discussed below are the metal-free polymers. The figure suggests that a two-dimensional network is formed. The more likely case is a "statistical" three-dimensional network produced by numerous out-of-plane reactions of the phthalonitrile end groups and containing also a large number of unreacted end groups. Ideally one would like to promote the continued reaction of the active end groups until the polymer existed as a single macromolecule. In such a single-molecule plastic, any discontinuity of the conduction path would be offset by a multitude of alternate pathways.

The cured dianil polyphthalocyanines are dark colored, rigid plastics, outwardly resembling an epoxy or phenolic. Like other thermosetting resins, they are primarily useful as structural materials.

EXPERIMENTAL TECHNIQUES

Samples for study were prepared by melting the crystalline monomer in a 2.5-cm diameter aluminum planchet and curing at 300°C in air for 25 hours or longer. The solid disk was removed from the planchet and its faces polished smooth on 600-grit paper to a thickness of about 2 mm. The faces were repolished as required after postcuring.

Our main interest was in the effect of postcuring or thermal annealing on the electrical resistivity of the specimens. After the initial 300°C cure, the polyphthalocyanine is an electrical insulator, reflecting the fact that molecular discontinuities are numerous. The polymer was postcured to promote the continued growth of the conjugated system. For this the specimens were either sealed in an evacuated vial or kept in a stream of inert gas, usually argon. The postcure is described in detail in the preceding paper by Walton.

Measurement of d.c. resistivity was done in either of two ways. For specimens of high resistance (≥ 100 ohm), the standard two-electrode technique was employed using a Keithley 610C electrometer. Gold electrodes, usually 1.9 cm in diameter, were vapor-deposited on each face of the specimens. They were housed in a well shielded oven and cycled between 22°C and 155°C. A continuous trace of resistance and temperature was made on a Houston Omnigraphic 3000 strip chart recorder. The volume resistivity was computed as:

$$\rho = \left(\frac{A}{d}\right) R,$$

where ρ is in ohm-cm, d is the sample thickness in cm, A is the area in cm^2 of an electrode (assuming the electrodes are of equal size), and R is the measured resistance in ohms.

The van der Pauw four-probe technique was used for low-resistance samples (< 100 ohm) (4). Contact was made with small copper clips at the perimeter of one face of the specimen. A Keithley 164TT digital multimeter was used in the milliohmmeter mode. The sample was allowed to equilibrate at various discrete temperatures between 22°C and 172°C.

RESULTS

The effect of the postcure temperature on the room temperature d.c. volume resistivity, ρ , of the metal-free dianil polyphthalocyanines is shown in Figure 2. Both meta and para isomers are included, the differences between them being insignificant. Of the fifteen samples illustrated, nine were held at the indicated temperature for 100 hours, five for 60 hours or longer, but the 850°C sample only for about 12

hours. The dwell time at a given postcure temperature is an important variable in the 450-650°C range, as is illustrated for 500°C in Figure 3. Our experience, however, has been that below or above this range changes in resistivity are quite small beyond 8 hours at temperature.

The corresponding changes in activation energy, E_a , with postcure temperature are shown in Figure 4. The change in ρ was measured as the sample was cycled between room temperature and 172°C (155°C for the high-resistance samples) and E_a was computed from the Arrhenius relation:

$$\rho = \rho_0 e^{E_a/kT},$$

where ρ_0 is a constant, k is the Boltzmann constant, and T is absolute temperature.

Figures 5-11 are plots of resistivity and temperature data representative of those which generated the curves in Figures 2 and 4 above.

The resistance-vs-temperature curve in Figure 5 is typical of the polymer postcured at 500°C. The same data are presented in an Arrhenius plot in Figure 6; the negative deviation from linearity at the higher temperatures should be noted for future reference. (The points on these two curves are merely values taken from the original strip-chart traces for the sake of replotting the data. The same holds for Figures 7 and 8 below).

Figure 7 illustrates the rather dramatic drop in resistivity that accompanies an increase in the postcure temperature of just 50°C. The hysteresis in the curve that appears during the first cycle is attributable mainly to loss of absorbed moisture from the sample. The Arrhenius plot in Figure 8 includes data from resin co-reacted with a small amount of SnCl_2 . The two sets of data yield the same E_a (within experimental error); the displacement of the SnCl_2 curve to slightly higher resistivity values is most probably due to a shorter time of postcure, viz., 30 hr for the SnCl_2 co-reacted polymer but 100 hr for the metal-free polymer. Hence, the SnCl_2 co-reactant, at least at this low level, seems to have no effect on the resistivity of the dianil polyphthalocyanine.

Figure 9 portrays another hundred-fold drop in resistivity following a further 50°C increase in postcure temperature to 600°C. (The points on the curve now represent individual measurements of ρ at equilibrium temperatures.) When we have reached a 900°C postcure (Figure 10), we are in the milliohm-cm range and measure only a 12% decrease in ρ upon heating the specimen to 168°C, which corresponds to $E_a = 0.010$ eV. If, however, the range of measurement is extended down to cryogenic temperatures with liquid helium cooling, as in Figure 11,

we see that the linearity of the Arrhenius plot is lost below -20°C . Indications of this negative deviation were just becoming manifest near room temperature in the earlier Arrhenius plots (Figures 6 and 8 above).

DISCUSSION

Reliability of the Resistivity Measurements

Figure 12 shows the increase in density that results from raising the postcure temperature. Over the same temperature range there is a corresponding linear shrinkage of about 15%. These rather drastic physical changes tended to cause very fine hairline cracks in the specimens, especially above 600°C . Because resistivities of samples postcured at 600°C or above were measured by the van der Pauw four-probe technique, a question arises as to the validity of the measurement, inasmuch as the technique rests on the assumption that the specimen contains no voids or cracks. One would expect to obtain apparent resistivity values higher than the true values if the sample contained voids or cracks. In an attempt to estimate whether our measured values were too high, we also made some resistivity measurements on selected samples using a collinear four-probe arrangement (5,6) in conjunction with a Keithley model 530 "Type All" system. The 1-mm spacing between the probes allowed the measurements to be made on small areas of sample surface that appeared to be free of any cracks. To our surprise, the values obtained in this fashion for samples postcured at 400° , 500° , 550° , and 700°C were higher than the van der Pauw values by roughly a factor of ten. This discrepancy was considerably larger than the variation that resulted from repositioning the collinear probes on the surface of the sample. Moreover, the collinear four-probe technique exhibited hysteresis upon reversal of the polarity, the deviation being as great as $\pm 21\%$ from the mean. No such hysteresis was ever observed with the van der Pauw technique.

A possible explanation for these apparent anomalies in the collinear four-probe measurement is that the sample surface is rough with respect to the very fine probe tips. (The 600-grit paper used to polish the specimens contains $17\text{-}\mu\text{m}$ diameter particles.) Thus, given the hardness of these polyphthalocyanines and the spring loading on each individual probe, it is conceivable that the probe tips are resting on asperities or even on particles of abrasive, thereby producing both the anomalously high resistances and rectification (hysteresis upon polarity reversal). As a test of this hypothesis, the measurements will be repeated after the samples have been given a much higher polish.

Until satisfactory resistivity measurements can be made on small, crack-free areas, the effect of cracks in the samples cannot be estimated. In general, though, one would anticipate slightly lower resistivity values for the high-temperature (i.e., $\geq 600^{\circ}\text{C}$) samples. The worst case would be met if cracks and perhaps internal voids would mask metallic conductivity. A situation of that sort occurred in the

investigation of polythiazyl, (SN)_x (7). Compressed pellets of polycrystalline (SN)_x exhibited a room-temperature resistivity of about 0.05 ohm-cm with a semiconductor-like temperature dependence that yielded an activation energy of about 0.02 eV. Single crystals of the same polymer, however, measured along their most highly conductive axis, gave a resistivity one-hundredth as large and showed a metallic temperature dependence ($E_a = 0$). The investigators concluded that in the polycrystalline material the metallic conduction within the crystallites was more than offset by the thermally activated transport (hopping) of electrons across the grain boundaries. By analogy, then, microscopic cracks in the polyphthalocyanine might be acting like grain boundaries and masking the intrinsic conduction mechanism.

With respect to the van der Pauw-type measurement, a colleague using silver-paste contacts and different electronics has obtained a resistivity for a 550°C p-dianil specimen in good agreement with the measurement reported here. Linearity in the I-V curve from 1 μ A to 400 μ A with no hysteresis upon reversal of polarity confirmed that the silver-paste contacts were indeed ohmic.

Activation Energy

The activation energy is the parameter known to solid-state physicists as the band gap. In computing E_a for the dianil polyphthalocyanines, the expression $\rho = \rho_0 \exp(E_a/kT)$ was used. This form does not necessarily suggest any particular conduction model and is generally suitable for amorphous semiconductors (8). For an intrinsic semiconductor, in which there is a hole carrier for every conduction electron, the relationship takes the form $\rho = \rho_0 \exp(\epsilon/2 kT)$, wherein the factor of 1/2 acknowledges that the current carriers are equally divided between electrons and holes. Some authors choose to characterize organic semiconductors by this latter expression (2,9). Our opinion, however, is that the a priori assumption of intrinsic conductivity, at least for the polyphthalocyanines, is not justified, in particular because they are principally amorphous and also because the level of impurities in nearly all organic materials is much higher than in electronic-grade silicon or germanium.

A general scheme for classifying materials by the activation energy of conduction is the following (10):

<u>Material</u>	<u>ϵ, eV</u>
Insulators	≥ 3
Most of the useful semiconductors	≈ 1
Thermoelectric and infrared detectors	≈ 0.1
Semimetals	≈ 0

Keeping in mind that ϵ translates as $2 E_a$, it is interesting to note that the activation energies shown in Figure 4, above, cover the entire range from useful semiconductors to semimetals. Thus, if one had an application that demanded a particular E_a , these dianil polyphthalocyanines could be matched to the need simply by the appropriate postcure.

Carrier Typing

The Keithley 530 "Type All" system with collinear four-probe head described earlier was used to help identify the majority charge carrier. The instrument utilizes two separate methods for this: the rectification method (preferred for high resistance materials) and the thermoelectric method (Seebeck voltage; for low resistances). The rectification method failed to give any meaningful response on the 400, 500, 550, and 700°C samples examined. The thermoelectric method, however, indicated p-type (hole) conductivity for all four samples. Because of the anomalies encountered in our resistivity measurements with the collinear four-probe arrangement, it seems premature to speculate at this point on the mechanism of the electrical conduction in the polyphthalocyanines.

Pyropolymer Formation

The high temperatures at which the dianil polyphthalocyanines are postcured are within the range of pyropolymer formation. A pyropolymer is just an organic polymer that has been converted by pyrolysis to an electrically conductive species. The term includes natural pyropolymers such as cokes, carbon blacks, and chars, and synthetic pyropolymers such as pyrolyzed polydivinylbenzene, polyvinylidene chloride, and aromatic polyimides. Carbon fibers, which are made from viscose rayon, polyacrylonitrile, or mesophase petroleum pitch, and which are finding widespread use as reinforcement for high-strength plastics, are examples of synthetic pyropolymers. The curves of $\log R$ - and E_a -vs-pyrolysis temperature for many of these polymers closely resemble the same curves for the dianil polyphthalocyanines (Figures 2 and 4) (11). It may well be, then, that postcuring of the phthalocyanines is converting them into pyropolymers in addition to stimulating continued growth of the polymer network. Pyropolymer formation involves the cleavage of less stable bonds—as evidenced by the evolution of gases like CO_2 and NH_3 —and the formation of semi-isolated regions of condensed polynuclear systems that eventually, as the temperature is increased, merge into a continuous network of fused aromatic rings in which an increasingly effective π -orbital overlap develops. Indeed the weight losses that occurred as the dianil polyphthalocyanines were postcured above 500°C were by themselves strong indicators that something considerably more drastic was happening than simply the progressive growth of the macromolecular network envisaged in the model described earlier in this paper.

Not all organic polymers form good pyropolymers and, of those that do, some develop electrical conduction at appreciably lower temperatures than others. Thus, for example, pre-oxidized polydivinylbenzene pyrolyzed at 700°C has a room-temperature conductivity of $\sim 10^{-7} (\text{ohm-cm})^{-1}$, whereas an aromatic polyimide pyrolyzed at the same temperature yields $\sim 0.1 (\text{ohm-cm})^{-1}$ (11). Similarly carbon fibers made from polynuclear aromatic petroleum pitch are more highly conductive than polyacrylonitrile-based carbon fibers produced at the same temperature. The dianil polyphthalocyanines appear to fall into the class of good pyropolymer formers. Considering the good structural integrity that survives the postcure (or pyrolysis), they might be considered three-dimensional analogs of the quasi-one-dimensional carbon fibers.

It is not uncommonly thought that pyropolymer formation is nothing more than progressive carbonization leading to graphitization. If that were indeed the case, heteroatoms like nitrogen and oxygen would be expected to hinder pyropolymer formation. It has been shown, however, that in an aromatic polyimide pyrolyzate considerable quantities of nitrogen and oxygen are retained even at 800°C (11). Similar findings are common in the technology of the polyacrylonitrile-based carbon fibers. Thus, graphitization is not an essential requirement for electrical conduction in pyropolymers and there would be no basis for dismissing the dianil polyphthalocyanines as pyropolymer formers because of their relatively high nitrogen content. Moreover, our postcure temperatures are lower by a few hundred degrees than the temperatures required for graphitization. Nevertheless, there may be signs of incipient graphitization in the X-ray diffraction scan of the polyphthalocyanines. The scans shown in Figure 13 were made using a General Electric XRD-6 diffractometer with Ni-filtered Cu:K α radiation. The broad peaks of the 300°C-cured specimen are typical of a semicrystalline polymer. The way the peaks grow progressively sharper with higher postcure temperatures is indicative of increasing structural order. The large peak at $2\theta = 25^\circ$ corresponds to a d-spacing of 3.56 Å (0.356 nm) which is approaching the 3.35 Å ($2\theta = 26.6^\circ$) spacing between the basal planes of graphite. Even this 25° peak, however, is much broader and much less intense than X-ray diffraction peaks from a high-grade graphite. In addition, the density of even the 900°C samples ($\sim 1.7 \text{ g/cm}^3$) is far from that of graphite (2.25 g/cm 3). Thus, the graphitic character of the postcured polyphthalocyanines is much too weak to account for their considerable electrical conductivity.

CONCLUSIONS

The metal-free dianil polyphthalocyanines, both the meta and para forms, show promise as a new class of organic semiconductors. They are network (i.e., three-dimensional) polymers, suitable for molding into structural components, and their conductivity is tunable by postcuring or annealing at the appropriate temperature over the range from insulators to semi-metals. Being insoluble and opaque, they have thus far defied all attempts at chemical analysis. The pattern of change in

various properties, including resistivity, weight loss, and density, as the materials are postcured at high temperatures is strongly suggestive of pyropolymer formation.

In continuing this work, our plans include examining polyphthalocyanines co-reacted with various metals. Besides the direct effect on conductivity that co-reacted metals might have, there is the beneficial influence on pyropolymer formation that metals might exert (12).

The extensive charge delocalization within the π -electron system of highly conjugated systems like these dianil polyphthalocyanines gives rise to the ability to form quite stable charge-transfer complexes with suitable electron donors and acceptors. Thus, the effect of various dopants will be part of our study. A variation on the doping technique is ion implantation, preliminary results from which already show great promise.

Modification of the "bridge" connecting phthalocyanine nuclei — the "bridge" being the -R- of Figure 1 — is another part of the study contemplated for the near future. Numerous options exist in addition to the dianil structure discussed in this paper, thereby offering some latitude in adjusting for desired mechanical properties as well as electrical properties. Also along the lines of modifying the basic monomer itself, we intend to investigate the possibility of solid-state polymerization of crystalline monomers. On this matter we take our cue from investigators like Tobin Marks (13) who have produced solids with highly anisotropic metallic properties by partial oxidation of non-polymeric phthalocyanines with iodine. Our purpose will be to impart mechanical strength and integrity to these highly conducting phthalocyanines.

ACKNOWLEDGEMENTS

I wish to acknowledge the major contribution of my co-worker Theodore R. Walton, to whom credit goes for the synthesis and post-curing of all the samples; and to J. R. Griffith and J. G. O'Rear, who first conceived and synthesized this class of polyphthalocyanines. Carmine A. Carosella of NRL's Radiation Technology Division assisted with the collinear four-probe measurements, made the independent van der Pauw measurement, and has done the preliminary ion implantation.

REFERENCES

1. T. R. Walton and J. R. Griffith, in Applied Polymer Symposium No. 26 (N. A. J. Platzter, editor), John Wiley and Sons, New York, 1975, p. 429.
2. A. Epstein and B. Wildi, in Symposium on Electrical Conductivity in Organic Solids (H. Kallmann and M. Silver, editors), Interscience, New York, 1961, p. 337.

3. C. J. Norrell, H. A. Pohl, M. Thomas, and K. D. Berlin, J. Polym. Sci. Polym. Physics Ed. 12, 913 (1974).
4. L. J. van der Pauw, Philips Res. Repts. 13, 1 (1958); Philips Tech. Rev. 20, 220 (1959).
5. L. B. Valdes, Proc. IRE 42, 420 (1954).
6. W. R. Runyan, Semiconductor Measurements and Instrumentation, McGraw-Hill, New York, 1975, pp. 69-72.
7. M. Akhtar, C. K. Chiang, M. J. Cohen, J. Kleppinger, and A. J. Heeger, U.S. NTIS, AD Rep. 1977, AD-A041976.
8. S. Kanda and H. A. Pohl, in Organic Semiconducting Polymers (J. E. Katon, editor), Marcel Dekker, New York, 1968, p. 90; C. Kittel, Introduction to Solid State Physics, 4th ed., John Wiley and Sons, New York, 1971, p. 394; E. P. Goodings, Endeavour 34, 123 (1975).
9. J. P. Suchet, Chemical Physics of Semiconductors, Van Nostrand, London, 1965, p. 161.
10. D. E. Hill, in Organic Semiconducting Polymers (J. E. Katon, editor), Marcel Dekker, New York, 1968, p. 28.
11. S. D. Bruck, Ind. Eng. Chem. 59, 18 (1967).
12. H. A. Pohl and S. L. Rosen, in Proc. Fifth Carbon Conf., Vol. 2, Pergamon Press, London, 1963, p. 113.
13. T. J. Marks, J. Coat. Technol. 1976, 48 (620), 53.

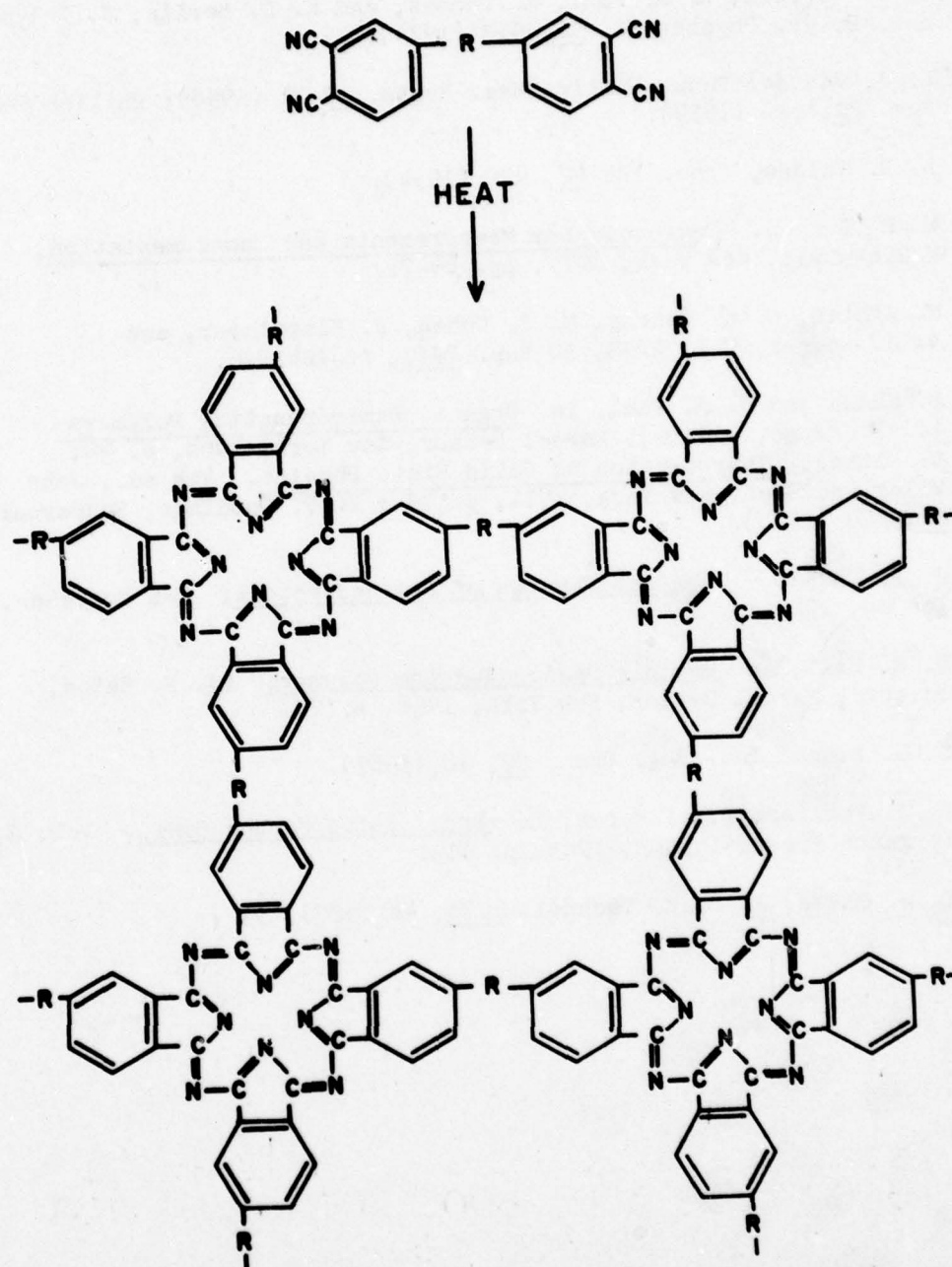


Figure 1 - The polymerization of phthalonitrile into polyphthalocyanine. In the present case, R represents either $-\text{N}=\text{CH}-\text{C}_6\text{H}_4-\text{CH}=\text{N}-$ (para) or $-\text{N}=\text{CH}-\text{C}_6\text{H}_3-\text{CH}=\text{N}-$ (meta).

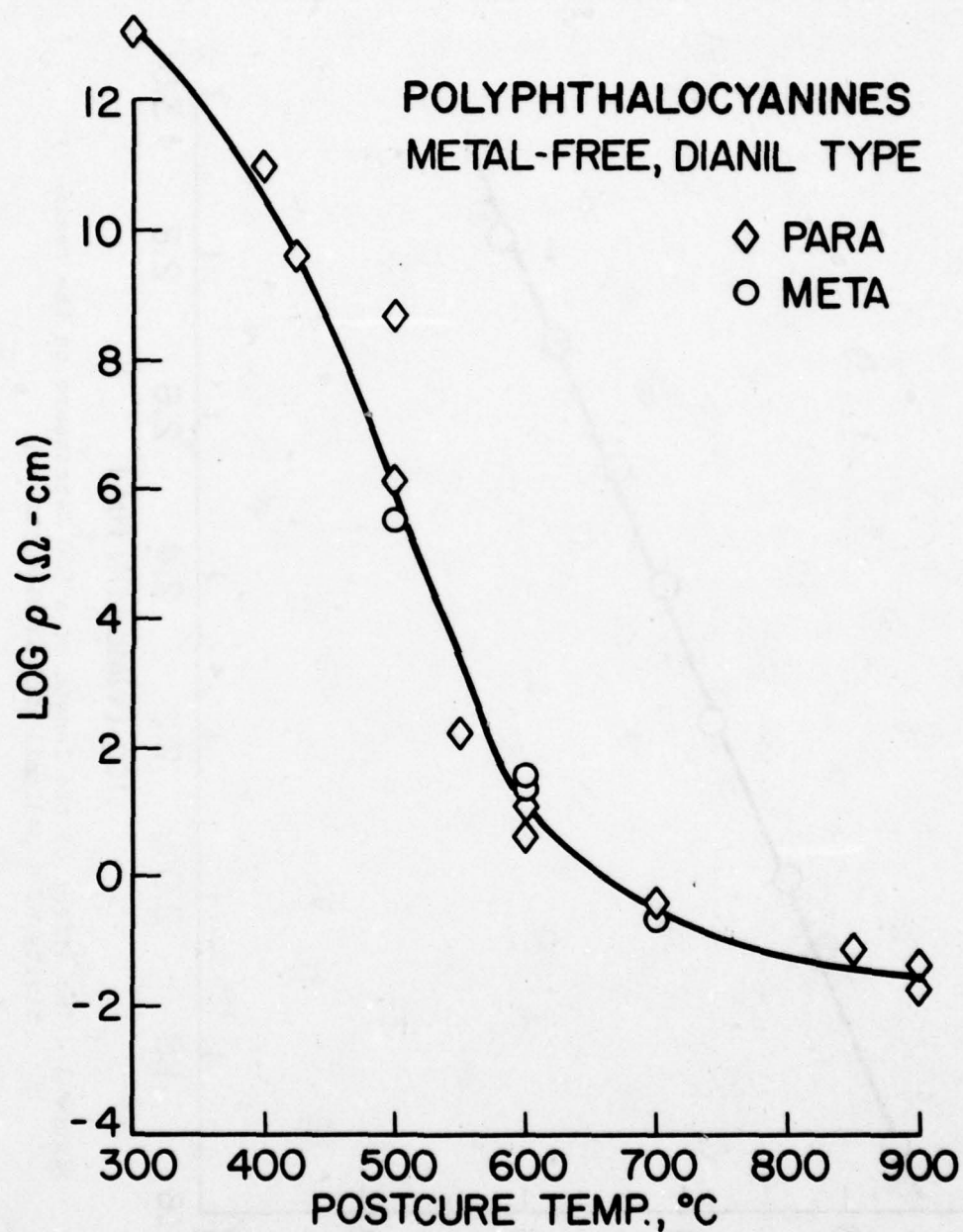


Figure 2 - The effect of postcure temperature on the electrical resistivity (measured at 23°C) of the dianil polyphthalocyanines.

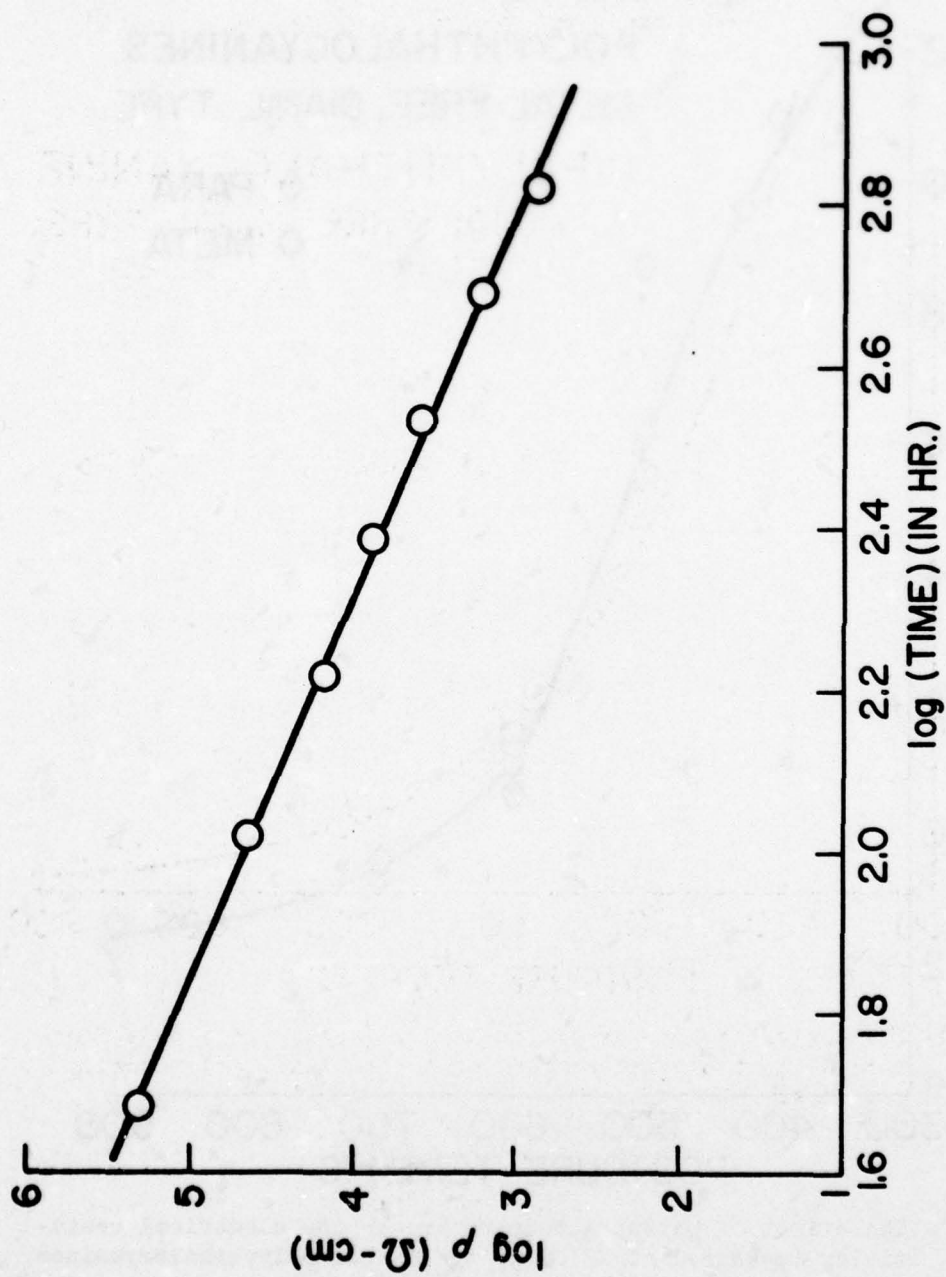


Figure 3 - The effect of the length of a 500°C-postcure on the resistivity of a p-dianil polyphthalocyanine.

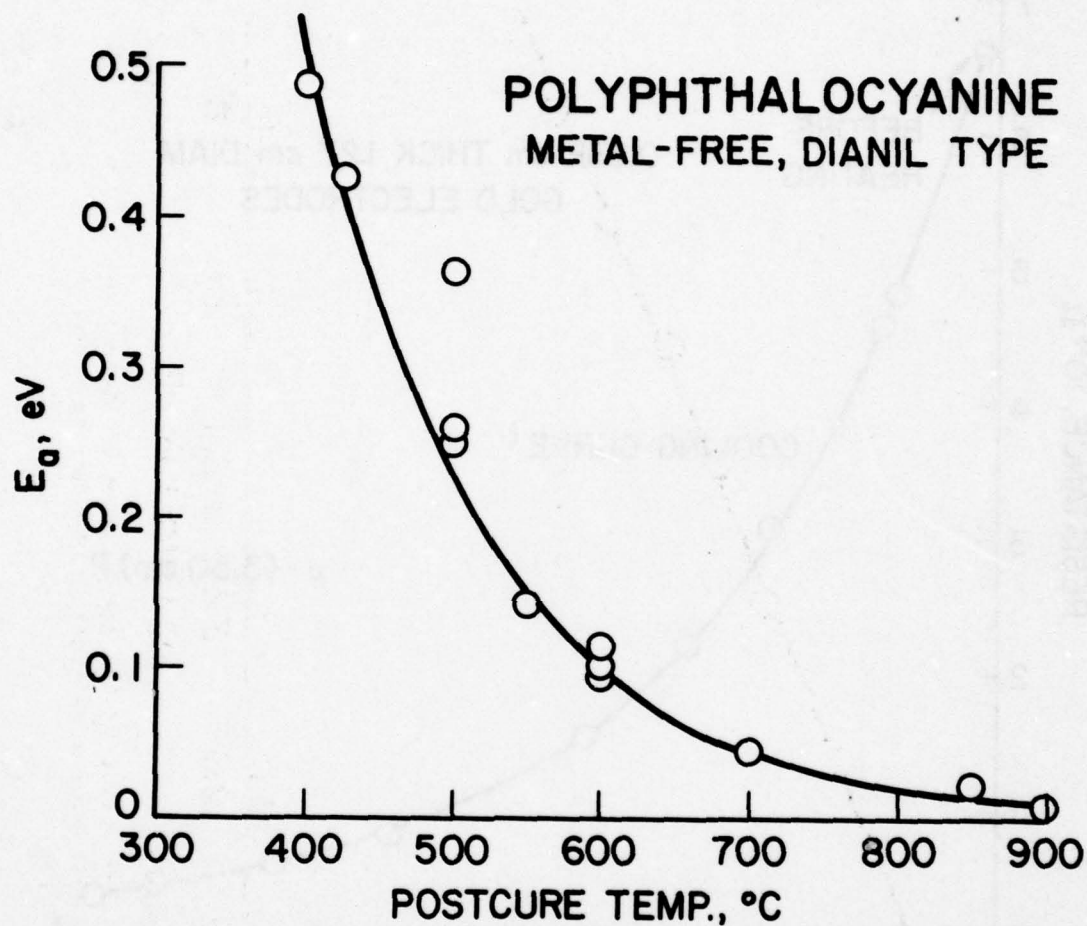


Figure 4 - The activation energy of conduction (energy gap) as a function of postcure temperature of the p-dianil polyphthalocyanines.

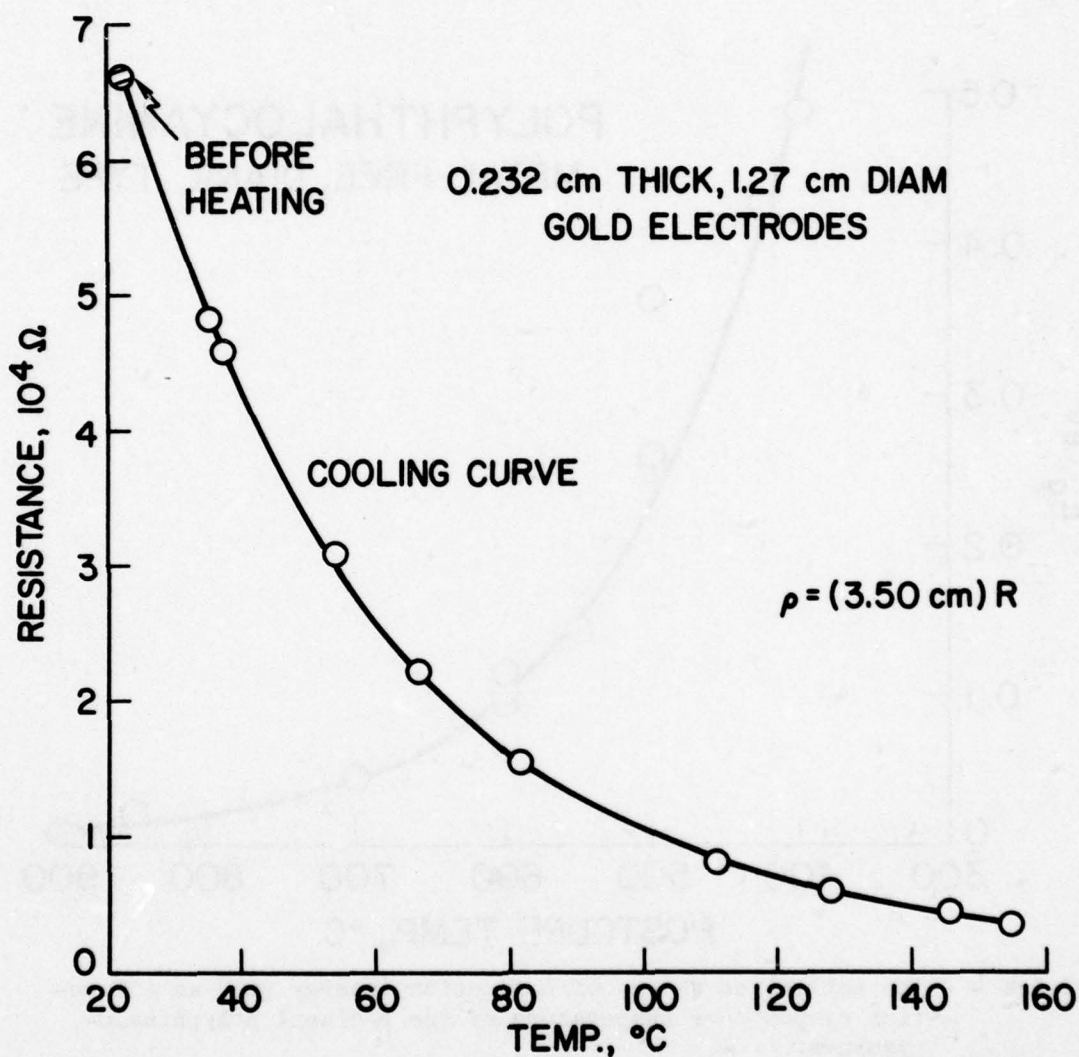


Figure 5 - A typical resistance-vs-temperature curve for a m-dianil polyphthalocyanine postcured at 500°C . Temperature as shown on the abscissa is the temperature of measurement.

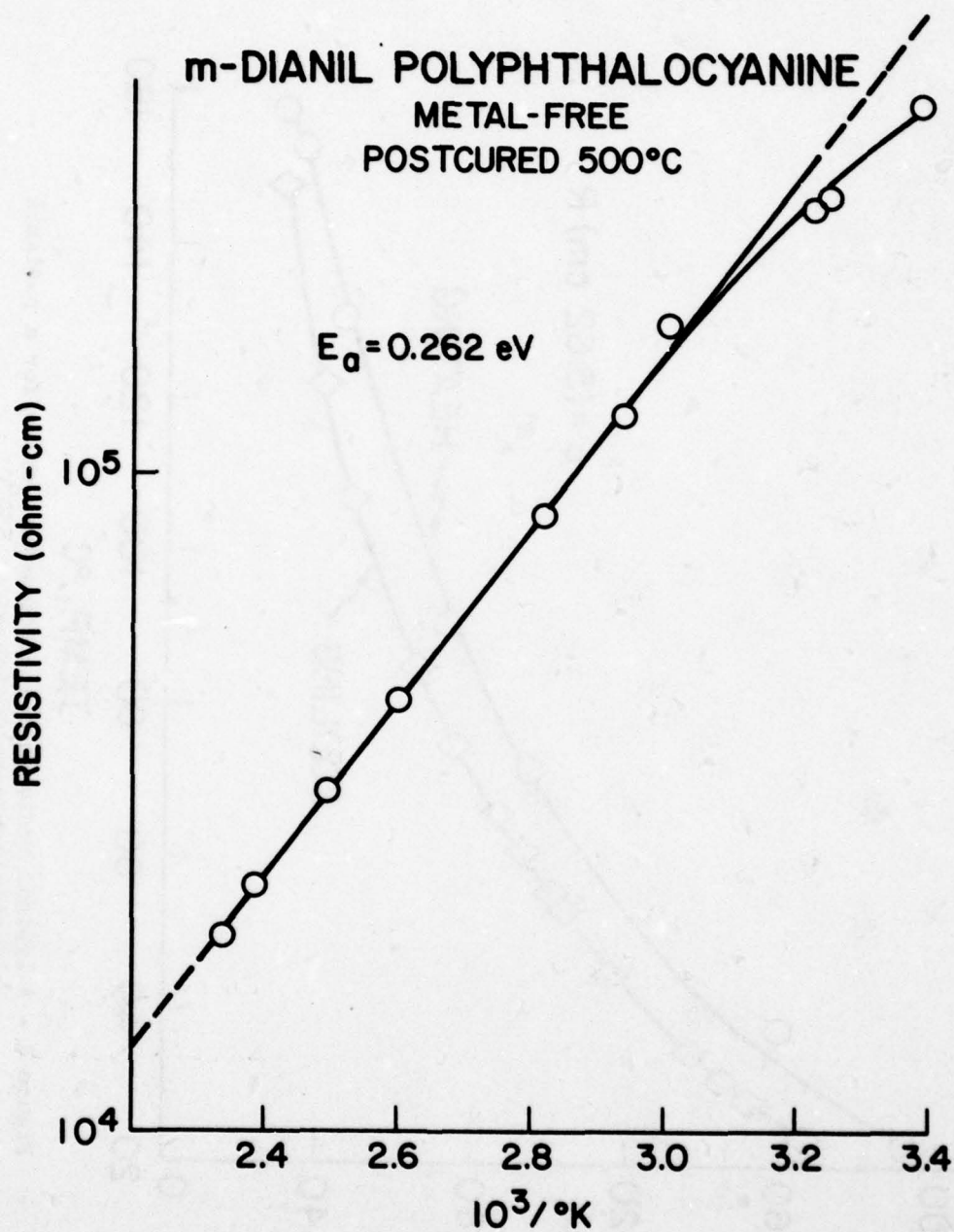


Figure 6 - Arrhenius plot of the data of the preceding figure. The linearity is characteristic of a semiconductor.

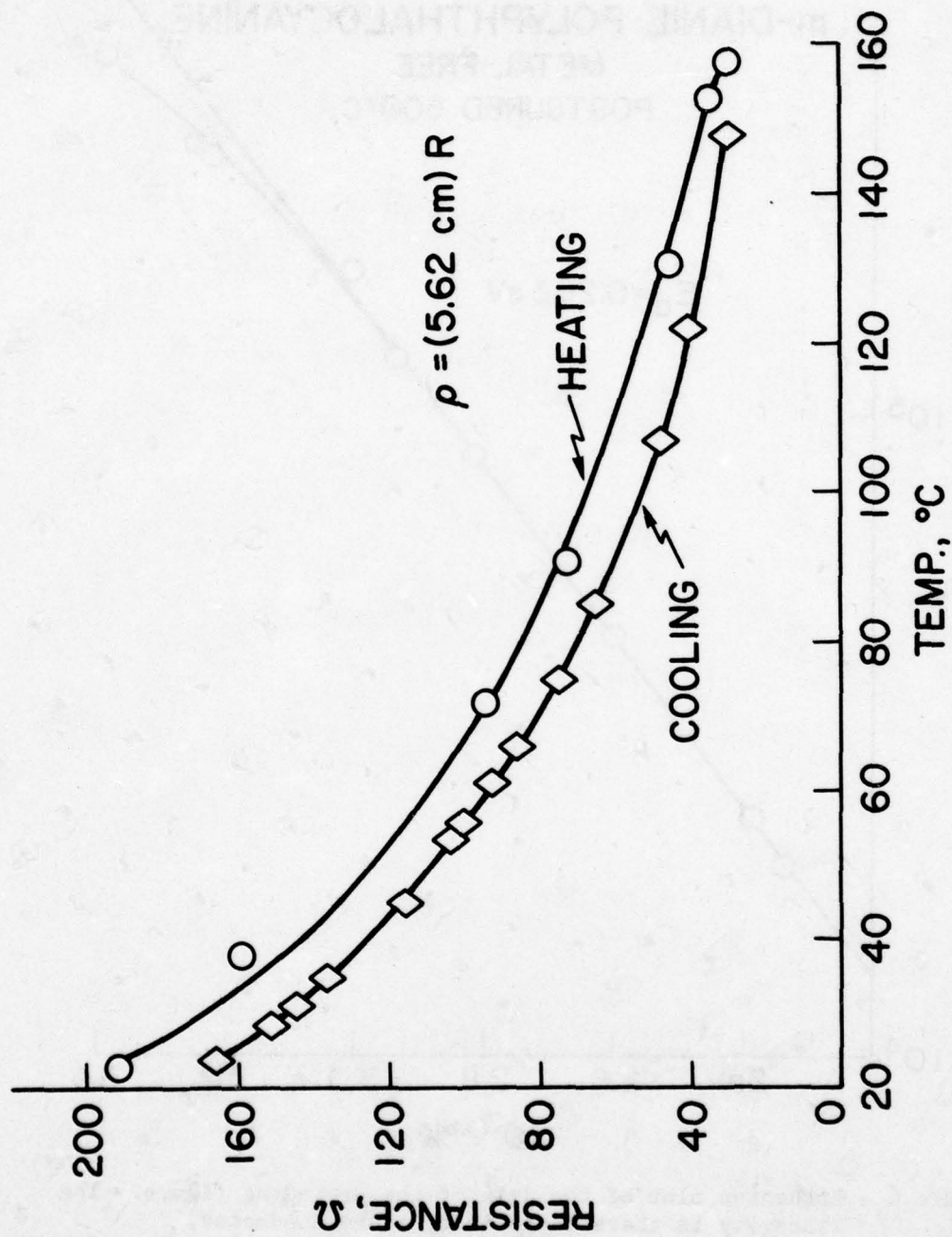


Figure 7 - A typical resistance-vs-temperature curve for a p-dianil polyphthalocyanine postcured at 550 $^{\circ}\text{C}$.

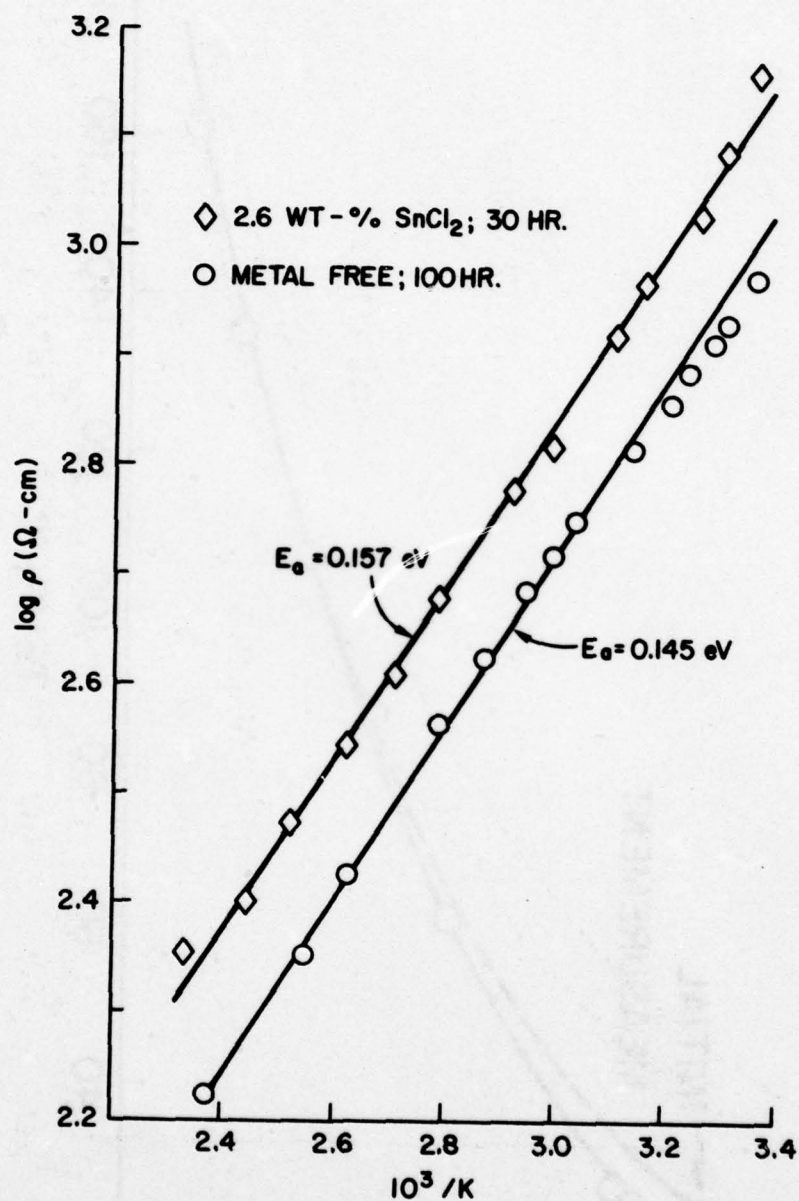


Figure 8 - Arrhenius plot of the resistivity data from samples postcured at 550°C.

**POLYPHTHALOCYANINE
METAL -FREE, p-DIANIL TYPE**

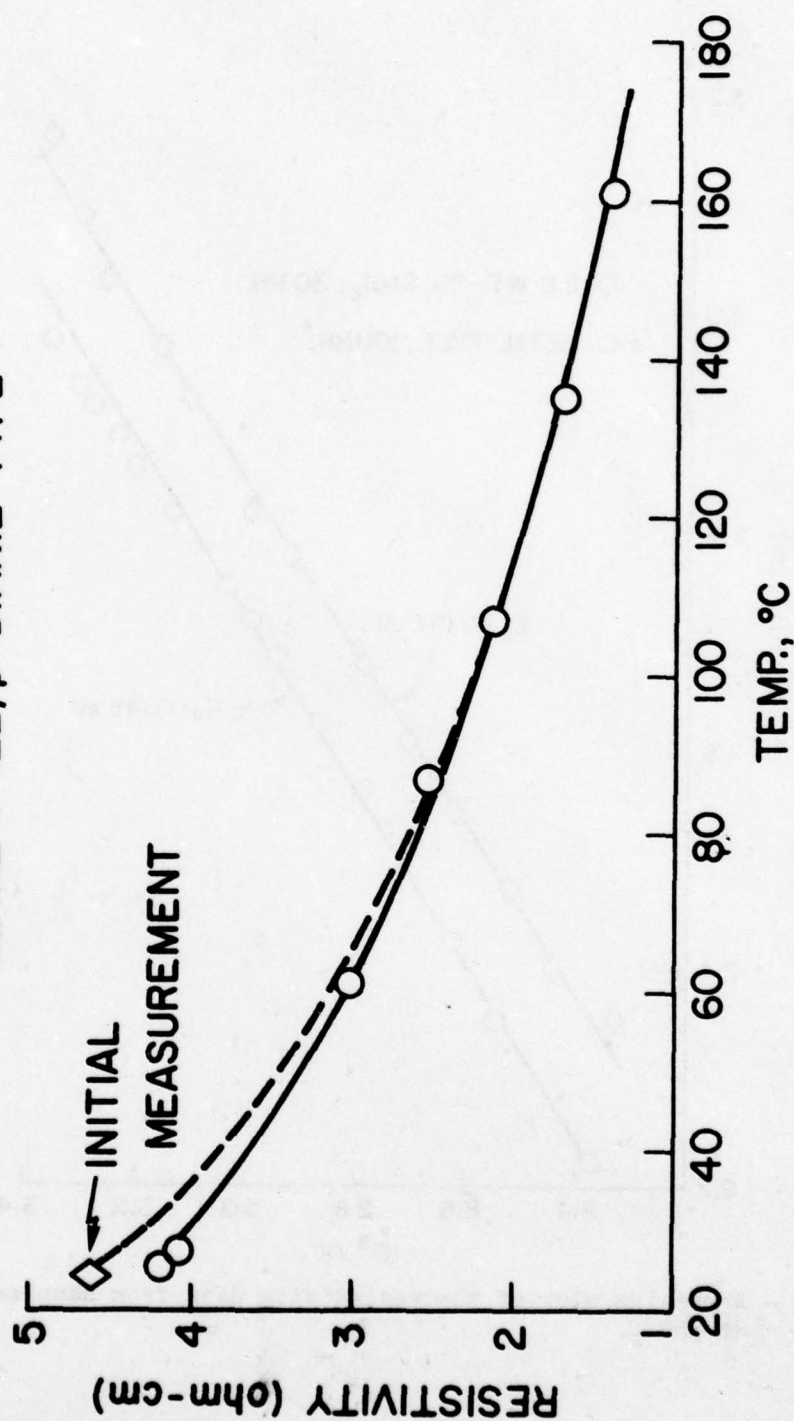


Figure 9 - Resistivity-vs-temperature of measurement of a p-dianil polypthalocyanine postcured at 600°C.

**POLYPHTHALOCYANINE
METAL-FREE, p-DIANIL TYPE**

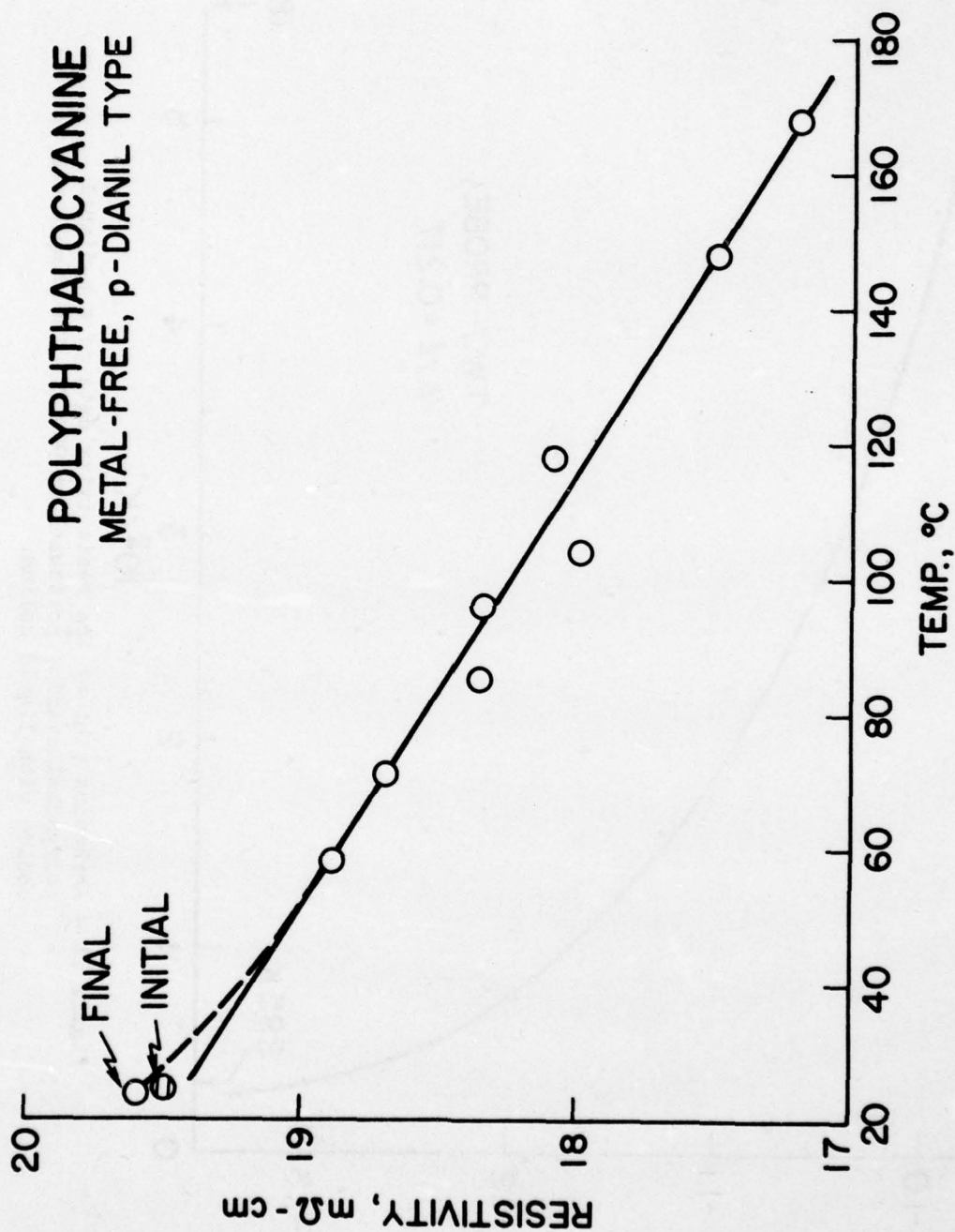


Figure 10 - Resistivity-vs-temperature of measurement of a p-dianil polypthalocyanine postcured at 900°C.

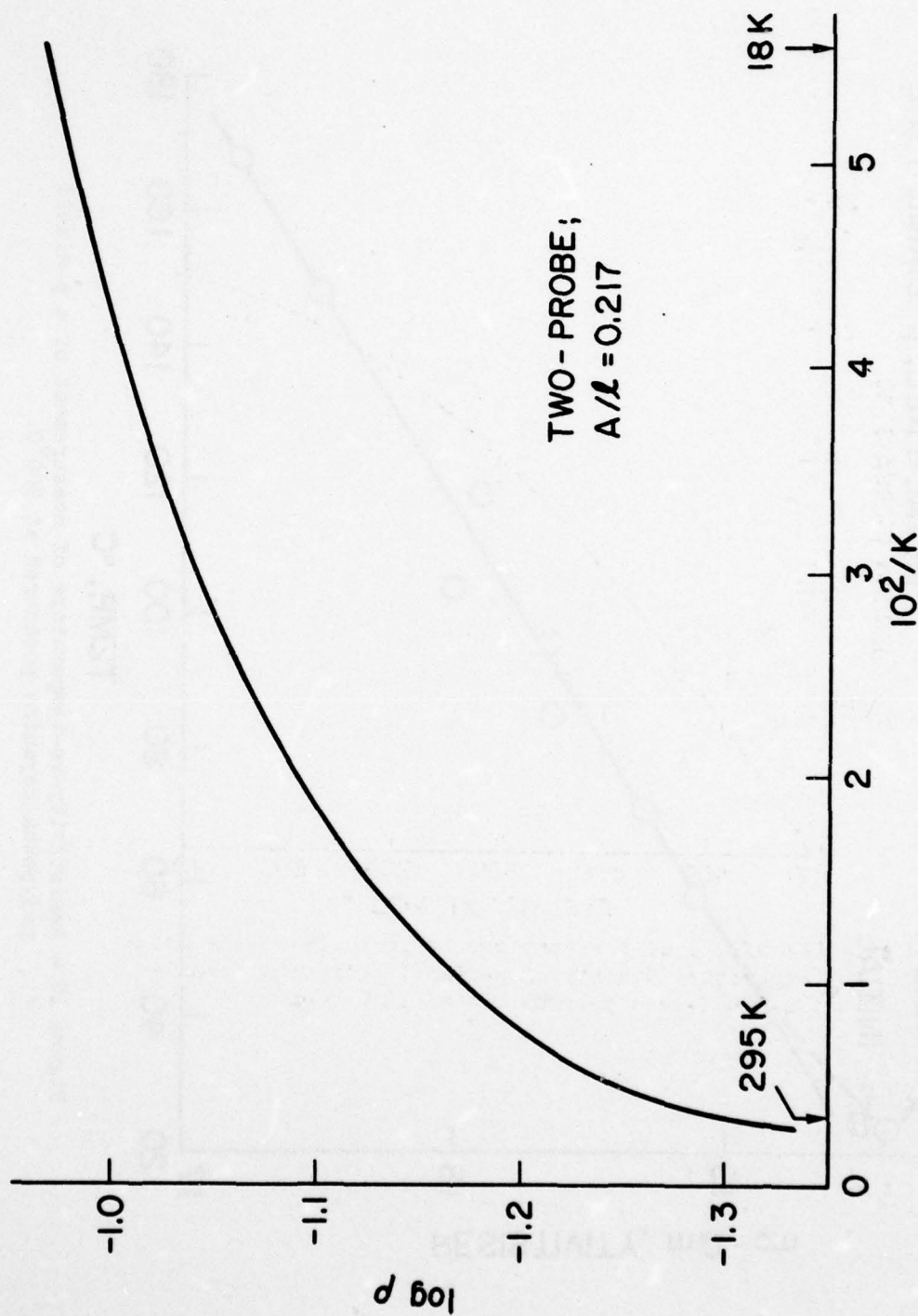


Figure 11 - Arrhenius plot of the resistivity data of a p-dianil polypthalocyanine postcured at 900°C. The sample was cooled with liquid helium.

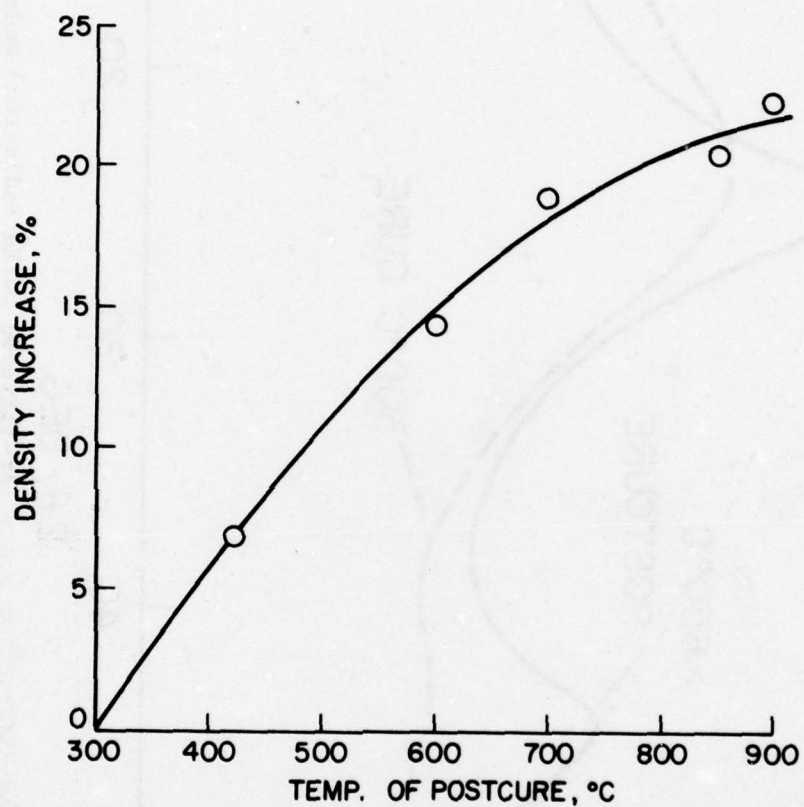


Figure 12 - The effect of the postcure temperature on the room-temperature density of p-dianil polyphthalocyanine. For the 300°C-cure polymer, $D_0 = 1.310 \text{ g/cm}^3$.

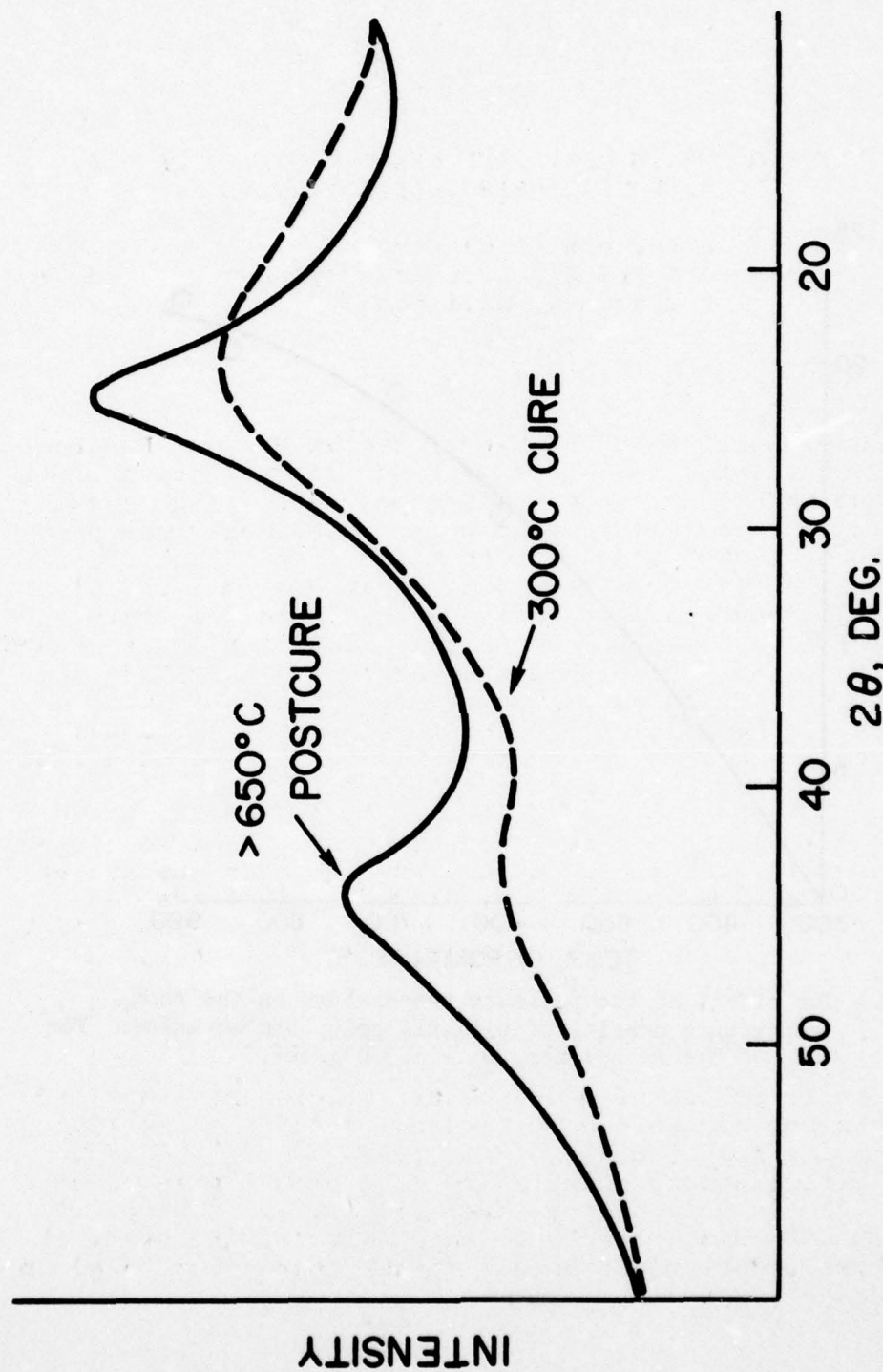


Figure 13 - X-ray diffraction scans (Ni-filtered Cu:K α radiation) made on solid disks of p-dianil polyphthalocyanines.

PROBLEMS AND PROSPECTS OF FUTURE ELECTROACTIVE POLYMERS
AND "MOLECULAR" ELECTRONIC DEVICES

Forrest L. Carter
Inorganic and Electrochemistry Branch
Chemistry Division

INTRODUCTION

A major portion of the Electroactive Polymer Program is directed toward the development of lightweight, thermally stable, metallically conducting polymers. Such novel materials, successfully developed and presumably composed primarily of light elements such as B, C, N, F, Si, P, S, and Cl, would (1) offer significant savings in cost and weight, (2) constitute an inexhaustible material source, and (3) provide new DoD opportunities in material usage and fabrication. Moreover, this program may well provide an entrance into a related subject whose possible future impact on the computer and electronics industry would far exceed what we currently conceive as the scope of the Electroactive Polymer Program.

In particular, the new subject concerns the development of future electronic devices whose dimensions are at the "molecular" level, that is, diodes, capacitors, and gates (or switches) whose dimensions are in the range of 10 Å to 500 Å. As will be indicated below, systems composed of arrays of such devices would correspond to computing speed and memory capacity increases several magnitudes beyond anything currently contemplated.

In anticipation of mid-1980 tri-service military needs, the DoD has allocated funding of \$150 million for a six-year period to develop VHSI (very high speed integrated) circuits corresponding to an eventual size reduction of 1/10 in chip pattern features (1,2). However, even with this size reduction, such switches are still at least three orders of magnitude larger than those based on a "molecular" approach.

In developing the theme of "molecular" electronic devices, the following points will be taken up in turn:

- We will review the problem areas in the current NRL effort to produce new polymeric conductors and offer some ideas for their resolution.

- Then we will discuss the importance of making good electrical contacts between such materials and the more conventional metallic conductors. At the "molecular" level of electronic devices, it is readily appreciated that the communication problem between the device and the external environment is of extreme importance.

- In the third section, we consider a host of problems in both the application of current quantum mechanical theory and in the development of a quantum mechanics for "molecular electronic devices."

- Next we discuss in outline form a variety of possible switching mechanisms operating at the molecular level, indicating in greater detail two phenomena of special interest, the sudden polarization effect and a very promising switching mechanism involving periodic tunnelling.

- This leads us to two highly speculative forecasts of how computers might be synthesized and operated in the far future (20-40 years).

- Finally, we note that a computer based on individual quantum effects might be expected to have a lower-than-hoped-for reliability per gate and might require a dramatic change in approach for the electronics engineer.

CURRENT MATERIAL PROBLEM AREAS

It is apparent from the current literature that, experimentally, considerable advances have been made in modifying the conductivity of such interesting polymeric compounds as polythiazyl, $(\text{SN})_x$, and polyacetylene, $(\text{CH})_x$. However, the current situation with respect to the preparation of metallically conducting polymers can be quickly grasped by noting the band structure type with which the parent material can be identified. For example, if a normal valence bond structure can be readily written, the material is probably a semiconductor (or insulator) with the Fermi level located at an energy gap ΔE_g , as in Fig. 1a. This includes such materials as crystalline benzene, naphthalene, polyacetylene $((\text{CH})_x)$, polydiacetylene $((\text{C}_4\text{H}_2)_x)$, and

the polyphthalocyanines. Thus, while the resistance of polyacetylene can be decreased many orders of magnitude by electron extraction from the valence band with Br_2 , this technique may not produce the highest metallic conductivity. The reason is that, in order to extract enough electrons from the band to obtain a high density of holes at the Fermi level, the electronegativity of the extracting reagent must be so large that other processes, like bond rearrangement, will occur first (as in the addition of F_2 to a double bond).

If the situation is similar to Fig. 1b, with the Fermi level falling at a zero band-gap region ($\Delta E_g=0$), electron extraction to a high density of states can be achieved with a less electronegative reagent. This is the situation with both graphite and with $(\text{SN})_x$, where the addition of Br_2 vapor enhances the conductivity significantly, but less dramatically, than in applications to materials appropriate to Fig. 1a. We note that the majority of isovalent analogs of $(\text{SN})_x$ will be similar to Fig. 1b, i.e., with a zero band gap.

For a good metallically conducting polymer, one would prefer the situation indicated in Fig. 1c where the filled valence band and the mostly empty conduction band overlap at the Fermi surface. This provides a large density of states in both the hole and electron conduction modes.

The primary question then is: "How does one achieve the overlapping of valence and conduction bands with the light elements of the first two rows?" In metals and inter-metallic compounds we note two relationships: (i) The metal atoms have more available atomic orbitals than valence electrons*; and (ii) The atoms have more bonded neighbors than valence electrons.

The first relationship suggests the incorporation of the electron-deficient element boron into the polymeric structure, and possibly phosphorus and sulfur as well, since these latter elements have some d-character available when they are in a positive charged state. Realiza-

* By valence electrons, we mean electrons involved in bond formation, rather than all electrons outside a noble gas core.

tion of the second relationship in polymers may not be readily possible since the elements H through Cl show a strong preference for having equal or fewer neighbors than they have valence electrons.

One aspect of the current NRL work in the conducting polymer area is directed toward preparing composite polymers containing B, S, and P, using, among other methods, atom-insertion reactions. The latter may lead to the second condition above, where some atoms will have more neighbors than valence electrons.

Since we have now outlined approximately the class of materials and properties desired, the second question becomes: "Can more specific indications be offered to the experimental chemists as to what exact compounds should be prepared?" At the moment, the answer is "No." However, before leaving the preparative chemist entirely to his own intuition, it is possible to eliminate certain classes of chemical bond sequences.

We will illustrate this possibility by comparing various S-N polymers with known S-P polymers using polyhedral atomic volume (PAV) results to make an estimate of charge transfer. The electron distribution among the energy levels in $(\text{SN})_x$ may be represented as in Fig. 2. In Fig. 2a we show two paired, unshared electrons each in a localized level on N and S, and two shared electrons each forming two σ bonds. In Fig. 2b, one electron is added to each atom to form the π bond. The remaining electron per S-N pair, which would normally reside on sulfur to give neutral S and N, however, is equally shared by N and S in an antibonding π bond in a highly delocalized molecular orbital (Fig. 2c). The distribution of approximately 1/2 a shared electron on N and S is supported by both ESCA and molecular orbital results, and indicates a very sensitive charge balance between the two atoms. Naively, but clearly, a more asymmetrical charge distribution is likely to lead to electron localization and strongly diminished conductivity. Chemically, electron localization might be expected to result in sulfurs with an unpaired electron which would react to form additional S-S bonds and hence a completely different insulating compound.

In looking for isovalent analogs to $(\text{SN})_x$, one naturally considers P as a substitute for N, especially since, as indicated earlier, the use of P might lead to overlapping valence and conduction bands if phosphorus d-character is involved. By comparing atomic volumes of related S-N compounds with S-P compounds, it appears that charge

To examine this latter question we drew on crystallographic data recently summarized (3) for metal atoms in the porphyrin structure, which is a highly conjugated ring system similar to that of the phthalocyanine ring (Fig. 5). The metal atom in both structures has four N neighbors in a planar or near planar configuration. The metal atom bonding can be considered as a resonance of two electronic structures, in each of which the metal atom forms single bonds with two opposite nitrogens (replacing two hydrogens) and forms two partial dative bonds with the remaining two nitrogens.

The interatomic metal-to-N distances for a series of metalloporphyrins support the simple picture above (Table II). From the bond distances, we can calculate the corresponding bond orders and metal valences by assuming the application of Pauling's metallic radii (4). We also show that the valence is very similar if the bonds are assumed covalent rather than metallic. In general, it appears that the metal atom is generally trivalent (with the exception of Mn) but not tri-positive, corresponding to the resonance of two metal-N single bonds with two metal-N "half-bonds." In the latter case, we may consider a "half-bond" to be the use of a single metal orbital and one electron to form bonds simultaneously with two N atoms. Figure 6 illustrates two different types of metal orbitals suitable for the formation of half-bonds (5).

The data in Table II suggest that: (a) The metal-nitrogen bonds are probably semiconducting in nature; (b) Although the transition metals use d-character in their bonds to nitrogen, the use of metals here does not introduce delocalized d-character into the band picture; (c) The polarization of the metal-nitrogen bonds transfers about one electron away from the metal atom, which corresponds to the formal transfer of one electron to the metal atom from the nitrogen unshared electron pairs in the formation of the two dative half-bonds; thus the metals are near neutral; and (d), In total, then, the replacement of two hydrogens in the phthalocyanine ring by a transition metal has little effect on the conductivity of phthalocyanine.

In returning to the question of how to make p-type polyphthalocyanine semiconductors, we should remember that the metal atom as discussed above is bonded by nitrogen in an approximate square planar configuration so that two sites (or at least one) are available for additional metal complexing. If such sites are occupied by mono-charged

TABLE II. METALLIC VALENCE IN METALLOPORPHYRINS

	<u>Bond Distance</u>	<u>Bond Order</u>	<u>Metal Valence</u>	<u>Covalent Valence</u>	<u>Charge Transfer via Bond Polarization</u>
Cr	2.033	.57	2.28	2.48	0.96
Mn	>2.083	<.44	1.76	1.99	0.86
Fe	1.972	.66	2.65	2.82	0.86
Co	1.949	.70	2.81	2.96	0.89
Ni	1.928	.74	2.95	3.09	0.93
Cu	1.981	.66	2.64	2.81	0.73
Zn	2.036	.72	2.87	3.01	1.17

anionic groups, like Br^- , then the metal-atom-anionic couple can act as an electron acceptor from the phthalocyanine ring and hence produce a p-type (hole-conducting) polyphthalocyanine.

Now the advantage of this approach is that the anionic groups are stabilized or "trapped" by the metal atom which transfers the electron-withdrawing effect of the anions to the ring system. Perhaps such materials can be made by either (1) polymerization of the phthalocyanine with the transition metal (very finely divided), followed by introduction of halogen, (2) ion implantation of both metal and halogen atoms, or (3) polymerization with cuprous or cupric salts (currently one technique in use).

Let us return now to the problem of the corrosive nature of the popular dopants (Br_2 , etc.) for polyacetylene $((\text{CH})_x)$, graphite, and $(\text{SN})_x$. From the polyphthalocyanine case above, it would appear desirable to insert in these materials a similar polar trap for the anionic species. This might be achieved in several ways as suggested above or by synthetically incorporating other trapping groups.

THE CONTACT PROBLEM

If the preparation of chemically produced "metallic" polymers is the primary current problem, then the succeeding important problem will be the development of reliable electrical contacts between such polymers and the more ordinary metallic conductors. In terms of future "molecular" electronic devices, the contact problem is again an extremely important one whose solution must be sought simultaneously with the development of the devices and their interconnecting conducting filaments.

In taking a larger view of the "contact" problem as one of communication with an array of molecular devices or memory cells, the use of optical techniques to communicate or prepare and read quantum states should not be overlooked. However, consideration of that prospect is beyond the scope of this article.

The usual contact problems between two conductors are associated with contact resistance, contact heating, rectification and then failure. When these considerations are applied to lower temperature, reactive materials like $(\text{SN})_x$ or doped $(\text{CH})_x$, it is to be appreciated that contact heating will lead to chemical reactivity and early

contact failure. Accordingly, it is to be understood that such contacts must be made with more than ordinary concern.

While the electrical properties of doped and undoped $(CH)_x$ and $(SN)_x$ specimens have been determined using silver-painted contacts, such contacts are usually employed at low-current conditions and are not likely to be stable contacts for high current and continuous use.

Ion-Implanted and Metal Atom Contacts

As an example of a near term approach that might prove useful, consider the contact indicated in Fig. 7 between an ion-implanted conducting layer and a metallic external conductor. If a dopant is implanted in a material at a single implanting potential, then the dopant has a Gaussian-like distribution below the surface. On the left of Fig. 7 we see the conducting implanted layer with a peaked dopant distribution about 1000 Å below the surface, but with a nonconducting surface. However, by spatially varying the energy of the impinging ions and/or by varying the impinging angle on the surface, the peak concentration of the dopant can be brought to the surface, as on the right side of Fig. 7. At this point, it is desirable to form a strong, cohesive bond with the polymer conductor by perhaps employing metal-atom techniques (6) where the highly reactive atomic species form strong conducting bonds at low temperatures with the conducting polymers. Over the layer deposited by the metal-atom technique, an evaporated metallic conductor is deposited. For most metals, of course, reactive metal atoms are produced by evaporation and then trapped in a cold neutral matrix. The picture just described for the preparation of a contact is within the current state-of-the-art.

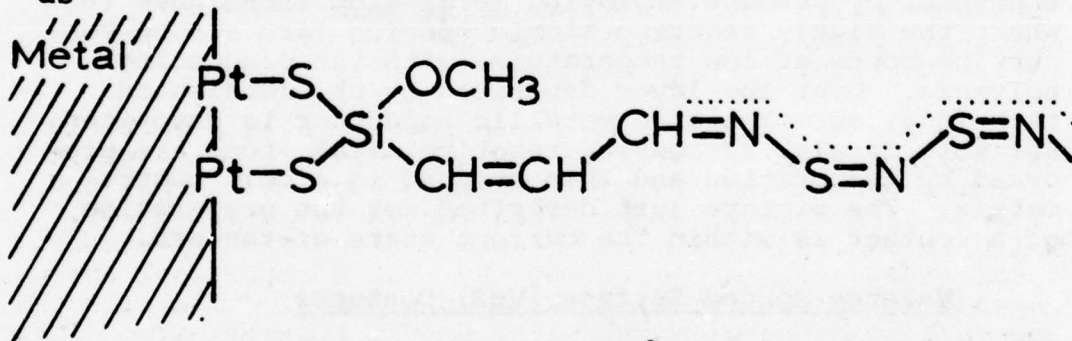
Valence-Bonded Surface (VBS) Contacts

This type of contact, in which the conducting filaments are to be covalently bonded to the metal substrate, is an area of high current interest to electrochemists and surface chemists (7). However, at the present time, the main research efforts involve covalent bonding of insulating materials to metal surfaces.

The general approach is illustrated in Fig. 8 where a specially prepared Pt-metal surface is exposed to a vapor of a reactive trimethoxy silane. In the right-hand side of Fig. 8, we note two possible modes of the attachment of the reagent to the Pt-metal surface, that is, by

either one or two covalent-bonded oxygen linkages. ESCA studies of this reaction at NRL show that the Pt surface is indeed involved in the surface reaction. Figure 9 shows the Pt 4f spectra and the very significant increase in the Pt peak widths, i.e., from a FWHM of 1.55 for Pt metal to a FWHM of 1.95 for the modified Pt surface. A Pt atom by itself would show a significant ESCA chemical shift; however, here a surface Pt atom sees not only the one or two oxygen linkages to silicon, but is also influenced by still being firmly attached to many other Pt atoms in the metal. Hence the charges on the attached Pt atom are strongly compensated for by the metallic Fermi sea of electrons.

ESCA results show, as suggested in Fig. 8, that during the reaction, the trimethylene chloride group is converted to a propylene group. Such a terminal reactive group permits extending the length of the propylene group by further reactions. This small beginning then suggests the feasibility of adapting this approach to form valence-bonded surface (VBS) contacts. Thus, firstly one would want to attach to the propylene group a conducting polymeric filament. Secondly, instead of the oxygen bridging link, one might prefer a thio-linkage, since kinetic studies suggest sulfur linkages are more conducting (8). Following these considerations, we might picture the Pt surface as



We note that a short section ($\approx 10 \text{ \AA}$) of the hetero polymer is semiconducting in nature. Accordingly, we suggest that clever surface chemists will find a way to minimize such a resistive chain element once the problem is posed.

If a strong VBS contact can be formed on a metal substrate, it would also appear possible to reverse the procedure and, by starting with a conducting polymer substrate, prepare VBS contacts to metal. This might be possible using a variation of metal-atom chemistry.

By such detailed attention to the preparation of electrical contacts, we hope in the future to be able to prepare and predict the nature of electrical contacts, not only between conducting polymers, but also within "molecular" electronic device arrays and between such arrays and the larger outside world.

THEORY: APPLICATION AND NEED

In this section we will first discuss current problems in the application of Molecular Orbital theory to the prediction of new metallic inorganic polymers and what might be done to improve prediction capabilities. Then, in a somewhat different vein, we will look to the future and consider areas of molecular electronic devices in which new theoretical considerations might play a useful and guiding role.

Present Needs

In the search for new, light, metallically conducting polymers, one must rely primarily on intuition and the rather vague suggestions of the theorist as outlined above. While Molecular Orbital (MO) theory and Band Structure (BS) calculations are widely touted and provide assistance in understanding known materials and properties, they are of little value in the prediction of new materials having specific unique properties. Several reasons exist for this situation.

MO and BS calculations are primarily single-particle calculations, and as such do not take adequate account of electron correlation energy (i.e., between the correlated motion of electrons). This electron correlation energy, which is defined as the difference between the experimental total energy of the system and the best Hartree-Fock energy, amounts to approximately 30 Kcal/mole per electron pair. However, bond energies are usually of a similar value, i.e. 20-30 Kcal/mole per single bond, and many very important phenomena depend entirely on even weaker bonds (like the hydrogen bond). Thus, while Hartree-Fock MO calculations can be very accurate percentagewise, they are not generally useful for predicting compound existence. However, such MO calculations are of value if performed on series of compounds, so that trends in properties can be observed. Otherwise, in calculations of heats of formation, one must depend on accidental cancellation of electron correlation energies, which is hardly a reassuring situation. This situation will only improve when valence-bond or electron-pair function calculations are systematically performed.

Another reason to be modest in one's expectations of MO or BS calculations is that, in general, only a few atoms in the asymmetric unit can be treated. Thus, most MO calculations can treat perhaps 60 electrons in the valence shell, corresponding to about 10 atoms (non-hydrogen). In fact, however, it would be desirable to treat more than 60 non-hydrogen atoms, with a total of several hundred electrons, in order to study the band-like properties of an electroactive polymer as one increases the number of repeat units to ten or more.

Another problem is that of having a sufficient number of basis functions, so that the results reflect something of reality and not just the built-in limitations of a restricted set of basis orbitals. Thus it is desirable to permit the use of some Si, P, or S d-character with a contracted radial character for bonding electrons, but with extended radial character for anti-bonding, delocalized, or unoccupied d orbitals.

While the prospects for performing ab initio calculations using hundreds of electrons are currently quite dim, the rapid increase in computer capacity and the recent introduction of array processors suggests that semi-empirical calculations involving large numbers of electrons are not so distant.

However, in the application of semi-empirical MO methods to the search for new metallically conducting polymers, one quickly finds new problems. Thus in Dewar's MINDO-3 programs, one has well-developed bonding parameters for C and H with B, N, O, S, F, P, S and Cl, but not for the latter group of elements with themselves. A second problem is that all the parameterization has been achieved with well-known and rather conventional compounds. Thus it is not clear that these semi-empirical approaches based on conventional materials will provide useful guidance in predicting the feasibility of compounds like $(\text{SN})_x$ that may be unique in their bond formation.

Future Needs

In anticipation of the development of "molecular" electronic devices, it is possible to indicate areas in which theoretical efforts might play an important and guiding role in the design of molecular conductors and devices.

1. Filamentary Conductors. The following questions can be asked concerning the structures of intermediate size involving many parallel molecular filaments, down to the single molecular conducting filament.

What is the nature of electrical conduction along filaments of molecular dimension and finite length, perhaps having 10-20 repeat units? Here we must remember that such filaments may involve zig-zag chains as well as straight chains of atoms. What is the effect of structural conformations on conduction and mobility? Are end or termination effects important? How detrimental are short distances of "insulating" bond character in the structure - can the problem be relieved by alternating single-double bond systems? While the physics of "free" electron conduction is well understood, and the effect of bond formation and bond direction upon the Fermi surface is qualitatively understood (5,9), the details of conduction at the molecular level in non-metal containing systems is in its infancy. Thus, for example, it is not yet clear whether conduction in conjugated molecular systems like TTF-TCNQ is via electrons, valence electron pairs (10), or holes.

2. Tunnelling Phenomena. In systems of molecular size, the phenomena of quantum mechanical "tunnelling" may be expected to play an important role. As indicated in the section below, it may lead to some powerful molecular devices or, alternatively, it may have a deleterious effect similar to the "cross-talk" phenomena in current semiconductor technology. In the area of conductors, one may pose queries involving electron tunnelling parallel to conducting fibers past atomic defects or short "saturated" areas in the conductor. Further, will tunnelling occur between two or more filamentary parallel conductors? or between a finite filament and a parallel conducting plate? or between a short filament and a perpendicular plate? One can pose similar questions concerning parallel-conducting layers and in regard to both the normal and the superconducting states. Many interesting questions and solutions await us in these areas.

3. Layered Clusters. One should not be concerned solely with filamentary structures, since layered devices are also interesting potential molecular devices (see below). Here one might consider planar structures, as in the porphyrins and phthalocyanine ring systems and their metal derivatives, in graphite-like systems, or in inorganic systems based on covellite or klockmannite in which metal-like Cu-S hexagonal layers are separated by insulating tetrahedral layers involving the semiconducting linkage Cu-S-S-Cu.

4. Quantum Mechanics of "Molecular Devices." Inasmuch as Quantum Mechanics (QM) is hardly able to handle as many as three electrons without neglecting electron correlation, it is clear that considerable simplification must occur in the formalism of QM if it is to be tractable and useful in discussing the gross features of networks of molecular devices. It will be necessary for theorists to develop analogs, at the molecular scale, of the electrical concepts of resistance, impedance, capacitance, etc. Further, it is to be expected that such a "network" analog will consist of finite one-dimensional solutions joined to others at the ends, where a quantum-mechanical analog of Kirchoff's law (for current flow) would apply. In addition, it is clear that both time-dependent and stationary solutions would be of great interest. Surely many new phenomena will be discovered as our understanding about "molecular-sized" gates, switches, and oscillators increases.

SIGNAL TRANSPORT AND MOLECULAR SWITCHES

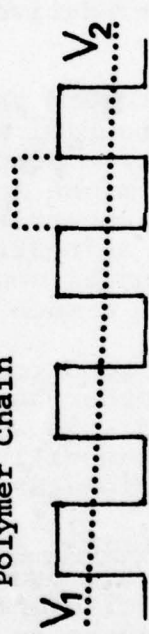
One of the most fascinating aspects of the concept of switching at the molecular level is the very wide variety of energy carriers that can be utilized. These can include excited molecules, ions, photons, phonons, excitons, and magnons, as well as holes and electrons. The variety of molecular switching phenomena that can be involved is even larger and can involve bond breaking and reformation, molecular transformation, conformation changes, electronic or magnetic excited states, as well as vibrational and rotational states.

Signal Transport Possibilities

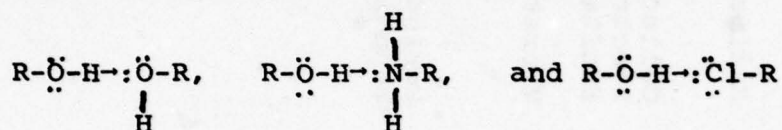
In this section we will treat some of the possible carriers of information and generally only sketch the particular phenomena involved. However, two phenomena, one chemical and one quantum mechanical in nature, will be treated more fully in the next sections, the Sudden Polarization Effect, and the phenomena of Periodic Tunnelling.

In Table III we list some of the ways in which a signal might be transported within a molecular device. The table summarizes the particles carrying the signal, the typical distance involved in a single step, the pertinent structural features, the phenomena, and the action required for utilization of the phenomena as a "switch."

TABLE III. TRANSPORT OF SIGNAL (WITHIN DEVICE)

<u>Particle</u>	<u>Dis-</u> <u>tance</u>	<u>Structure</u>	<u>Phenomena</u>	<u>Switch</u>
1. H^+ , H^-	3 Å	Asy. Hydrogen Bond	Particle Tun- nelling "Mole- cular Diode"	Reverse Poten- tial
2. Photon	35 Å	Dipole-Dipole	Excimer	Rotate Dipole
3. Exciton	50 Å	1,2,3-d Structure	Collective Electronic Excitation	Alter- nate Trap
4. Phonon	100 Å	Polymer Chain	Vibration	Discon- nect Chain
5. Electron	300 Å	 $V_1 > V_2$	Periodic Tunnelling	Well ~ Barrier

1. Proton and Hydride-Ion Particle Tunnelling. As a first example, we might consider proton (H^+) or hydride ion (H^-) transfer. The motion of such light particles might occur as either a vibration phenomena or one involving particle tunnelling. In biological systems, great use is made of the asymmetrical hydrogen bonds not only as weak bonds tying together long strands of nucleic acids and polypeptides to form DNA, RNA and proteins, but also as one-way conductors (11) and as photoactivated proton pumps through a membrane as in the bacterium "halobacterium halobium" (12). In hydrogen bonds such as



the amount of asymmetry varies considerably between the -O-H bond and the weaker dative bond ($-H \cdots \underset{\underset{H}{|}}{\ddot{O}}-$) where the

hydrogen is attracted toward the unshared electron pair of O, N, or Cl. If a potential were imposed across the hydrogen bond (i.e., the dative bond) such that the $R\ddot{N}H_2$ group was more negative, one might anticipate the proton (H^+) tunnelling through the potential barrier, picking up an electron and returning as neutral hydrogen. Current flow under the reverse potential would require a hydride ion to jump to the $R\ddot{N}H_2$ group, a much less favorable process.

Thus the hydrogen bond could act as a molecular diode or rectifier. On the other hand, hydride ion (H^-) transfer to carbonium ions $C^+ \equiv (R)_3$ is well known, and could similarly provide a particle tunnelling mechanism for conduction and switching at the molecular levels.

2. Excimer and Exciplex Energy Transport. If two identical chromophores are properly oriented, the photon energy sufficient to excite one to a singlet state can be shared with the chromophore in the ground state via a dipole-dipole coupling mechanism, if they are sufficiently close, i.e., $\approx 45\text{\AA}$. We note that excimer fluorescence is slightly less energetic than the fluorescent radiation of a single chromophore. The interesting aspect of the creation of this excited pair is that the probability of creation is quite sensitive to the relative orientation of the two chromophores via the dipole-dipole interaction. Accordingly, excimer formation could be turned off by literally "turning" one chromophore by 90° . Later in this section we discuss a mechanism for doing this via the "Sudden Polarization" effect.

If the two chromophores are not identical but closely related, the shared excited state is called an "exciplex" rather than an excimer. Finally, we note that non-radiative energy transfer between similar chromophores can occur up to distances of 150 Å via the dipole-dipole coupling mechanism but without excimer formation. Energy transfer by this phenomenon can also be turned off by rotating one of the involved chromophores by 90° about the appropriate axis.

3. Exciton Energy Transport. The "exciton" is a collective electronic excitation in a crystalline material which has been optically generated and is associated with a crystal wave vector of $k \approx 0$. If, for a molecular crystal, the thermal energy, E_T , is large compared to the exciton band width so that a wide range of k values is involved, then the physical extent of the exciton can vary from several lattice spacings wide down to a single large molecule (14). The half-life of the exciton can vary enormously, depending both on the concentration of exciton traps and on the exciton spin states; thus for a triplet spin state, half-lives several seconds long have been observed, while singlet lifetimes can be five to nine orders of magnitude smaller. During the longer half-lives, the exciton can travel (diffuse) distances readily measured in millimicrons.

For our current purpose, we are interested in excitons which are close to molecular size and which can transport the electronic excitation energy distances of ≈ 1000 Å. When an exciton is trapped, the energy can be released as delayed fluorescence radiation, thermal energy, electronic charge separation, etc. Since exciton trapping is relatively easy, the switching mechanism can involve the preparation of alternate trapping sites. While exciton behavior has been well studied in three-dimensional semiconductors and organic crystals, it would be of considerable interest for our present purposes to understand exciton transport in materials with strong one- or two-dimensional aspects.

4. Phonon Propagation in Polymer Systems. Energy transport along polymer chains (meaning extended linear molecules) could also be achieved by means of phonon propagation over distances involving hundreds of Angstroms. The phonon might be generated by optical absorption at a chromophore or by non-radiative decay of an excited electronic state, e.g., perhaps from a trapped exciton. As a switching mechanism, one might consider either a chain-breaking process involving a hydrogen bond or a pair of

them as in Fig. 10, or by a damping process, wherein the polymer chain is coupled to the wall, perhaps by the formation of a charge-transfer complex which would give rise to an electrostatic attraction. In either case, it is clear that phonon propagation along the polymer chain would be interrupted, but in a manner which could be reversed.

5. Electron Transport via Periodic Tunnelling. In 1962, Pshenichnov (15) showed by quantum mechanical arguments that the transmission of particles through a series of identical potential barriers can be anomalously high under certain conditions. Normally, the transmission coefficient, $Q(E)$, for an electron of energy E through a potential barrier of height V declines exponentially with $|\sqrt{V - E}|$ and with the barrier thickness. However, for a system of periodic barriers, quasi-stationary states of energy E_i exist between each succeeding pair of barriers.

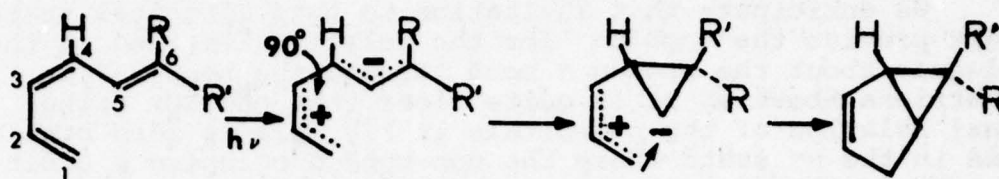
Now if the energy E of the incoming electron matches that of one of these quasi-stationary states, then the transmission coefficient $Q(E)$ approaches 1.0, i.e., perfect transmission. However, by changing one of the potential wells, one can spoil the perfect match and achieve a very fast cutoff of transmission. This then becomes both a very effective switching mechanism as well as a signal transport mechanism over distances of several hundred Angstroms. This is perhaps one of the most promising of molecular device mechanisms and as such will be further considered after a discussion of the Sudden Polarization Effect.

The Sudden Polarization Effect

The sudden polarization effect is of particular interest in this discussion because it is a photochemical effect which often results not only in the rotation of a molecular moiety about a normally rigid double bond, but also results in the unexpected separation of charge. Theoretical chemist Prof. L. Salem has further suggested that this recently discovered effect plays an important role in the mechanism of human sight (16).

W. G. Dauben, the chemist primarily responsible for the discovery of the effect, is an experimental photochemist who in 1970 proposed a reaction mechanism involving a zwitterionic intermediate to explain some highly stereospecific photocyclization products of nonpolar precursors (17). This rather daring proposal and zwitterionic intermediate (i.e., with charge separation and bond rotation)

is illustrated below for a hexatriene.



For the above reaction, Dauben (18) proposed that the photon excites the π bond at position 3-4 and that the two portions of the molecule rotate about the bond by 90° ; he further proposed that charge separation takes place and is distributed over the remaining double bonds via resonance forms. Once this has occurred, the reaction rearrangement can proceed as indicated above.

The theoretical studies have given valuable clues as to the three conditions necessary for this development of the zwitterionic intermediate. These have been summarized by Salem (16) as follows:

- The overlap of the π systems to the left and the right of the "broken" (rotated) double bond should be orthogonal, as indicated in Fig. 11a.

- Charge separation occurs only when the angle of rotation is within a degree of 90° , as indicated in Fig. 12. It is this very "sudden" change in charge separation as the rotation angle approaches 90° that gives rise to the term "sudden polarization effect." In fact, this second condition is in accord with the first condition concerning orthogonal π systems and allows the mixing of the two wave functions Z_1 and Z_2 of Fig. 11b. Only then do these highly polarizable Z_1 states result in charge separation.

- The wavefunction mixing is only stabilized if the two ends of the molecule are somewhat dissimilar. Here we note that, in a π system of alternating single and double bonds, the presence of an extra electron (due to a π -bond rupture) or absence of a π electron (hole) is readily delocalized on the π system, as was indicated above for hexatriene. In addition, and more directly related to the

sudden polarization effect, there is an excited antibonding diradical state of comparable energy to the zwitterionic states.

We anticipate that excitation to this diradical state might provide the impetus for the relative twisting of the molecule about the broken π bond (around the bond 3-4 in hexatriene above). It is quite clear that the 90° orthogonal relation of the p orbitals in Fig. 11a is more stable than in the π^* state where the non-bonded occupied p orbitals are in the same plane.

Although we have paid special attention to the "sudden polarization effect" as a mechanism leading to both charge separation and molecular rotation (and rearrangement), we now call attention to the fact that it may be an important mechanism in the conversion of cis-polyacetylene to the more stable trans- form.

When acetylene is first polymerized at low temperature, its IR spectra indicates it is entirely cis-polyacetylene. However, if it is heated or allowed to remain at room temperature, it gradually converts to the trans-form (19). In Fig. 13 we note that each of these two forms has a resonant equivalent structure (near equivalence in the cis case) that tends to restrict all atoms to the plane of the paper. Two simple arguments suggest that the trans version is the more stable form: (1) for long chains, the two resonant forms are equivalent, giving rise to a greater stability, and (2) the hydrogens in the cis-form provide a steric hindrance that is not present in the trans-form.

In Fig. 14 we postulate a photocatalyzed conversion of the cis to the trans form employing the "sudden polarization effect." In Fig. 14b, we illustrate the zwitterionic state with two carbons and their hydrogens rotated as a group 90° out of the plane of the paper. We show the negative charge localized and the plus charge distributed, although it is not clear which is the more favorable state. The energy for rotation might be of thermal origin or from the repulsive interaction of the two p electrons in the diradical antibonding π^* state, as discussed above. However, once having reached the 90° rotation state, further rotation by 90° would give the favorable trans conformation, as in Fig. 14c. At this point, a shift in electrons, also as indicated in Fig. 14c, could provide a further charge separation and a rotation of two more carbons with their hydrogens into the 90° plane. This process can repeat indefinitely, each time converting two cis π bonds into the trans configuration, until it terminates at the end

the chain or meets a charged state coming from the right. In order to understand this process, it is important to remember that the resonance of a p-orbital hole (plus charge) over a small portion of the carbon chain appreciably decreases the restoring force with which the resonating π system tends to keep all the carbons in the same plane.

Finally we note that, in Prof. Salem's application of the "sudden polarization effect" to visual excitation of the rhodopsin molecule, there is both a transformation of the conjugated retinal skeleton to the all trans form, as well as a very real separation of charge. In the latter case, a mobile electron on the conjugated chain is neutralized by a quaternary imino group attached at the end of the conjugated chain, Fig. 15.

Tunnelling in Periodic Structures

We have just seen how the "sudden polarization effect" can give rise to the rotation of a molecular moiety in structural transformation, as well as to charge separation, all via a photochemical-quantum effect. As such, it represents only part of a potential molecular electronic device. For example, the moiety rotation might be employed to turn on (or off) excimer formation between two chromophores coupled via the dipole-dipole interaction.

However, in contrast, we can draw almost immediately a parallel between modern microcircuitry and the molecular devices based on Pschenichnov's study (15) of tunnelling in periodic structures. The basic ideas are indicated in Fig. 16, where we have four identical wells periodically spaced. Assume that the dimensions of the well are such that a single well would have two stationary states, one deep and one relatively near the surface. If the four such potential wells are adjacent, it is anticipated that the upper levels will be split by the interaction, while the splitting of the lower level is negligible as suggested by Fig. 16a. Now imagine that on either side of the set of four wells, the potential is dropped, as indicated by the heavy dashed lines. The four split levels then correspond to the pseudo-stationary states discussed by Pschenichnov. Then the transmission probability, $Q(E)$, for an electron of energy (E) penetrating the periodic structure is indicated schematically in Fig. 16b. If the particle energy E is not close to one of the energies, E_1 , E_2 , E_3 and E_4 , of the pseudo-stationary states, then the transmission probability is virtually zero; even close to the resonant energies E_i , the fall-off of $Q(E)$ is a strong

exponential. However, at the energies E_i , the transmission is perfect, i.e., $Q(E_i) = 1$. It is clear then that any change in potential at any well is likely to induce a precipitous decline in the transmission probability.

The perfect transmission at $E = E_i$ and the sharp probability drop for any disturbance of the wells then provide an ideal opportunity for a molecular switching device. In Fig. 17 we indicate the usual circuitry for a "NAND" gate and a "NOR" gate. For the "NAND" gate, the potential at the output drops only when there is input at both input transistors such that current flows from the positive potential to ground. An analogous situation is obvious using the quantum tunnelling through periodic barriers. For example, the addition or subtraction of an electron at any of the deep levels in the four wells would reduce transmission through the structure to zero.

In Fig. 16c, we suggest a molecular device that uses the periodic tunnelling approach to generate a highly monochromatic beam of electrons. Here the potential drop between each well must match the energy difference ($E_{i+1} - E_i$) between succeeding pseudo-stationary states.

The molecular systems which might function as periodic tunnelling devices are currently poorly defined. However, as linear systems, perhaps something as simple as a short linear copolymer involving alternate chromophoric aromatic groups serving as the potential wells, linked by methylene groups as potential barriers, might be appropriate. The wells could then be either influenced optically to form charge-transfer states, or perhaps even induction effects might be quite effective. A more rigid linear system might involve stacked metal ligand systems like $\text{Pd}(\text{dpg})_2\text{I}_x$ or $\text{Ni}(\text{Pc})\text{I}$ (20) (where dpg = diphenylglyoximate and Pc = phthalocyanine) or the halogen-bridged copper complexes of thiazole (21). Here the organic ligands of the stacked systems provide handy access to modify the metal atom potential (the well) while the metal-metal distance can be readily varied by either the choice of ligand or by degree of oxidation by iodine.

If quantum tunnelling of periodic structures occurred perpendicular to the lamella in layered structures, one can easily imagine molecular analogs to the "NOR" gate of Fig. 17c. For example, in the covellite (CuS) and klockmannite (CuSe) structure, semiconducting layers and metallically conducting layers alternate in a periodic fashion. Such a structural arrangement, as in Fig. 17d and employing quantum tunnelling between layers, provides a ready "NOR" gate analogy.

ON GROWING AND OPERATING THE COMPUTER OF THE 1990s

One of the impressive aspects of the U.S. computer industry has been its ability to mass produce electronic circuitry of diminishing size with ever-increasing complexity, reliability, and operating speeds (22). Even so, the industry not only sees a technological threat from like industries in Japan, but also is currently struggling with technological limitations to further reduce active component sizes. Before considering the benefits that might be associated with a computer based on molecular-sized electronic components, it is desirable to consider three problems associated with the current larger computers.

Problems in Current Computer Technology

The problems are the increased cost and performance degradation associated with wiring the Central Processor Unit (CPU) and memory chips together and heat generation by the ever-present resistive elements, as suggested by the NAND and NOR gates of Fig. 17. While tens of thousands of active elements can now be routinely placed on a single silicon chip, it now costs more to assemble these chips onto printed circuit boards and then assemble these boards into a working computer than to produce the chips. In 1977 it was estimated (23) that the chip cost was only 3.4% of the total cost of the assembled and tested electronic systems. As illustrated in Fig. 18, this is primarily because of the two-dimensionality of both the silicon chips and of their assembly. This leads to another related problem, namely the operating speed of the computer. Since the speed of an electrical impulse is no greater than 0.3 mm per picosecond, the length of the wires hooking together chips provides a clear limitation on the ultimate speed of a computer. One well-known successful computer architect, Seymour Cray, has built very fast large computers with this limitation very much in mind (thus no wire in the computer is longer than 3-1/2 ft.) (24). One obvious way to circumvent this problem in the future is to build three-dimensional rather than two-dimensional microcircuitry. If, for example, all the microcircuitry could be included in a three-dimensional block, 1 cm on a side, the transport of information from one element to another would take no longer than 34 picoseconds, compared to 3.5 nanoseconds for a 3-1/2 ft. wire, an improvement of a hundred-fold. We further note that most silicon devices are limited by the drift velocities of holes and electrons in silicon, whereas molecular devices could have pico and sub-pico response times (25,26).

Thus, if it were possible to form a three-dimensional array of microcircuitry elements, it would be possible to enhance the operating speed many-fold while virtually eliminating the wiring costs.

The third problem that plagues modern large computers is the heat generated by the resistive elements in the microcircuitry. For example, the current Cray supercomputer uses 1/10 megawatt of electrical power (24). For adequate cooling, the Cray computer has a built-in refrigerator while others imbed their circuitry in the Freon cooling fluid itself. In the prior section treating molecular devices based on tunnelling of periodic barriers, we indicated that switching the gate on or off might be controllable by just a few individual electrons or particles. This suggests that the enormous heat load of modern computers might be avoidable in the future by making use of "molecular electronic gates," etc.

Density of Switches vs. Switch Size

The enormous number of elements, indicated in powers of ten, that might be contained in one cubic centimeter are indicated in Fig. 19 as a function the size of the active element. The time parameter indicating approximate past, current, and projected future gate densities is indicated on the curve itself. It is apparent that if a switching element plus its insulation could be contained in a cubic molecular volume 100 Å on a side, a cubic centimeter of molecular circuitry could exceed the sum of all memory elements manufactured to date. Obviously, the potentials are enormous. A highly speculative description of how a forerunner of such a computer might be made is indicated in the next section.

The Chemical Growth of a Computer

In the development of a three-dimensional array of electrical "molecular" elements on the order of 100 to 1000 Å on edge (center to center), one can readily imagine at least two approaches. The first is closely related to current microprocessor technology, while the second is much more chemical in nature, and as a newer concept, will be developed more fully.

1. Computer via Vapor Deposition, etc. In the first approach, one would employ the use of laser or x-ray lithographic techniques to develop a set of active elements on a substrate surface. On top of these elements would be

superimposed another substrate $\sim 1000 \text{ \AA}$ thick, which would include electrical leads through the substrate circuitry to elements to be developed on this second substrate. Here the process to develop the molecular circuitry would be repeated, with a third substrate deposited, and the process repeated until the desired number of elements and their conductors had been prepared. Material deposition would be presumably achieved by some combination of evaporation, sputtering deposition, and/or vapor-phase chemical reaction and deposition. In terms of this first model, the difficulties include (1) deposition of the second and succeeding substrate layers over the active elements in such a way that the substrate would be perfect enough for the development of succeeding active elements; (2) the process of developing conducting paths through the substrate from active elements below to active elements on top, and (3) the problem of the registry of the conducting filament to the switches above and below.

Conducting linear filaments through insulating materials are a subject of considerable current interest. For example, consider the stacked metal complexes such as $\text{K}_2\text{Pt}(\text{CN})_4\text{BrO}_{0.30} \cdot 3 \text{ H}_2\text{O}$ and $\text{Ni}(\text{Pc})\text{I}^*$ where planar complexes of transition metal atoms are stacked, one complex on the other, so that the metal atoms form a continuous, sometimes conducting, chain (20). By controlling the thickness of the ligand complexes and the oxidation of the metal, one can modify the metal-metal distance and hence the conductivity. Moreover, by controlling the size of the ligand, one can control within limits the separation of the conducting metal chains. Having made a molecular crystal of such a metal complex, it may be possible to crosslink the ligands between metal strands by optical excitation and subsequent solid-state reaction. This, however, would undoubtedly require ligands which had appropriately reactive side groups in anticipation of the crosslinking reaction, as has been done in the multilayer polymerization of tricoso-10,12-dienoic acid (27).

A second possible source of conducting filaments with a periodic repeat separation is the so-called "modulated" structure where carefully controlled non-stoichiometry produces long-period modulations. In ceramic materials, these modulations have a shear plane attribute associated with a local non-stoichiometry and metal-metal contacts. It is likely that modulated materials will be

* Pc = phthalocyanines

found such that the metals form a conducting path through the insulator substrate, where the periodicity between conducting paths is long, perhaps 100-1000 Å. In addition to linking two planar assemblies of molecular gates on either side of such a modulated substrate, such a material might be useful for constructing a field emitter array, as indicated in Fig. 20.

2. Computer via Chemical Growth. In this second hypothesized approach to manufacturing a three-dimensional array of molecular switches, i.e., a computer, considerable use is made of solution reactions, sometimes catalyzed in selected regions near the growing surface by a laser beam of selected wavelengths.

To appreciate and imagine how a computer might be synthesized or grown in solution, it will be useful to acquaint the reader with the process known as the Merrifield Method of polypeptide synthesis (28). This highly successful technique of biochemistry is now a standard method for producing long polypeptide chains in high yield. Furthermore, these polypeptide chains, perhaps a hundred amino acid units long, might be composed of many different amino acids linked together in a very specific and pre-selected order. The process of building the polypeptide chain is initiated by preparing a substrate, usually in the form of plastic beads, with a link to the first amino acid that can later be broken. Then, using a system of automatic controlled valves, various reagents and solutions containing the appropriate amino acids are reacted with the polypeptide growing on the bead substrate. When the desired polypeptide is achieved, the linkage to the substrate is broken and the polypeptide collected.

The proposed process for growing an array of molecular devices is similar, except that in different areas of the now planar substrate, one is producing regions of different character, i.e., conductors, insulating material, and components which will be active molecular devices. Different solutions will be introduced, reacted and rinsed away for each layer of each function.

A schematic overview of the process is suggested by Fig. 21. By employing optical lithography, large electrical contacts to the external environment would be developed on a substrate of high thermal conductivity. Then, by using the technique of forming valence bonds between a molecule and a metal surface, described in an earlier section above, specific areas would be covered

with molecules destined to become conducting filaments and paths, while the remaining surface is covered with insulating material. Each new layer contains reactive sites for chemically bonding the succeeding layers. The fine graphic detail necessary here might be achieved using x-ray lithography. At this point, the prepared substrate would be introduced into the "reaction cell," into which the flow of reagents, solutions, and rinses is controlled by a computer (upper left). Thus, layer by layer, active elements, conducting filaments, and insulating materials are built up just as a long chain polypeptide is built up in the Merrifield method. In some instances, the reactions would be catalyzed in certain regions by the "reaction laser" shown. Ultimately, additional electrical contacts to the external environment would be developed on the outer surfaces.

Such a process presumes, of course, that the chemistry of each step is well understood and controlled. Incomplete reactions are difficult to tolerate in such a case. Enough duplication must be built in so that there is a finite overlap of functions. Thus, a conducting filament might involve several strands of $(SN)_x$ molecules.

Operation of the Advanced Chemical Computer

The conditions under which the proposed chemical computer of the future would operate are indicated in Fig. 22. Here we see that the central processor unit and memory of the future supercomputer has a volume of a cubic centimeter and is mounted on a support cooled by a helium refrigerator. The electrical leads are relatively few, with most of the input timing control pulses and numerical input data being transmitted via optical pulses through cooled masks. Output illustrated here is envisioned as being via multichannel optical techniques in which each channel source would be highly directional.

At the microscopic or molecular level, such a highly directional output might be achieved as follows: Assume that one has developed a linear array of oriented chromophores which, when excited, will radiate in preferred directions (i.e., dipole). Further, that these dipoles are parallel and reinforce each other as in Fig. 23. Now if several of these chromophores could be excited nearly simultaneously, the spontaneous radiation of one might stimulate the remainder to also radiate, producing in essence, a small, highly directional laser source.

Another possible output source for the CPU of a chemical computer might take advantage of the sensitivity of a

two-dimensional charge-coupled device (CCD) built into the side of the chemical computer. Usually, of course, the receiver cells of the CCD detect charged particles or electrons which have been photoemitted. As currently imagined, electron impulses can be injected into the receiver cells over a small potential barrier using the molecular tunnelling device of Fig. 16b, which can be readily switched on or off by a very small signal. Such a use of a CCD as an output device provides a high density of output channels for a low controlling charge input.

Benefits to be Derived from a Chemical Computer

As a summary of the advantages of a computer based on molecular level electronic devices, we recall the following points:

(a) In going from a modern-day, two-dimensional computer to three-dimensional fabrication, chassis and wiring costs would be significantly decreased and fabrication more fully automated.

(b) By reducing the switching elements to molecular size, the memory density could be increased by several orders of magnitude and power input very significantly reduced.

(c) Three-dimensional construction, plus switching elements of molecular size, could enhance computer speed by several orders of magnitude.

These possible advantages are all very significant, and now is an appropriate time for chemists, physicists, and engineers to be sensitized to the possibility of useful switching devices at the molecular level. However, there exist disadvantages to be considered, as indicated in the last section.

RETHINKING COMPUTER ENGINEERING

The principal reason for the success of the modern-day computer technology is the enormous reliability that has now been built into the individual switching elements of a computer. For example, compared to the vacuum tube of the early 1950's, the failure rate per gate has decreased by a factor of 10^5 (29). If, however, the computer is to be based on quantum mechanical devices, with the dimension of large molecules, i.e., $100 - 1000 \text{ \AA}$, then it should be anticipated that the failure rate will

go up until a learning period has indicated how reliable molecular switches should be constructed and operated. However, it is entirely possible that molecular switches will never be as reliable as microscopic switches.

In such a case, in order to gain the enormous advantages conceived above for molecular electronic devices, it will be necessary to rethink the computer engineering and architecture. Some obvious concepts which might be incorporated to regain reliability are:

- Duplicate circuitry, where the same function is performed by components in parallel.

- Duplicate calculations where the same elemental calculation (addition, etc.) is performed in duplicate, either by different circuits or by the same circuit several times.

- Reserve computing capacity wherein faulty circuitry is automatically recognized and switched out by the computer and circuits which constitute an initially built-in reserve are switched in.

Here, two points are of interest. First is the question of whether a circuit of molecular electronic devices is repairable or not? The second is the observation that the above considerations are based on a strict adherence to the principles of Boolean logic - and the resultant question: is such adherence necessary?

The question of repairability, by way of contrast to disablement and replacement by reserve capacity, is a very challenging one. An interesting possibility would be to use laser techniques to selectively break or induce bond rearrangement in special molecular moieties built into strategic positions in the active circuitry. In order to enhance the spatial resolution available with optical techniques, it is clear that a wide range of such "repair" moieties should be available, each sensitive to a particular wavelength with an insensitivity to all other "repair" wavelengths.

If the above question is one of special challenge to the chemist and spectroscopist, then the second question concerning the necessity of strict adherence to the principles of Boolean logic should be an equally challenging question for future computer engineers. At what part of computer technology is approximate adherence to Boolean logic possible? Obviously, one area might be in the

least significant digits of a numerical calculation which are affected by round-off problems. However, special circuitry for the lesser significant digits may not be economically attractive. On the other hand, information transport in biological nervous systems, as pointed out in detail many years ago by the mathematician and father of the modern electronic computer, J. Von Neumann, is certainly not a system of Boolean logic (30). The beauty and logic of biological systems for a moderately complex feedback circuitry has been recently exemplified by the description of the control system for a swimming leech (31). Perhaps the computer engineers might take inspiration for re-engineering the computer architecture for molecular electronic devices from their famous predecessor and by looking to examples from the living world.

REFERENCES

1. A. L. Robinson, *Science*, 201, 1112 (1978).
2. A. L. Robinson, *Science*, 202, 405 (1978); *ibid.*, 200, 1364 (1978).
3. W. R. Scheidt, *Accounts of Chem. Res.*, 10, 339 (1977).
4. L. Pauling, "The Nature of the Chemical Bond," Cornell Univ. Press, Ithaca, N.Y., 3rd Ed., 1960.
5. F. L. Carter, in "Electronic Density of States," Ed. by L. H. Bennett, Nat. Bur. of Standards Special Publication No. 323 (1971), p. 385.
6. P. L. Timms, "Techniques of Preparative Cryochemistry" in "Cryochemistry," Eds. M. Moskovits and G. Ozin, Wiley-Interscience, John Wiley & Sons, N.Y., 1976, p. 61.
7. W. R. Heineman and P. T. Kissinger, *Anal. Chem.* 50, 166R (1978).
8. G. J. Kennard and E. Deutsch, *Inorg. Chem.*, 17, 2225 (1978).
9. F. L. Carter in "Proc. 8th Rare Earth Research Conference," Ed. R. E. Lindstrom, held at Reno, Nevada, 19-22 April 1970, p. 460.
10. Y-N. Chiu and F. E. Wang, *Chemical Physics*, 18, 301 (1976).

11. P-O. Lowdin, Rev. Modern Phys., 35, 724 (1963).
12. J. F. Nagle and H. J. Morowitz, Proc. Natl. Acad. Sci., 75, 298 (1978).
13. R. F. Cozzens in "Photoconductivity in Polymers," Eds. A. V. Patsis and D. A. Seanor, Technomic Publishing Co. Inc., Westport, Conn., 1976, p. 189.
14. V. Ern and M. Schott, in "Localization and Delocalization in Quantum Chemistry," Vol. II, Eds., O. Chalvet, et al., D. Reidel Publishing Company, Dordrecht, Holland, 1976, p. 249.
15. E. A. Pschenichnov, Soviet Physics - Solid State, 4, 819 (1962).
16. L. Salem in "Excited States in Organic Chemistry and Biochemistry," Eds. B. Pullman and N. Goldblum, D. Reidel Publishing Co., Dordrecht, Holland, 1977, p. 163.
17. W. G. Dauben and J. S. Ritscher, J. Amer. Chem. Soc. 92, 2925 (1970).
18. W. G. Dauben, M. S. Kellogg, J. I. Seeman, N. D. Wietmeyer, P. H. Wendschuh, Pure Appl. Chem., 33, 197 (1973).
19. T. Ito, H. Shirakawa, and S. Ikeda, J. Polymer Sci., 13, 1943 (1975).
20. T. J. Marks, Annals of N. Y. Acad. Sci., 313, 595 (1978).
21. W. E. Estes, D. P. Gavel, W. E. Hatfield, and D. J. Hodgson, Inorg. Chem., submitted.
22. For several good reviews of microelectronics, see the Sept. issue 1977 Scientific American, 237, No. 3.
23. I. E. Sutherland and C. A. Mead, Scientific American, 237, 210 (1977).
24. W. D. Metz, Science, 199, 404 (1978).
25. E. P. Ippen, C. V. Shank, A. Lewis and M. A. Marcus, Science, 200, 1281 (1978).
26. P. M. Rentzepis, Science, 202, 174 (1978).

27. B. Ticke, G. Wegner, D. Naegele and H. Ringsdorf, *Angew. Chem. Int. Ed. Engl.*, 15, 764 (1976).
28. M. Bodanszky, Y. S. Kausner, and M. A. Ondetti, "Peptide Synthesis," 2nd Ed., John Wiley & Sons, N.Y., 1976.
29. I. E. Sutherland and C. A. Mead, *Scientific American*, 237, 210 (1977).
30. J. von Neumann, "Probabilistic Logics," lectures delivered at Calif. Inst. of Tech., 4-15 Jan. 1952, Notes by R. S. Pierce; see also J. von Neumann, "Theory of Self-Reproducing Automata," Ed. and completed by A. W. Burks, Univ. of Ill. Press, Urbana and London, 1966.
31. G. S. Stent, W. B. Kristan, Jr., W. O. Friesen, C. A. Ort, M. Poon, R. L. Calabrese, *Science*, 200, 1348 (1978).

BAND STRUCTURE TYPE

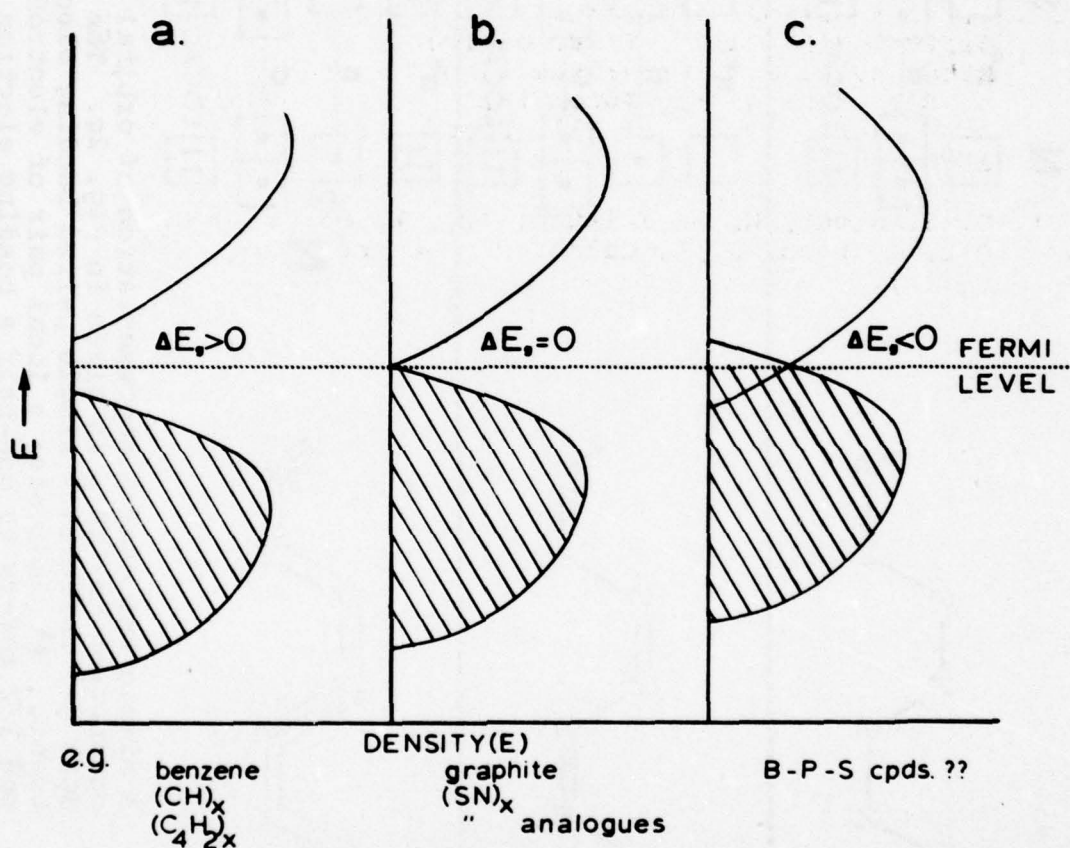


Fig. 1. Materials having all saturated or only alternating single and double bonds are band structure type a with a finite band gap, $\Delta E_g > 0$. Graphite and analogs of $(SN)_x$ will likely be of type b, with a zero band gap. What is sought is type c, with overlapping conducting and valence bands. This might be achieved by the atoms having more orbitals and neighbors than bonding electrons.

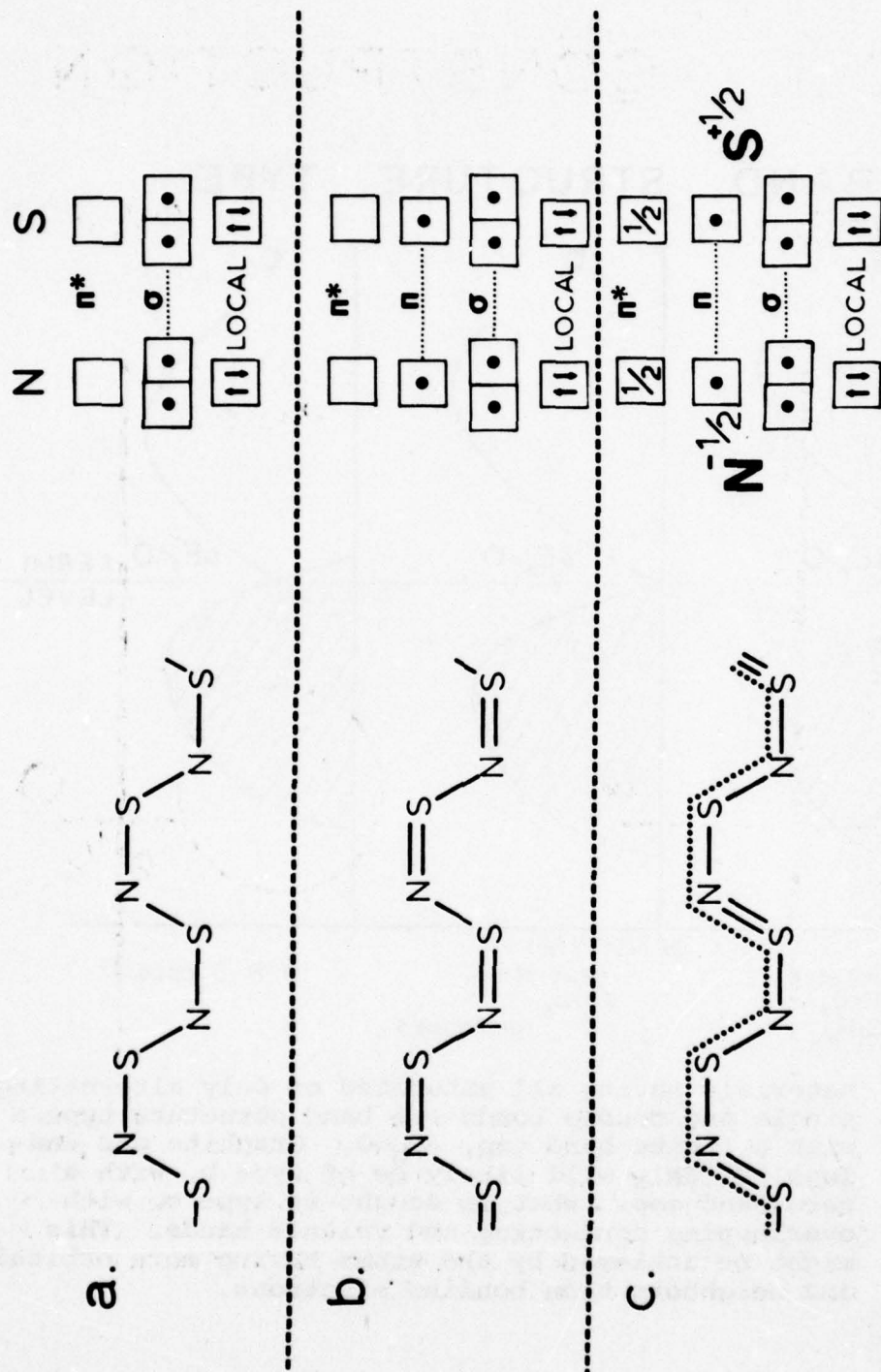


Fig. 2. A simple but useful representation of orbital occupation in $(SN)_x$ is given in Fig. 2c. The dots (.) refer to single paired bonding electrons, $\uparrow\downarrow$ indicates a local pair of electrons, and $1/2$ refers to one-half a bonding electron (dot).

CELL CONSTRUCTION

VORONOI

PAV

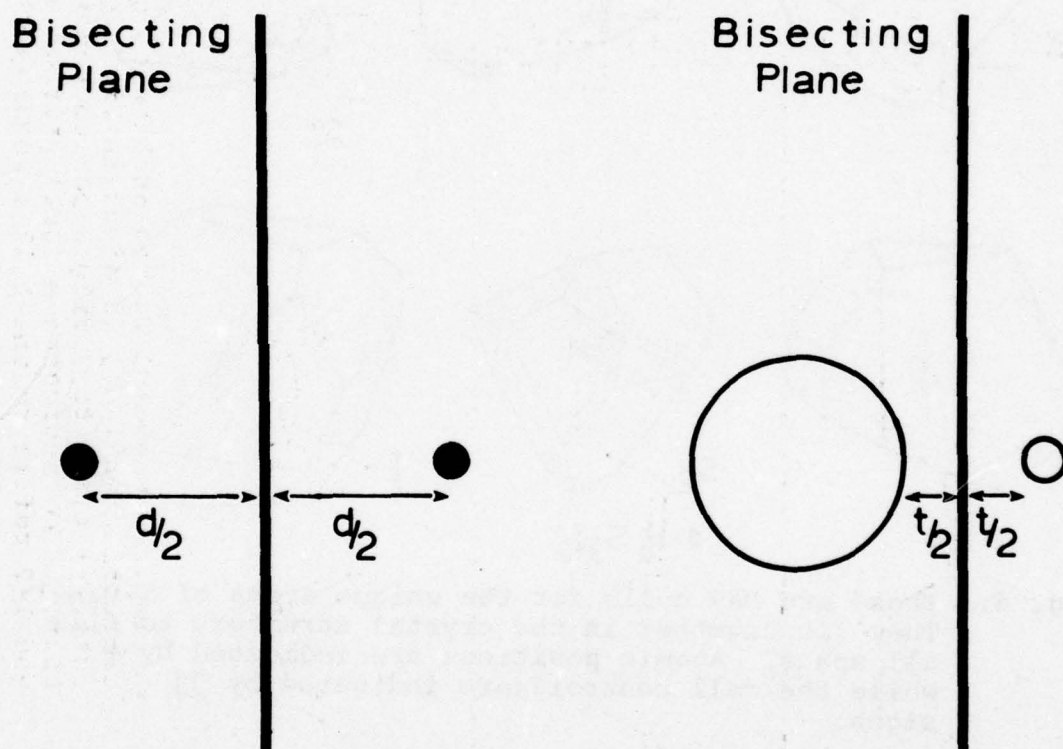


Fig. 3. In the construction of Voronoi cells, the planes perpendicular to the interatomic vectors are placed midway between the atom positions. For Polyhedral Atomic Volume (PAV) cells, these planes are midway between the outer spheres of the atoms assuming a single bond radius. Voronoi cells are space-filling and PAV cells usually so.

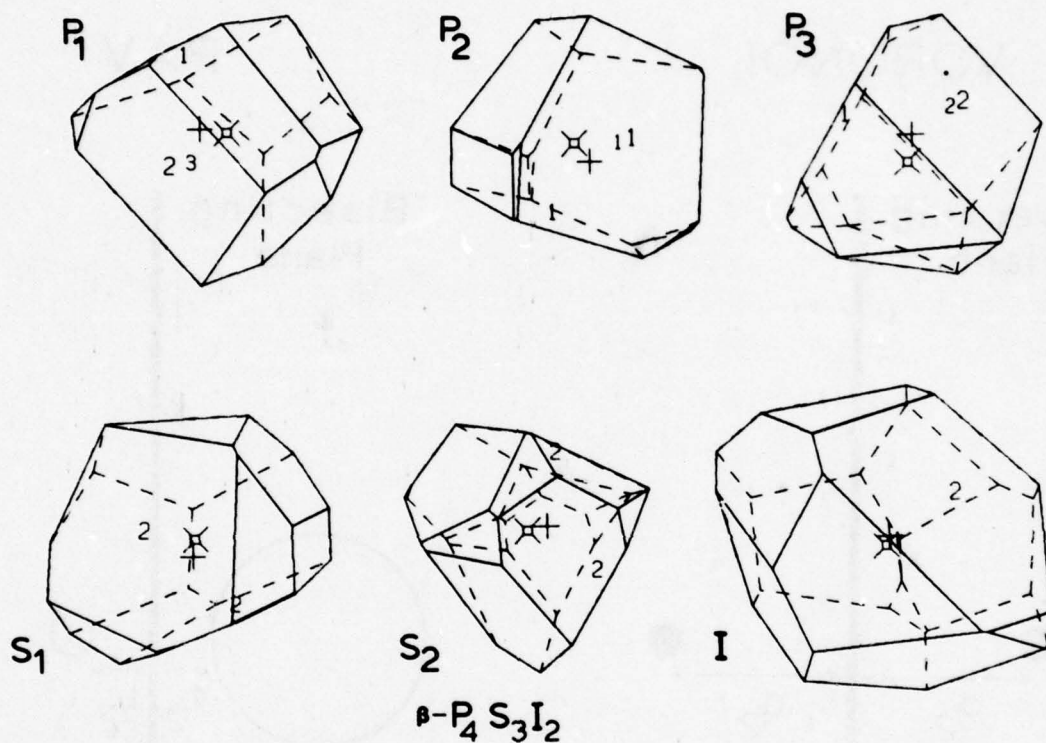
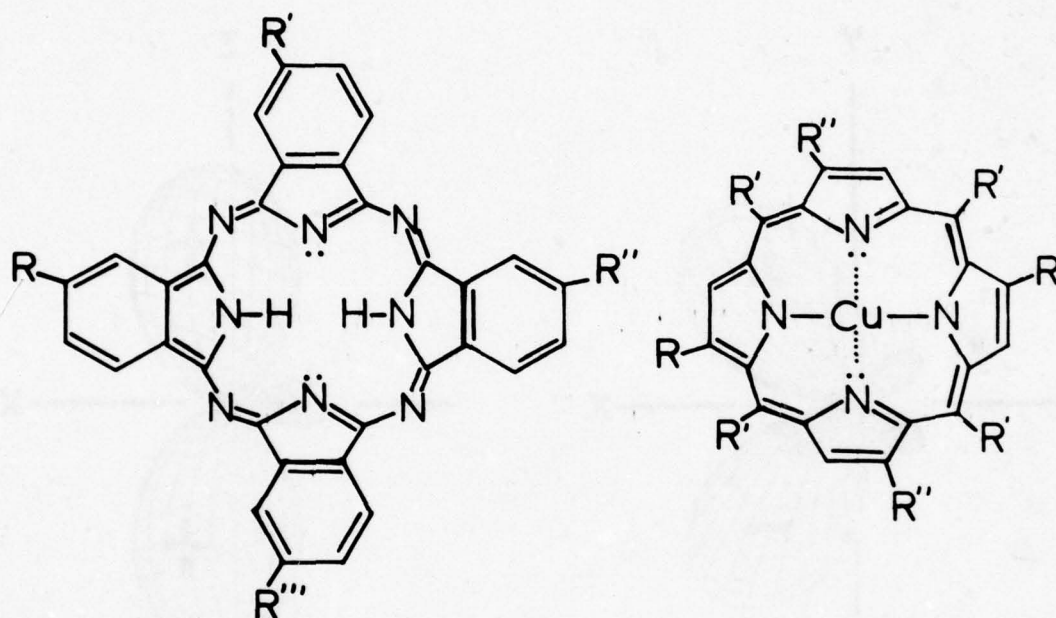


Fig. 4. These are PAV cells for the unique atoms of $\beta\text{-P}_4\text{S}_3\text{I}_2$. They fit together in the crystal structure to fill all space. Atomic positions are indicated by + while the cell centroids are indicated by \boxplus signs.



Phthalocyanine group

Metalloporphyrin

Fig. 5. The phthalocyanine group and the porphyrin group are shown. In the latter case, the hydrogens on nitrogen have been replaced by copper to form a metalloporphyrin where the Cu-N bonds resonate with the dative N:...Cu bonds to give four equivalent half-bonds. The R, R', etc., groups are hydrogen or side chains.

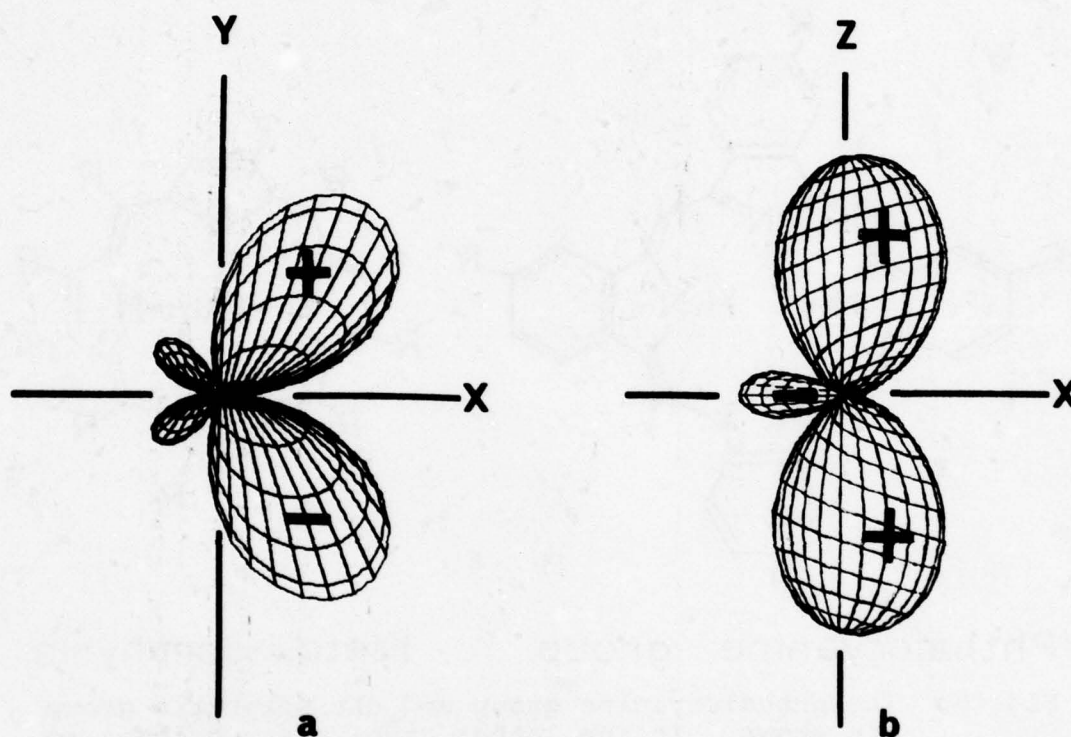


Fig. 6. Transition metal atoms can form hybrid orbitals in which the angular part of the electron density is well concentrated into two lobes suitable for forming half-bonds with suitably located neighbors. C orbital is a p_y - d_{xy} hybrid, while a G orbital is a s - d_{z^2} - p_x hybrid.

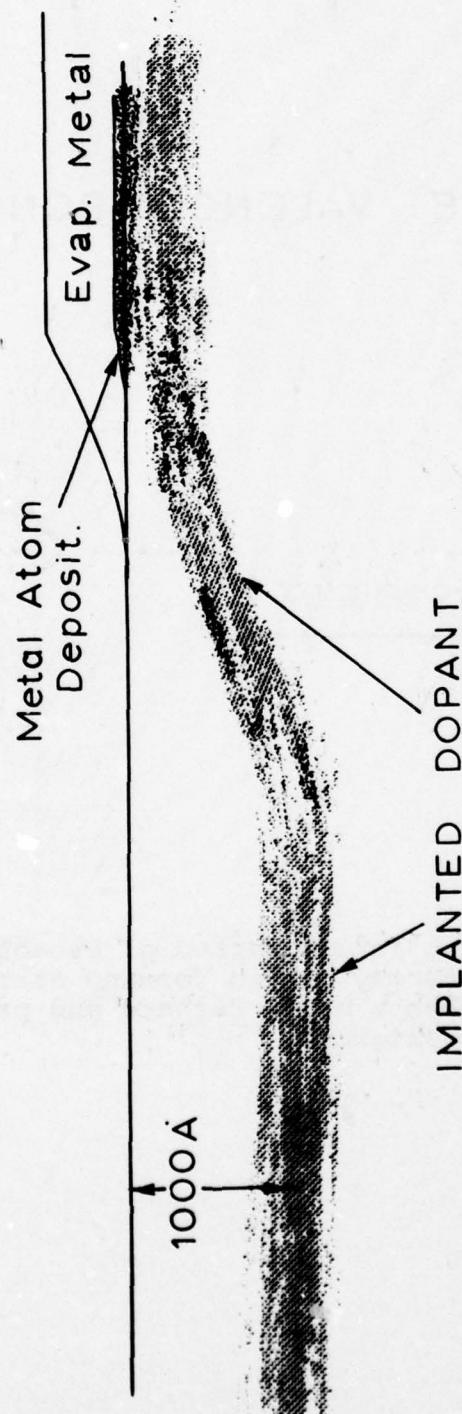


Fig. 7. An implanted doped conducting layer 1000 Å below the surface can be brought to the surface via control of the implanting ion kinetic energy and/or incident angle. On this surface-conducting area can then be deposited active metal atoms and overlapped with an evaporated metal film.

SURFACE VALENCE BONDING

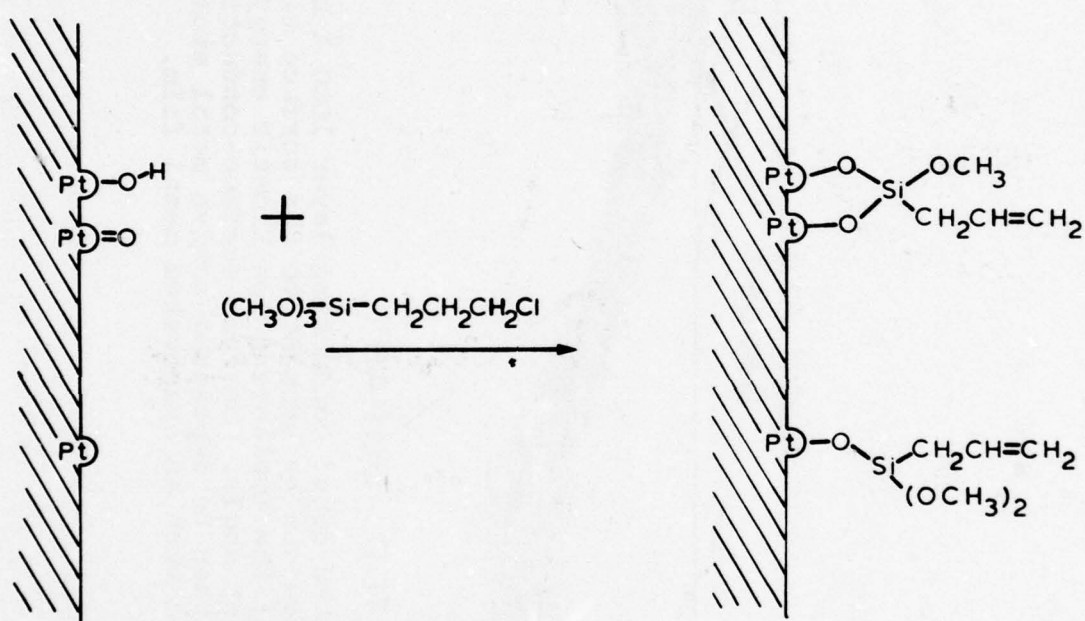


Fig. 8. An important future method of establishing electrical contacts may be via forming strong valence bonds between a metal surface and precursor of a conducting oligomer.

PLATINUM 4f SPECTRA

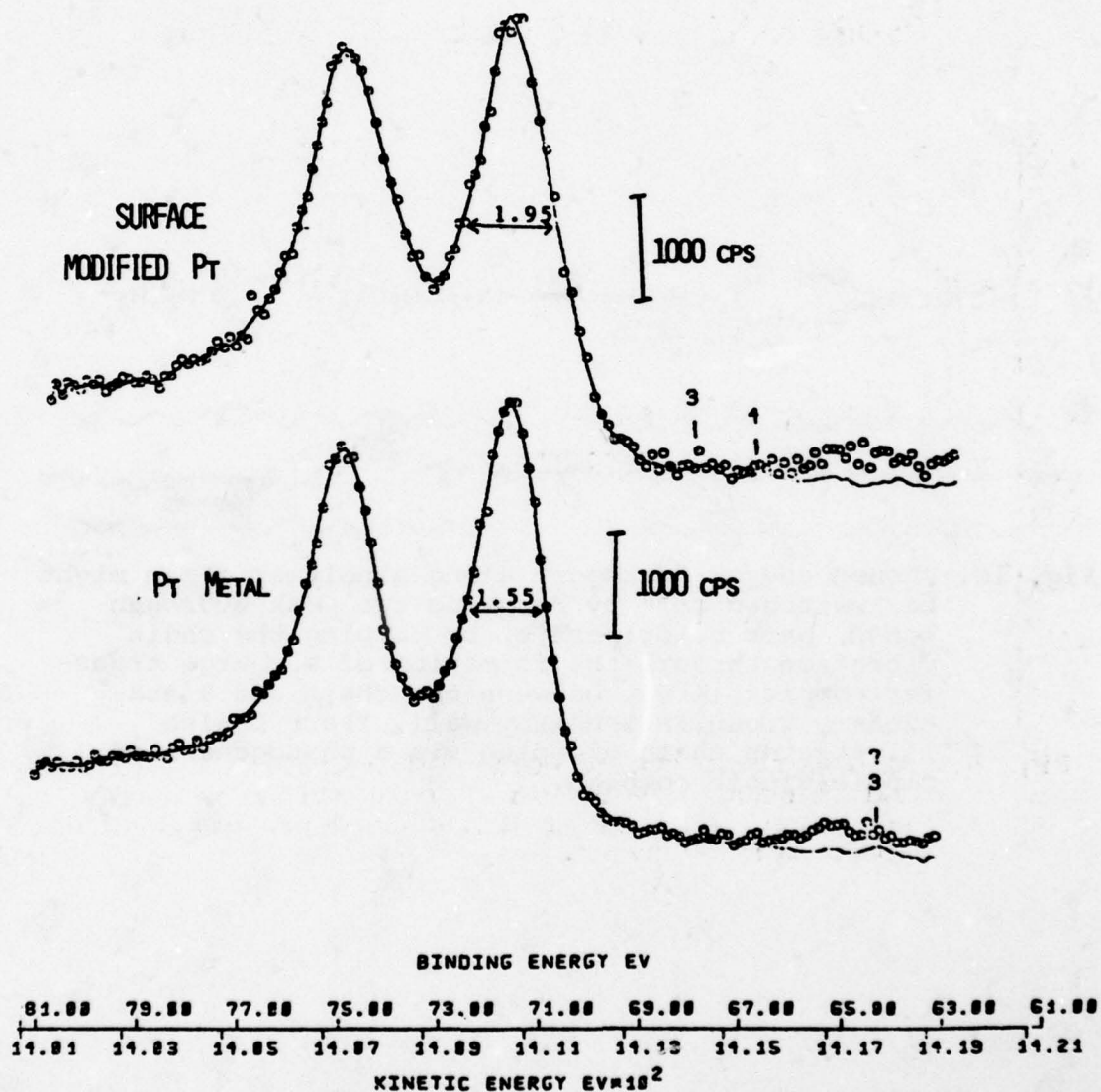


Fig. 9. The large increase in the FWHM of the Pt(4f) spectra (1.55 \rightarrow 1.95 eV) indicates that a surface layer of Pt atoms has indeed been metal-bonded to methoxysilane as suggested in Fig. 8.

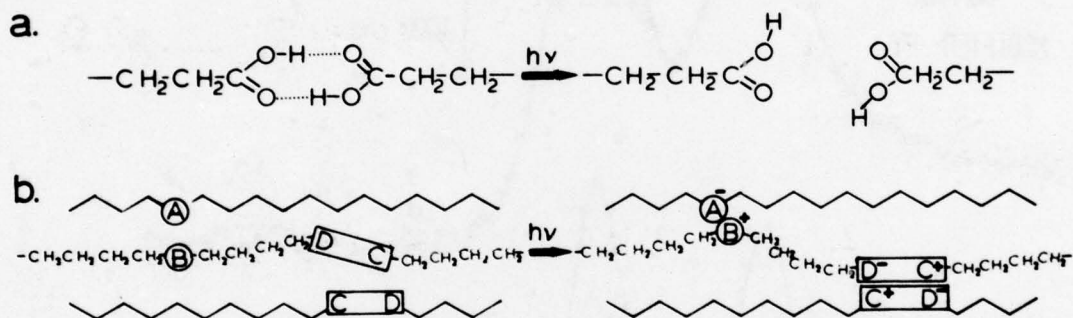
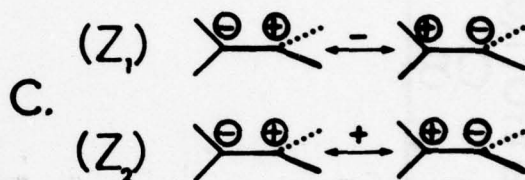
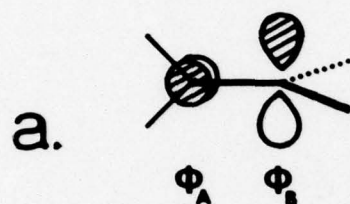


Fig. 10. Phonon energy transport along a polymer chain might be "switched off" by breaking two weak hydrogen bonds, part a, or part b, by damping the chain vibration through the formation of a charge transfer complex, $A^{\cdot-}B^{\cdot+}$, between the chain and a stationary group in a nearby wall. Part b also illustrates chain clamping via a photogenerated dipole-dipole complex.



b.

$$(Z_1) \quad \Psi = \Phi_A(1) \Phi_A(2) - \Phi_B(1) \Phi_B(2)$$

$$(Z_2) \quad \Psi = \Phi_A(1) \Phi_B(2) + \Phi_B(1) \Phi_A(2)$$

Fig. 11. Figure 11a illustrates the two p orbitals of an excited π bond after a 90° rotation about the bond. The wavefunctions Z_1 and Z_2 of Fig. 11b represent ionic ways of distributing the excited electrons (shown schematically in Fig. 11c). The zwitterionic states correspond to linear combinations of Z_1 and Z_2 .

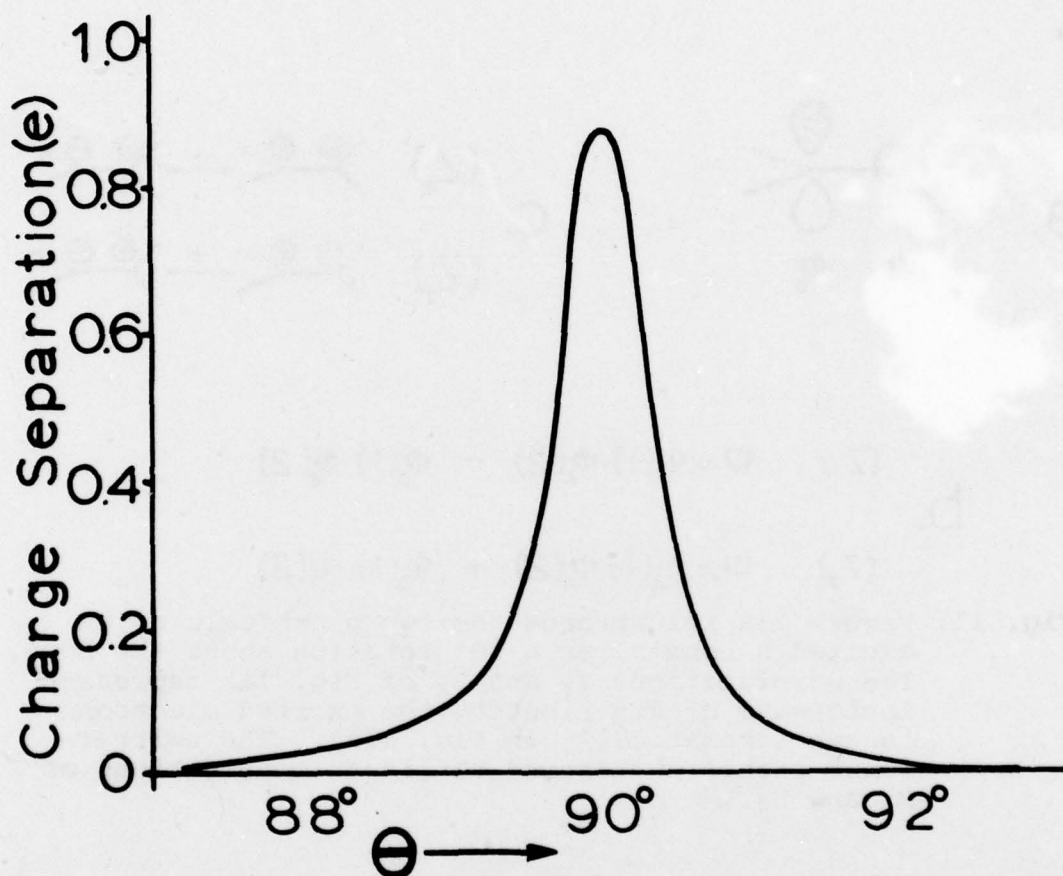


Fig. 12. The charge transfers in the zwitterionic states depend very much on angle of rotation θ about the excited double bond, especially near 90° . It is this surprising angular dependence that gives rise to the term "Sudden Polarization Effect." This figure is adapted from that of Salem, Ref. 16.

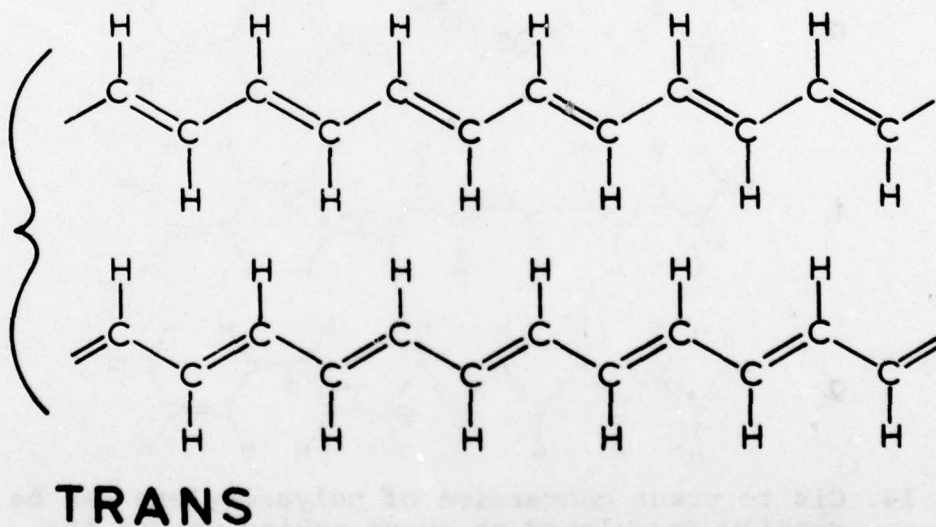
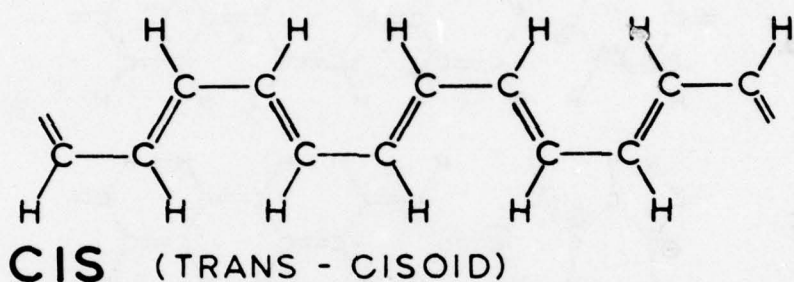
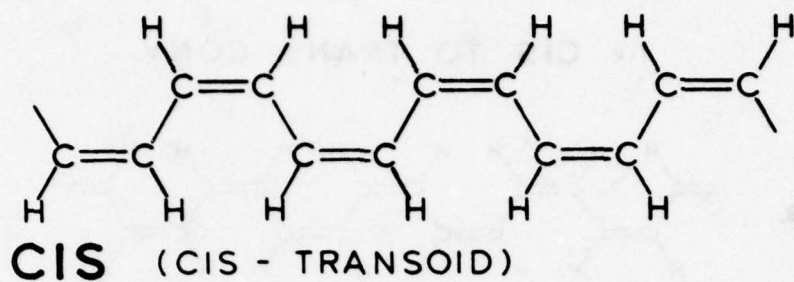


Fig. 13. The two related resonance forms of the cis isomer of polyacetylene are compared to the equivalent resonance forms of the trans- isomer. By rotating the trans- cisoid form repeatedly about the single bonds, one can hypothetically convert this form to one of the trans forms; however, this is a very unlikely route of cis to trans conversion due to steric hindrance.

hv CIS TO TRANS CONV.

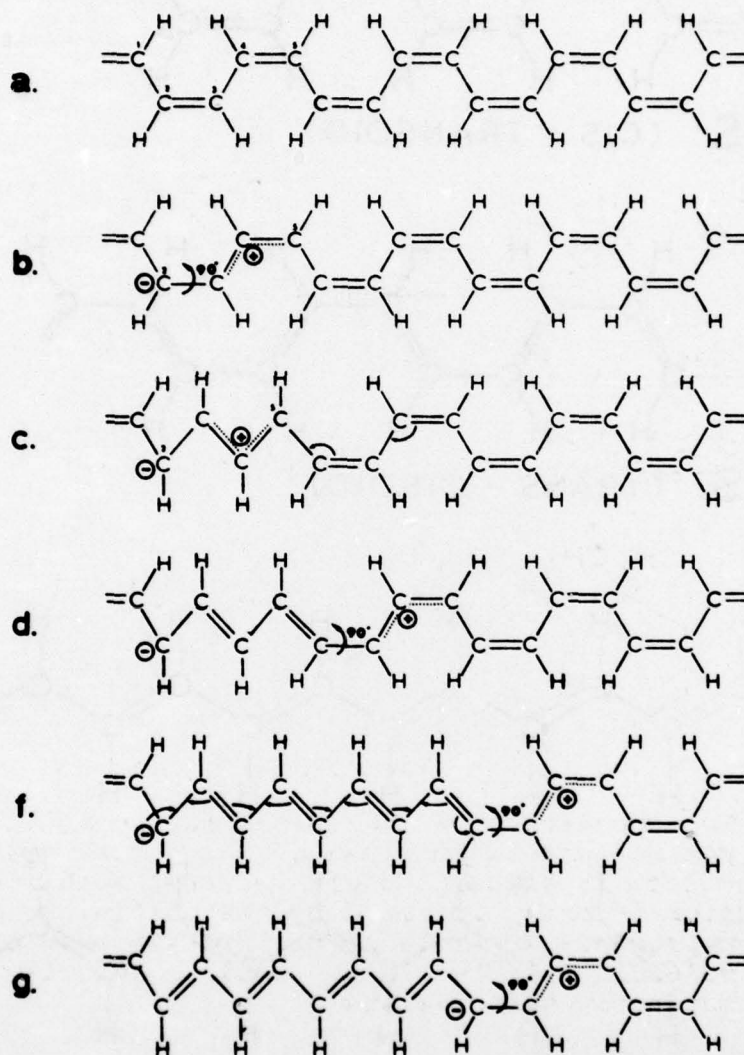


Fig. 14. Cis to trans conversion of polyacetylene can be readily formulated as above making use of the sudden polarization effect and sequential rotation of carbon atom pairs. The first rotation involves carbons 3 and 4 about an axis joining carbons 2 and 5. The omitted step e is essentially the same as step c with the + charge four carbons further right. The electron rearrangement indicated in step f-g suggests extended charge separation is not necessary.

March

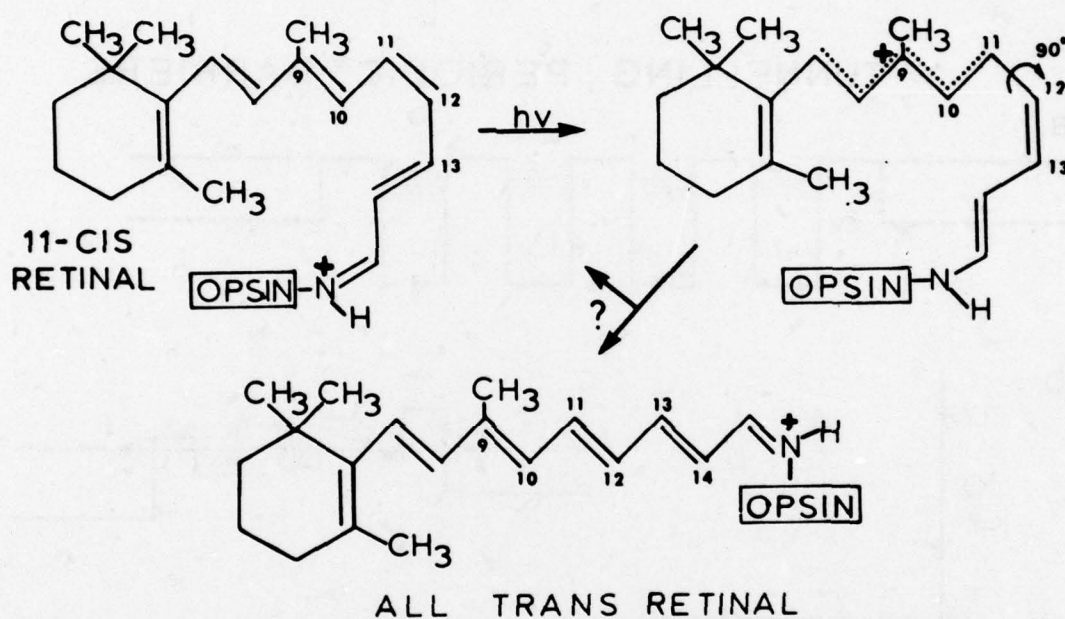


Fig. 15. The conversion of 11 cis-retinal to all trans retinal via Salem's use of the sudden polarization effect is associated with extensive charge separation strongly assisted by the quaternary imino-nitrogen. The role of the protein part of the molecule (OPSIN) in the optical activity is currently controversial.

TUNNELLING PERIODIC BARRIERS

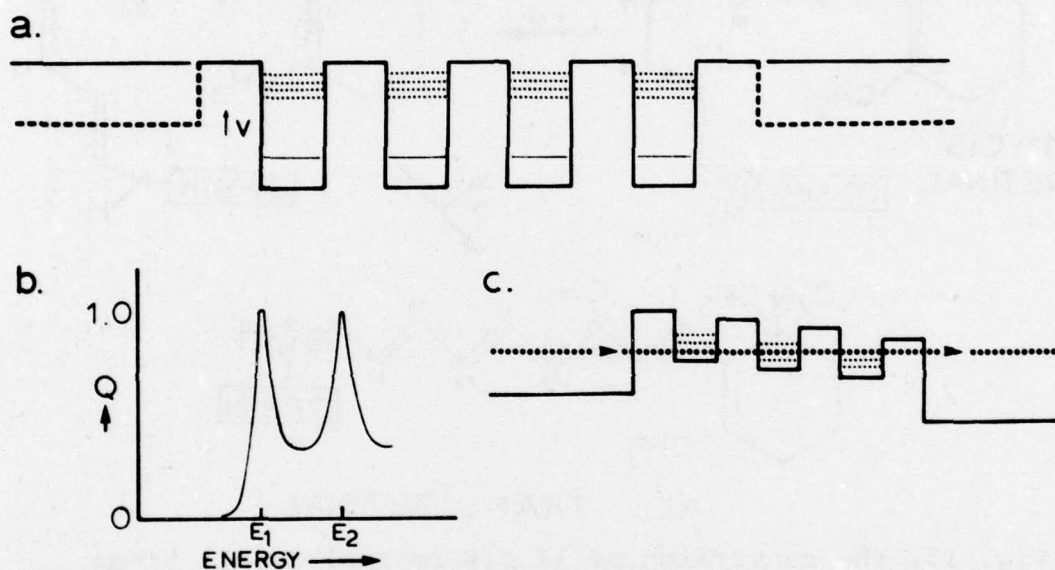


Fig. 16. In part a, the splitting of upper energy levels into the E_i values is indicated by the dotted lines. The rapid fall-off in transmission $Q(E)$ as one deviates from an E_i value is schematically indicated in part b. Part c suggests use of periodic tunnelling to accelerate electrons to a monochromatic beam.

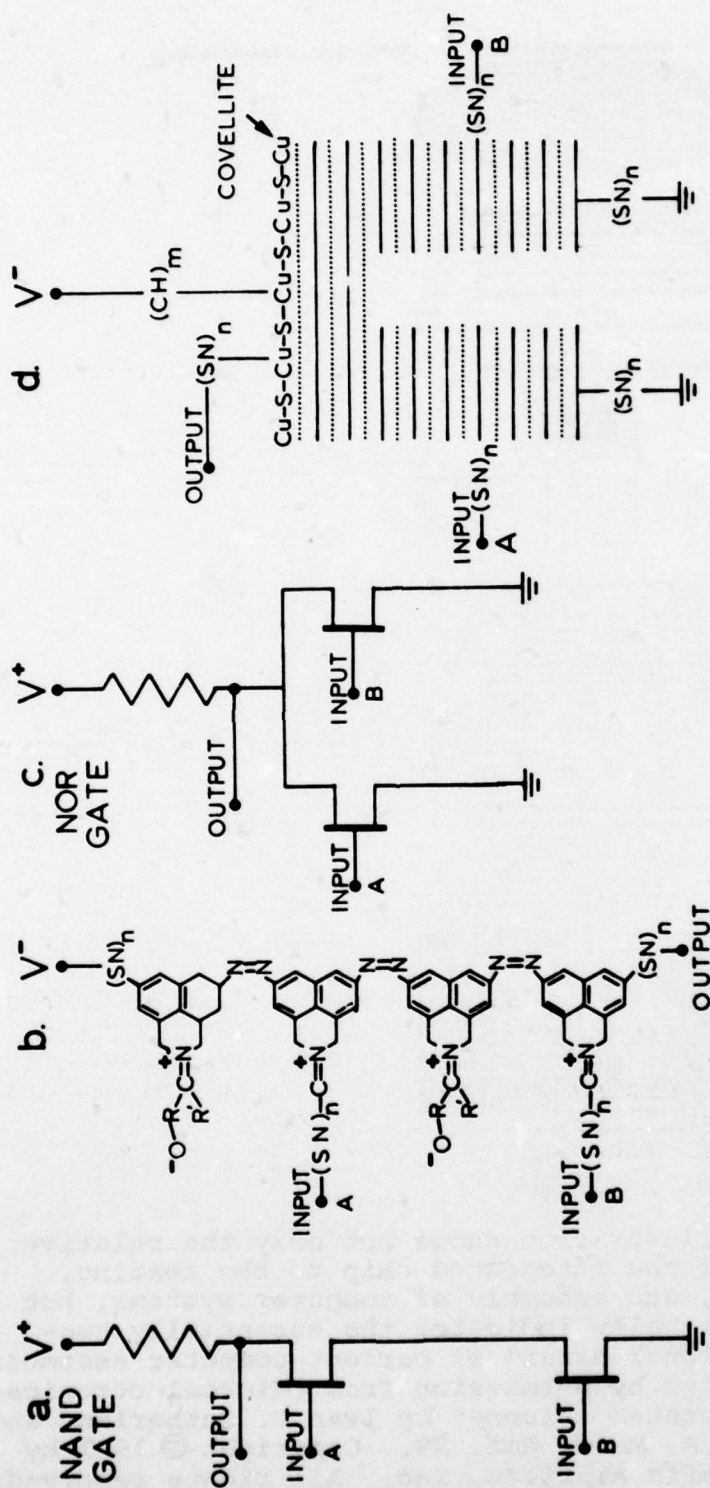


Fig. 17. Molecular analogs to the "NAND" and "NOR" gates of conventional electronic circuitry, Figs. 17a and 17c, respectively, are readily imagined by making use of periodic barrier tunnelling. In Fig. 17b, note that the usual resistive element is absent. The solid parallel lines in Fig. 17d represent hexagonal conducting $(Cu-S)_n$ layers while the dotted lines represent insulating tetrahedral $(CuS)_n$ layers.

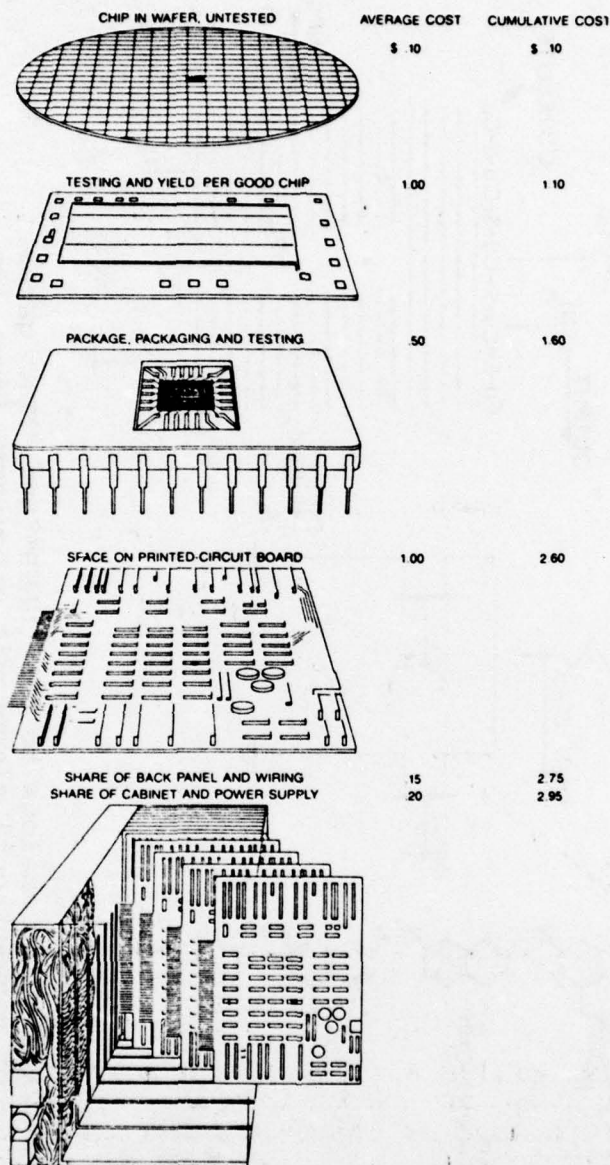


Fig. 18. This illustration shows not only the relative cost of the integrated chip to the testing, hookup, and assembly of computer systems, but also visually indicates the essentially two-dimensional nature of current computer assemblies. Reprinted by permission from "Microelectronics and Computer Science" by Ivan E. Sutherland and Carver A. Mead, Ref. 29. Copyright © 1977 by Scientific American, Inc. All rights reserved.

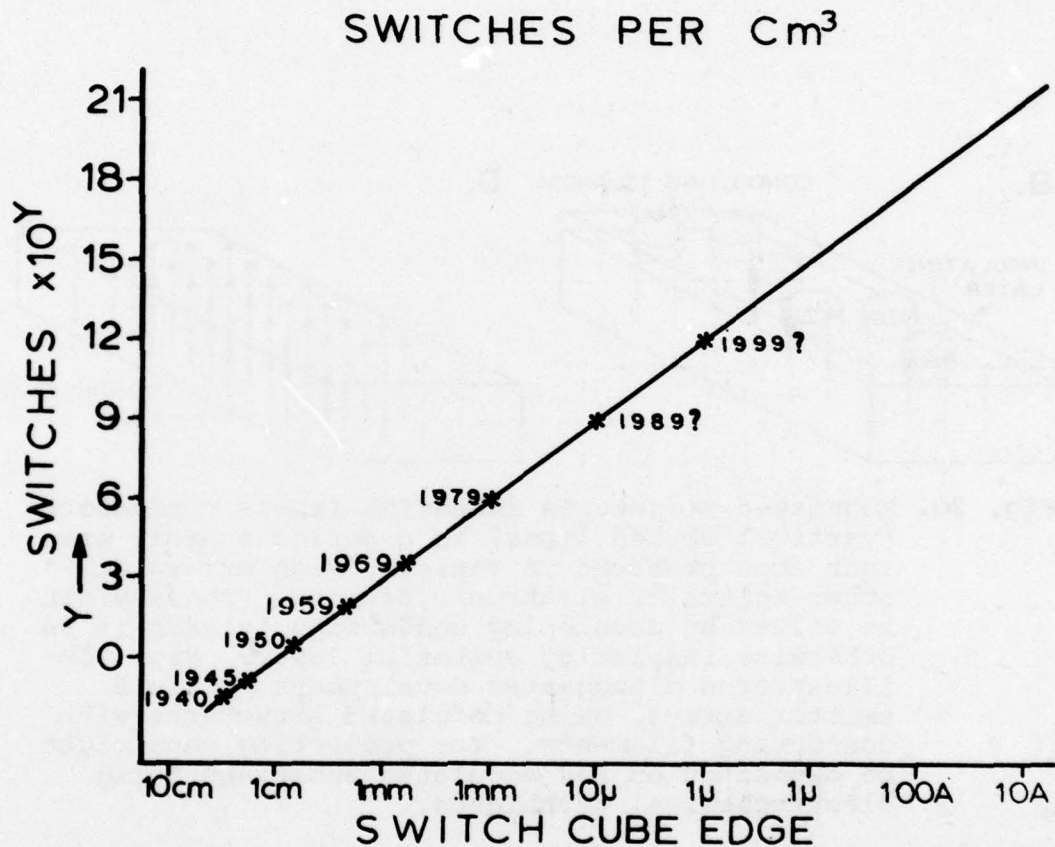


Fig. 19. If molecular electronic gates can be produced in the range of 100 to 1000 Å on an edge, the enormous number of components per cubic centimeter (10^{18} to 10^{15}) would produce a revolution in computer technology if three-dimensional assembly were achievable.

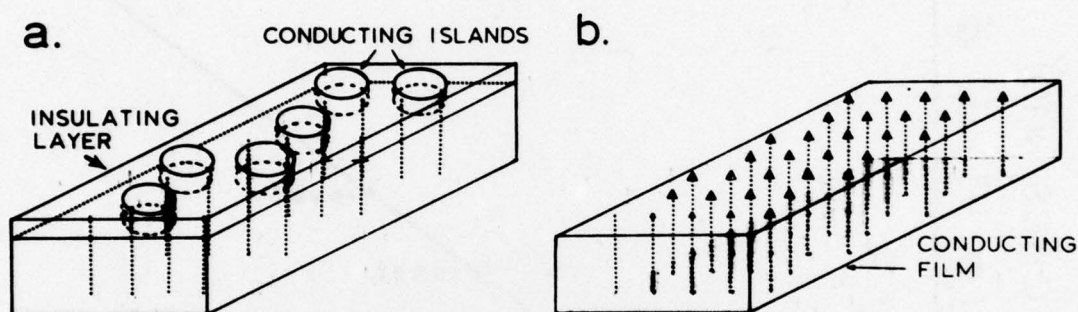


Fig. 20. Modulated structures imbedding linear conductors (vertical dotted lines) in a periodic array present some problems in registry with arrays of other molecular electronic devices. These might be solved by developing conducting islands in an otherwise insulating epitaxial layer. Fig. 20b illustrates a suggested development of field emitter arrays, using modulated structures with conducting filaments. The projecting caps might be deposited on the modulated substrate using electrochemical techniques.

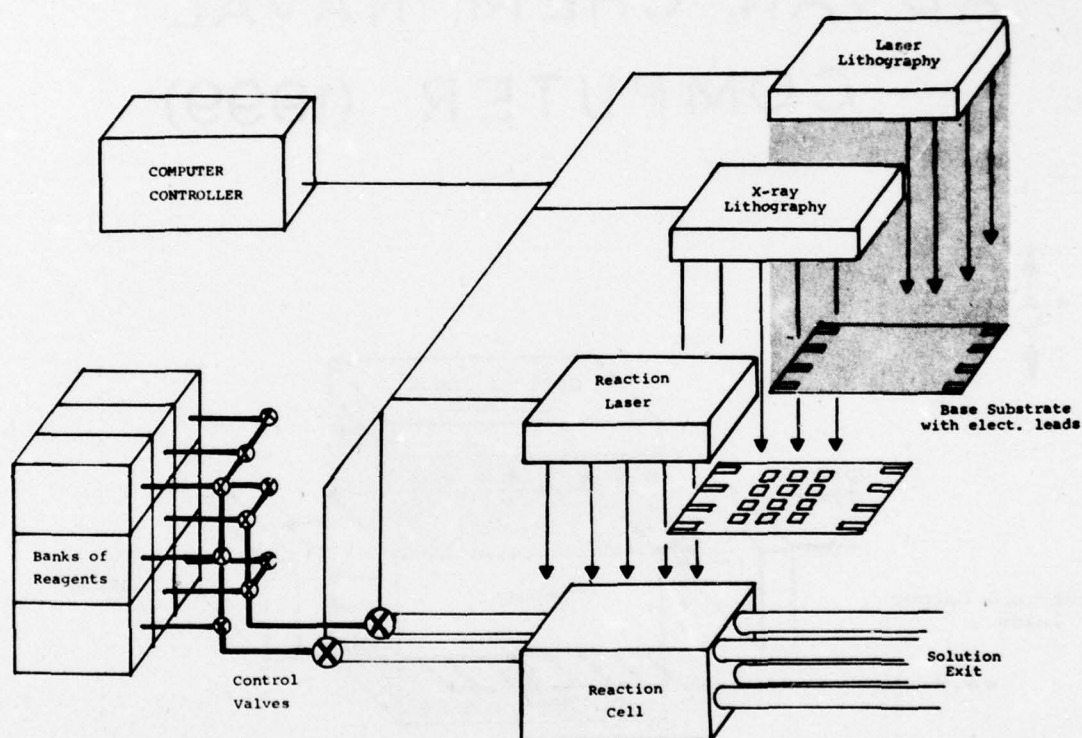


Fig. 21. A schematic for the chemical growth of the computer of the future assumes use of a variety of current techniques including the Merrifield method of long chain protein synthesis.

ADVANCED CHEMICAL NAVAL COMPUTER (1999)

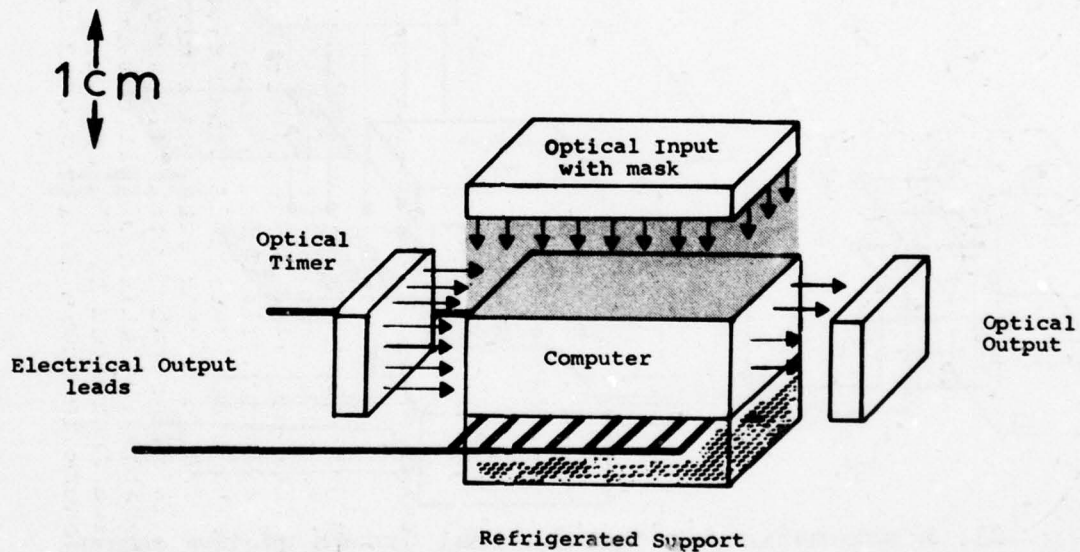
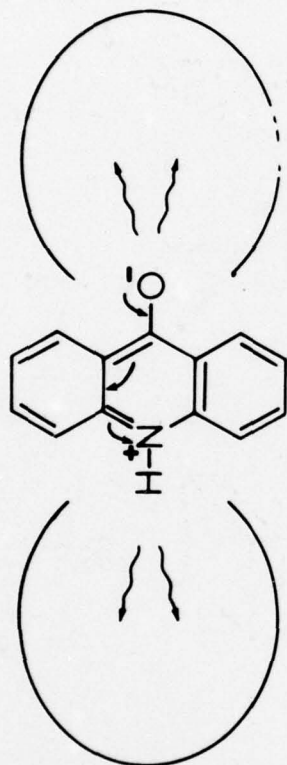


Fig. 22. A supercomputer of the 1990's is pictured as miniscule by comparison with current models. Such a computer would have low power consumption and optical input and output devices.



a.

b.

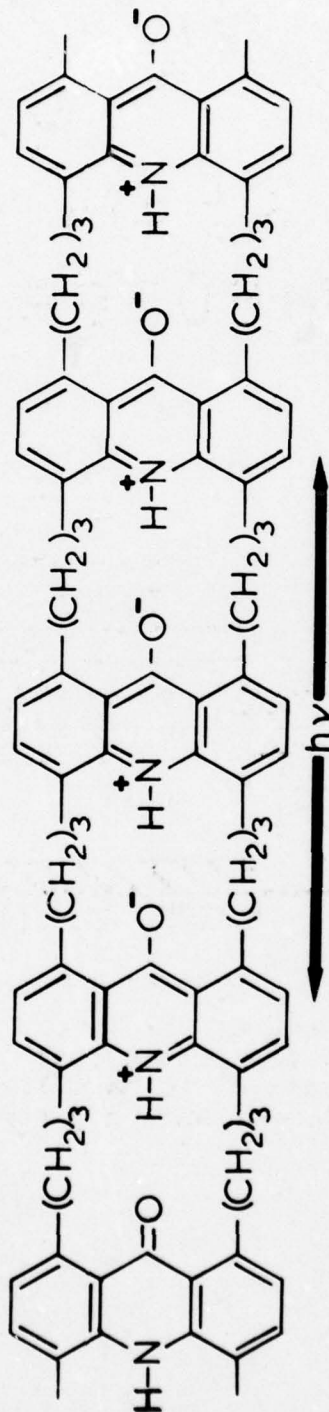


Fig. 23. A linear array of excited chromophores may be able to radiate in a highly directional mode similar to the current laser devices. In Fig. 23a, the dipole radiation field for a single chromophore undergoing deactivation is schematically indicated. In Fig. 23b, a linear array of excited chromophores is illustrated with aligned dipole fields. The probable radiation directions for the excited array are indicated by the arrows. The left-most chromophore is shown in its ground state.